

TURKISH JOURNAL OF AGRICULTURAL ENGINEERING RESEARCH



VOLUME:5 ISSUE:1 YEAR:2024

TURKAGER

2024



e-ISSN:2717 - 8420

<https://dergipark.org.tr/tr/pub/turkager>



TURKISH JOURNAL OF AGRICULTURAL ENGINEERING RESEARCH



TURKAGER

e-ISSN: 2717 - 8420

<https://dergipark.org.tr/tr/pub/turkager>

Turkish Journal of Agricultural Engineering Research
(*Turk J Agr Eng Res, TURKAGER*)

Volume 5,
Issue 1,
Year 2024

Indexing / Abstracting



Source Index



DIRECTORY
OF OPEN ACCESS
SCHOLARLY
RESOURCES



ADVANCED SCIENCE INDEX



BASE
Bielefeld Academic Search Engine



Directory of
Research Journal
Indexing



ASOS
indeks



ROOTINDEXING
JOURNAL ABSTRACTING AND INDEXING SERVICE



TIB
LEIBNIZ INFORMATION CENTRE
FOR SCIENCE AND TECHNOLOGY
UNIVERSITY LIBRARY



Scientific Indexing Services

Quality Open Access Market



TURKISH JOURNAL OF AGRICULTURAL ENGINEERING RESEARCH



TURKAGER

e-ISSN: 2717 - 8420

<https://dergipark.org.tr/tr/pub/turkager>

Turkish Journal of Agricultural Engineering Research (*Turk J Agr Eng Res, TURKAGER*)

PUBLISHER

Prof. Dr. Ebubekir ALTUNTAŞ

Tokat Gaziosmanpaşa University, TÜRKİYE

ABOUT

Turkish Journal of Agricultural Engineering Research (Turk J Agr Eng Res, TURKAGER) is an international open-access online, and peer double-blind reviewed journal. TURKAGER publishes the original English and Turkish research articles and a very limited number of review articles. There are no page charges for manuscript publishing in this journal. TURKAGER has an open access system and online journal published twice a year in June and December.

Turk J Agr Eng Res (TURKAGER) is a peer double-blind reviewed journal and an interdisciplinary journal concerned with all parts of Agricultural Engineering (Horticulture, Plant Protection, Biosystems Engineering, Field Crops, Agricultural Economics, Soil Science and Plant Nutrition, Aquaculture, Animal Science), Food Science and Technology, Biology, and Environment.

Turkish Journal of Agricultural Engineering Research is indexed/abstracted in CABI, EBSCO, Information Matrix for the Analysis of Journals (MIAR), CAS Source Index (CASSI), Food Science & Technology Abstracts (FSTA), BASE, Directory Research Journals Indexing (DRJI), ROAD (Directory of Open Access Scholarly Resources), WorldCat, ResearchBible, Beluga-Catalogue of Hamburg Libraries, Advanced Science Index (ASI), Scientific Literature (Scilit), Scholar Article Journal Index (SAJI), IJIFACTOR Indexing, Electronic Journals Library (EZB), SJIF Master Journals List, International Institute of Organized Research (I2OR), Cite Factor, International Services for Impact Factor and Indexing (ISIFI), ASOS INDEX, Cosmos, Technical Information Library (TIB), ROOTINDEXING, Scientific Indexing Services (SIS), Journal Tables of Contents, Quality Open Access Market.

Turkish Journal of Agricultural Engineering Research is licensed (CC-BY-NC-4.0) under a Creative Commons Attribution 4.0 International License.



TURKISH JOURNAL OF AGRICULTURAL ENGINEERING RESEARCH



TURKAGER

e-ISSN: 2717 - 8420

<https://dergipark.org.tr/tr/pub/turkager>

Turkish Journal of Agricultural Engineering Research (*Turk J Agr Eng Res, TURKAGER*)

EDITORIAL BOARD TEAM

EDITOR-in-CHIEF

Prof. Dr. Ebubekir ALTUNTAŞ / *Tokat Gaziosmanpaşa University, TÜRKİYE*

ASSISTANT EDITORS

Prof. Dr. Sedat KARAMAN / *Tokat Gaziosmanpaşa University, TÜRKİYE*

Dr. Bahadır ŞİN / *Sakarya University of Applied Sciences, TÜRKİYE*

TECHNICAL EDITOR

Dr. Bahadır ŞİN / *Sakarya University of Applied Sciences, TÜRKİYE*

LANGUAGE EDITORS

Assoc. Prof. Dr. Gülay KARAHAN / *Çankırı Karatekin University, TÜRKİYE*

Dr. Manoj Kumar MAHAWAR, *ICAR-Central Institute, Res. Cotton Tech., INDIA*

Prof. Dr. Fatih YILMAZ / *Tokat Gaziosmanpaşa University, TÜRKİYE*

STATISTICS EDITOR

Assoc. Prof. Dr. Yalçın TAHTALI / *Tokat Gaziosmanpaşa University, TÜRKİYE*

Dr. Lütfi BAYYURT, *Tokat Gaziosmanpaşa University, TÜRKİYE*

SECRETARIAT

Dr. Burcu AKSÜT *Tokat Gaziosmanpaşa University TÜRKİYE*

Researcher Hamide ERSOY, *Tokat Gaziosmanpaşa University, TÜRKİYE*

Dr. Esra Nur GÜL, *Tokat Gaziosmanpaşa University, TÜRKİYE*

Researcher Emine POLAT, *Tokat Gaziosmanpaşa University, TÜRKİYE*

Dr. Ayse Nida KAYAALP, *Muş Alparslan University, TÜRKİYE*

(*): The list is based on the surname of the editors in alphabetical order



TURKISH JOURNAL OF AGRICULTURAL ENGINEERING RESEARCH



TURKAGER

e-ISSN: 2717 - 8420

<https://dergipark.org.tr/tr/pub/turkager>

Turkish Journal of Agricultural Engineering Research (*Turk J Agr Eng Res, TURKAGER*)

SECTION EDITORS (*)

Prof. Dr. Zümrüt AÇIKGÖZ, *Animal Science, Ege University, TÜRKİYE*

Prof. Dr. Bilge Hilal ÇADIRCI EFELİ, *Biology, Tokat Gaziosmanpaşa University, TÜRKİYE*

Assoc. Prof. Dr. Hasan Gökhan DOĞAN, *Agricultural Economics, Kırşehir Ahi Evran University, TÜRKİYE*

Assoc. Prof. Dr. Gülay KARAHAN, *Land Scape and Architecture, Çankırı Karatekin University, TÜRKİYE*

Dr. Ayşe ÖLMEZ, *Fisheries Engineering, Tokat Gaziosmanpaşa University, TÜRKİYE*

Dr. Mahir ÖZKURT, *Field Crops, Muş Alparslan University, TÜRKİYE*

Assoc. Prof. Dr. Ahmet ÖZTÜRK, *Horticulture, Ondokuz Mayıs University, TÜRKİYE*

Prof. Dr. Bahadır SAYINCI, *Biosystems Engineering, Bilecik Şeyh Edebali University, TÜRKİYE*

Prof. Dr. Serkan SELLI, *Food Engineering, Cukurova University, TÜRKİYE*

Prof. Dr. Osman SÖNMEZ, *Soil Science and Nutrition, Erciyes University, TÜRKİYE*

Dr. Şerife TOPKAYA, *Plant Protection, Tokat Gaziosmanpaşa University, TÜRKİYE*

(*): The list is based on the surname of the editors in alphabetical order.

ADVISORY BOARD (*)

- Prof. Dr. Şenol AKIN, *Yozgat Bozok University, TÜRKİYE*
Prof. Dr. Omar Ali AL-KHASHMAN, *Al-Hussein Bin Talal University, Ma'an-JORDAN*
Assoc. Prof. Dr. Tewodros AYALEW, *Hawassa University, ETHIOPIA*
Dr. İlkey BARITÇI, *Dicle University, TÜRKİYE*
Prof. Dr. Zeki BAYRAMOĞLU, *Selçuk University, TÜRKİYE*
Assoc. Prof. Dr. Abdullah BEYAZ, *Ankara University, TÜRKİYE*
Assoc. Prof. Dr. Hatem BENTAHHER, *Electromechanical Systems, Sfax University, TUNISIA*
Assoc. Prof. Dr. Özer ÇALIŞ, *Akdeniz University, TÜRKİYE*
Prof. Dr. Ahmet ÇELİK, *Atatürk University, TÜRKİYE*
Prof. Dr. Aslıhan DEMİRDÖVEN, *Tokat Gaziosmanpasa University, TÜRKİYE*
Prof. Dr. Alper DURAK, *Malatya Turgut Ozal University, TÜRKİYE*
Assoc. Prof. Dr. Ramadan ELGAMAL, *Agricultural Engineering, Suez Canal University, EGYPT*
Dr. Hamideh FARIDI, *University of Tehran, IRAN*
Prof. Dr. Simon V. IRTWANGE, *University of Agriculture, Makurdi, NIGERIA*
Prof. Dr. Ali İSLAM, *Ordu University, TÜRKİYE*
Prof. Dr. Tomislav JEMRIC, *University of Zagreb, CROATIA*
Dr. Avinash Suresh KAKADE, *Univ.of Vasantrao Naik Marathwada Krushi Vidyapeeth, INDIA*
Dr. Zdzisław KALINIEWICZ, *Uniwersytet Warmińsko-Mazurski, ul. Olsztyn, POLAND*
Dr. Manal H.G. KANAAN, *Middle Technical University, Baghdad, IRAQ*
Dr. Muhammad Wasim Jan KHAN, *Institute of Southern Punjab (ISP), Multan, PAKISTAN*
Assist. Prof. Dr. Alltane J KRYEZIU, *University of Prishtina, Pristina, REPUBLIC OF KOSOVO*
Dr. Ahmed Moustafa Mohamed Ibrahim MOUSA, *Al-Azhar University, Cairo, EGYPT*
Assoc. Prof. Dr. Shahid MUSTAFA, *University of Sargodha, Sargodha, PAKISTAN*
Dr. Muhammad Ather NADEEM, *University of Sargodha, Sargodha, PAKISTAN*
Assoc. Prof. Dr. Seyed Mehdi NASIRI, *Shiraz University, Shiraz, IRAN*
Assoc. Prof. Dr. Chinenye Macmanus NDUKWU, *Michael Okpara Univ. of Agriculture, NIGERIA*
Assoc. Prof. Dr. Zhongli PAN, *California University, Davis, California, USA*
Assoc. Prof. Dr. Gheorghe Cristian POPESCU, *Pitesti University, ROMANIA*
Dr. Monica POPESCU, *University of Pitesti, ROMANIA*
Prof. Dr. Y. Aris PURWANTO, *IPB University, INDONESIA*
Prof. Dr. Hidayet OĞUZ, *Necmettin Erbakan University, TÜRKİYE*
Prof. Dr. Esen ORUÇ, *Tokat Gaziosmanpasa University, TÜRKİYE*
Dr. Shafiee SAHAMEH, *Tarbiat Modares University, Tehran, IRAN*
Prof. Dr. Mehmet Ali SAKİN, *Tokat Gaziosmanpasa University, TÜRKİYE*
Prof. Dr. Şenay SARICA, *Tokat Gaziosmanpasa University, TÜRKİYE*
Prof. Dr. Gordana SEBEK, *University of Montenegro, Podgorica, MONTENEGRO*
Assoc. Prof. Dr. Marisennayya SENAPATHY, *Wolaita Sodo University, Ethiopia, EAST AFRICA*
Dr. Feizollah SHAHBAZI, *Lorestan University, Khoram Abad, IRAN*
Prof. Dr. İsmail SEZER, *Ondokuz Mayıs University, TÜRKİYE*
Prof. Dr. Metin SEZER, *Karamanoğlu Mehmetbey University, TÜRKİYE*
Dr. Alaa SUBR, *University of Baghdad, IRAQ*
Hilary UGURU, *Delta State Polytechnic, Ozoro, Delta State, NIGERIA*

(*): The list is based on the surname of the editors in alphabetical order.



TURKISH JOURNAL OF AGRICULTURAL ENGINEERING RESEARCH



TURKAGER

e-ISSN: 2717 - 8420

<https://dergipark.org.tr/tr/pub/turkager>

Turkish Journal of Agricultural Engineering Research (*Turk J Agr Eng Res, TURKAGER*)

Volume 5,
Issue 1,
June 30, 2024

REFEREES (*)

- Sefa ALTIKAT, *Iğdır University, TÜRKİYE*
Mehmet Emin BİLGİLİ, *East Mediterranean Agricultural Research Institute, TÜRKİYE*
Necati ÇETİN, *Ankara University, TÜRKİYE*
Maney Ayalew DESTA, *Ethiopian Institute Agricultural Research, ETHIOPIA*
Emrah DAĞLI, *Bülent Ecevit University, TÜRKİYE*
Mahmut DURGUN, *Tokat Gaziosmanpaşa University, TÜRKİYE*
Tülin EKER, *Osmaniye Korkut Ata University, TÜRKİYE*
Can ERTEKİN, *Akdeniz University, TÜRKİYE*
Ömer ERTUĞRUL, *Kırşehir Ahi Evran University, TÜRKİYE*
Mohamed GHONIMY, *Cairo University, EGYPT*
Esra Nur GÜL, *Tokat Gaziosmanpaşa University, TÜRKİYE*
Zeki GÖKALP, *Erciyes University, TÜRKİYE*
Önder KABAS, *Akdeniz University, TÜRKİYE*
Özlem KILIÇ BÜYÜKKURT, *Osmaniye Korkut Ata University, TÜRKİYE*
Manoj MAHAWAR, *Indian Council of Agricultural Research, INDIA*
Funmilayo OGUNNAIKE, *The Federal Polytechnic, NIGERIA*
Muyiwa Abiodun OKUSANYA, *The Federal Polytechnic Ilaro, NIGERIA*
Gülden ÖZGÜNALTAY ERTUĞRUL, *Kırşehir Ahi Evran University, TÜRKİYE*
Alaattin SAKCALI, *Atatürk University, TÜRKİYE*
Onur SEVİNDİK, *Çukurova University, TÜRKİYE*
Muhammed TAŞOVA, *Tokat Gaziosmanpaşa University, TÜRKİYE*
Hilary UGURU, *Delta State University of Science and Technology, NIGERIA*
Elçin YEŞİLOĞLU CEVHER, *Ondokuz Mayıs University, TÜRKİYE*
Taner YILDIZ, *Ondokuz Mayıs University, TÜRKİYE*

(*): The list is based on the surname of the editors in alphabetical order.



TURKISH JOURNAL OF AGRICULTURAL ENGINEERING RESEARCH



TURKAGER

e-ISSN: 2717 - 8420

<https://dergipark.org.tr/tr/pub/turkager>

Turkish Journal of Agricultural Engineering Research (*Turk J Agr Eng Res, TURKAGER*)

Volume 5, Issue 1, June 30, 2024

Research Article

No	Articles	Author/s	Pages
1	Manufacturing of Healthy and Functional Savoury Flavours Using Over-Fermented Tempeh Hydrolisate Flour	Wignyanto WIGYANTO <u>Mujianto MUJIANTO</u>	1-20
2	Moisture-Dependent Physical and Aerodynamics Properties of Cowpea Seeds	<u>Olufemi Adeyemi ADETOLA</u> Adenike Mary ADEROTOYE Marvellous Oluwaseun LAWAL	21-34
3	Development of a Mechanical System to Produce Animal Feed from Rice Straw	<u>Mohamed GHONIMY</u> Ahmed SULIMAN Mohamed MORSY Ahmed ABDEEL-ATTY Ahmed ALZOHEIRY	35-48
4	Performance Evaluation of Diesel Engine Operated Cassava Grating Machine	<u>Amanuel Erchafo ERTEBO</u>	49-65
5	Study on Dielectric Properties of Rice Husk Ash Stabilized Soil	Ogaga AKPOMEDAYE <u>Friday Elohor ODOH</u> Helen JUWAH	66-75
6	Gravimetric characteristics and friction parameters of common bean (<i>Phaseolus vulgaris</i> L.)	<u>Biniam Zewdie GHEBREKIDAN</u> Adesoji Matthew OLANIYAN Amana Wako KOROSO Alemayehu Girma TADESSE Dereje Alemu ANAWTE Tamrat Lema NURGIE	75-93
7	Development of a Solar-Powered Barley Sprouting Room	<u>Ahmed Shawky EL-SAYED</u> AbdelGawad SAAD Mohamed Ali Ibrahim AL-RAJHI Maisa Moneir MEGAHED	94-116

Review Article

8	A Review of Hybrid and Green House Type Solar Dryers	<u>Promise ETIM</u> Akindele ALONGE David ONWE Inimfon OSSOM	117-130
---	--	---	---------



Turkish Journal of
Agricultural
Engineering Research
(Turk J Agr Eng Res)
e-ISSN: 2717-8420



Manufacturing of Healthy and Functional Savoury Flavours Using Over-Fermented Tempeh Hydrolysis Flour

Wignyanto WIGYANTO^a , Mujianto MUJIANTO^{b*} 

^aDepartment of Agriculture Industry Technology, Faculty of Agriculture, Technology University of Brawijaya, Malang, INDONESIA

^bDepartment of Agriculture Industry Technology, Faculty of Engineering, University of Wijaya Kusuma Surabaya, Surabaya, INDONESIA

ARTICLE INFO: Research Article

Corresponding Author: Mujianto MUJIANTO, E-mail: mujianto@uwks.ac.id

Received: 28 May 2023 / Accepted: 20 December 2023 / Published: 30 June 2024

Cite this article: Wignyanto, W and Mujianto M (2024). Manufacturing of Healthy and Functional Savoury Flavours Using Over-Fermented Tempeh Hydrolysis Flour. *Turkish Journal of Agricultural Engineering Research*, 5(1), 1-20. <https://doi.org/10.46592/turkager.1304379>

ABSTRACT

This research aims to: 1) determine the closeness of the properties of overfermented tempeh protein hydrolyzate flour to the properties of 11 cooking spices, 2) determine the potential of overfermented tempeh protein hydrolyzate flour as a raw material for the cooking spices industry. Fourier Transform Infrared (FTIR) Spectroscopy absorbance patterns were analyzed using principal component analysis (PCA) and hierarchical cluster analysis (HCA). Based on the PCA, the study's findings indicated that over-fermented tempeh hydrolysis flour 19/25H with a loading factor value of 0.617, 22/12H with a loading factor value of 0.609, 5/1H with a loading factor value of 0.533, 14/7H with a loading factor value of 0.533, 15/8H with a loading factor value of 0.528, 20/17H with a loading factor value of 0.513, As the primary ingredient for the savoury flavors of grilled chicken (SF01), over-fermented tempeh hydrolysis flour 4/15H with a loading factor value of 0.504 and 9/10H with a loading factor value of 0.505 both offer potential flavor character, Balado (SF02), Barbeque (SF03), Spicy Corn (SF04), Cheese (SF05), Salty Cheese (SF06), Sweet Spicy (SF07), Roasted Beef (SF08) and Tiramisu (SF09). Based on the result of hierarchical cluster analysis of over-fermented tempeh hydrolysis flour 9/10H and 23/23H, they have flavour character and functional properties as the main ingredient for the Savoury Flavours of Grilled Chicken (SF01) with closeness value of 453.406 (9/10H) and 465.536 (23/23H), Balado (SF02) with closeness value of 506.061 (9/10H) and 544.227 (23/23H), Barbeque (SF03) with a closeness value of 593.029 (9/10H) and 652.165 (23/23H), Spicy Corn (SF04) with closeness value of 595.097 (9/10H) and 632.614 (23/23H), Cheese (SF05) with closeness value of 482.596 (9/10H) and 520.814 (23/23H), Salty Cheese (SF06) with closeness value of 469.605 (9/10H) and 475.465 (23/23H), Sweet Spicy (SF07) with closeness value of 515.754 (9/10H) and 563.700 (23/23H), Roasted Beef (SF08) with closeness value of 526.120 (9/10H) and 525.428 (23/23H) and Tiramisu (SF09) with closeness value of 520.196 (9/10H) and 551.815 (23/23H).

Keywords: Fourie Transform Infrared (FTIR), Hierarchical Cluster Analysis (HCA), Principal Component Analysis (PCA), Savoury flavors



INTRODUCTION

Tempeh is a fermented food made of soybeans. It is a nutritious, affordable, and sustainable functional source of protein. Tempeh has been a widely accepted fermented product ([Ahnan-Winarno *et al.*, 2021](#)). Savoury flavour is flavour which gives taste to dry food (snacks), such as those made of potato (*Solanum tuberosum*), cassava (*Manihot utilissima*), banana (*Musa balbisiana*), sweet potato (*Ipomoea batatas*), breadfruit (*Artocarpus incissus*), melinjo chips (*Gnetum gnemon*), gayam fruit (*Inocarpus edulis*), corn (*Zea mays*), peanut (*Arachis hypogaea*), bean (*Canavalia gladiata*), pruriens (*Dolichos lablab*), chickpeas (*Pisum sativum*), bogor beans (*Voadzeia subterranea*), and biscuits and fruits which are generally sliced thinly and fried. The savoury flavours distributed in commercial markets are available in various tastes, such as salty savoury, grilled chicken, barbeque chicken, onion chicken, black pepper chicken, roasted chicken, citrus-scented balado, red balado, super red balado, orange balado, roasted balado, spicy balado, barbeque, spicy barbeque, chocolate tiramisu seasoning, grilled squid, green tea seasoning, grilled corn, sweet corn, chicken broth, balado chili sauce, green chili sauce, black pepper beef, roasted beef and many other taste variants. The savoury flavour is defined as far as possible and discussed with examples of delicious foods. According to a study, there is a direct causal relationship between 2 variations of MSG and 9 (nine) brands of seasoning (savory flavors) created from food additives and supportive materials with eigenvalues equal to 8.854 or 98.374 of variant. The seasonings with grilled chicken flavor (SF7), salted cheese flavor (SF5), roasted beef flavor (SF3), barbeque flavor (SF9), tiramisu flavor (SF6), spicy corn flavor (SF10), and monosodium glutamate (MSG) with eigenvalues score of 7.416 or 67.416% of variant all exhibit this direct causative correlation. Balado flavored seasoning (SF8), cheese flavored seasoning (SF4), sweet, spicy flavored seasoning (SF11), and Chinese flavor enhancing ingredients have direct causality with Chinese flavor enhancing ingredients, with eigenvalues scores of 1.517 or 13.792% of the variant. Monosodium glutamate (SF1) and Chinese flavor enhancing ingredient have similar eigenvalues score, which is 1.108 or 10.071% of variant ([Mujianto *et al.*, 2020](#)). It was characterized by the complexity of its taste, odour and trigeminally mediated attributes as by its combination of stimulation by mouth with lack of sweetness ([Land, 1994](#)) the moisture content of white bean (55.20%) and red lentil (55.99%) tempeh was similar to that of soy tempeh (55.45%) ([Erkan *et al.*, 2020](#)).

The characteristics of protein hydrolyzed from enzymatic hydrolysis process of rejected tempeh. The result of this study indicates that the highest Hydrolysis Level (HL) belongs to Flavorzyme enzyme (10.3% HL), Protamex (8.4% HL) and Calotropin (7.1% HL). The enzymatic reaction rate for Flavorzyme enzyme is V max, as much as 0.01727 mg per ml per minute, while the content of glutamate acid in hydrolyzed over fermented-tempeh reaches 15.95% ([Mujianto *et al.*, 2018](#)). Several groups of microorganism from fermented food such as tempeh and tape were reported; the potential LAB (Lactic Acid Bacteria) derived from those food sources is limited ([Novarina *et al.*, 2020](#)). Tempeh aroma and texture showed strong correlation between the numbers of bacterial population during the period or stages of tempeh maturation ([Nur *et al.*, 2020](#)). For centuries, fermented soy foods have been dietary staples in Asia and, now, in response to consumer demand, they are available

throughout the world. Fermentation produces unique flavors, boosts nutritional values, and increases or adds new functional properties (Cao *et al.*, 2019). The content of polyphenols and the antioxidative properties were determined in soybean tempeh fermented by four strains of *Rhizopus oligosporus* (Kuligowski *et al.*, 2017). In 2004, the value of savoury snack market in Thailand was expected to be worth 10-12 billion baht and this market consisted of puffed snacks (40%), potato chips (30 %), puffed rice (9%), prawn crackers (8-9%), fish snacks (8%), and others flavors for snack-food application (Wangcharoen *et al.*, 2006). The need for high nutritional value and healthy savoury flavors opens up opportunities for industries made from over fermented tempeh hydrolysate flour.

MATERIALS and METHODS

Materials

This study uses 9 (nine) kinds of savoury flavor, 1. Grilled Chicken (SF01), 2. Balado (SF02), 3. Barbeque (SF03), 4. Spicy Corn (SF04), 5. Cheese (SF05), 6. Salted Cheese (SF06), 7. Sweet Spicy (SF07), 8. Roasted Beef (SF08) and, 9. Tiramisu (SF09). Several savoury flavor stores in Surabaya provided the nine (9) different types of savoury flavors. Other ingredients include over-fermented tempeh flour (TTA01), over-fermented tempeh flour is made by crushing over-fermented tempeh obtained from traditional markets in Sidoarjo. Xingtai Sinobest Biotech Co.LTD is the manufacturer of the enzymes used, which include mannase (M), cellulose neutral enzyme (NC), and neutral protease enzyme (NP) and 2 (two) variants of monosodium glutamate, namely: 1. Monosodium glutamate (MSG) and, 2. Chinese Vetsin (VC).

Methods

Research method with Central Composite Design (CCD) model Quadratic Response Surface Method (QRSM) using Design Expert for Design of Experiment (DOE) software version 7.1. Data from Absorbance observations from Fourier Transform Infrared (FTIR) spectroscopy was processed using OriginLab software version 8.5. For PCA and HCA using SPSS software version 25.

RESULTS AND DISCUSSION

The descriptive statistic analysis results of 27 (twenty-seven) experiment units, 9 (nine) savoury flavours, 2 (two) types of MSG and over-fermented tempeh flour as seen in Table 2, which indicates that 23/23 H experiment unit has minimal absorbance average value of 27.4601 ± 9.06326 . Meanwhile, cheese flavor or SF02 has a maximum absorbance average value of 66.3262 ± 27.13280 . The total absorbance point observation from those 39 (thirty-nine) variables was 72.852 (seventy-two thousand eight hundred and fifty-two).

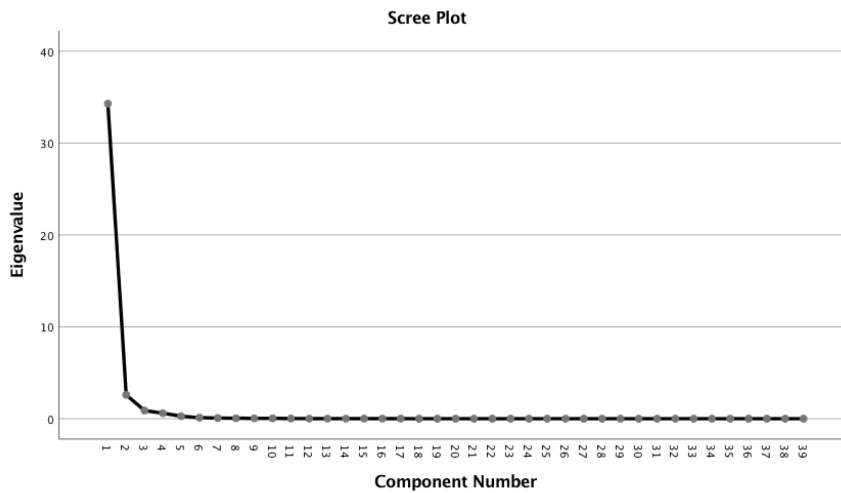


Figure 1. The correlation between eigenvalues and the 39 (thirty-nine) Principal Component.

Figure 1 shows the correlation between eigenvalue and 39 principal components. The correlation between the eigenvalues score and the principal component in the above figure shows that up to the 10th principal component (F10), the eigenvalues score approaches 0 (zero). Cumulatively, the percentage (%) of variants explained was 99.903%. For nine (9) savory flavors, the KMO test result was 0.949 and the Bartlett's test result was 421,242,458 with degrees of freedom of 741, suggesting that the data was normally distributed. The test result of KMO score > 0.50 is $0.949 > 0.500$, which means that the variable can be predicted and further analysed. Bartlett's test < 0.05 is $0.000 < 0.050$ indicating that inter-variables have a high correlation.

Component Plot in Rotated Space

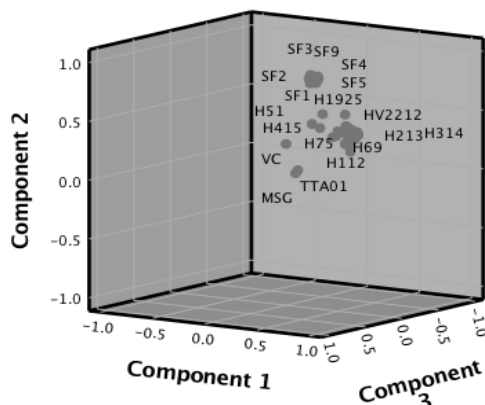


Figure 2. Correlation between the first principal component (F1), second principal component (F2) and third principal component (F3) of 27 (twenty-seven) experiment units, 2 (two) MSG Variants, over-fermented tempeh flour and 9 (nine) savoury flavours from FTIR absorbance observation result.

Based on the Figure 2, from 39 (thirty-nine) variables of principal component constituent, 54.56% is in the 1st (first) principal component, 36.825% is in the 2nd (second) principal component, and 8.615% is in the 3rd (third) principal component.

The suitability of attenuated total reflection (ATR) mid-infrared (MIR) spectroscopy, combined with principal component analysis (PCA) and partial least squares (PLS) regression, was evaluated as a rapid analytical technique for the classification of sparkling wine style and quality (Culbert *et al.*, 2015). Principal Component Analysis (PCA) is frequently used to display and discover patterns in SNP data from humans, animals, plants, and microbes, especially to elucidate population structure. Given the popularity of PCA, one might expect that PCA is understood well and applied effectively (Gauch *et al.*, 2019). FTIR-ATR combined with chemometrics analysis such as hierarchical cluster analysis (HCA), principal component analysis (PCA) and partial least squares-discriminant analysis (PLS-DA) was used for classification and discrimination of gelatin gummy candies related to their gelatin source (Cebi *et al.*, 2019). Principal component analysis and hierarchical cluster analysis can be used to determine the similarity or proximity of material characteristics. Table 1 below shows the multi-enzyme hydrolysis surface response design layout of over-fermented tempeh flour.

Table 1. Multi-enzyme hydrolysis surface respond design layout of over-fermented tempeh flour.

No	Std	RUN	Block	A T°C	B L/S (%)	C NP (%)	D NC (%)	E M (%)
1	4	15	Block 1	50	0.4	2	1	1
2	13	4	Block 1	45	0.3	1.5	1.5	1.5
3	3	14	Block 1	40	0.4	2	1	2
4	10	6	Block 1	40	0.4	2	2	1
5	6	9	Block 1	50	0.2	1	2	2
6	8	3	Block 1	40	0.4	1	2	2
7	1	12	Block 1	50	0.4	1	2	1
8	5	1	Block 1	50	0.4	1	1	2
9	14	7	Block 1	45	0.3	1.5	1.5	1.5
10	9	10	Block 1	50	0.2	2	1	2
11	2	13	Block 1	50	0.2	2	2	1
12	15	8	Block 1	45	0.3	1.5	1.5	1.5
13	12	11	Block 1	45	0.3	1.5	1.5	1.5
14	11	2	Block 1	40	0.2	1	1	1
15	7	5	Block 1	40	0.2	2	2	2
16	20	17	Block 2	45	0.3	0.58942	1.5	1.5
17	19	25	Block 2	45	0.482116	1.5	1.5	1.5
18	17	18	Block 2	54.1058	0.3	1.5	1.5	1.5
19	21	27	Block 2	45	0.3	2.41058	1.5	1.5
20	24	24	Block 2	45	0.3	1.5	1.5	0.58942
21	26	16	Block 2	45	0.3	1.5	1.5	1.5
22	16	19	Block 2	35.8942	0.3	1.5	1.5	1.5
23	25	26	Block 2	45	0.3	1.5	1.5	2.41058
24	23	23	Block 2	45	0.3	1.5	2.41058	1.5
25	22	22	Block 2	45	0.3	1.5	0.58942	1.5
26	27	21	Block 2	45	0.3	1.5	1.5	1.5
27	18	20	Block 2	45	0.117884	1.5	1.5	1.5

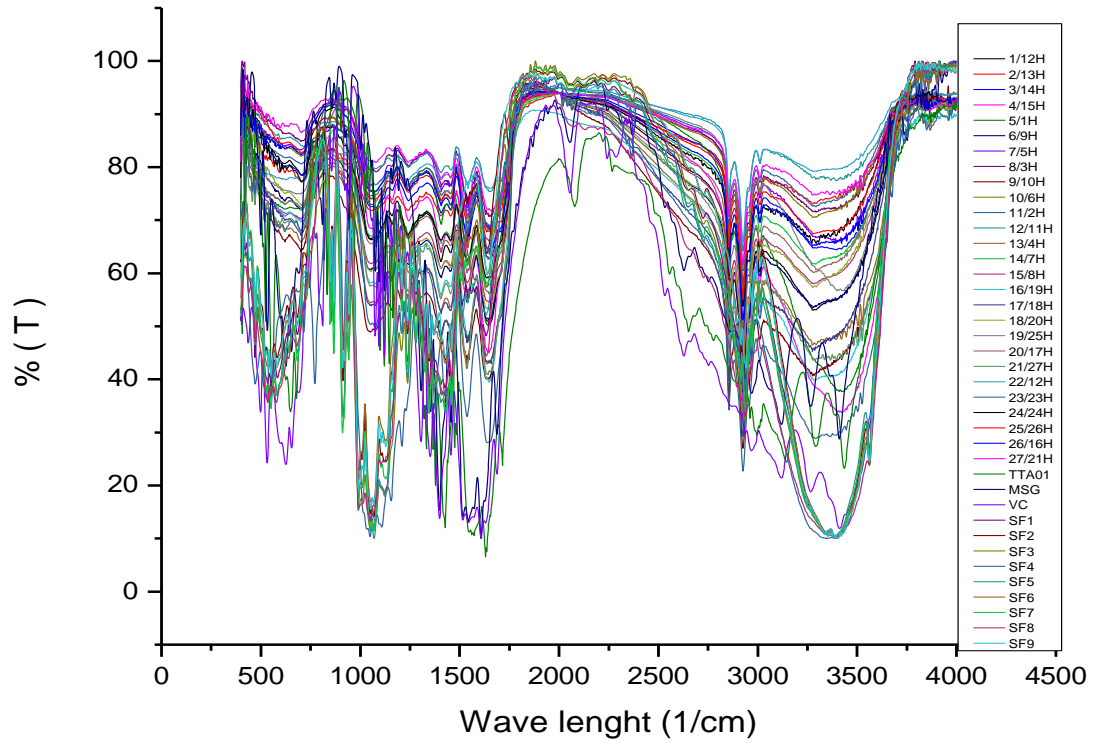


Figure 3. The absorbance pattern of 27 (twenty-seven) experiment units, over-fermented tempeh flour (TTA01), 2 (two) MSG variants and 9 (nine) savoury flavours in Indonesia.

Table 2. *The descriptive statistics of 27 (twenty-seven) experiment units, 9 (nine) savoury flavours, 2 (two) MSG variants and over-fermented tempeh flour (TTA01).*

No	Variable	Descriptive Statistics		
		Mean	Std. Deviation	N Analysis
1	1/12H	76.6104	14.20904	1868
2	2/13H	81.4654	8.20171	1868
3	3/14H	80.6243	9.85148	1868
4	4/15H	73.4221	17.79953	1868
5	5/1H	76.5199	16.25822	1868
6	6/9H	73.9939	13.88617	1868
7	7/5H	83.4050	9.03077	1868
8	8/3H	84.6223	7.87576	1868
9	9/10H	66.9074	18.14567	1868
10	10/6H	83.5856	8.48006	1868
11	11/2H	83.9339	7.89538	1868
12	12/11H	85.9742	5.93450	1868
13	13/4H	69.8087	16.12828	1868
14	14/7H	77.7141	11.14317	1868
15	15/8H	75.1172	12.60613	1868
16	16/19H	69.6567	16.52951	1868
17	17/18H	69.9997	16.82641	1868
18	18/20H	75.0469	12.86786	1868
19	19/25H	80.6327	10.49047	1868
20	20/17H	77.0628	11.73228	1868
21	21/27H	70.6065	16.57611	1868
22	22/12H	84.9985	6.66885	1868
23	23/23H	65.7346	21.61881	1868
24	24/24H	79.5129	10.59181	1868
25	25/26H	82.1704	9.00046	1868
26	26/16H	81.3369	9.91432	1868
27	27/21H	85.3122	7.00052	1868
28	TTA01	58.4175	23.21023	1868
29	MSG	67.3225	23.42716	1868
30	VC	54.8081	27.70221	1868
31	SF1	62.4048	27.22395	1868
32	SF2	66.3262	27.13280	1868
33	SF3	61.4711	28.48600	1868
34	SF4	60.3558	27.67728	1868
35	SF5	61.1741	27.51418	1868
36	SF6	65.7723	26.78064	1868
37	SF7	62.4748	27.94771	1868
38	SF8	58.7726	27.04615	1868
39	SF9	65.6665	27.08503	1868

Table 3. The result of FTIR absorbance pattern variable interpretation of over-fermented tempeh flour, 27 (twenty-seven) experiment units and 2 (two) MSG variants from 59,776 observation points.

No	Variable	Factor	Eigen Values	Loading Factor	% Variance	Cumulative %	
1	2/13H			0.855			
2	24/24H			0.848			
3	18/20H			0.833			
4	12/11H			0.824			
5	10/6H			0.821			
6	27/21H			0.820			
7	11/2H			0.814			
8	25/26H			0.805			
9	17/18H			0.803			
10	6/9H	The similarity of flavour character and material functional properties with over-fermented tempeh flour, 27 (twenty-seven) over-fermented tempeh hydrolysisate flour and 2 (two) MSG variants (F1)		0.796			
11	8/3H			0.793			
12	20/17H			0.790			
13	15/8H			0.790			
14	1/12H			18.107	0.786	46.428	46.428
15	26/16H				0.782		
16	13/4H				0.781		
17	14/7H				0.778		
18	9/10H				0.775		
19	3/14H				0.775		
20	21/27H			0.735			
21	16/19H			0.720			
22	7/5H			0.710			
23	22/12H			0.702			
24	23/23H			0.701			
25	4/15H			0.573			
26	19/25H			0.572			
27	TTA01			0.596			
28	MSG			0.616			
29	VC			0.502			
30	5/1H			0.499			

Figure 3 above shows the absorbance pattern of 27 (twenty-seven) experimental units, over-fermented tempeh flour (TTA01), 2 (two) MSG variants and 9 (nine) savory flavors in Indonesia. The 1st principal component (F1), after variable extraction and rotation using varimax method, has 30 (thirty) variables of the 1st principal component (F1) with eigenvalues score more than or equivalent to 0.50 respectively as follows:

Based on Table 3, the equation for the 1st principal component (F1) is the function of flavour character similarities and material functional properties 18/20H, 12/11H, 10/6H, 27/21H, 11/2H, 25/26H, 17/18H, 6/9H, 8/3H, 20/17H, 15/8H, 1/12H, 26/16H, 13/4H, 14/7H, 9/10H, 3/14H, 21/27H, 16/19H, 7/5H, 22/12H, 23/23H, 4/15H, 19/25H, TTA01, MSG, VC and 5/1H with eigenvalues score of 18.107 and total with over-

fermented tempeh flour, 27 (twenty-seven) over-fermented tempeh hydrolisate flour of the 1st (first) variant and 2 (two) MSG variants as in equation (1) below :

$$F1 = 0.855 (2/13H) + 0.848 (24/24H) + 0.833 (18/20H) + 0.824 (12/11H) + 0.821 (10/6H) + 0.820 (27/21H) + 0.814 (11/2H) + 0.805 (25/26H) + 0.803 (17/18H) + 0.796 (6/9H) + 0.793 (8/3H) + 0.790 (20/17H) + 0.790 (15/8H) + 0.786 (1/12H) + 0.782 (26/16H) + 0.781 (13/4H) + 0.778 (14/7H) + 0.775 (9/10H) + 0.775 (3/14H) + 0.735 (21/27H) + 0.720 (16/19H) + 0.710 (7/5H) + 0.702 (22/12H) + 0.701 (23/23H) + 0.573 (4/15H) + 0.572 (19/25H) + 0.596 (TTA01) + 0.616 (MSG) + 0.502 (VC) + 0.499 (5/1H) \quad (1)$$

Remark:

F1 = The Similarity of Flavour Character and Material Functional Properties of Over-Fermented Tempeh Flour (TTA01), 27 (twenty-seven) Over-Fermented Tempeh Hydrolisate Flour, and 2 (two) MSG Variants.

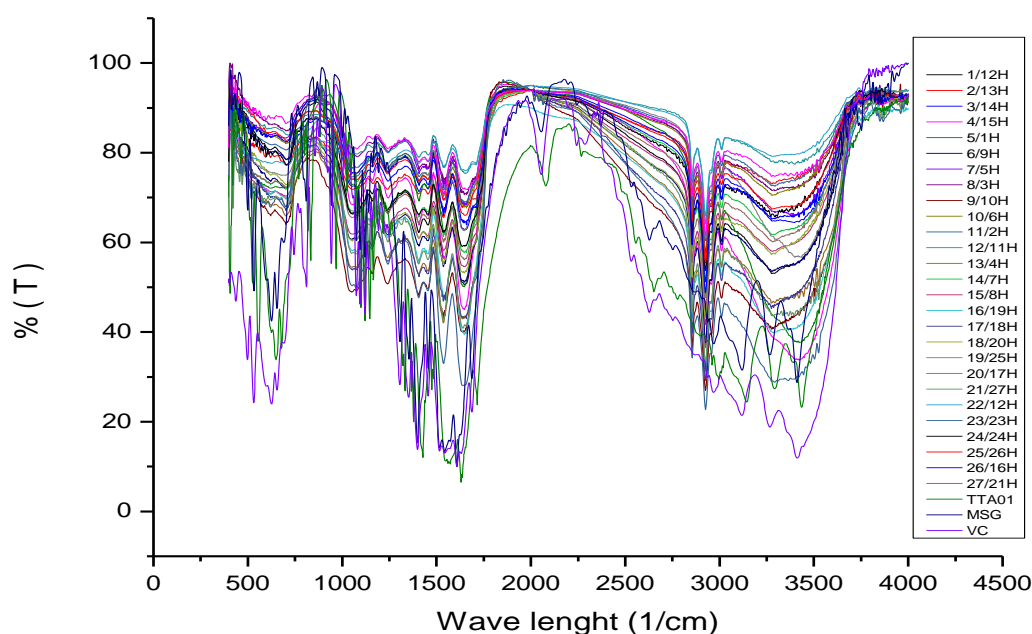


Figure 4. The absorbance pattern of the 1st principal component constituent variable (F1).

Figure 4 above shows the absorbance pattern of the 1st principal component constituent variable (F1). Based on equation (1) above, there are 9 (nine) variables with coefficient value (NK) of $0.803 \leq NK \leq 0.855$, namely 2/13H, 24/24H, 18/20H, 12/11H, 10/6H, 27/21H, 11/2H, 25/26H and 17/18H. There are 14 (fourteen) variables with coefficient value (NK) of $0.701 \leq NK \leq 0.796$, namely 6/9H, 8/3H, 20/17H, 15/8H, 1/12H, 26/16H, 13/4H, 14/7H, 9/10H, 3/14H, 21/27H, 16/19H, 7/5H, 22/12H and 23/23H. There are 6 (six) variables with coefficient value (NK) of $0.499 \leq NK \leq 0.616$, namely 4/15H, 19/25H, TTA01, MSG, VC and 5/1H. The closeness of coefficient value (NK) indicates the proximity of flavour characteristic properties and material functional properties.

The analytical method using infrared spectrophotometry requires a little sample preparation, and evaluation of the spectrogram was carried out in the protein and carbohydrate absorbance area (Kos *et al.*, 2016). Spectral information can also be exploited for strain typing purposes, which are particularly important for epidemiological analyses and some technological applications. Accordingly, in recent years, FTIR spectroscopy has been increasingly used for typing and classifying microorganisms below the species level (Wenning and Scherer, 2013).

Table 4. FTIR absorbance pattern variable interpretation of over-fermented tempeh flour and 22 (twenty-two) experiment units and 9 (nine) savoury flavours from 57,908 observation points.

No	Variable	Factor	Eigen Values	Loading Factor	% Variance	Cumulative %	
1	2/13H			0.455			
2	18/20H			0.454			
3	12/11H			0.473			
4	10/6H			0.447			
5	11/2H			0.497			
6	17/18H			0.457			
7	6/9H			0.484			
8	20/17H			0.513			
9	15/8H			0.528			
10	13/4H	The similarity of flavour character and material functional properties of 19 (Nineteen) over-fermented tempeh hydrolysisate flour of the 1 st variant with 9 (nine) savoury flavours (F2)		0.499			
11	14/7H			0.533			
12	9/10H			0.505			
13	3/14H			0.473			
14	21/27H			13.283	0.491	34.058	80.487
15	16/19H				0.449		
16	7/5H				0.463		
17	22/12H				0.609		
18	4/15H				0.504		
19	SF9				0.903		
20	SF2				0.898		
21	SF3				0.895		
22	SF6				0.880		
23	SF7				0.879		
24	SF4				0.872		
25	SF5				0.860		
26	SF1				0.855		
27	SF8				0.850		
28	19/25H				0.617		
29	5/1H			0.533			

The 2nd principal component (F2), after doing variable extraction and rotation using varimax method, has 29 (twenty-nine) 2nd principal components (F2) with eigenvalues score more than or equivalent to 0.50 respectively as follows: 2/13H, 18/20H, 12/11H, 10/6H, 11/2H, 17/18H, 6/9H, 20/17H, 15/8H, 13/4H, 14/7H, 9/10H, 3/14H, 21/27H, 16/19H, 7/5H, 22/12H, 4/15H, SF9, SF2, SF3, SF6, SF7, SF4, SF5, SF1, SF8, 19/25H and 5/1H with eigenvalues score of 13.283 and total cumulative variant of 34.058%. Based on Table 4 above, the equation for the 2nd principal component (F2) that is the function of flavour character similarities and material functional properties of 20 (twenty) over-fermented tempeh hydrolysisate flour of the 2nd variants with 9 (nine) savoury flavours is in equation (2). The present review

describes the implementation of these complementary vibrational spectroscopy techniques and their potentials, advantages and disadvantages for GAG analysis (Mohamed *et al.*, 2017).

$$F2 = 0.455 (2/13H) + 0.454 (18/20H) + 0.473 (12/11H) + 0.447 (10/6H) + 0.497 (11/2H) + 0.457 (17/18H) + 0.484 (6/9H) + 0.513 (20/17H) + 0.528 (15/8H) + 0.499 (13/4H) + 0.533 (14/7H) + 0.505 (9/10H) + 0.473 (3/14H) + 0.491 (21/27H) + 0.449 (16/19H) + 0.463 (7/5H) + 0.609 (22/12H) + 0.504 (4/15H) + 0.903 (SF9) + 0.898 (SF2) + 0.895 (SF3) + 0.880 (SF6) + 0.879 (SF7) + 0.872 (SF4) + 0.860 (SF5) + 0.855 (SF1) + 0.850 (SF8) + 0.617 (19/25H) + 0.533 (5/1H) \quad (2)$$

Remark :

F2 = The similarity of flavour character and material functional properties of 20 (twenty) over-fermented tempeh hydrolysisate flour of the 1st (first) variant with 9 (nine) savoury flavours.

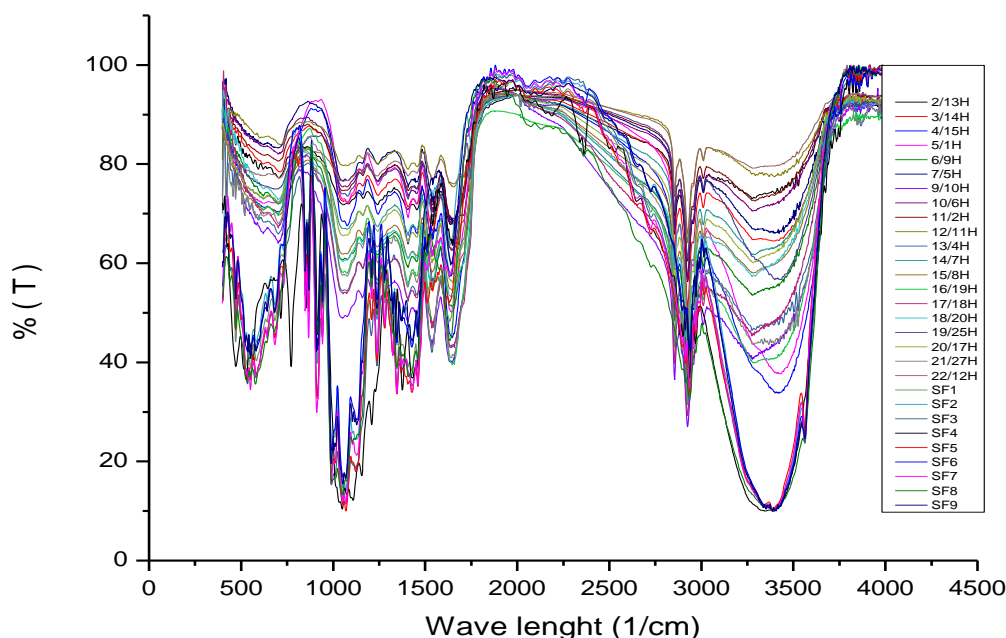


Figure 5. Absorbance pattern of the 2nd principal component constituent variable (F2).

Figure 5 above shows the absorbance pattern of the 2nd principal component constituent variable (F2). Based on equation (1) above, there are 9 (nine) variables with coefficient value (NK) of $0.850 \leq NK \leq 0.903$, namely SF8, SF1, SF5, SF04, SF7, SF6, SF3, SF2 and SF9. There are 12 (twelve) variables with coefficient value (NK) of $0.447 \leq NK \leq 0.499$, namely 10/6H, 16/19H, 18/20H, 2/13H, 17/18H, 7/5H, 3/14H, 12/11H, 6/9H, 11/2H, 21/27H, and 13/4H. There are 7 (seven) variables with coefficient value (NK) of $0.504 \leq NK \leq 0.617$, namely 4/15H, 9/10H, 20/17H, 15/8H, 14/7H, 22/12H, and 19/25H. The closeness of coefficient value (NK) indicates the closeness of flavour characteristic properties and the closeness of material functional properties, that is, the flavour characteristic and functional properties of over-fermented tempeh hydrolysisate flour with 9 (nine) savoury flavours. The extraction of

FS from *S. binderi* was further optimized with central composite design (CCD) using RSM (Hii *et al.*, 2014).

Previous studies have reported that the umami taste of monosodium l-glutamate (MSG) and saltysmelling odors (e.g., soy sauce, bacon, sardines) enhance the perception of saltiness. This study aimed to investigate the neural basis of the enhancement of saltiness in human participants using functional near-infrared spectroscopy (Onuma *et al.*, 2018). Using Response Surface Methodology (RSM), we evaluated the culture conditions (nitrogen source, carbon source, pH and agitation rate) that increase the biomass of *Acidocella facilis* strain USBA-GBX-505 and therefore enhance the production of its lipolytic enzyme, 505 LIP (Bernal *et al.* 2017). Principal component analysis and partial least regression models were developed using the first derivative DRIFT spectra (400–4000 cm⁻¹) to predict fructose and glucose sugars (Olale *et al.*, 2017). Enzymatic mungbean meal protein hydrolysate with PCA showed that 72.87% of the total variance confirmed the correlation between DH, S0, DPPH, ABTS, sensory characteristics and volatile flavour compounds (Sonklin *et al.*, 2018).

Table 5. Interpretation Results of over-fermented tempeh flour and 2 (two) MSG variants FTIR absorbance pattern variable from 3,372 (three thousand three hundred and seventy two) observation points.

No	Variable	Factor	Eigen Values	Loading Factor	% Variance	Cumulative %
1	TTA01	Similarities of flavour character and material		0.722		
2	MSG	functional properties of over-fermented tempeh flour with 2 (two) MSG variants	4.230	0.720	10.847	91.334
3	VC			0.718		
(F3)						

The 3rd principal component (F3), after variable extraction and rotation using the varimax method, has 3 (three) 3rd principal components (F3) with eigenvalues score more than or equivalent to 0.50, respectively, as follows: TTA01, MSG and VC with eigenvalues score of 4.230 and total cumulative variant of 10.847%. Based on Table 5 above, the equation for the 3rd principal component (F3) is the function of flavour character similarities and material functional properties of MSG and VC with over-fermented tempeh hydrolysate flour (TTA01) as in Equation (3) below:

$$F3 = 0.722 (TTA01) + 0.720 (MSG) + 0.718 (VC) \quad (3)$$

Remark :

F3 = The similarity of flavour character and material functional properties of over-fermented tempeh flour with 2 (two) MSG Variants

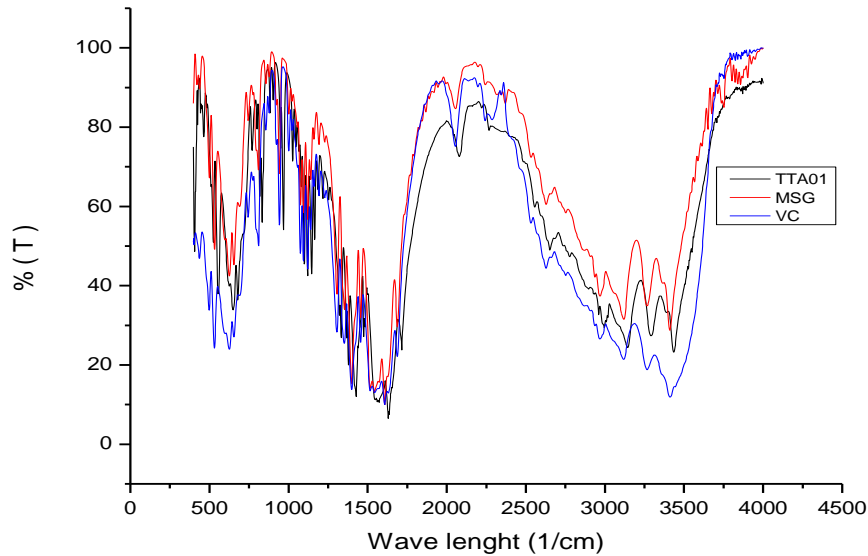


Figure 6. Absorbance pattern of the 3rd principal component constituent variable (F3)

Table 6. Interpretation results of 1 (one) experiment unit FTIR absorbance pattern variable from 1,868 observation points.

No	Variable	Factor	Eigen Values	Loading Factor	% Variance	Cumulative %
1	5/1H	Similarities of flavour character and material functional properties with over-fermented tempeh hydrolysisate flour of the 3 rd variant (F4)	2.7031	0.553	7.031	98.364

Figure 6 above shows the absorbance pattern of the 3rd principal component constituent variable (F3). The 4th principal component (F4), after doing variable extraction and rotation using varimax method, has 1 (one) 4th principal component (F4) with eigenvalues score more than or equivalent to 0.50 respectively as follows: 5/1H with eigenvalues score of 2.7031 and total cumulative variant of 7.031%. Based on Table 6 above, the equation for the 4th principal component (F4) is the function of flavour character similarities and material functional properties with over-fermented tempeh hydrolysisate flour of the 4th (fourth) variants as in equation (4) below:

$$F4 = 0.553 (5/1H) \quad (4)$$

Remark :

F4 = The similarities of flavour character and material functional properties with over-fermented tempeh hydrolysisate flour of the 3rd (third) variants.

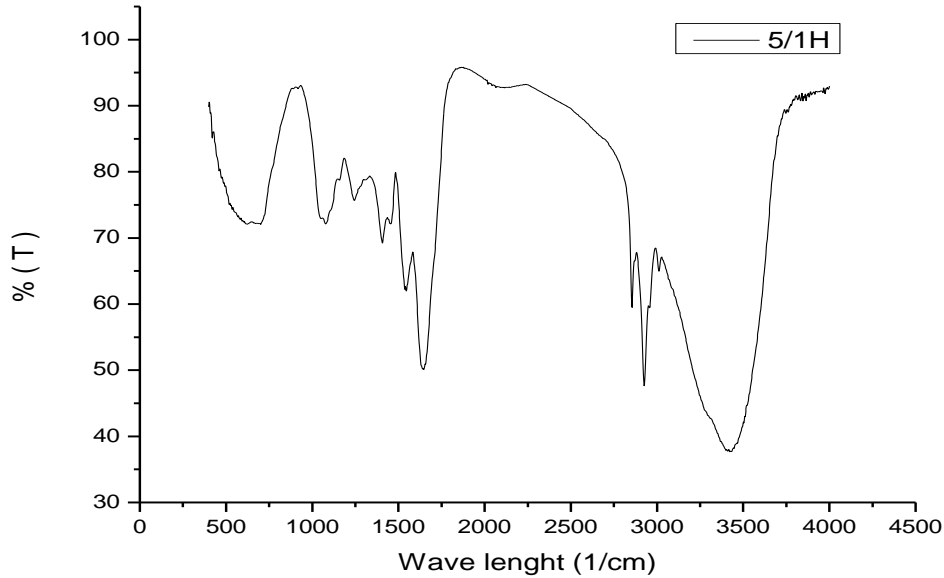


Figure 7. Absorbance pattern of the 4th principal component constituent variable.

Figure 7 above shows the absorbance pattern of the 4th principal component constituent variable. Table 7 below shows the component matrix after varimax rotation. Figure 8 below shows the dendrogram of 27 (twenty-seven) experimental units, 9 (nine) savory flavors, over-fermented tempeh flour (TTA01) and 2 (two) MSG variants, 1) over-fermented tempeh hydrolysate flour, 2) over-fermented tempeh flour, and 2 (two) MSG variants, 3) 9 (nine) savory flavors.

Table 7. Matrix component after varimax rotation.

	Rotated Component Matrix ^a			
	1	2	3	4
2/13H	0.855	0.455	0.233	-0.023
24/24H	0.848	0.424	0.271	0.112
18/20H	0.833	0.454	0.27	0.125
12/11H	0.824	0.473	0.203	0.177
10/6H	0.821	0.447	0.272	0.225
27/21H	0.82	0.318	0.293	0.356
11/2H	0.814	0.497	0.256	0.134
25/26H	0.805	0.42	0.267	0.311
17/18H	0.803	0.457	0.305	0.194
6/9H	0.796	0.484	0.29	0.201
8/3H	0.793	0.369	0.278	0.385
20/17H	0.79	0.513	0.303	0.124
15/8H	0.79	0.528	0.292	0.095
1/12H	0.786	0.392	0.308	0.353
26/16H	0.782	0.382	0.308	0.373
13/4H	0.781	0.499	0.313	0.192
14/7H	0.778	0.533	0.296	0.111
9/10H	0.775	0.505	0.292	0.186
3/14H	0.775	0.473	0.284	0.302
21/27H	0.735	0.491	0.345	0.298
16/19H	0.72	0.449	0.346	0.396
7/5H	0.71	0.463	0.289	0.438
22/12H	0.702	0.609	0.196	-0.18
23/23H	0.701	0.439	0.368	0.409
4/15H	0.573	0.504	0.354	0.528
SF9	0.336	0.903	0.149	0.216
SF2	0.352	0.898	0.151	0.203
SF3	0.401	0.895	0.139	0.111
SF6	0.359	0.88	0.202	0.22
SF7	0.403	0.879	0.201	0.123
SF4	0.392	0.872	0.118	0.16
SF5	0.441	0.86	0.218	0.106
SF1	0.439	0.855	0.219	0.145
SF8	0.4	0.85	0.24	0.184
19/25H	0.572	0.617	0.317	0.366
TTA01	0.596	0.176	0.722	0.197
MSG	0.616	0.203	0.72	0.156
VC	0.502	0.415	0.718	0.163
5/1H	0.499	0.533	0.359	0.553

Extraction Method: Principal Component Analysis.

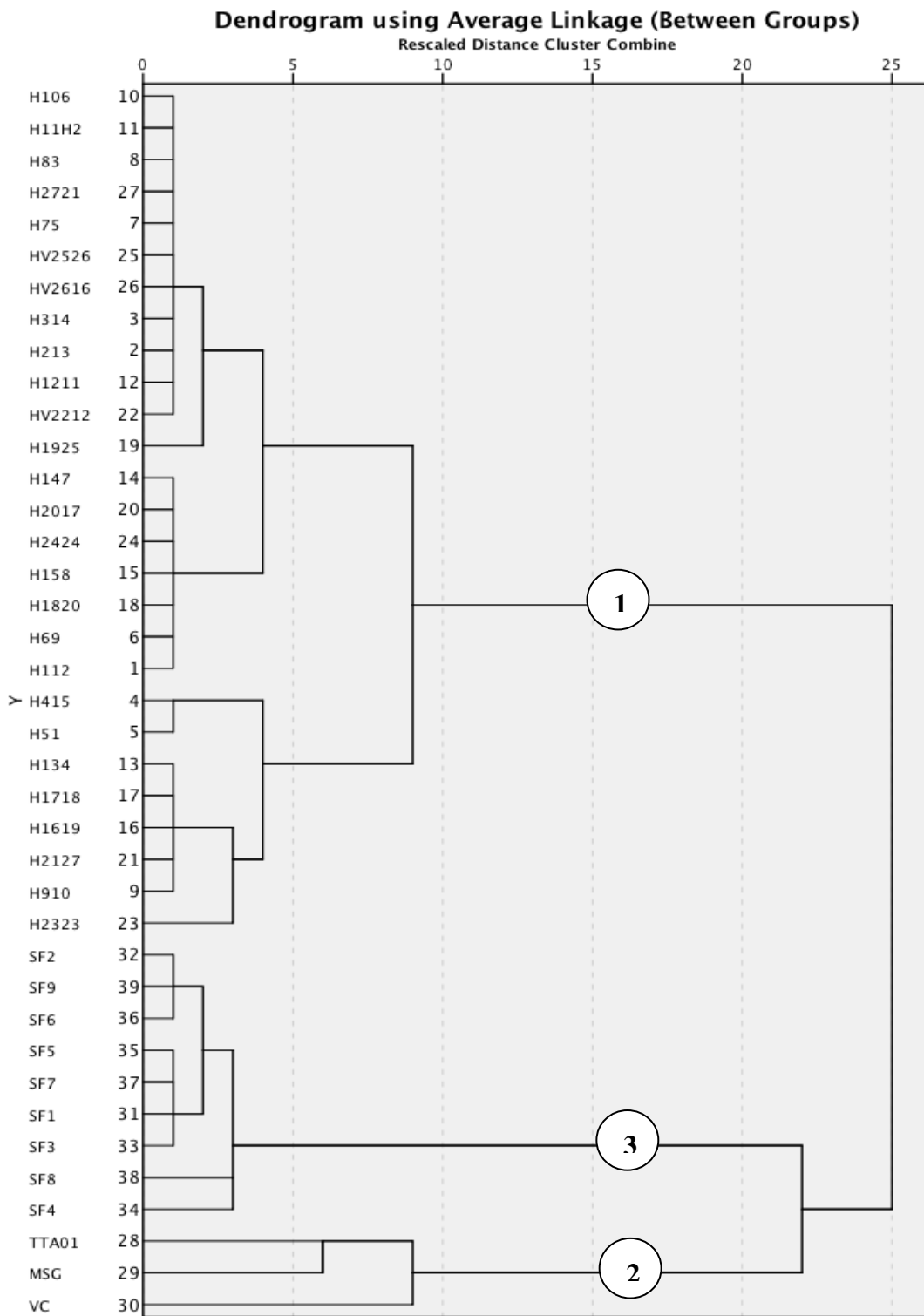


Figure 8. Dendrogram of 27 (twenty-seven) experiment units, 9 (nine) savoury flavors, over-fermented tempeh flour (TTA01) and 2 (two) MSG variants, 1) over-fermented tempeh hydrolysisate flour, 2) over-fermented tempeh flour, and 2 (two) MSG variants, 3) 9 (nine) savoury flavours.

Table 8. Closeness of functional properties and flavour character of 27 (twenty-seven) experiment units and 9 (nine) savoury flavours, 2 (two) MSG variants, and over-fermented tempeh flour.

Case	TTA01	MSG	VC
1/12H	976,872.52	512,297.52	1,472,312.01
2/13H	1,588,322.37	961,598.81	2,222,509.79
3/14H	1,416,467.25	826,040.41	2,003,459.91
4/15H	810,350.01	467,060.21	1,112,303.80
5/1H	1,053,677.75	610,795.41	1,409,830.62
6/9H	847,189.55	461,095.48	1,268,478.76
7/5H	1,696,063.28	1,018,682.09	2,342,049.08
8/3H	1,845,458.95	1,126,285.97	2,551,162.88
9/10H	507,303.17	339,872.04	740,207.11
10/6H	1,727,745.46	1,035,887.41	2,389,502.88
11/2H	1,800,856.72	1,097,041.12	2,466,659.83
12/11H	2,098,851.12	1,336,128.50	2,832,728.26
13/4H	598,267.22	344,988.94	903,143.34
14/7H	1,170,788.66	667,537.57	1,665,964.94
15/8H	962,336.08	539,293.72	1,395,609.83
16/19H	554,829.53	320,844.64	884,027.69
17/18H	592,598.74	330,721.66	923,927.89
18/20H	941,212.90	517,183.79	1,420,882.81
19/25H	1,456,227.85	869,570.32	1,976,431.19
20/17H	1,101,325.15	615,192.64	1,578,289.86
H2127	610,472.35	338,362.49	907,450.61
22/12H	2,049,736.57	1,311,738.47	2,712,758.53
23/23H	412,620.60	299,421.94	583,485.00
24/24H	1,308,228.82	744,997.72	1,899,505.33
25/26H	1,576,321.05	935,151.67	2,224,049.56
26/16H	1,460,196.38	848,496.05	2,071,357.44
27/21H	1,946,456.91	1,204,332.28	2,676,168.16
TTA01	0.00	270,781.21	318,027.15
MSG	270,781.21	0.00	511,428.97
VC	318,027.15	511,428.97	0.00
SF1	1,001,661.57	953,618.13	811,731.55
SF2	1,268,717.63	1,107,104.91	1,134,018.22
SF3	1,244,703.62	1,237,744.35	1,000,691.97
SF4	1,225,055.12	1,271,692.03	992,494.01
SF5	1,011,645.21	994,867.61	803,018.33
SF6	1,143,963.16	991,629.56	1,001,238.34
SF7	1,117,982.78	1,063,922.35	909,226.60
SF8	975,607.37	1,065,292.30	703,497.57
SF9	1,264,075.83	1,135,857.22	1,115,278.29

Table 8 above shows the closeness of functional properties and flavor characteristics of 27 (twenty-seven) experimental units and 9 (nine) savory flavors, 2 (two) MSG variants, and over-fermented tempeh flour.

The clustering of 39 (thirty-nine) variables which consists of 27 (twenty-seven) experiment units, 9 (nine) savoury flavours, 2 (two) MSG variants and over-fermented tempeh flour results in 3 (three) clusters was as follows :

1. The 1st (first) cluster indicated the similarities of flavour character and material functional properties of 27 (twenty-seven) over-fermented tempeh hydrolysisate flour as the product of multi enzyme hydrolysis as shown on Figure 9, point 1 (one).
2. The 2nd (second) cluster indicated the similarities of flavour character and material functional properties of 2 (two) MSG variants with over-fermented tempeh flour (TTA01) as shown in Figure 9, point 2 (two).
3. The 3rd (third) cluster indicated the similarities of flavour character and material functional properties of 9 (nine) savoury flavors as shown in Figure 9, point 3 (three).

The HCA indicated that those 3 (three) clusters in more details can be seen in Figure 9 of flavor character dendrogram and material functional properties, which are the results of cluster analysis hierarchy using agglomerative method, namely the average linkage method. ELISA and high content analysis (HCA) were employed to examine the disruptive effects of MSG on the secretion of enteroendocrine hormone glucagon-like peptide-1 (GLP-1) and GLP-1 receptor (GLP-1R), respectively ([Shannon et al., 2017](#)). Detection of L-Cysteine in wheat flour was accomplished successfully using Raman microscopy combined chemometrics of PCA and HCA ([Cebi et al., 2017](#)).

CONCLUSION

Based on the results of the research with the experimental design above, the conclusions are:

1. The results of principal component analysis of 28 (twenty-eight) experiment units, 2 (two) MSG variants and 9 (nine) savoury flavours in Indonesia, over-fermented tempeh hydrolysisate flour 19/25H with loading factor value of 0.617, 22/12H with loading factor value of 0.609, 5/1H with loading factor value of 0.533, 14/7H with loading factor value of 0.533, 15/8H with loading factor value of 0.528, 20/17H with loading factor value of 0.513, 9/10H with loading factor value of 0.505 and over-fermented tempeh hydrolysisate flour 4/15H with loading factor value of 0.504, show that they have potential flavour character and functional properties as the main ingredient for the Savoury Flavors of Grilled Chicken (SF01), Balado (SF02), Barbeque (SF03), Spicy Corn (SF04), Cheese (SF05), Salty Cheese (SF06), Sweet Spicy (SF07), Roasted Beef (SF08) and Tiramisu (SF09).
2. The results of hierarchical cluster analysis of 28 (twenty-eight) experiment units and 9 (nine) savoury flavours in Indonesia, over-fermented tempeh hydrolysisate flour 9/10H and 23/23H, show that they have flavour character and functional properties as the main ingredient of Savoury Flavours of Grilled Chicken (SF01) with closeness value of 453.406 (9/10H) and 465.536 (23/23H), Balado (SF02) with closeness value of 506.061 (9/10H) and 544.227 (23/23H), Barbeque (SF03) with closeness value of 593.029 (9/10H) and 652.165 (23/23H), Spicy Corn (SF04) with closeness value of 595.097 (9/10H) and 632.614 (23/23H), Cheese (SF05) with closeness value of 482.596 (9/10H) and 520.814 (23/23H), Salty Cheese (SF06) with

closeness value of 469.605 (9/10H) and 475.465 (23/23H), Sweet Spicy (SF07) with closeness value of 515.754 (9/10H) and 563.700 (23/23H), Roasted Beef (SF08) with closeness value of 526.120 (9/10H) and 525.428 (23/23H) and Tiramisu (SF09) with closeness value of 520.196 (9/10H) and 551.815 (23/23H).

ACKNOWLEDGMENTS

This expression of gratitude is sent to Republic of Indonesia Finance Department Research Fund Management Institution that has provided research grant funding.

DECLARATION OF COMPETING INTEREST

The authors declare that they have no conflict of interest.

CREDIT AUTHORSHIP CONTRIBUTION STATEMENT

Wignyanto Wignyanto: Investigation, methodology, conceptualization, formal analysis, data curation, validation, writing-original draft, review, and editing, visualization.

Mujianto Mujianto: Investigation, methodology, conceptualization, formal analysis, data curation, validation, writing-original draft, review, and editing, visualization.

ETHICS COMMITTEE DECISION

This article does not require any ethical committee decision.

REFERENCES

- Ahnan-Winarno AD, Cordeiro L, Winarno FG, Gibbon J and Xia H (2021). Tempeh: A semicentennial review on its health benefits, fermentation, safety, processing, sustainability, and affordability. *Comprehensive Review Food Science and Food Safety*, 20: 1717–1767.
- Bernal LF, Lopez G, Ruiz M, Vera-Bravo R, Reyes A and Baena S (2017). Response Surface methodology (RSM) for analysing culture conditions of acidocella facilis strain USBA-GBX-505 and partial purification and biochemical characterization of Lipase 505 LIP. *Universitas Scientiarum*, 22(1): 45-70. <https://doi.org/10.11144/Javeriana.SC22-1.rsmr>
- Cao ZH, Green-Johnson JM, Buckley ND, and Lin Q-Y (2019). Bioactivity of soy-based fermented foods: A review. *Biotechnology Advances*, 37(1): 223-238. <https://doi.org/10.1016/j.biotechadv.2018.12.001>
- Cebi N, Dogan CE, Develioglu A, Altuntop Yayla ME and Sagdic O (2017). Detection of L-Cysteine in wheat flour by raman microspectroscopy combined chemometrics of HCA and PCA. *Food Chemistry*, 228: 116-124. <https://doi.org/10.1016/j.foodchem.2017.01.132>
- Cebi N, Dogan CE, Ekin Mese A, Ozdemir D, Arıcı M and Sagdic A (2019). A rapid ATR-FTIR spectroscopic method for classification of gelatin gummy candies in relation to the gelatin source. *Food Chemistry*, 277: 373-381. <https://doi.org/10.1016/j.foodchem.2018.10.125>
- Culbert J, Cozzolino D, Ristic R and Wilkinson K (2015). Classification of sparkling wine style and quality by MIR spectroscopy. *Molecules*, 20(5): 8341-8356. <https://doi.org/10.3390/molecules20058341>
- Erkan SB, Gürler HN, Bilgin DG, Germec M and Turhan I (2020). Production and characterization of tempehhs from different sources of legume by Rhizopus Oligosporus. *LWT*, 119(October):108880. <https://doi.org/10.1016/j.lwt.2019.108880>

- Gauch HG, Sheng Q, Piepho HP, Zhou L and Chen R (2019). Consequences of PCA Graphs, SNP codings, and PCA variants for elucidating population structure. *PLoS ONE*, 14(6): 1-26. <https://doi.org/10.1371/journal.pone.0218306>
- Hii, SL, Kong FL, Yoon TL and Wong CL (2014). Statistical optimization of fermentable sugar extraction from the Malaysian brown alga sargassum binderi.” *Journal of Applied Phycology*, 27(5):2089-2098. <https://doi.org/10.1007/s10811-014-0480-6>
- Kos G, Sieger M, McMullin D, Zahradnik C, Sul yok M, Öner T, Mizaikoff B and Krska R (2016). A novel Chemometric classification for FTIR spectra of mycotoxin-contaminated maize and peanuts at regulatory limits. *Food Additives and Contaminants-Part A Chemistry, Analysis, Control, Exposure and Risk Assessment*, 33(10): 1596-1607. <https://doi.org/10.1080/19440049.2016.1217567>
- Kuligowski M, Pawłowska K, Jasińska-Kuligowska I and Nowak J (2017). Isoflavone composition, polyphenols content and antioxidative activity of soybean seeds during tempehh fermentation.” *CyTA-Journal of Food*, 15(1): 27-33. <https://doi.org/10.1080/19476337.2016.1197316>
- Land DG (1994). Savoury flavours-an overview. *Understanding Natural Flavors*, 298-306.
- Mohamed HT, Untereiner V, Ganesh D.S and Brézillon S (2017). Implementation of infrared and raman modalities for glycosaminoglycan characterization in complex systems. *Glycoconjugate Journal*, 34(3): 309-323. <https://doi.org/10.1007/s10719-016-9743-6>
- Mujiyanto M, Witono Y, Wignyanto W, Kumalaningsih S and Auliani'am (2018). Hydrolysis characteristics of over fermented tempeh (Fermented soybean cake) product hydrolyzed by enzymatic hydrolysis as natural flavor source (Flavor enhancer). *The Indian Journal of Nutrition and Dietetics*, 55(1): 29. <https://doi.org/10.21048/ijnd.2018.55.1.18062>
- Mujiyanto M, Wignyanto W, Kumalaningsih S and Aulianni'Am (2020). The causality of monosodium glutamate Fourier Transform Infrared (FTIR) absorbance pattern with wave peaks from several seasoning product (Savoury flavors). *Journal of Physics: Conference Series* 1569(3). <https://doi.org/10.1088/1742-6596/1569/3/032030>
- Novarina I, Inawati, Dinoto A, Julistiono H, Handayani R and Saputra S (2020). Assessment of potential probiotic lactic acid bacteria from tempeh and tape. The 9th International Symposium for Sustainable Humansphere, IOP Conf. Series: *Earth and Environmental Science*, 572, 012026
- Nur N, Meryandini A, Suhartono MT and Suwanto A (2020). Lipolytic bacteria and the dynamics of flavor production in Indonesian tempeh. *Biodiversitas Journal of Biological Diversity*, 21(8): 3818-3825. <https://doi.org/10.13057/biodiv/d210850>
- Olale K, Walyambillah W, Mohammed SA, Sila A and Shepherd K (2017). Application of DRIFT-FTIR spectroscopy for quantitative prediction of simple sugars in two local and two floridian mango (*Mangifera Indica* L .) cultivars in Kenya. *Journal of Analitical Science and Technology*, 8: 21. <https://doi.org/10.1186/s40543-017-0130-0>
- Onuma T, Maruyama H and Sakai N (2018). Enhancement of saltiness perception by monosodium glutamate taste and soy sauce odor: A near-infrared spectroscopy study. *Chemical Senses*, 43(3): 151-167. <https://doi.org/10.1093/chemse/bjx084>
- Shannon M, Green B, Willars G, Wilson J, Matthews N and Lamb J, Gillespie and Connolly L (2017). The endocrine disrupting potential of Monosodium Glutamate (MSG) on secretion of the Glucagon-like Peptide-1 (GLP-1) gut hormone and GLP-1 receptor interaction. *Toxicology Letters*, 265: 97-105. <https://doi.org/10.1016/j.toxlet.2016.11.015>
- Sonklin C, Laohakunjit N, Kerdchoechuen O and Ratanakhanokchai K (2018). Volatile flavour compounds, sensory characteristics and antioxidant activities of mungbean meal protein hydrolysed by bromelain. *Journal of Food Science and Technology*, 55(1): 265-277. <https://doi.org/10.1007/s13197-017-2935-7>
- Wangcharoen W, Ngarmsak T and Wilkinson BHP (2006). The product design of puffed snacks by using Quality Function Deployment (QFD) and Reverse Engineering (RE) techniques. *Kasetsart Journal - Natural Science*, 40(1): 232-239.
- Wenning M and Scherer S (2013). Identification of microorganisms by FTIR spectroscopy : Perspectives and limitations of the method. *Applied Microbiology and Biotechnology*, 97: 7111-71120. <https://doi.org/10.1007/s00253-013-5087-3>



Turkish Journal of
Agricultural
Engineering Research
(Turk J Agr Eng Res)
e-ISSN: 2717-8420



Moisture-Dependent Physical and Aerodynamics Properties of Cowpea Seeds

Olufemi Adeyemi ADETOLA^{a*} , Adenike Mary ADEROTOYE^a ,
Marvellous Oluwaseun LAWAL^a 

^aDepartment of Agricultural Engineering, School of Engineering and Engineering Technology, Federal University of Technology Akure, Ondo State, NIGERIA

ARTICLE INFO: Research Article

Corresponding Author: Olufemi Adeyemi ADETOLA, E-mail: oaadetola@futa.edu.ng

Received: 19 October 2023 / Accepted: 8 January 2024 / Published: 30 June 2024

Cite this article: Adetola OA, Aderotoye AM, Lawal MO (2024). Moisture-Dependent Physical and Aerodynamics Properties of Cowpea Seeds. *Turkish Journal of Agricultural Engineering Research*, 5(1): 21-34. <https://doi.org/10.46592/turkager.1378321>

ABSTRACT

This study focuses on the significant impact of moisture content on the engineering properties of cowpea seeds, which is vital for designing effective agricultural tools, equipment, and machines. We specifically examined two cowpea seed varieties, SAMPEA-16 and SAMPEA-14, across different moisture levels (10, 15, 20, 25, and 30% wb). Our findings show distinct variations in the physical characteristics of these seeds as the moisture content changes. For both SAMPEA-16 and SAMPEA-14, we observed changes in average length, width, and thickness at each moisture level. At moisture contents ranging from 10% to 30% wb, the dimensions for SAMPEA-16 were 11.20 mm by 9.10 mm by 8.61 mm, gradually changing to 10.60 mm by 8.80 mm by 8.50 mm, and for SAMPEA-14, they ranged from 8.30 mm by 6.50 mm by 6.50 mm to 8.40 mm by 6.50 mm by 6.40 mm. Significantly, the 1000 seed mass for SAMPEA-16 increased from 302.30 g to 404.80 g within the 15% to 30% moisture range, while the sphericity varied from 0.849 to 0.877. For SAMPEA-14, similar trends were observed with the sphericity shifting from 0.848 to 0.852. Additionally, the true density for SAMPEA-14 and SAMPEA-16 changed from 1034.12 kg m⁻³ to 1074.40 kg m⁻³ and 1089.61 kg m⁻³ to 1116.87 kg m⁻³, respectively. Another notable finding is the increase in the angle of repose with moisture content. For SAMPEA-16, it rose from 22.40° to 30.23°, and for SAMPEA-14, from 23.22° to 34.28°, as moisture content increased from 10% to 30%. Furthermore, the terminal velocity for both varieties increased with moisture, with SAMPEA-14 ranging from 4.92 to 5.25, and SAMPEA-16 from 5.72 to 6.16, at 10% to 25% moisture content. The insights from this study are crucial for the design of agricultural machinery, processing units, and storage facilities, aiming to enhance the quality and quantity of cowpea produce.

Keywords: Density, Evaluate, Repose, Sphericity, Terminal Velocity, Varieties



INTRODUCTION

In Africa, Latin America, South-East Asia, and the southern United States, cowpea (*Vigna unguiculata* L.), an annual legume crop with African origins, is a common crop (Adekanye and Olaoye, 2018). Cowpea, an annual diploid legume, is renowned for its high protein content, which ranges from 18-25%, comparable to various types of meat (Narayana and Angamuthu, 2021). Due to the unique agronomic structure of its seeds, cowpea is particularly susceptible to the impact of loading and is significantly affected during threshing with iron beaters (Adewumi *et al.*, 2007). Often referred to as the 'hungry-season crop,' cowpea is harvested before grains and plays a crucial role in bridging food gaps. In Nigeria, cowpea production serves as a direct or indirect source of income for many individuals. Furthermore, cowpea contributes significantly to agricultural sustainability in sub-Saharan Africa. It offers multiple agronomic benefits, such as ground cover and plant residue, nitrogen fixation, and weed suppression. These qualities not only enhance soil fertility, particularly in marginal lands, but also support the livelihoods of numerous small-holder farmers in the region (Muhammed-Bashir *et al.*, 2018).

Cowpea is a versatile crop in Africa since it may be grown for human use, animal food, and to encourage the growth of other crops. Cowpeas, often known as "blackeyed peas" in the Americas, are mostly consumed in West Africa and are highly high in protein. Attempts to pinpoint the origin of cowpea cultivation are hampered by inadequate archeological documents (Gómez, 2004). When prepared (either boiled, grinded and made into "Akara ball," "moinmoin," etc.), cowpea is eaten in a variety of ways. Among the crucial processes in agricultural processing are post-harvest procedures include cleaning, grading, drying, dehydrating, storing, milling, handling and transport, and thermal processing of foods. Agricultural materials' engineering qualities are crucial for processing (Chukwu and Sunmonu, 2010). Engineers, food scientists, and processors must investigate these qualities in order to build efficient techniques and instruments. Numerous studies have been conducted to define some of the engineering features necessary in handling agricultural products after production in their dry condition without taking the impact of moisture into account. Loss in the quality and deterioration in the threshed seeds occurs when properties are not considered before developing the threshers. According to Timothy and Olaoye (2013), high moisture content of cowpea seeds increases the mechanical damage while low moisture content reduces the mechanical damage. They also report moisture content affects the machine efficiency and the percentage damage. In spite of the economic importance of cowpea, there is little knowledge on its physical properties because it appears that there is not much published research on the physical properties of cowpea seed that are dependent on moisture. This has affected the effectiveness of the developed machines, leading to little or no progress in the mechanization of cowpea processing. Davies and Zibokere (2011) reported that most of the cowpea processing are done manually. As the domestic and industrial use of cowpea continues to expand, so does the need for efficient processing equipment and machines for unit operations required. As a result, this study examined the impact of moisture content on the physical and aerodynamic characteristics of cowpea seeds, which would help engineers create better equipment for mechanizing the production of cowpeas.

MATERIALS and METHODS

Materials

One of the earliest crops to be domesticated is the cowpea. Cowpeas grow well in up to 85% sand soil and do well in arid, unfavorable environments. Since cowpeas grow best at 30°C, they are only available as a summer crop in most of the world. It thrives in areas with 400-700 mm of annual precipitation. Compared to most other crops, it can withstand infertile and acid soils better in sandy soils. For erect varieties, 133,000 seeds are typically planted per hectare, while for climbing and trailing varieties, 60,000 seeds are planted per hectare. After roughly 100 days, the seeds can be collected, and after 120 days, the entire plant can be used for fodder. In this study, a variety of equipment, instruments, and materials were utilized, including a KD-TBE-1200 electronic weighing balance and a Gallenkamp laboratory oven. Measurement tools comprised a compass, a ruler, and a vernier caliper, alongside a thermometer for temperature monitoring. Chemical and storage materials included toluene and desiccators, as well as a measuring cylinder for volume measurements. The angle of repose was determined using a specialized device, and air flow was measured with a hot wire anemometer. Additionally, a measuring can was used, and the subject of our study was cowpea.

Collection and Preparation of Samples

Two varieties of cowpea seeds were procured from Oba Ile, Ondo State, South Western Nigeria, after quality assurance test was carried out. Each sample was inspected for infested seeds as well as other foreign objects like dust, stones, chaff, immature, broken, and damaged seeds. Two hundred (200) seeds were selected randomly from each of the variety and were numbered to avoid repetition of measurements.

Determination of moisture content of the cowpea seeds

To determine the moisture content of the cowpea pods, we employed a laboratory oven, digital weighing balance, and sample tray. Initially, the weight of the freshly harvested, wet samples denoted as (W_w) was recorded. These samples were then dried at a temperature of 105°C. The moisture content was calculated using Equation 1, following the guidelines recommended by the Association of Official Analytical Chemists ([AOAC, 1995](#)). This process ensures accurate and standardized moisture content determination for the cowpea pods.

$$M_c = \frac{W_w - W_d}{W_d} 100\% \quad (1)$$

Where M_c is the moisture content of seeds (dry basis) in %, W_w is the wet weight of the cowpea seeds in g and W_d is the dry weight of the cowpea in g.

The initial moisture content of the seeds used was 10.0% db. It was conditioned to enable samples of different moisture levels and thereafter kept in the refrigerator at 5°C for at least 24 hours to ensure evenly distribution of moisture.

Experimental Procedures

Determination of the physical properties of the cowpea seeds

To accurately measure the dimensions of the cowpea seeds, we used a vernier caliper with a precision of 0.01mm. This instrument was employed to determine the length (L), width (W), and thickness (T) of 60 randomly selected seeds. Each of these dimensions was meticulously recorded. This measurement process was replicated thrice at moisture contents of 20%, 25%, and 30%. Furthermore, we assessed both the mass and the angle of repose of the sample at varying moisture levels, specifically at 15%, 20%, 25%, and 30%. These measurements are crucial for understanding how moisture content affects the physical properties of cowpea seeds.

Sphericity

Sphericity is defined as the ratio of the diameter of a sphere with the same volume as the particle to the diameter of the smallest sphere that can completely enclose the particle, or more commonly, to the particle's maximum diameter. Essentially, it is a measure of how closely an object resembles a perfect sphere. For our study, the sphericity of the cowpea seeds was calculated using Equation 2, as outlined by [Olukunle and Akinnuli \(2012\)](#), and subsequently cited by [Adetola *et al.* \(2020\)](#).

The ratio between the diameter of a sphere with the same volume as the particle and the diameter of the smallest circumscribing sphere or, more commonly, the particle's maximum diameter-is known as sphericity. It is the measure of how spherical (round) an object is. The sphericity of the cowpea was calculated using Equation 2 [Olukunle and Akinnuli \(2012\)](#) cited by [Adetola *et al.* \(2020\)](#).

$$S = \frac{D_g}{L} \quad (2)$$

Where S is the sphericity in percent, D_g is the seed's geometric mean diameter in centimeters, and L is the seed's length in centimeters.

The Geometric mean diameter (D_g)

Equation 3 was used to get the geometric mean Diameter (D_g) [Olukunle and Akinnuli \(2012\)](#) quoted by [\(Adetola *et al.* 2020\)](#).

$$D_g = (LWT)^{1/3} \quad (3)$$

Where, D_g is the geometric mean diameter in centimeters, L is the length of the seed in centimeters, W is the width of the seed in centimeters, and T is the thickness of the seed in centimeters.

Determination of gravimetric properties of cowpea seeds

[Krishnakumar \(2019\)](#) emphasizes that the knowledge of density, specific gravity, and porosity is crucial in designing equipment and systems for separation, handling, drying, processing, storage, and transport of agricultural products. Understanding these properties ensures the efficiency and effectiveness of such equipment and processes.

True density

The liquid displacement method was used to calculate the true density using Equation 4 as recommended by [Olukunle and Akinnuli \(2012\)](#). Cowpeas of a known mass were placed within a measuring cylinder that was completely filled with toluene. The volume of the cowpea seed was discovered to be the volume of toluene that was displaced. Because seeds absorb toluene less thoroughly than water, it was used instead of water. Additionally, because of its low surface tension and poor dissolution power ([Mohsenin, 1978](#)) referenced by [Isa and Aderotoye \(2017\)](#) it fills even small dips in the cowpea seeds.

$$\rho_t = \frac{W_t}{V_t} \quad (4)$$

Where ρ_t is the true density in kg m^{-3} , W_t is the actual weight in kilograms (kg), and V_t is the actual volume (m^3).

Determination of Angle of Repose of Cowpea Seeds

Tilting box which consist of an iron rod for the frame, a plywood box with a fixed stand attached, a protractor was used to determine angle of repose for cowpea seeds, and an adjustable plate at the surface. In order for the seed to follow and acquire a natural slope, it was placed on the adjustable surface and allowed to progressively incline ([Tabatabaeefar, 2003](#); [Heidabeigi *et al.*, 2009](#)). Four different surfaces-wood, mild steel, stainless steel, and galvanized sheet-were used for these. One of the criteria used to calculate the angle of inclination of the hopper or chute for cowpea discharge is the value of the angle of repose.

Static Friction Calculation

The static coefficients of friction for cowpea seeds were evaluated on four different surfaces: mild steel, galvanized sheet, wood, and stainless steel. To determine these coefficients, we employed Equation 5, as outlined in the study by [Heidabeigi *et al.* \(2009\)](#).

$$\mu = \tan \alpha \quad (5)$$

Where μ is the coefficient of static friction and α is the angle of repose in degrees.

Determination of the Aerodynamic Properties of the Cowpea Seeds

To determine the terminal velocity of cowpea seeds, we utilized a vertical air tunnel at the agricultural engineering workshop of the Federal University of Technology, Akure. For each test, a single seed was released from the top of the air tunnel into the air stream. The speed of the blower's connected fan was gradually increased to raise the airflow rate until the seed remained suspended in the air stream. A hot wire anemometer, with a precision of 0.1 m s^{-1} , was used to measure the air velocity that effectively suspended the seed.

A total of twenty seeds, selected based on their moisture level, were tested. Each sample underwent three replications, in line with methodologies established by

[Sacilik *et al.* \(2003\)](#) and [Gupta and Das \(1997\)](#). The terminal velocity values for the cowpea seeds were meticulously recorded.

Statistical analysis

The analysis of variance (ANOVA) and Duncan Post-Hoc Multiple Comparison Test test were performed on the data acquired from the three replications at each moisture content using Mini Tab Software.

RESULTS AND DISCUSSION

Physical Properties of Cowpea Seeds

The findings detailing the impact of moisture content on various physical and aerodynamic properties of cowpea seeds are systematically presented in Tables 1 to 8 and Figures 1 to 4. These results demonstrate that the moisture content significantly influences both the physical and aerodynamic characteristics of the cowpea seeds.

Dimensions of the cowpea seeds

The average length, width and thickness of the cowpea seeds increased with an increase in the moisture content. At 10% moisture content, the average length and breadth were 9.00 mm, and 8.00 mm for SAMPEA-16 variety respectively. After conditioning, their dimensions were: 10.40 mm and 8.20 mm; 10.70 mm and 8.50 mm; 10.60 mm and 8.70 mm; 11.20 mm and 8.80 mm at moisture content of 15% wb; 20% wb; 25% wb and 30% wb respectively (Table 1). The result obtained in Table 1 is in agreement with the result reported by [\(Davies and Zibokere, 2011\)](#). Table 2 shows the average length, width and thickness for the SAMPEA-14 variety for the 10% moisture content was 8.10 mm, 6.30 mm and 6.20 mm, there was in increase in the seed dimensions at the 15%, 20%, 25% and 30% moisture content having the average value of 8.20 mm, 6.40 mm and 6.30 mm at 15%, 8.30 mm, 6.50 mm and 6.30 mm at 20%, 8.40 mm, 6.50 mm and 6.40 mm at 25%, 8.50 mm, 6.70 mm and 6.50 mm at the 30%.

Table 1. Physical properties of SAMPEA-16 of cowpea at different moisture content.

Dimension	Moisture content	Maximum Value	Minimum Value	Mean	Standard Deviation
Length	10	12.9	8.00	9.00	0.09
	15	13.00	8.60	10.40	0.09
	20	13.10	9.10	10.70	0.10
	25	16.00	9.20	10.60	0.08
	30	17.80	9.50	11.20	0.08
Width	10	12.90	7.0	8.00	0.05
	15	9.80	7.10	8.20	0.05
	20	9.90	7.00	8.50	0.05
	25	9.90	7.20	8.70	0.05
	30	10.20	7.60	8.80	0.06

Table 2. Physical properties of SAMPEA-14 of cowpea at different moisture content.

Dimension	Moisture content	Maximum	Minimum Value	Mean	Standard Deviation
Length	10	10.00	7.00	8.10	0.05
	15	10.00	6.60	8.20	0.06
	20	10.00	6.90	8.30	0.05
	25	10.01	8.40	8.40	0.08
	30	9.90	6.00	8.50	0.06
Width	10	7.80	4.30	6.30	0.07
	15	8.10	5.50	6.40	0.04
	20	8.30	5.60	6.50	0.05
	25	8.50	5.80	6.60	0.04
	30	8.50	5.90	6.70	0.04
Thickness	10	7.70	1.90	0.65	0.06
	15	8.00	5.00	0.62	0.04
	20	8.00	5.10	0.63	0.04
	25	8.20	5.80	0.64	0.04
	30	8.30	5.70	0.64	0.04

Volume

The volume of the Cowpea seeds has a linear relationship with moisture. This result is in line with the result obtained by [Davies and Zibokere \(2011\)](#). When the moisture content changed from 10.0% to 30.0% wb, the volume increased from 0.3424 mm³ to 0.4038 mm³ for SAMPEA-16 and from 0.1997 mm³ to 0.2122 mm³ for SAMPEA-14. The increase in volume is a result of the increase in moisture. This is depicted in Figure 1. Table 3, the effect of volume on the two varieties of cowpea, SAMPEA-16 and SAMPEA-14, was statistically significant ($p < 0.05$).

Table 3. Analysis of variance for volume for varieties 1 and 2.

Source	DF	Seq SS	Contribution	Adj SS	Adj MS	F-Value	P-Value
MC	4	0.020447	72.77%	0.020447	0.005112	6.68	0.007
Error	10	0.007650	27.23%	0.007650	0.000765		
Total	14	0.028096	100.00%				
Source	DF	Seq SS	Contribution	Adj SS	Adj MS	F-Value	P-Value
MC	4	0.016071	64.71%	0.016071	0.004018	4.58	0.023
Error	10	0.008765	35.29%	0.008765	0.000876		
Total	14	0.024836	100.00%				

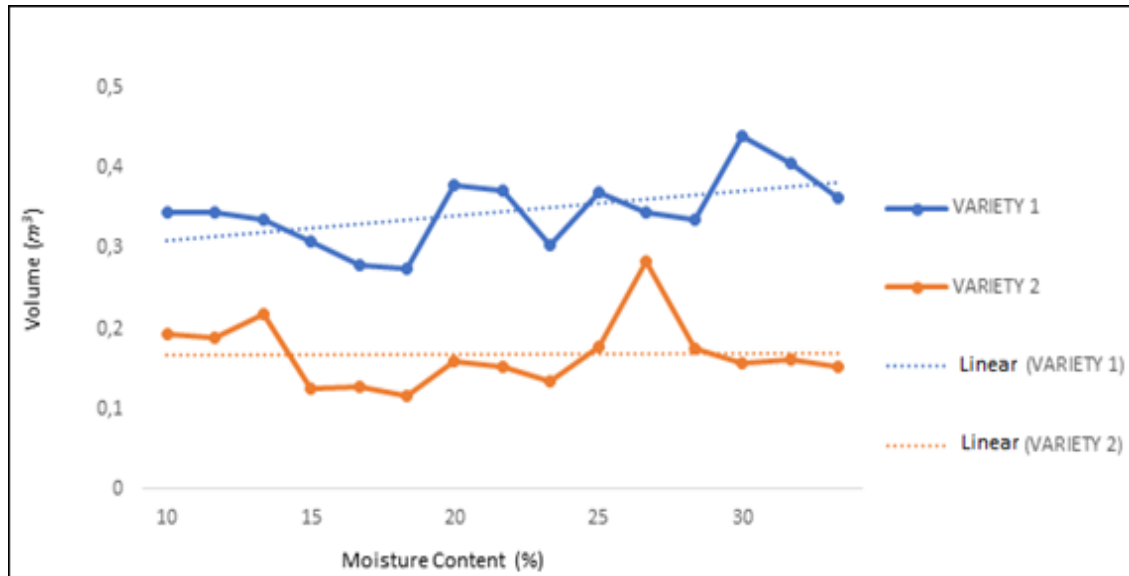


Figure 1. Effect of moisture content in % on volume in m³.

Sphericity

Between 10% and 15% moisture content, the effect of moisture content on the sphericity of SAMPEA-16 increased from 0.849 to 0.877; however, at 20% and 25% moisture content dry basis, the effect of moisture content decrease to 0.8730 and 0.866 respectively; and finally, it increased to 0.877 at 30% moisture content. For SAMPEA-14, the moisture content range between 10% and 15% showed a linear reduction from 0.848 to 0.838, but later increased at 20% to 25% from 0.842 to 0.852 and at 20% moisture content dry basis, before decreasing to 0.838 at 30% moisture content (Figure 2). [Yalçın \(2007\)](#) reported that sphericity of cowpea has a direct relationship with the moisture content of cowpea. The sphericity of cowpea increases as the moisture content of cowpea increases. [Aydin *et al.* \(2002\)](#) for Turkish mahaleb, [Gupta and Das \(1997\)](#) for sunflower seed, [Sacilik *et al.* \(2003\)](#) for hemp seed, [Baumler *et al.* \(2006\)](#) for safflower, and [Dursun and Dursun \(2005\)](#) for caper seed have all reported similar trends. While the increase reported in IAR-339-1 and Ife brown seeds is consistent with that obtained by [Davies and El- Okene \(2009\)](#) for soybean, the decline in sphericity of seeds is in line with that obtained by [Adejumo *et al.* \(2007\)](#) for the Kano White variety of bambara groundnut, [Altuntas and Yildiz \(2007\)](#) for faba bean, and [Cetin \(2007\)](#) for barbungia. A similar result was obtained by [Olawale *et al.* \(2018\)](#) and [Isa and Aderotoye \(2017\)](#). Table 4, the effect of moisture on SAMPEA-16 cowpea was statistically significant ($p < 0.05$) while Table 5 shows that SAMPEA-14 cowpea was not statistically significant ($p < 0.05$).

Table 4. Analysis of Variance of Sphericity for Variety 1 Cowpea, SAMPEA-16

Source	DF	Seq SS	Contribution	Adj SS	Adj MS	F-Value	P-Value
MC	4	0.001728	64.84%	0.001728	0.000432	4.61	0.023
Error	10	0.000937	35.16%	0.000937	0.000094		
Total	14	0.002665	100.00%				

Table 5. Analysis of Variance of Sphericity for Variety 2 Cowpea, SAMPEA-14.

Source	DF	Seq SS	Contribution	Adj SS	Adj MS	F-Value	P-Value
MC	4	0.000444	30.21%	0.000444	0.000111	1.08	0.416
Error	10	0.001026	69.79%	0.001026	0.000103		
Total	14	0.001470	100.00%				

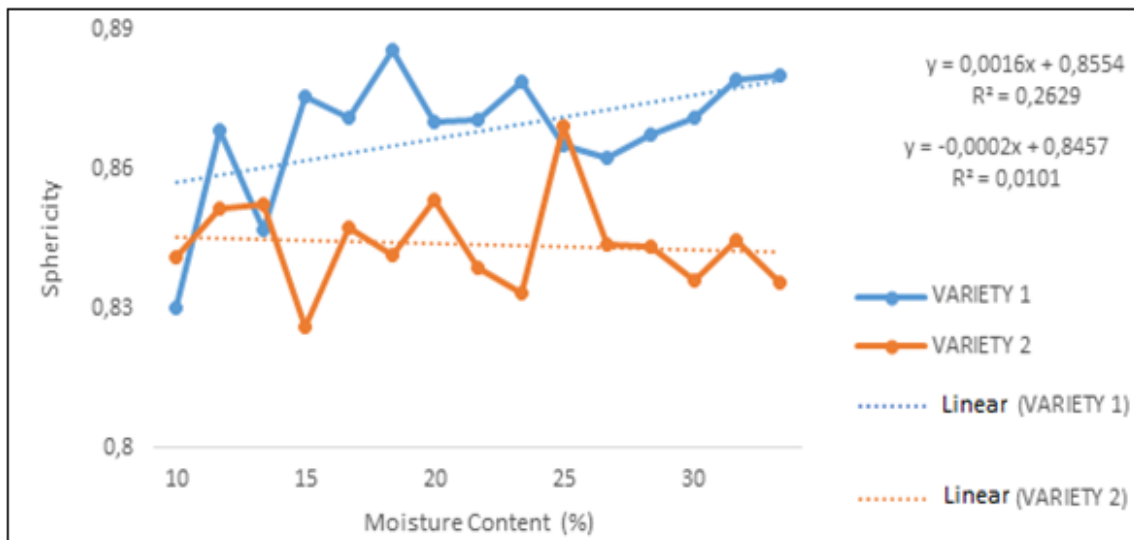


Figure 2. Effect of moisture content in % on the sphericity.

True Density

True densities increased as moisture levels rose from 1034.12 to 1074.40 kg m⁻³ for SAMPEA-14 and SAMPEA-16, respectively, and from 1089.61 to 1116.87 kg m⁻³ for SAMPEA-16. Figure 3 demonstrates that the real densities of the two varieties grew and then declined as moisture levels rose. This indicates that initially, due to moisture absorption, the relative rise in cowpea weight was equal to the corresponding volumetric increase, but with an increase in moisture, the relative increase in weight was not equal to the corresponding increase in volume. The true density decreases as the moisture content of cowpea seed increases. Similar results were obtained for cotton seed by [Ozarslan \(2002\)](#), hemp seed by [Sacilik et al. \(2003\)](#), soybean by [Deshpande et al. \(1993\)](#), and hemp seed by [Abalone et al. \(2004\)](#); [Davies and Zibokere \(2011\)](#) also noted a negative association between true density and moisture content. According to Table 6's statistical analysis, there was a significant difference in the true density for SAMPEA-14 but not for SAMPEA-16, as indicated by the P-value.

Table 6. Analysis of variance of true density for SAMPEA-16 and SAMPEA-14 cowpea varieties.

Source	DF	Seq SS	Contribution	Adj SS	Adj MS	F-Value	P-Value
MC	4	0.01014	36.21%	0.01014	0.002535	1.42	0.297
Error	10	0.01787	63.79%	0.01787	0.001787		
S	14	0.02801	100.00%				
Source	DF	Seq SS	Contribution	Adj SS	Adj MS	F-Value	P-Value
MC	4	0.06870	73.73%	0.06870	0.017175	7.02	0.006
Error	10	0.02447	26.27%	0.02447	0.002447		
Total	14	0.09318	100.00%				

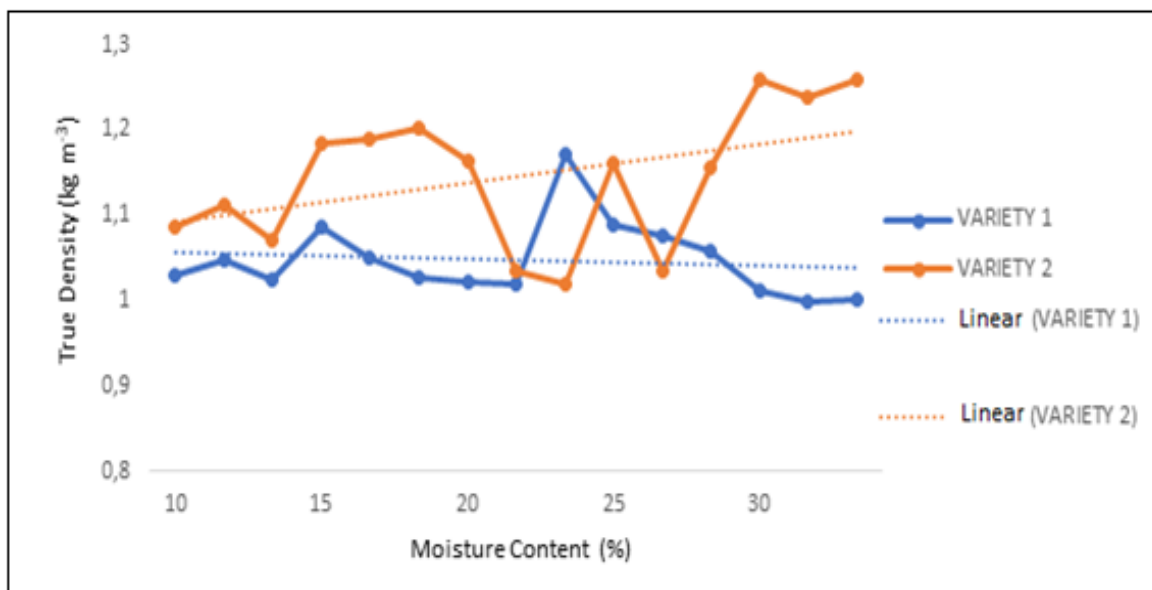


Figure 3. Effect of moisture content in % on the true density in $kg\ m^{-3}$.

Angle of repose

Table 7's statistical analysis reveals from the P-value that the angle of repose for the SAMPEA-16 and SAMPEA-14 cowpea types was significantly different from one another. The two types' angles of repose grew as the moisture content grew. When the moisture content increased from 10% to 30%, Table 8 shows that the angle of repose for the SAMPEA-16 increased from $22.40^{\circ} \pm 0.82^b$ to $30.23^{\circ} \pm 0.52^a$. The angle of repose went from $23.22^{\circ} \pm 0.50^d$ to $34.28^{\circ} \pm 0.81^a$ for the same increase in moisture in SAMPEA-14. [Olalusi *et al.* \(2009\)](#) and [Davies and Zibokere \(2011\)](#) reported that the primary cause of the increase in angle of repose for these cowpea varieties is the larger size of the seeds. This suggested that, in comparison to cowpea seeds, the forces of solid friction at the grain-material interface were generally lower in oil bean seeds. This is comparable to the data on Tiger nut published by [Olalusi *et al.* \(2009\)](#).

Table 7. Analysis of variance of angle of repose for SAMPEA-16 and SAMPEA-14 cowpea variety.

Source	DF	Seq SS	Contribution	Adj SS	Adj MS	F-Value	P-Value
MC	4	141.532	94.85%	141.532	35.3830	46.09	0.000
Error	10	7.677	5.15%	7.677	0.7677		
Total	14	149.209	100.00%				

Source	DF	Seq SS	Contribution	Adj SS	Adj MS	F-Value	P-Value
MC	4	228.947	97.34%	228.947	57.2368	91.33	0.000
Error	10	6.267	2.66%	6.267	0.6267		
Total	14	235.214	100.00%				

Table 8. Mean values for the physical properties for SAMPEA-16 and SAMPEA-14 cowpea varieties.

Property	Moisture Content (%)	Variety 1	Variety 2
True density	10	1.03±0.01 ^a	1.09±0.02 ^b
	15	1.05±0.03 ^a	1.20±0.01 ^{ab}
	20	1.07±0.09 ^a	1.07±0.08 ^b
	25	1.07±0.02 ^a	1.12±0.07 ^b
	30	1.00±0.01 ^a	1.25±0.01 ^a
Angle of repose	10	22.40±0.82 ^b	23.23 ±(0.50 ^d)
	15	23.56±0.89 ^b	25.69 ±(0.96 ^c)
	20	24.57±1.34 ^b	25.90 ±(0.31 ^c)
	25	28.91±0.56 ^a	30.12 ±(1.11 ^b)
	30	30.23±0.52 ^a	34.28 ±(0.81 ^a)
Volume	10	0.34±(0.01 ^{ab})	0.20±0.02 ^{ab}
	15	0.29±(0.02 ^b)	0.12±0.006 ^b
	20	0.35±(0.04 ^{ab})	0.15±0.012 ^{ab}
	25	0.35±(0.02 ^{ab})	0.21±0.06 ^a
	30	0.40±(0.04 ^a)	0.16±0.004 ^{ab}
Sphericity	10	0.85±0.02 ^b	0.85±(0.01 ^a)
	15	0.88±0.01 ^a	0.84±0.01 ^a
	20	0.87±0.005 ^{ab}	0.84±0.01 ^a
	25	0.86±0.002 ^{ab}	0.85±0.01 ^a
	30	0.88±0.005 ^a	0.84±0.005 ^a

Values are means of triplicate and standard error. Means values having different superscript within the same row are significantly different (P<0.05).

Aerodynamic properties of cowpea seeds

Figure 4 reveals that as the moisture increased, terminal velocity of the cowpea seeds for the two varieties increased. The terminal velocity of each variety increased with the increase in moisture. The terminal velocity of SAMPEA-14 increased from 4.92 m/s to 5.25 m s⁻¹, and the terminal velocity for SAMPEA-16 increased from 5.72 m s⁻¹ to 6.16 m s⁻¹ at 10% to 25% moisture content. The finding was to that of

cowpea studies conducted by [Aderinlewo *et al.* \(2011\)](#). In the cases of sunflower, karingda, cumin, lentil, and melon seeds, respectively, similar findings were reported by [Gupta and Das \(1997\)](#), [Suthar and Das \(1996\)](#), [Singh and Goswami \(1996\)](#), [Carman \(1996\)](#).

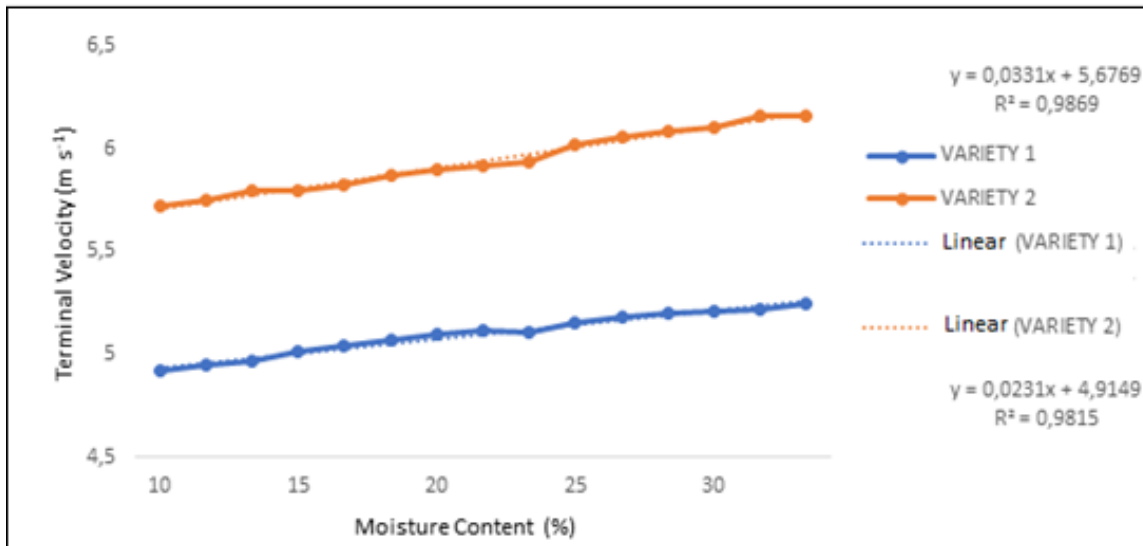


Figure 4. Impact of moisture content on the terminal velocity.

CONCLUSION

The study's findings indicate a linear relationship between the dimensions of cowpea seeds and their moisture content. As moisture increases, there is a corresponding growth in the seed's length, width, and thickness. However, it's important to note that regardless of the moisture level, the shape of the cowpea seeds, as indicated by their sphericity results, remains significantly non-spherical. This implies that cowpea seeds would not effectively pass through a separating machine equipped with circular holes. Additionally, moisture content positively correlates with the volume of the seeds; an increase in moisture leads to an expansion in volume. This study also observed that the angle of repose for the seeds increased on all tested surfaces as moisture content rose. Furthermore, there is a positive relationship between the terminal velocity of the cowpeas and their moisture content, indicating that as moisture increases, so does the terminal velocity.

DECLARATION OF COMPETING INTEREST

The authors declare that they have no conflict of interest

CREDIT AUTHORSHIP CONTRIBUTION STATEMENT

The authors declared that the following contributions are correct.

Olufemi Adeyemi ADETOLA: Conceptualization, writing-original draft, review, and editing and validation.

Adenike Mary ADEROTOYE: Writing-original draft and data curation.

Marvellous Oluwaseun LAWAL: Investigation, methodology, formal analysis, writing-original draft and data curation.

ETHICS COMMITTEE DECISION

This article does not require any ethical committee decision.

REFERENCES

- Abalone R, Cassinera A, Gaston A and Lara MA (2004). Some physical properties of amaranth seeds. *Biosystems Engineering*, 89(1): 109-117. <https://doi.org/10.1016/j.biosystemseng.2004.06.012>
- Adejumo OI, Alfa AA and Mohammed A (2007). Physical Properties of Kano white Variety of Bambara Groundnut. *Nigerian Academic Forum*, (12)1: 68-77.
- Adekanye AT and Olaoye JO (2018). Performance evaluation of motorized and treadle cowpea threshers. *Agricultural Engineering International: The CIGR Journal (CIGR)*, 15(4): 300-306.
- Aderinlewo AA, Raji AO and Olayanju TMA (2011). Effect of variety and moisture content on aerodynamic properties of four Nigerian cowpea (*Vigna unguiculata*) varieties. *Journal of Natural Sciences, Engineering and Technology*, 10(1): 106-115.
- Adetola OA, Olukunle OJ, Olalusi AP and Olubanjo OO (2020). Effect of tillage practices on selected engineering properties of cassava (*Manihot esculenta*) tubers. *Nigerian Journal of Technological Development*, 17(3): 205-216. <http://dx.doi.org/10.4314/nitd.v17i3.7>
- Adewumi BA, Ademosun OC and Ogunlowo AS (2007). Design, fabrication and preliminary testing of athresher-cleaner for grain legume. *Journal of Food Science and Technology*, 44(3): 276-280.
- Altuntas E and Yildiz M (2007). Effect of moisture content on some physical and mechanical properties of faba bean (*Vicia faba* L.) grain. *Journal of Food Engineering*, 78:174-183. <https://doi.org/10.1016/j.jfoodeng.2005.09.013>
- AOAC (1995). Association of Official Analytical Chemists.
- Aydin C, Ogut H and Konak M (2002). Some physical properties of Turkish Mahaleb. *Biosystems Engineering*, 82(2): 231-234. <https://doi.org/10.1006/bioe.2002.0062>
- Baumler E, Cuniberti A Nolasco SM and Riccobene IC (2006). Moisture dependent physical and compression properties of safflower seed. *Journal of Food Engineering*, 73: 134-140. <https://doi.org/10.1016/j.jfoodeng.2004.11.029>
- Carman K (1996). Some physical properties of lentil seeds. *Journal of Agricultural Engineering Research*, 63(2), 87-92. <https://doi.org/10.1006/jaer.1996.0010>
- Cetin M (2007). Physical properties of barbunia bean (*Phaseolus Vulgaris* L. cv. burbuniz) seed. *Journal of Agricultural Engineering Research*, 80: 353-362. <https://doi.org/10.1016/j.jfoodeng.2006.06.004>
- Chukwu O and Sunmonu MO (2010). Determination of selected engineering properties of cowpea (*Vigna unguiculata*) related to design of processing machines. 2(6): 373-377.
- Davies RM and El-Okene AM (2009). Moisture-dependent physical of soybeans. *International Agrophysics*, 23: 299-303.
- Davies RM and Zibokere DS (2011). Effect of moisture content on some physical and mechanical properties of three varieties of cowpea (*Vigna unguiculata* L. Walp). *Agricultural Engineering International: CIGR*, 13(1): 1-16.
- Deshpande SD, Bal S and Ojha TP (1993). Physical properties of soybean. *Journal of Food Engineering*, 56: 89-98. <https://doi.org/10.3923/ja.2006.74.78>
- Dursun E and Dursun I (2005). Some physical properties of caper seed. *Biosystems Engineering*, 92(2), 237-245. <https://doi.org/10.1016/j.biosystemseng.2005.06.003>
- Gómez C (2004). COWPEA Post-harvest Operations. In *FAO*.
- Gupta RK and Das SK (1997). Physical properties of sunflower seeds. *Journal of Agricultural Engineering Research*, 56(1): 49-57. <https://doi.org/10.3923/ijar.2007.677.686>
- Isa J and Aderotoye MA (2017). Effect of moisture content on the physical and aerodynamics properties of cashew nut. *Journal of Engineering and Engineering Technology*, 11(2): 96-102. <https://doi.org/10.13140/RG.2.2.35988.94082>

- Krishnakumar T (2019). Engineering properties of agricultural materials. <https://doi.org/10.13140/RG.2.2.20324.83842>
- Mohsenin NN (1978). Physical properties of plant and animal materials. *Gordon and Breach Publ. Inc.*, New York. 758 pages.
- Muhammed-Bashir O, Oriola KO, Ogundeji BA and Adesokan MA (2018). Fabrication and performance evaluation of cowpea thresher for small scale cowpea farm holders in Nigeria. *Current Journal of Applied Science and Technology*, 31(6): 1-11. <https://doi.org/0.9734/CJAST/2018/43751>
- Narayana M and Angamuthu M (2021). The beans and the peas, Woodhead Publishing, Pages 241-272.
- Olalusi AP, Bolaji OT and Adebayo SS (2009). Some Engineering Properties of Tiger Nut. *Journal of 3rd International Conference of WASAE and 9th International Conference of NIAE*. p. 244-248.
- Olawale C, Aderibigbe D, and Femi O (2018). Effect of soaking time on some engineering properties of cowpea (*Vigna unguiculata*). *Agricultural Engineering International: The CIGR Journal (CIGR)*, 20(1): 143-149.
- Olukunle OJ and Akinnuli BO (2012). Investigating some engineering properties of coffee seeds and beans. *Journal of Emerging Trends in Engineering and Applied Sciences*, 3(5): 743-747. <https://doi.org/10.1016/j.aaspro.2015.01.052>
- Ozarslan C (2002). Physical properties of cotton seed. *Biosystems Engineering*, 83(2): 169-174. <https://doi.org/10.1006/bioe.2002.0105>
- Sacilik K, Ozturk R and Keskin R (2003). Some physical properties of hemp seed. *Biosystems Engineering*, 86(2): 191-198. [https://doi.org/10.1016/S1537-5110\(03\)00130-2](https://doi.org/10.1016/S1537-5110(03)00130-2)
- Singh KK and Goswami TK (1996). Physical properties of cumin seed. *Journal of Agricultural Engineering Research*, 64(2): 93-98. <https://doi.org/10.1006/jaer.1996.0049>
- Suthar SH and Das SK (1996). Some physical properties of karingda [*Citrullus lanatus* (thumb) mansf] seeds. *Journal of Agricultural Engineering Research*, 65(1): 15-22. <https://doi.org/10.1006/jaer.1996.0075>
- Tabatabaeefar A (2003). Moisture-dependent physical properties of wheat. *International Agrophysics*, 17: 207-211.
- Timothy A and Olaoye JO (2013). Performance evaluation of motorized and treadle cowpea threshers. *Agricultural Engineering International: The CIGR Journal (CIGR)*, 15(4): 300-306.
- Yalçın İ (2007). Physical properties of cowpea (*Vigna sinensis* L.) seed. *Journal of Food Engineering*, 79(1): 57-62. <https://doi.org/10.1016/j.jfoodeng.2006.01.026>



Turkish Journal of
Agricultural
Engineering Research
(Turk J Agr Eng Res)
e-ISSN: 2717-8420



Development of a Mechanical System to Produce Animal Feed from Rice Straw

Mohamed GHONIMY^{a*} , Ahmed SULIMAN^b ,
Mohamed MORSY^c , Ahmed ABDEEL-ATTY^d , Ahmed ALZOHEIRY^e 

^aDepartment of Agriculture and Biosystems Engineering, College of Agriculture and Food, Qassim University, P.O.Box 6622, Buraydah, Al-Qassim 51452, Saudi Arabia; Agricultural Engineering Dept., Faculty of Agriculture, Cairo University, Giza, EGYPT

^bDepartment of Agricultural Engineering, Faculty of Agriculture, Cairo University, Giza, EGYPT

^cDepartment of Animal Production Faculty of Agriculture, Cairo University, Giza, EGYPT

^dAgricultural Engineer, Private Sector, EGYPT

^eDepartment of Agriculture and Biosystems Engineering, College of Agriculture and Food, Qassim University, Buraydah, Saudi Arabia. Department of Natural Resources and Agricultural Engineering, Faculty of Agriculture, Damanshour University, Damanshour, EGYPT

ARTICLE INFO: Research Article

Corresponding Author: Mohamed GHONIMY, E-mail: mohamed.ghonimy@agr.cu.edu.eg

Received: 6 February 2024 / **Accepted:** 3 April 2024 / **Published:** 30 June 2024

Cite this article: Ghonimy M, Suliman A, Morsy M, AbdeEl-Atty A and Alzoheiry A (2024). Development of a Mechanical System to Produce Animal Feed from Rice Straw. *Turkish Journal of Agricultural Engineering Research*, 5(1): 35-48. <https://doi.org/10.46592/turkager.1432932>

ABSTRACT

Rice straw stands out as the primary agricultural residue posing significant challenges for both farmers and the Egyptian government. Its volume accounts for approximately 18% of the total annual waste generated. Livestock farmers typically harvest the straw and feed it to their animals. However, the process of manually mixing molasses, urea, and salts with the straw often leads to inconsistent blending and uneven distribution of the mixture. This inconsistency poses a considerable risk to the health of the animals, potentially resulting in fatalities. Thus, a mechanical system for producing animal feed (rice straw cutting mixed with additives of urea, minerals and molasses) was developed. This system consists of a chopping unit, mixing unit, and pumping & distribution unit. Measurements included the uniformity of the cut rice straw pieces within the preferred size, the uniformity of the dissolved additives mixture and the uniformity of the additives distribution on cut rice straw. Crude protein and urea percentages were measured in the final product. The results showed a maximum production rate of 0.6 ton h⁻¹ the suitability of the developed system for mixing the additives with the cut rice straw. The suitability of the developed system was determined through the uniformity of the distribution of the additives on the cut rice straw. The results showed that the optimum content of crude protein of 6.2% was found at urea content of 5% and a mixing unit shaft speed of 300 rpm and 5 min mixing time. Also, the developed system achieved a rate of return of 19% and a payback period of about two years.

Keywords: Additive, Animal feed, Rice straw, Mechanical system



INTRODUCTION

Egypt cultivates about 400,000 ha of rice every year, which produce 3.39 million tons of rice straw. This quantity presents a sizable problem to the farmers, government and the environment (CMAE, 2020). In Egypt, animal feed resources are not sufficient to meet the nutritional requirements of the livestock. This shortage of feed and low genetic potential of the local animals is the major factors causing the low productivity of the indigenous breeds. Rice straw is a poor-quality fibrous material, which is not suitable for use as an animal feed without treatments to change its physical structure. Cutting rice straw and adding supplements, such as non-protein nitrogen plus molasses and minerals, will encourage animals to consume it. These treatments will also increase the digestibility and nutritive value of this type of feeding. Nowadays, farmers cut rice straw by machines and manually add a mixture of molasses and urea. This primitive process is very harmful to the animals, since the product is not homogeneous and some parts will have high percentage of urea which is toxic when consumed by the animals. Wang *et al.* (2021) found that treating rice straw with 5% urea increased the crude protein (CP) content from 3.42% to 8.07%. Mu *et al.* (2022) observed that processing and neutralizing cut rice straw, whether chopped into lengths of 2-3 cm or 15-20 cm, significantly enhanced the digestibility of crude protein (CP) and dry matter (DM). Chopping the straw into 2-3 cm lengths prior to treatment yielded superior outcomes compared to longer-cut straw. Neutralization also affected the chemical composition of the straw and increased its Sulphur content. Mohammed Aliyi (2021) studied the effect of urea treatment of rice and wheat straw on feed intake and milk yield of buffaloes. Chemical treatment of straw increased dry matter intake (DMI) over untreated straw and improved milk yield. Availability of urea was the major limitation to the process. Radwan (2000) developed a feed preparation unit, which chops the crop residual, and mix the chopped material with the additives determined for the feed ration. He found that the output decreased from 1320, 760 and 508 kg h⁻¹ to 1400, 800 and 600 kg h⁻¹ for corn stalks, corn Stover and rice straw respectively. Adding molasses increased the mean weight length (MWL) by 31%. Radwan (2000) developed a feed preparation unit which chops the crop residual to the desired sizes and mixes the chopped materials with the additives determined for the feed ration. He found that the chopper speed should surpass 1400 rpm, while the mixing speed should range between 60 rpm and 100 rpm. Mohamed *et al.* (2001) developed a rice straw chopper and they found that the productivity of the developed machine was 0.95 ton h⁻¹ at 2000 rpm rotor speed. Patel *et al.* (2023) evaluate and optimize the chopping unit of straw chopper cum mixture machine for paddy straw management. The effect of operational parameters i.e., blade type, rotational and forward speed of the machine, and crop parameters i.e. days after harvesting (DAH) on the power requirement was determined. They found that the cutting torque was significantly affected by the rotational speed, forward speed and DAH of the paddy straw. A straw management system (SMS) serrated blade operating at rotational and forward speed of 900 rpm and 1 km h⁻¹ respectively with average cutting torque of 3.8 Nm was found to be optimal for cutting the paddy straw. The objective of this research is to develop a mechanical system for producing animal feed by cutting the rice straw then mixing it with additives, such as urea, molasses and minerals.

MATERIALS and METHODS

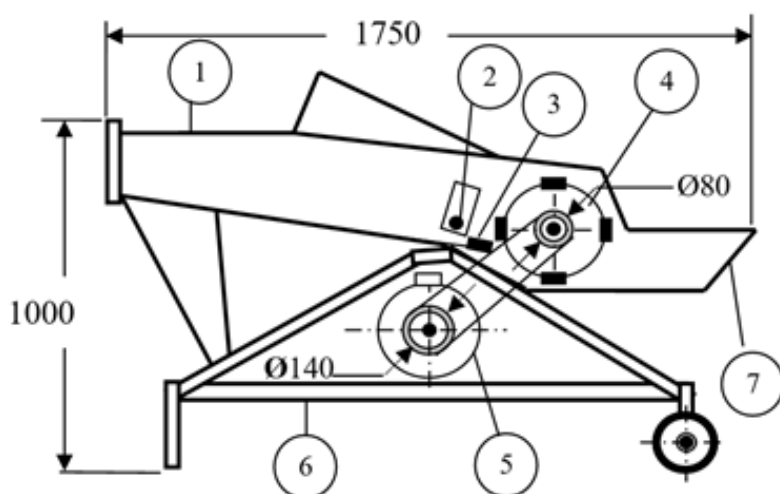
The developed system consists of chopping unit, mixing unit, and pumping & distribution unit.

The chopping unit

A diagram showing the components of the chopping unit is shown in Figure (1). The cutting-head is a cylinder drum type. The chopping mechanism consists of fixed knife and a cutting head equipped with four movable knives, the angle between each two knives is 90 degrees. This unit is used for chopping crop residues such as maize stalks and rice straw. The overall dimensions of chopping unit are 1750 mm long, 400 mm wide and 1000 mm high. The chopping unit consists of:

1. Cutting-head

The cutting head, Figure (2), has four parallel knives which are mounted on a cylinder. The cutting head consists of four cutting knives which are fixed to the rotating axis. Each knife is fastened by five bolts and rotates with high speed corresponding to a lower speed of feeding drums. The fixed knife length, width and thickness are 300, 60 and 5 mm, respectively. The chopping cylinder has a diameter of 300 mm and is 300 mm long.



1. Feeding hopper, 2. Feeding drum, 3. Fixed knife, 4. Cutting drum, 5. Electric motor, 6. Frame, 7. Outlet dimensions in mm

Figure 1. The chopping unit.

2. Feeding drum

The feeding drum, Figure (2), pushes the rice straw to the cutting-head. The feeding drum length, outside diameter, and thickness were 300, 40, and 5 mm respectively. The cutting head and feeding drum are operated by an electric motor fixed on the machine frame.

3. Source of power

The chopping unit is powered by an electric motor, 7.35 kW (10 HP), 3 phase and with a rotating speed 1400 rpm.

4. Transmission system

The transmission system of the chopping unit consists of two units. The first unit transmits the motion from the electric motor to the cutting drum. The second unit transmits the motion from the cutting drum to the feeding drum. V-belts are used to transmit the motion between driving and driven pulleys.

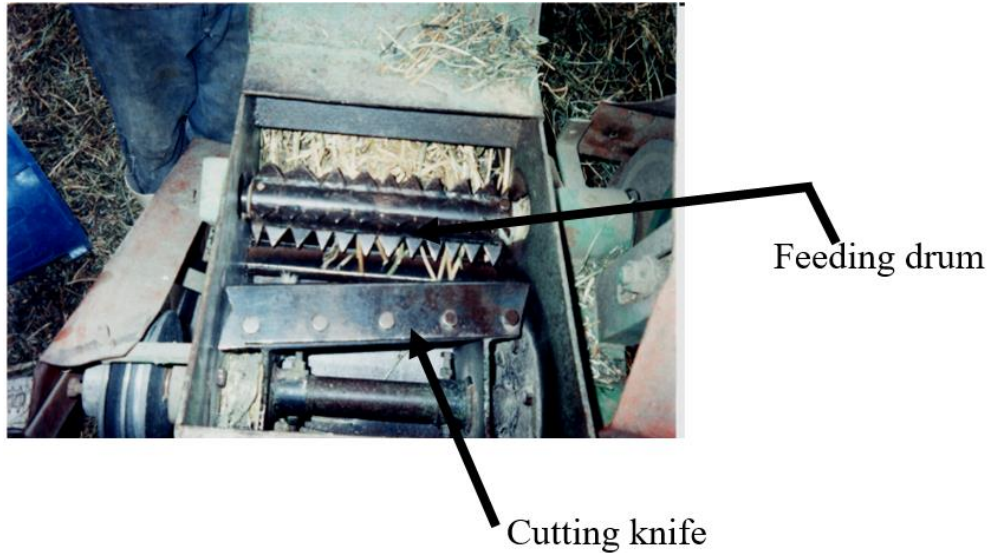


Figure 2. *The chopping machine.*

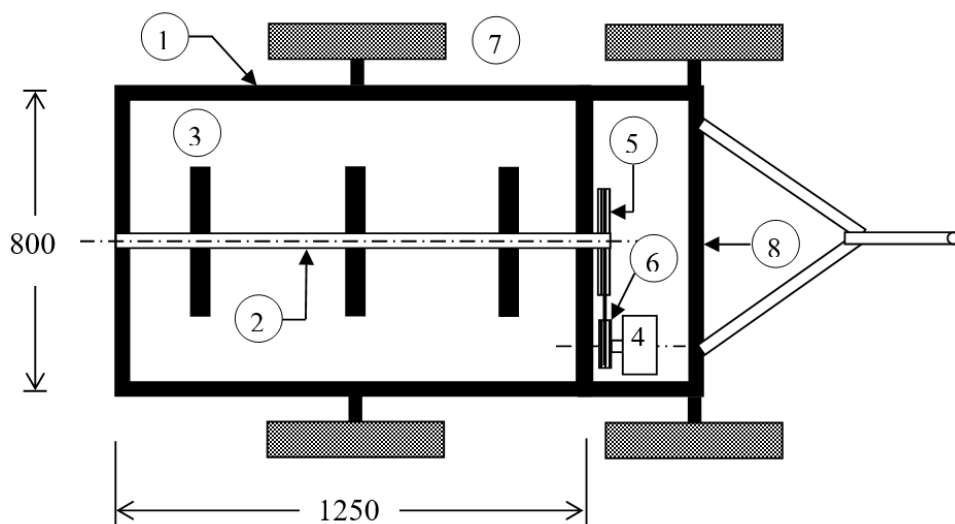
The chopping unit was tested to chop rice straw at three rotating speeds of 1450, 1550 and 1650 rpm equivalent to liner speed (22.8, 24.3 and 25.9 m s⁻¹) (Younis *et al.*, 2002) and three levels of clearances between the fixed knife and cutter head drum of 1, 2 and 3 mm.

The mixing unit

The mixing unit, Figure 3, consisted of:

1. Frame and hitching

The frame of mixing unit was manufactured from steel 50, U section 100 mm and 6 mm thickness. The mixing unit is attached to the tractor by draw bar pull. The frame length, width and height are 1850, 1000 and 1000 mm respectively. Four tires 15×15 ×85 cm were used to trail this frame.



1. Tank, 2. Mixing shaft, 3. Blade vane, 4. Motor, 5. Driven pulley, 6. Driving pulley, 7. Tire, 8. Frame dimensions in mm

Figure 3. The mixing unit.

2. Tank

The tank, Figure (4), consists of steel hollow cylinder, diameter 800 mm, 1250 mm long and with 4.3 mm thickness. The tank has a 400 mm diameter orifice for the introduction of the additives. The tank capacity is 600 liters.

3. Mixing shaft

The mixing shaft, Figure (5), is a 40 mm diameter steel 50 rod. Three blade vanes were welded on the shaft for mixing the additives. The blade dimensions are 50 mm wide, 400 mm long and 2 mm thickness. The mixing shaft rotates on two ball bearings size 6206.



Figure 4. The mixing tank

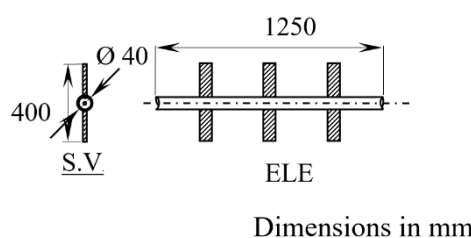


Figure 5. The mixing shaft

4. Power

Diesel engine, 2.94 kW (4 HP) at 1000 rpm, was used to transmit the power to the mixing shaft. Belt drive and pulley was used to reduce the speed transmitted from the engine to the mixing shaft.

5. Power transmission system

V-belts are used to transmit the motion between driving and driven pulleys. The length of the V-belts was calculated according to [Tinder \(2022\)](#) and meets the ANSI

American standards. The mixing unit was evaluated at three levels of rotating speeds 100, 200 and 300 rpm and at three mixing time intervals of 5, 10 and 15 minutes.

Pumping and distribution unit

The components of pumping and distribution unit are pump, pipes, sprinklers and limit electric switch.

1. Pump

Gear pump was used to move the dissolved additives mixture through pipes to sprinklers. This pump was adjusted to discharge 85 Lh^{-1} equivalent to 118.5 kg mixture per hour at a head of 20 m. This pump is operated by a motor 0.37 kW (0.5 HP) at 2860 rpm rotating speed. A speed reducer was used to control the discharge of the pump by controlling the rotating speed of the motor.

2. Pipes

The pipes in the distribution unit were one-inch diameter rubber tubes. There are two parts, one connected between the dissolving unit and the pump to take in the dissolved additives mixture from the dissolving unit, (150 mm length). The other part is connected between the pump and cutting machine for delivering the mixture to sprinklers, (100 mm length).

3. Sprinklers

Three sprinklers, 3 mm in diameter, were used to distribute the dissolved additives mixture on the rice straw. These sprinklers were fixed in a pipe 200 mm length at the outlet of the chopping unit. The end of the pipe is connected with a tube to return the excess additives to the tank.

4. Limit electric switch

A limit electric switch (model XCK-P 106, 220V and 3A), is used to transmit the electric current to the pump motor during operation when the rice straw touches the switch. The switch is mounted at the entrance of cutting unit Figure (6). The chopping unit, the mixing unit and the pumping and distribution unit are assembled in compacted system as shown in Figure (7).



Figure 6. The limit electric switch



Figure 7. The developed mechanical system

Measurements and calculations:1. Mass of residues

The weight of the machine output was determined using a spring balance, 500 N capacity, with 5 N accuracy.

2. Cutting length and diameter of residues

The cutting length and diameter of the residue were measured using vernier caliper, accuracy ± 0.1 mm.

3. Cutting head rotating speed

The rotating speed of the cutting head was determined using hand-held mechanical tachometer, accuracy 1-6 rpm.

4. Chopping unit productivity (P_c)

The chopping unit productivity (P_c) was calculated from the Equation 1.

$$P_c = \frac{M}{T} \quad (1)$$

Where: P_c is chopping unit productivity, kg h^{-1} ; M is mass of chopped material, kg; T is operating time, h.

5. The uniformity of the dissolved additives mixture

Chemical analyses were performed at the Animal Production Research Institute, Agric. Research Center, Ministry of Agriculture, Giza, Egypt. This analysis was done to determine the uniformity of the dissolved additives mixture by determination of the ratio of urea in the dissolved additives mixture. The samples of the dissolved additives mixture were taken from inside the tank at three levels (bottom from 0 to 250 mm, middle from 250 to 500 mm and top from 500 to 800 mm). Twenty-five samples were taken from each level.

6. The uniformity of the additives distribution on cut rice straw

The uniformity of the additives distribution on cut rice straw was determined by the calculation of the percentage of crude protein (CP) in the samples. Three percentages of urea 1, 3 and 5% were distributed on the chopped rice straw (according to [Abreu et al., 2022](#)). Five samples (S_1, S_2, S_3, S_4 and S_5) were taken from the final product for each urea percentage. Chemical analyses were performed to compute the crude protein.

7. Cost analysis and economic evaluation

The cost analysis ([Oida, 1997](#)) was performed in two steps. The first step was to calculate the cost of the materials and the fabrication. The second step was to calculate the mechanical system operating cost. In order to evaluate the financial viability of the developed system, three parameters were computed and were analyzed. These parameters include developed system operating cost, the internal rate of return (IRR) and the pay back period (PBP).

RESULTS AND DISCUSSION

Physical and chemical properties of rice straw

The ranges of the stem diameter and length of the rice straw were 2-4 mm, and 50-110 cm respectively. Chemical analysis of the rice straw and molasses are shown in Table (1). Table (1) shows the average values of the percentage of crude fiber (*CF*), ether extract (*EE*), crude protein (*CP*), nitrogen free extract (*NFE*), ash (*Ash*) and the moisture content (*MC*).

Table 1. Chemical analysis of rice straw and molasses

Components, %	<i>CF</i>	<i>EE</i>	<i>CP</i>	<i>NFE</i>	<i>Ash</i>	<i>MC</i>
Rice straw	33.40	1.90	3.35	36.36	17.99	7.00
Molasses	0.00	0.00	4.90	60.10	12.00	23.00

The performance of the chopping unit

Effect of cutting head speed on chopping unit productivity

The average values of the chopping unit productivity (*Pc*) are shown in Figure (8). It is clear that the *Pc* was increased by increasing the cutting head speed from 1450 rpm (22.8 m s⁻¹) to 1650 rpm (25.9 m s⁻¹) at the same clearance. Meanwhile, the *Pc* was decreased by increasing of clearance at the same speed. The maximum value of *Pc* of 600 kg h⁻¹ was found at speed 1650 rpm (25.9 m s⁻¹) and clearance 1 mm. Meanwhile, the minimum value of *Pc* of 400 kg h⁻¹ was found at speed 1450 rpm (22.8 m s⁻¹) and clearance 3 mm. This agree with what [Hashem *et al.* \(2022\)](#) reported they found that the productivity of the chopping unit decreased with reducing the clearance and increased with the increase of the chopping drum rotational speed. They achieved a maximum capacity of 350 kg h⁻¹ at a chopping drum rotational speed of 1200 rpm. These results are also similar to those found by ([Arif and Elaiwa, 2009](#); [Abo-Habaga *et al.*, 2019](#); [Jiang *et al.*, 2021](#)). [Abo-Habaga *et al.* \(2019\)](#) reported that the maximum chopper productivity of 1.2 Mg h⁻¹ was achieved using a chopping-drum speed of 2350 rpm and a feeding-mechanism speed of 0.42 m s⁻¹. Conversely, the minimum chopper productivity of 0.92 Mg h⁻¹ was observed with a chopping-drum speed of 1450 rpm and a feeding-mechanism speed of 0.26 m s⁻¹, regardless of the type of cutting knives used. Also, [Arif and Elaiwa \(2009\)](#) indicated that the maximum productivity of 171 kg h⁻¹ was achieved by employing two knives with a clearance of 4 mm, a cutting drum speed of 18.7 m s⁻¹. Employing two knives on the cutting drum resulted in higher machine productivity compared to using three or four knives. [Hashish *et al.* \(1994\)](#) conducted a study investigating various factors influencing the performance of chopping, crushing, and grinding equipment for field raw material. Their findings indicated several key conclusions: Firstly, they identified an optimum PTO speed of 700 rpm across the three different raw materials examined. Secondly, they observed that the highest production rates and efficiency were achieved at low moisture content levels, specifically 2.5% for rice straw, 5.3% for cotton stalks, and 6.26% for maize stalks. Lastly, they noted that equipment modifications led to improvements in both fineness degree and productivity, increasing from 37% to 48%.

At a cutting head speed 1450 rpm (22.8 m s^{-1}), the P_c increased by 15% by decreasing the clearance from 3 to 2 mm, and increased by 8.69% by decreasing the clearance from 2 mm to 1 mm. The same trend was also observed at cutting head speed 1550 rpm (24.3 m s^{-1}) and 1650 rpm (25.9 m s^{-1}).

The maximum chopping unit productivity was achieved when the cutting head speed was 1650 rpm (25.9 m s^{-1}) and 1 mm clearance. For these conditions the chopper productivity was 600 kg h^{-1} .

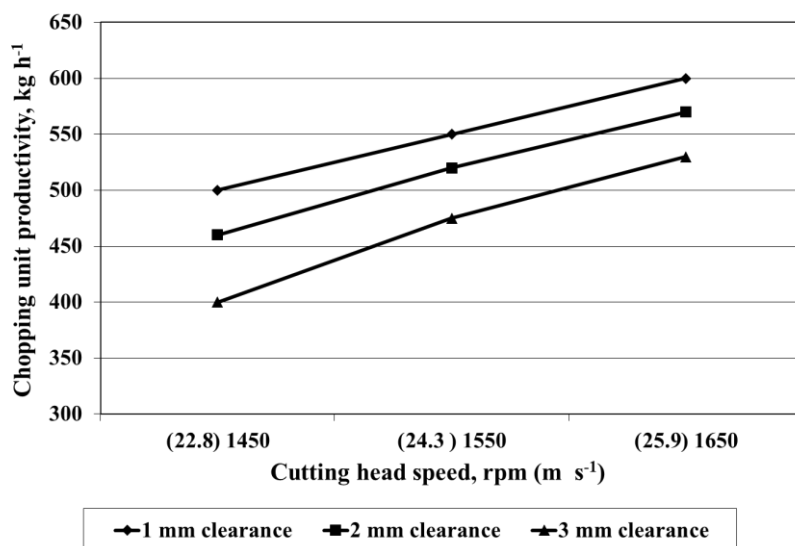


Figure 8. Effect of cutting head speed and clearance on the chopping unit productivity.

Effect of cutting head speed on the rice straw cutting length

The length of the cut rice straw was classified into three groups, the first was less than 20 mm, the second (favorite length) was from 20 to 80 mm, and the third was greater than 80 mm. The results of cutting length distribution at different speeds and clearances are shown in Table (2).

Table 2. Effect of cutting head speed and clearance on the percentage of rice straw cutting lengths.

Speed, rpm (m s^{-1})	Clearance, mm	Cutting length, %		
		<20 mm	20 to 80 mm	> 80 mm
1450 (22.8)	1	0	50	50
1550 (24.3)	1	2	63	35
1650 (25.9)	1	4	81	15
1450 (22.8)	2	0	40	60
1550 (24.3)	2	1	54	45
1650 (25.9)	2	2	73	25
1450 (22.8)	3	0	25	75
1550 (24.3)	3	0	35	65
1650 (25.9)	3	0	50	50

At clearance 1 mm, the percentage of rice straw cutting length <20 mm was zero % at cutting head speed 1450 rpm (22.8 m s⁻¹) but it was increased to 2% and 4% when the cutting head speed increased to 1550 rpm (24.3 m s⁻¹) and 1650 rpm (25.9 m s⁻¹). The percentage of favorite cutting length (20 to 80 mm) increased from 50% to 63 and 81% when the cutting head speed increased from 1450 rpm (22.8 m s⁻¹) to 1550 (24.3 m s⁻¹) and 1650 rpm (25.9 m s⁻¹) respectively. Also, the percentage of cutting length of > 80 mm was decreased from 50% to 35 and 15% when the speed increased from 1450 rpm (22.8 m s⁻¹) to 1550 rpm (24.3 m s⁻¹) and 1650 rpm (25.9 m s⁻¹) respectively. The same trend was found at clearances 2 and 3 mm.

The highest percentage of favorite length of the cut rice straw from 20 to 80 mm was achieved with cutting head speed of 1650 rpm (25.9 m s⁻¹) and 1 mm clearance. For these conditions, favorite length of the cut rice straw percentage was 81%. [Abo-Habaga *et al.* \(2019\)](#) reported an average cutting length of 91.2 mm at a cutting speed of 1450 rpm and they said that the average decreased to 33.1 mm when the rotational speed was increased to 2350 rpm. They reported that although the increase in the speed of the chopping drum reduced the average cutting length and increased the productivity it also raised the power requirement from 3.51 kW at 1450 rpm to 8.24 kW at 2350 rpm.

Evaluation of the mixing unit

The mixing unit was evaluated by determining the urea percentage in the dissolved additives mixture. Any increase in this ratio may be harmful to the health of the animals.

The average values of urea percentage at mixing shaft rotating speeds (100, 200 and 300 rpm) and dissolve time (5, 10 & 15 min) are shown in Figure (9). It is clear that the urea percentage has increased at the bottom of tank more than the top and middle. Also, the urea percentage was increased by increasing both of the dissolving time and mixing shaft rotating speed. At 5 min dissolve time, the urea percentage increased by increasing of mixing shaft rotating speed.

At the bottom of tank, the urea percentage increased by 0.9 and 1.4% by increasing the mixing shaft rotating speed from 100 to 200 and 300 rpm respectively. At the middle of tank, the percentage of urea increased by 1.0% and 1.5% while the mixing shaft rotating speed increased from 100 rpm to 200 and 300 rpm respectively. At the top of tank, the urea percentage increased by 0.9 and 1.6% by increasing the mixing shaft rotating speed from 100 rpm to 200 and 300 rpm respectively. The same trend was found at dissolve times 10 and 15 min.

At mixing shaft speed 100 rpm, the urea percentage at the bottom of tank was increased from 2.9% to 3.4 and 4.0% by increasing the dissolving time from 5 min. to 10 and 15 min. respectively. The urea at the middle of tank was increased from 2.5% to 3.2 and 3.8% by increasing the dissolving time from 5 min. to 10 and 15 min respectively. In addition, the ratio of urea at the top of tank was increased from 2.2% to 2.6 and 3.5% by increasing the dissolving time from 5 min. to 10 and 15 min. respectively. The highest value of urea percentage, 4.8%, was found at mixing shaft rotating speed 300 rpm and 15min. dissolving time at the bottom of tank.

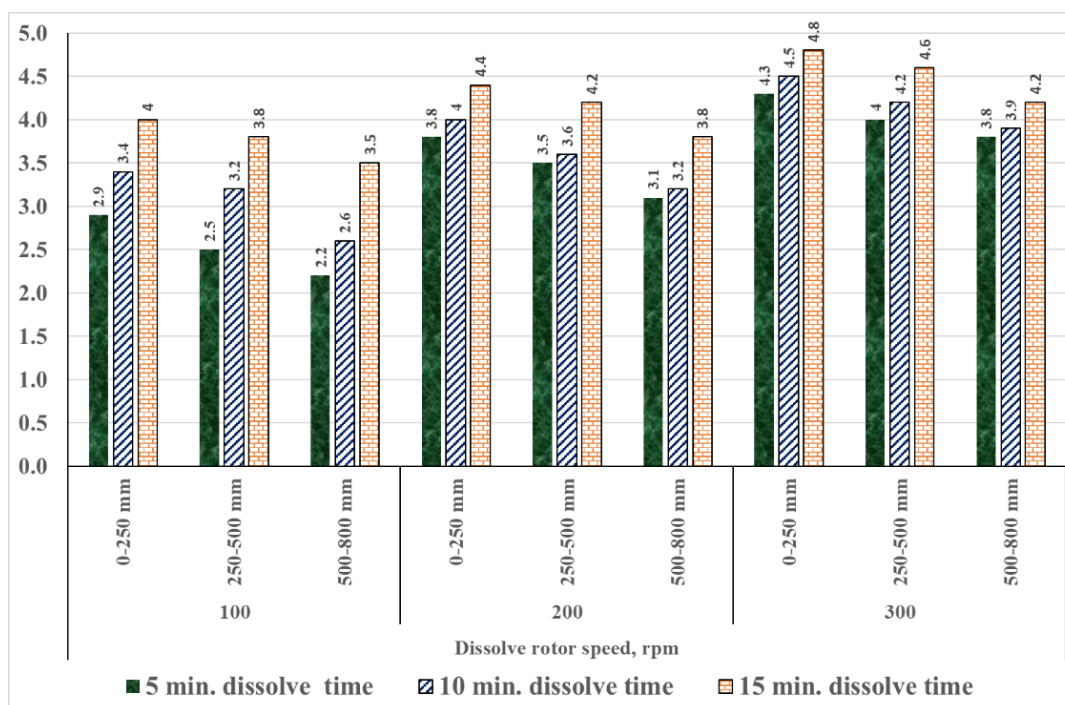


Figure 9. Effect of mixing shaft rotating speed on urea percentage at different dissolved times

The uniformity of the additives distribution on cut rice straw

The mechanical system included chopping unit, mixing unit and pumping and distribution unit was operated at the cutting head rotating speed of 1650 rpm, one mm clearance, 300 rpm mixing shaft rotating speed and 15 min. dissolving time. The uniformity of the additives distribution on cut rice straw was measured by the determination of the crude protein percentage (*CP*) in the final product. Five samples S_1 , S_2 , S_3 , S_4 and S_5 were taken from the final product to determine the crude protein percentage. The results of crude protein percentage at three levels of urea percentage 1, 3 and 5% are shown in Table (3). The average values of crude protein were 3.6, 4.9 and 6.2% at urea percentage 1, 3 and 5 respectively. The coefficient of variations (*CV*) of urea percentage for samples at 1, 3 and 5 were 4.22, 4.99 and 5.46% respectively for S_1 , S_2 , S_3 , S_4 and S_5 . These values indicate that there are no differences in the uniformity of the additives distribution on cut rice straw at different levels of urea percentage. The maximum value of crude protein of 6.2% was found at 5% urea.

Table 3. The effect of urea percentage on the crude protein percentage.

Sample	Urea concentration, %		
	1	3	5
S_1	3.55	4.60	5.80
S_2	3.58	5.10	6.40
S_3	3.70	4.80	6.60
S_4	3.40	5.20	5.90
S_5	3.80	4.80	6.30
Ave.	3.60	4.90	6.20
STDEV	0.15	0.24	0.33
CV	4.2	5.0	5.5

Economic viability

The total fabrication cost of the developed system including workshop cost was 83,478 LE at 2020 prices. The developed system achieved an internal rate of return (*IRR*) of 19%. The developed system *IRR* shows that the investment is worthy. The developed mechanical system indicated the pay back period (*PBP*) was about two years.

One way to benefit from the rice straw is to use it in manufacturing unconventional animal feed after cutting it and treating it with urea, molasses, and mineral salts to try to bridge the gap in animal feed. This treatment leads to an increase in the percentage of protein and a decrease in the percentage of fiber, transforming the straw from just a filling feed into a fodder with a higher nutritional value, in addition to protecting the environment from serious damage ([Abreu *et al.*, 2022](#)). In this research, an automated system was developed for cutting rice straw, mixing nutritional additives (urea, molasses, mineral salts), and distributing the mixture to the straw during the cutting process. The mechanical system included three units: cutting unit, mixing unit, and the unit for distributing the mixture to the straw during the cutting process. The results indicated that the favorite cutting length of 20 to 80 mm was 81% at a cutting head speed 1650 rpm (25.9 m s^{-1}) and one mm knife clearance. These results are similar to those found by ([Younis *et al.*, 2002](#); [El Shal and El Didamony, 2018](#); [Singh *et al.*, 2020](#); [Jiang *et al.*, 2021](#)). [El Shal and El Didamony \(2018\)](#) reported that the optimum knife speed of 2150 rpm (61.92 m s^{-1}), the chopping length of 15 mm, and chopping efficiency was 79.37%. The results also showed that the CP in rice straw after mixing the additive increased from 3.3 to 6.2%. Increasing the percentage of crude protein in the supplemented diet which may leads to improving the animal's rumination, and feed efficiency of dry matter ([Mendes *et al.*, 2015](#)). [Abreu *et al.* \(2022\)](#) mentioned that the feed supplementation is a powerful tool to adjust nitrogen (N) levels in the diet of ruminants during critical periods. Urea is commonly used as a source of non-protein nitrogen in molasses supplements. This dietary protein provides amino acids as well as nitrogen for microbial protein synthesis. Moreover, molasses has organoleptic characteristics, such as palatability, increasing dry matter intake, through microbial growth, especially for fiber-digesting bacteria.

CONCLUSION

A mechanical system for producing animal feed (cutting rice straw mixed with the additives of urea, minerals and molasses) was developed. This system consists of a chopping unit, mixing unit, and pumping & distribution unit. Cutting head speed of 1650 rpm and 1 mm clearance between fixed and the movable knives gave the highest chopping unit productivity of 600 kg h^{-1} , 81% favorite cutting length of 2 to 8 cm. The optimum content of crude protein of 6.2% was found at urea content of 5% and was obtained at mixing shaft rotating speed 300 rpm and 15 min dissolving time at the bottom of tank. The developed system achieved a rate of return of 19% and a pay back period of about two years.

DECLARATION OF COMPETING INTEREST

The author(s) must declare that they have no conflict of interest

CREDIT AUTHORSHIP CONTRIBUTION STATEMENT

This research work was carried out in collaboration with the authors (Ghonimy, Suliman, Morsy, Abdeel-Atty and Alzoheiry).

Mohamed Ghonimy contributed equally in various roles including setting research goals, development of methodology, performing the experiments, analyzing data, and writing the artical and also coordinated the activities with the co-author.

Ahmed Suliman contributed equally in various roles including setting research goals, development of methodology, performing the experiments, analyzing data, and writing the artical.

Mohamed Morsy contributed equally in various roles including setting research goals, development of methodology, performing the experiments, analyzing data, and writing the article.

Ahmed AbdeEl-Atty contributed equally in various roles including setting research goals, development of methodology, performing the experiments, analyzing data, and writing the article.

Ahmed Alzoheiry contributed equally in various roles including setting research goals, development of methodology, performing the experiments, analyzing data, and writing the article.

ETHICS COMMITTEE DECISION

This article does not require any ethical committee decision.

REFERENCES

- Abo-Habaga MM, Yehia I and Abo-Elasaad GA (2019). Study some factors affecting the design of rice straw bales chopper. *Journal of Soil Sciences and Agricultural Engineering*, 10(8): 471-475.
- Abreu D, Dubeux JJC, Queiroz LD, Jaramillo D, Da Silva Santos ER, van Cleef F, Vela-Garcia D, Dilorenzo N and Ruiz-Moreno M (2022). Supplementation of molasses-based liquid feed for cattle fed on limpgrass hay. *Animals*, 12(17): 1-19. <https://doi.org/10.3390/ani12172227>
- Arif AM and Elaiwa AA (2009). Rice straw chopping for animal feed. *Egyptian Journal of Agricultural Research*, 87(4): 1109-1118.
- CMAE (Central Management of the Agricultural Economy) (2020). Estimations of the agricultural crops residues. Ministry of Agriculture and Land Reclamation, Egypt. <https://moa.gov.eg/en/>
- El Shal A and El Didamony M (2018). Performance of a maize chopping machine with an attached sharpener unit. *Journal of Soil Sciences and Agricultural Engineering*, 9(12): 793-798. <https://doi.org/10.21608/JSSAE.2018.36533>
- Hashem FR, Ibrahim MM and Nasr GM (2022). Modification of a machine for chopping rice straw using circular saw. *Agricultural Engineering International: CIGR Journal*, 24(4): 230-243.
- Hashish AE, Hassan MA and Abd El-Mottaleb AF (1994). Some factors affecting on performance of chopping and grinding equipment for field raw materials. *Misr Journal of Agricultural Engineering*, 11(3): 669-682.
- Jiang W, Xiaoyan W, Hongwen L, Jin H, Caiyun L and Di L (2021). Design and experiment of rice straw chopping device for agitation sliding cutting and tearing. *Nongye Jixie Xuebao/Transactions of the Chinese Society of Agricultural Machinery*, 52(10): 41-50.

- Mendes FBL, Silva RR, de Carvalho GGP, da Silva FF, Lins TOJD, da Silva ALN, Macedo M, Filho GA, de Souza SO and Guimarães JO (2015). Ingestive behavior of grazing steers fed increasing levels of concentrate supplementation with different crude protein contents. *Tropical Animal Health and Production*, 47: 423-428. <https://doi.org/10.57447/ca.2019.v15.n5.a328>
- Mohamed TH, Younis SM, Ghonimy MI and Baiomy MA (2001). *Development of rice straw chopper*. In Proceedings of the 9th Conference of Misr Society of Agricultural Engineering (pp. 9-11).
- Mohammed Aliyi K (2021). *Effects of Feeding Urea-Molasses, Urea-Lime and Effective Micro-organism Treated Wheat Straw Basal Diets on Feed Intake and Growth Performance of Weaned Friesian-Borana Female Calves at Holetta Research Center, Ethiopia* (Doctoral dissertation, Addis Ababa University).
- Mu L, Wang Q, Cao X and Zhang Z (2022). Effects of fatty acid salts on fermentation characteristics, bacterial diversity and aerobic stability of mixed silage prepared with alfalfa, rice straw and wheat bran. *Journal of the Science of Food and Agriculture*, 102(4): 1475-1487. <https://doi.org/10.1002/jsfa.11482>
- Oida A (1997). Using personal computer for Agricultural machinery management. Kyoto University. Japan. *Jica Publ.*
- Patel A, Singh KP and Roul AK (2023). Laboratory investigation on rotary impact cutter blade parameters for multistep cutting of paddy straw. *Indian Journal of Ecology*, 50(2): 519-525. <https://doi.org/10.55362/IJE/2023/3929>
- Promma S, Tasaki I, Cheva IB and Indratula T (1994). Stabilization with sulfuric acid of the crude protein in urea-treated rice straw. *Asian-Australasian Journal of Animal Science*, 7(4): 481-486. <https://doi.org/10.5713/ajas.1994.481>
- Radwan HA (2000). Development of small self-driven untraditional feed-mill. Ph.D. Thesis, Fac. of Agric., Moushtohor, Zagazig Univ.
- Singh M, Goyal R, Verma A, Singh R and Singh M (2020). Comparative performance of different types of choppers for managing rice straw. *Agricultural Research Journal*, 57(4): 598-604. <https://doi.org/10.5958/2395-146X.2020.00086.1>
- Tinder R (2022). *Asynchronous Sequential Machine design and analysis: A comprehensive development of the design and analysis of Clock-Independent State Machines and Systems*. Springer Nature.
- Wang W, Tan X, Imtiaz M, Wang Q, Miao C, Yuan Z, and Zhuang X (2021). Rice straw pretreatment with KOH/urea for enhancing sugar yield and ethanol production at low temperature. *Industrial Crops and Products*, 170: 113776. <https://doi.org/10.1016/j.indcrop.2021.113776>
- Younis SM, Ghonimy MI, Baiomy MA and Mohamed TH (2002). Techno-economic evaluation of a developed field crop residues chopper. *Misr Journal of Agricultural Engineering*, 9(4): 63-80.



Turkish Journal of
Agricultural
Engineering Research
(Turk J Agr Eng Res)
e-ISSN: 2717-8420



Performance Evaluation of Diesel Engine Operated Cassava Grating Machine

Amanuel Erchafo ERTEBO* 

*Department of Mechanical Engineering, School of Mechanical, Chemical and Materials Engineering, Adama Science and Technology University, Adama, ETHIOPIA

ARTICLE INFO: Research Article

Corresponding Author: Amanuel Erchafo ERTEBO, E-mail: amanbaaman40@gmail.com

Received: 16 January 2024 / Accepted: 22 April 2024 / Published: 30 June 2024

Cite this article: Ertebo AE (2024). Performance Evaluation of Diesel Engine Operated Cassava Grating Machine. *Turkish Journal of Agricultural Engineering Research*, 5(1): 49-65.
<https://doi.org/10.46592/turkager.1420986>

ABSTRACT

This research work was carried out to assess the performance of a diesel engine-operated cassava grating machine. The factorial design was used to conduct the experiment and the collected data were analysed using Statistix 8 software. The results of the analysis of variance revealed that the speed, feeding rate, as well as their interaction effect, were significant at the 5% level. The highest throughput capacity of 471.4 kg h⁻¹ was observed at a speed of 1400 r min⁻¹, at a feeding rate of 5 kg min⁻¹, while the lowest throughput capacity was 272.5 kg h⁻¹ observed at a speed of 1100 r min⁻¹, at a feeding rate of 5 kg min⁻¹. The highest grating efficiency of 97.3% was observed at a speed of 1400 r min⁻¹, at a feeding rate of 15 kg min⁻¹, while the lowest grating efficiency was 81.6% observed at a speed of 1100 r min⁻¹, at a feeding rate of 5 kg min⁻¹. The lowest percentage of mechanical loss of 2.45% was observed at a speed of 1400 r min⁻¹, at a feeding rate of 15 kg min⁻¹, while the highest percentage of mechanical loss was 18.4% observed at a speed of 1100 r min⁻¹, at a feeding rate of 5 kg min⁻¹. The fuel consumption of the machine was measured as 1.82 L h⁻¹. Finally, the regression analysis results for throughput capacity showed that 95% of throughput capacity was recorded with both independent variables together, $F(2, 33) = 311.17$, $R = 0.974$, $p = 0.000$. This machine was recommended for cassava grating at an operating drum speed of 1400 r min⁻¹.

Keywords: Throughput capacity, Efficiency, Percentage of loss, Grating time, Physical properties

INTRODUCTION

Cassava (*Manihot esculenta* Crantz) is a year-round plant with a delicious root, that is produced globally in different climatic regions. Cassava is one of the most popular foods in Africa and served as the foundation of food sources for Africans due to its significance and adaptability. Approximately one billion people worldwide consume cassava ([Musa et al., 2022](#)). The majority of the cassava farmed in Africa is utilized



for food consumption, with 50% being processed and 38% being used fresh or boiled; the remaining 12% being used as animal feed ([Amelework et al., 2021](#)). Cassava is the biggest supplier of carbohydrates as food in the world, with Africa being its primary production region ([Musa et al., 2022](#)).

Cassava has a significant role in feeding a sizeable section of the Ethiopians in day-to-day life. It is also an important staple food well known in the south and southwest regions ([Sarka et al., 2017](#)). In the southern area of Ethiopia, cassava was grown on 195,055 ha, a production of 501,278.5 tons annually in total in 2013 ([Feyisa, 2021](#)). Cassavas makes major contributions to assuring year-round access to sustainable food, revenue generation, resource conservation, and food security.

The critical drawback of cassava tuber is fast physiological degradation. The crop should need processing quickly because of its extreme perishability. Degradation usually begins from forty-eight to seventy-two hours when it is removed from the field ([Musa et al., 2022](#)). Cassava has historically been the most perishable of all root tubers when the tubers are cut off from the main plant, they become unpleasant two to three days after harvest, resulting in post-harvest physiological decline ([Okoli and Okonkwo, 2019](#)). The cyanide (cyanogenic glucosides) that the cassava plant generates is dangerous and when taken can cause nausea, vomiting, headaches, dizziness, and exhaustion hence, it is critical that the tubers are processed as initially as possible ([Fadeyibi and Ajao, 2020](#)). The presence of hydrogen cyanide in cassava is the primary worry of the consumer during use therefore unit operation of the cassava tuber reduces hydrogen cyanide concentration it is toxic ([Doydora et al., 2017](#)). Also, upon harvest, cassava is massive and holds a high amount of moisture, estimated as 70%, and both the roots and leaves contain changeable amounts of cyanide, which is toxic to human health ([Nyamekye, 2021](#)).

Grating cassava with manual method results in time-consuming, less effective, low quality and quantity of product, and exposes mold development on the skins ([Krishnakumar et al., 2022](#)). To hand grate, one tonne of freshly peeled cassava roots generally requires 10 to 15 man days of effort ([Moreno et al., 2021](#)). However, a mechanical grater of cassava can grate the cassava on a large scale; improve the speed of cassava processing, save labor input, avoid direct contact, and save time. Mechanized grating of fresh cassava into mash contributes to reducing postharvest losses of cassava, increasing its shelf life, and improving food security. The main benefit of an engine-operated cassava grater was reducing human power requirements and easy grating operation.

Currently, the use of advanced technology in agriculture is crucial since the demand for agricultural products increased globally. Therefore, this study aimed to evaluate engine-operated cassava grater in terms of performance indicators, fill the technology gap in cassava processing in cassava growing areas of Ethiopia, avail the technology for future intervention, and generate information about machine performance for end users. The other purpose of this work was to reduce women's drudgery and grating the tuber in high quality and quantity in a short time by replacing manual grating with the machine.

MATERIALS and METHODS

Study area

The investigation for performance evaluation of the cassava grating machine was conducted in southern areas, it is situated 341 km from Addis Ababa, the capital city of Ethiopia. This region is located between 4°27' and 8°31' north latitude and 34°11' east longitude, altitude of the region varies from 376 to 4207 m above sea level.

Materials

Experimental materials

A sample of cassava (Figure 1) was obtained from southern areas, farmer's fields of the Wolayta, offa, and Sodo districts to calculate the physical characteristics and to conduct initial and detailed tests on cassava grater.



Figure 1. Cassava tuber samples.

Measurement device and tools

Various devices and techniques were utilized to perform various measurements on the cassava. The length of the cassava tuber was measured using a tape meter this measuring tape can measure a minimum length up to 0.5 cm, therefore, its sensitivity is 0.5 cm. The tuber diameters were measured with a Vernier caliper with its 0.01 mm accuracy; the sensitivity of the Vernier Caliper is 0.02 mm which means that the smallest measurement that can be read using this instrument is 0.02 mm. The weighing balance could be used to take the mass of the root both earlier and subsequently when it was grated. The sensitivity of a digital weighing balance is 1 mg; this means that a weight of at least 1.0 mg is needed to move the pointer over one scale and the smallest weight that the scale can measure. A smartphone stopwatch app was used to take time during the evaluation of the grater. The machine's drum speed was measured using a non-contact type of tachometer. The sensitivity of the tachometer is 0.043 v rad⁻¹ sec this means that the minimum

measurement that can be read using this tachometer is $0.043 \text{ v rad}^{-1} \text{ sec}$, a measuring distance of 50 mm to 500 mm and a measuring range of 2 r min^{-1} to $99,999 \text{ r min}^{-1}$. Additionally, a knife was used by hand to partially reduce the size of the cassava tuber. Therefore, a stopwatch, digital weighing balance, digital Vernier caliper, knife, tachometer, and pocket meter were used in the experiment.

Methods

Determination of physical characteristics

The first producer in automated cassava processing, [Adetan et al. \(2005\)](#) state that a thorough understanding of its physical characteristics is essential. A thorough understanding of the physical characteristics of agricultural products is important for operating post-harvest machinery. For the determination of each physical property such as geometric mean diameter, length, sphericity, bulk density, moisture content, and angle of repose, an experimental sample was randomly selected as 32, 26, 32, 28, 22, and 24 respectively. Therefore, the following physical properties have been studied:

Geometric mean diameter

A digital Vernier caliper with a 0.01 mm precision and a 0.00 to 150.00 mm measurement range was used to measure the diameters of cassava tubers. Based on the shape of cassava tubers, this was done at the major diameter (head), where "a" was taken, the intermediate diameter (middle), "b," and the minor diameter (tail), "c." An average amount for the geometric mean diameter of cassava root can be determined using Equation 1 ([Joshua and Simonyan, 2015](#)).

$$GMD = \sqrt[3]{a \times b \times c} \quad (1)$$

Where GMD is geometric mean diameter (mm), a is major diameter (mm), b is intermediate diameter (mm), and c is minor diameter (mm).

Sphericity

The sphericity of cassava tuber samples was determined using the formula by ([Edeh et al., 2022](#)) given in Equation 2.

$$\text{Sphericity} = \frac{GMD}{a} \quad (2)$$

Where GMD is the geometric mean diameter (mm) and a is the major diameter (mm).

Bulk density

The bulk density of tubers was determined by weighing the cassava tubers packed in a container of known weight and volume. The container having a volume in liters and a mass in kilo gram was filled with cassava tuber in a way that it might be at the top level of the containers. Then the container together with samples of cassava tuber to be weighted by a weighting balance of accuracy of 0.1 g and a capacity of 15 kg ([Joshua and Simonyan, 2015](#))

Moisture content for cassava tuber

According to an oven drying procedure approved by the AOAC (Memmert Ule500, Germany), the samples were dried for 24 hours at 105°C to measure the moisture content (AOAC, 2005). For the determination of the moisture content of cassava tuber, the following method was used as given in Equation 3 (Ndirika and Oyeleke, 2006).

$$M_c (wb) \% = \frac{W_w - W_d}{W_w} \times 100 \quad (3)$$

Where W_w is weight for wet tuber in gram, W_d is weight for dried tuber in gram and M_c is moisture content of tuber.

Angle of repose

The cassava tuber was set on the angle of repose device and gradually raised until the force of gravity overcame the frictional force between the tuber and the test surface, which was made of sheet metal, glass, and wood, allowing the tuber to start to down the slope. A graduated protractor attached to the apparatus measured the angle at which the cassava roots begin to slip or the angle at which the cassava roots start to slide, was read from a graduated protractor attached to the device which was the angle of repose of the cassava tuber.

Experimental procedure

The initial test of the grater can be carried out at four different speeds as well as three different feeding rates based on drum speeds of 1100 r min⁻¹ (46.08 m s⁻¹), 1200 r min⁻¹ (50.3 m s⁻¹), 1300 r min⁻¹ (54.5 m s⁻¹), and 1400 r min⁻¹ (58.6 m s⁻¹) corresponding to feed rates 5 kg min⁻¹, 10 kg min⁻¹, and 15 kg min⁻¹ before conducting the detailed test of the cassava grater. The drum speeds were selected for evaluating the grater performance on cassava tuber according to studies by Esteves *et al.* (2019). For performance evaluation of the grater, three hundred sixty kilograms (360 kg) of freshly harvested cassava root Hawassa variety without any degradation could be utilized for experimenting. The machine was started, and the speed was adjusted to 1100 r min⁻¹ (46.08 m s⁻¹), 1200 r min⁻¹ (50.3 m s⁻¹), 1300 r min⁻¹ (54.5 m s⁻¹), and 1400 r min⁻¹ (58.6 m s⁻¹) by using a tachometer. A weighing scale was used to measure the freshly harvested cassava tuber in batches of 5 kg, 10 kg, and 15 kg for each drum speed after the tuber was manually peeled with knives and cleaned with water for hygienic purposes.

Evaluation of the grating machine

Evaluation of the grater (Figure 2) was carried out considering the grating capacity, efficiency, percentage of mechanical loss, grating time, and quality of mash. The following formulas were used to evaluate engine-operated cassava grater using the Philippines Agricultural Engineering Standardization (PAES) (2004) techniques of testing for related machineries.

$$\text{Throughput capacity (kg h}^{-1}\text{)} = \frac{W_f}{T} \quad (4)$$

$$\text{Grating efficiency (\%)} = \frac{W_f}{W_i} \times 100 \quad (5)$$

$$\text{Percentage of loss} = \frac{W_i - W_f}{W_i} \times 100 \quad (6)$$

$$\text{Quality performance efficiency} = \frac{G}{G+B} \times 100 \quad (7)$$

Where W_f is final weight collected in kilogram, W_i is initial weight in kilogram, T is time duration required grating root in hour, G is good quality or fine grated mash (kg), and B is bad quality or coarse grated mash (kg).
is bad quality or coarse grated mash (kg).



Figure 2. Machine during operation.

Economic analysis

The analysis of fixed and running costs for the cassava grating machine was done by the selling price of the machine, interest, depreciation, labor, and fuel costs. While running cost for the working model of cassava grater were calculated in Ethiopia Birr using the standard procedure, the calculations were based on the [Philippines Agricultural Engineering Standards \(PAES\) \(2004\)](#).

$$Dp = \frac{SP - SV}{EL} \quad (8)$$

$$IC = \frac{SP + SV}{2U} \times I\% \quad (9)$$

$$LW = \frac{DLW}{DWH} \quad (10)$$

Where Dp is depreciation (EB h^{-1}), SP is selling price of grater, SV is salvage values, EL is economic life, IC is interest on capital (EB h^{-1}), U is annual use, I is interest, LW is labor wages (EB h^{-1}), DLW is daily labor wage, and DWH is daily working hours.

Statistical analysis

The experimentation was conducted using factorial design while the machine speeds were considered as the blocking variable as well as the four levels of speeds with three levels of feeding rate taken as treatment combination or treatment ($4 \times 3 = 12$). Each experiment to be replicated thrice there were 36 experimentation units ($4 \times 3 \times 3 = 36$). The collected data were analyzed using Statistix 8 software. The confidence intervals of 95% were utilized to indicate a significant effect of an independent variable on the dependent variable. A two-way analysis of variance was implemented on the data by following an appropriate procedure for the design of the experiment (Gomez & Gomez, 1984).

RESULTS AND DISCUSSION

Physical properties for cassava tuber

Table 1 shows that the mean physical characteristics of the cassava tuber samples for the Hawassa variety were calculated. So, results indicated that the mean value for geometric mean diameter was 14.05 mm while the highest as well as lowest amounts were 15.5 and 13.19 mm, respectively. The minimum value for the bulk density was 2.08 g cm^{-3} while the maximum value was 2.25 g cm^{-3} with a mean of 2.18 g cm^{-3} based on a result obtained for cassava tuber. According to the findings, the mean moisture content of 52.9% in a wet basis for the fresh sample was determined and the maximum value was 53.8% and the minimum value was 52%. The maximum angle of repose of 30° was obtained whereas the minimum angle of repose of 28.7° was obtained with its mean of 29.4° .

Table 1. Physical characteristics for cassava tuber.

Properties	Mean	SD	Mean \pm SD	Max	Min	CV
Length (mm)	316.7	135.0	316.7 \pm 135.0	450.0	180.0	42.6
Geometric mean diameter (mm)	14.05	1.279	14.05 \pm 1.27	15.5	13.19	9.1
Sphericity	0.89	0.024	0.89 \pm 0.024	0.91	0.87	2.6
Bulk density (g cm^{-3})	2.18	0.090	2.18 \pm 0.090	2.25	2.08	4.2
Moisture content (%)	52.9	0.9	52.9 \pm 0.9	53.8	52	1.7
Angle of repose ($^\circ$)	29.4	0.665	29.4 \pm 0.665	30.0	28.7	2.3

CV = Coefficient of variation, SD = Standard deviation

The test result showed that grating worked better when the tuber's moisture content was higher. It was also found that the higher moisture level of the root increased the grating quality of the grater. The grated mash was found to be cohesive during the test; at increasing moisture content, it spreads flatter. This indicated that to move the mash granules inside the machine, the mash needed more inclination. The findings showed that a cohesive mash was indicated by a higher angle of repose, whereas a lower angle indicated a free-flowing mash.

The performance of the grater was evaluated at four levels of drum speeds and three levels of feed rates with respect to throughput capacity, efficiency, mechanical loss, grating time, as well as quality performance efficiency. Once the machine had finished grating, measurements were taken of the final output mash, grating time, good quality, and bad quality mash were measured. Based on the test results, it was found that every batch of cassava root that was put into the machine was grated. During performance evaluation, the specific energy consumption of the machine was calculated as 0.004 L kg^{-1} .

Throughput capacity

Table 2 shows an analysis of variance (ANOVA) for effect of speed, feeding rate, as well as interaction effect on the capacity of the grating machine. Therefore, analysis of variance revealed that effect of speed, feeding rate, as well as interaction effect was significant at a 5% level based on a result obtained (Table 2) because the p values were lower than 0.05 ($P < 0.05$). The findings implied that the throughput capacity of a machine was affected by operating drum speed, feed rate, and interaction effect.

Table 2. Analysis of variance for throughput capacity of the grating machine.

Source	DF	Sum of squares	Mean squares	F-value	P-value	Remark
Block	2	18	9.1			
Drum speed	3	129708	43235.9	589.27	0.0000	Significant
Feed rate	2	3519	1759.4	23.98	0.0000	Significant
Speed×Feed	6	3267	544.4	7.42	0.0002	Significant
Error	22	1614	73.4			
Total	35	138125				

CV = 2.39, grand mean = 358.55, $P < 0.05$, significant at 5 % level, DF = degrees of freedom.

As shown in Figure 3 the average throughput capacity of the machine ranged from 272.5 kg h^{-1} to 471.4 kg h^{-1} . As the increasing speed from 1100 r min^{-1} to 1400 r min^{-1} , throughput capacity increased from 272.5 to 471.4 kg h^{-1} . When the capacity of the grater tended to increase with the increase in speed but it decreased through a feeding rate (Figure 3). This result means throughput capacity had a direct relationship to the drum speed and was inversely related to material feed rate.

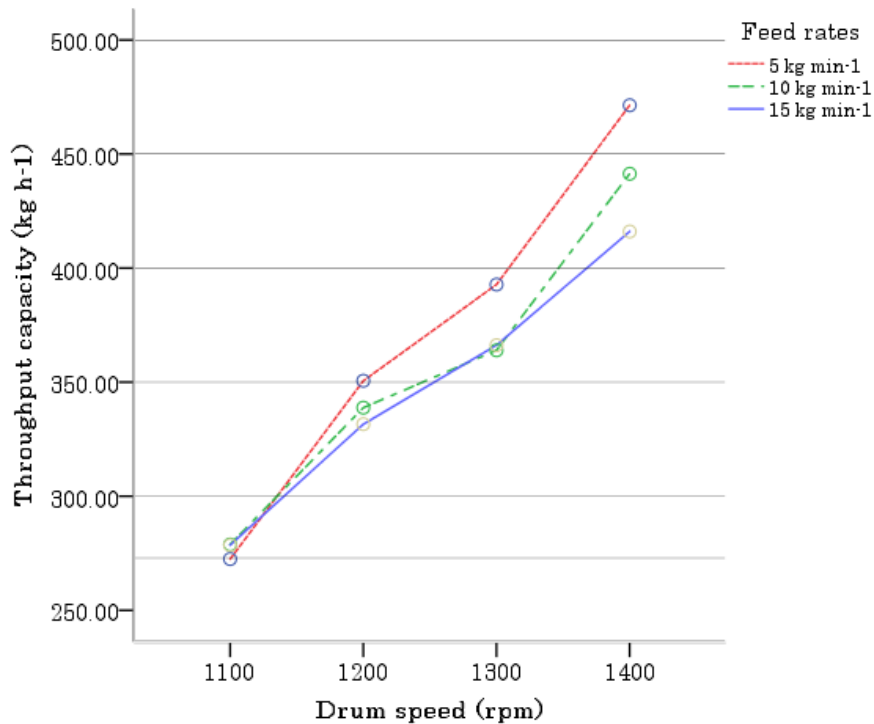


Figure 3. Effect of speed and feed rate on capacity.

The highest throughput capacity of 471.4 kg h⁻¹ was observed at a speed of 1400 r min⁻¹ as well as feeding rate of 5 kg min⁻¹, while the lowest throughput capacity was 272.5 kg h⁻¹ observed at a speed of 1100 r min⁻¹ and feeding rate of 5 kg min⁻¹.

The throughput capacity obtained in this study was higher compared to the value of 114.94 kg h⁻¹ reported by [Temam \(2020\)](#). In comparison, [Esteves et al. \(2019\)](#) reported an average grating capacity of 283.26 kg h⁻¹ at 1424.30 r min⁻¹ when testing the performance of a motor-operated cassava grater. [Ogunjirin et al. \(2020\)](#) stated the grating capacity of 250 kg h⁻¹ at 78.4 r min⁻¹ when grating cassava with a cassava grater. [Malomo et al. \(2014\)](#) reported a machine output of 80 kg h⁻¹ while assessing the performance of an automated grater. [Bello et al. \(2020\)](#) stated an output of 158.9 kg h⁻¹ when testing an electric motor-powered machine.

Grating efficiency

Table 3 shows an analysis of variance for speed, feeding rate, as well as their interaction effect on the efficiency of the machine. While analysis of variance revealed that the main effect of speed, feeding rate, as well as their interaction effect was significant at a 5% level because the p value obtained in (Table 3) was less than 0.05 ($P < 0.05$). Therefore, the results implied that effect of speed, feeding rate, as well as their interaction effect did affect the grating efficiency of a grating machine.

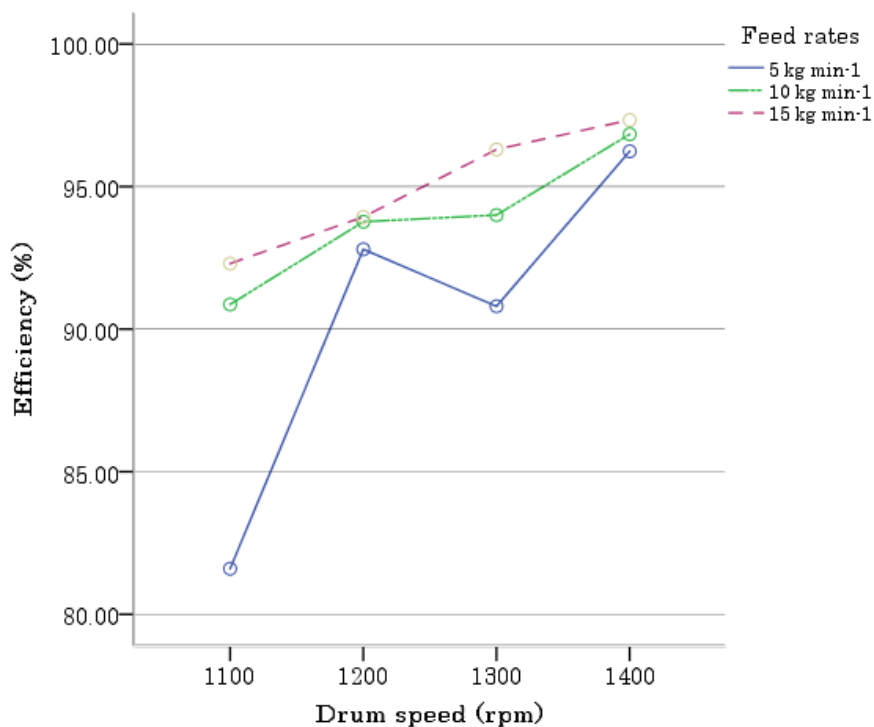
Table 3. Analysis variance for grating efficiency of grating machine.

Source	DF	Sum of squares	Mean squares	F-value	P-value	Remark
Block	2	0.285	0.143			
Drum speed	3	339.010	113.003	137.87	0.0000	Significant
Feed rate	2	138.868	69.434	84.72	0.0000	Significant
Speed×Feed	6	113.186	18.864	23.02	0.0000	Significant
Error	22	18.032	0.820			
Total	35	609.382				

CV = 0.97, grand mean = 93.063, $P < 0.05$, significant at 5 % level, DF = degrees of freedom.

As shown in Figure 4 it was found that an average grating efficiency for grater ranged from 81.6% to 97.3%. With increasing drum speed from 1100 r min⁻¹ to 1400 r min⁻¹, grating efficiency increased from 81.6% to 97.3%. The grating efficiency of the machine tended to increase with an increase in speed as well as feed rate. This means grating efficiency had a direct relationship to the speed as well as feeding rate of cassava tuber.

From the test results, the efficiency of the machine was increased with an increase in drum speed but is sudden drop or decrease of efficiency at drum speed of 1300 r min⁻¹ and at a feed rate of 5 kg min⁻¹ was observed. So, the decrease in efficiency occurred because of the low output recorded during the testing machine at a feeding rate of 5 kg min⁻¹. This low output was obtained when the drum was rotated, it returned the feeds back.

**Figure 4.** Effect of drum speed and feed rate on grating efficiency.

The highest grating efficiency of 97.3% was observed at a speed of 1400 r min⁻¹ as well as feeding rate of 15 kg min⁻¹, while the lowest grating efficiency was 81.6% observed at a speed of 1100 r min⁻¹ as well as feeding rate of 5 kg min⁻¹. The grating efficiency obtained in this study was higher compared to the value of 91.9% reported by [Ndaliman \(2006\)](#). In comparison, [Esteves et al. \(2019\)](#) reported an average grating

efficiency of 91.56% at 1424.30 r min⁻¹ while assessing a motor-operated grater. [Ogunjirin et al. \(2020\)](#) reported a grating efficiency of 84% at 78.4 r min⁻¹ when grating cassava with a cassava grater. [Malomo et al. \(2014\)](#) reported a machine efficiency of 89.7% while assessing cassava grater.

Percentage of mechanical loss

Table 4 shows an analysis of variance for speed, feeding rate, as well as their interaction effect on mechanical loss of the grater. Based on the results shown in (Table 4), an analysis of variance showed that the speed, feeding rate, as well as interaction effect were significant at a 5% level since the p-value was lower than 0.05 (P < 0.05). According to the results, a machine's percentage of mechanical loss was influenced by the feed rate, operational drum speed, and interaction effect.

Table 4. Analysis variance for percentage loss of the grating machine.

Source	DF	Sum of squares	Mean squares	F-value	P-value	Remark
Block	2	0.392	0.196			
Drum speed	3	357.243	119.081	136.81	0.0000	Significant
Feed rate	2	132.011	66.006	75.83	0.0000	Significant
Speed×Feed	6	120.575	20.096	23.09	0.0000	Significant
Error	22	19.150	0.870			
Total	35	629.371				

CV = 13.60, grand mean = 6.86, P < 0.05, significant at 5 % level, DF = degrees of freedom.

As shown in Figure 5 it was observed that the average percentage of mechanical loss of the machine ranged from 2.45% to 18.4%. With increasing drum speed from 1100 r min⁻¹ to 1400 r min⁻¹, the percentage of mechanical loss decreased from 18.4% to 2.45%. The percentage of mechanical loss of the machine tended to decrease with an increase in speed as well as feeding rate. This means the percentage of mechanical loss had an inverse relationship to the speed as well as feed rate of cassava tuber.

The test results showed that as drum speed increased, the machine's percentage loss decreased. However, at 1300 r min⁻¹ and at a feed rate of 5 kg min⁻¹, there was a sudden increase in loss was recorded when evaluating the grater at a feeding rate of 5 kg min⁻¹. A decrease in efficiency or low output was recorded when the drum rotated, returning the feeds back. Due to a decrease in efficiency or low output was obtained, leading to an increase in loss.

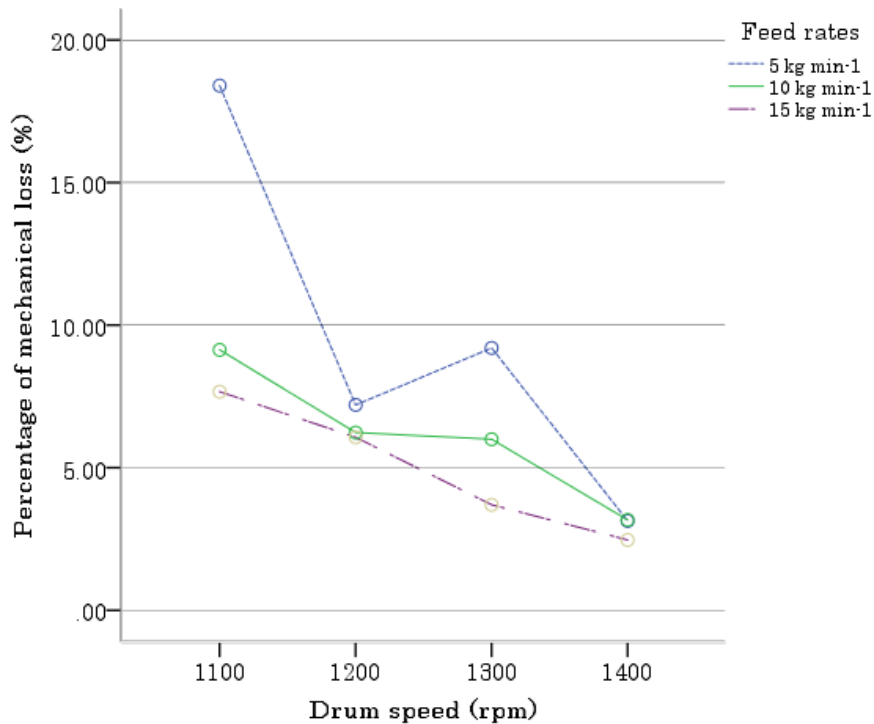


Figure 5. Effect of speed and feed rate on mechanical loss

The lowest percentage of mechanical loss of 2.45% was observed at a speed of 1400 r min⁻¹ as well as feeding rate of 15 kg min⁻¹, while the highest percentage of mechanical loss was 18.4% observed at a speed of 1100 r min⁻¹ as well as feeding rate of 5 kg min⁻¹. Since the drum speed of 1400 r min⁻¹ had the lowest percentage of loss among the other drum speed.

The percentage of mechanical loss recorded in this study was lower compared to the value of 8.45% at 1424.30 r min⁻¹ reported by [Esteves et al. \(2019\)](#). In comparison, [Ogunjirin et al. \(2020\)](#) reported a percentage loss of 10.9% at 78.4 r min⁻¹ when grating cassava with a cassava grater. [Apodi et al. \(2018\)](#) reported percentage loss of 5.5% when testing the performance of grater. [Malomo et al. \(2014\)](#) reported a loss of 10.3% while evaluating a grater.

Grating time

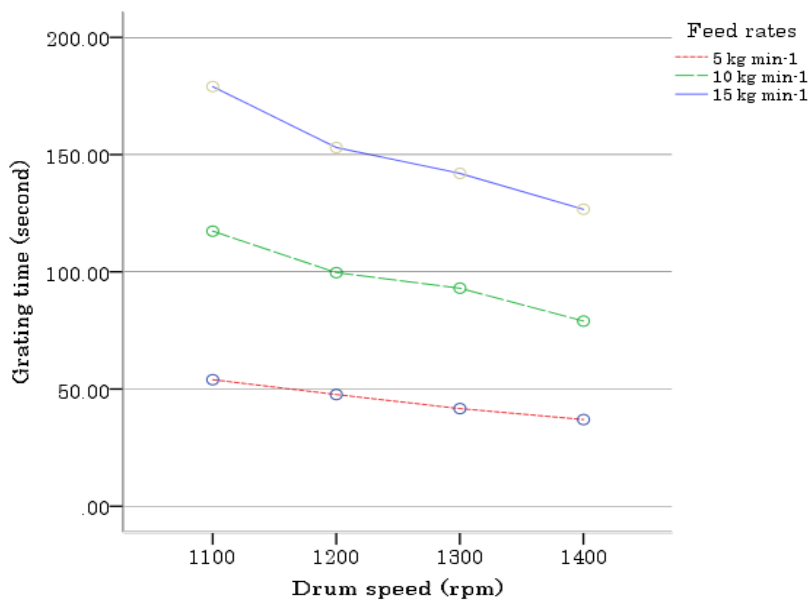
Table 5 shows the results for an analysis of variance for effect of speed, feeding rate, as well as interaction effect on the grating machine's grating time. Since the p value found in (Table 5) was less than 0.05 ($P < 0.05$), an analysis of variance indicated that the speed, feeding rate, as well as interaction effect, were significant at a 5% level. Thus, the results suggested that a grating machine's grating time was influenced by the feed rate, drum speed, and interaction effect.

Table 5. Analysis of variance for grating time of the grating machine.

Source	DF	Sum of squares	Mean squares	F-value	P-value	Remark
Block	2	0.2	0.1			
Drum speed	3	6140.1	2046.7	390.98	0.0000	Significant
Feed rate	2	66256.2	33128.1	6328.37	0.0000	Significant
Speed×Feed	6	1005.4	167.6	32.01	0.0000	Significant
Error	22	115.2	5.2			
Total	35	73517.0				

CV = 2.35, grand mean = 97.50, P < 0.05, significant at 5 % level.

As shown in Figure 6 it was recorded that the average grating time of the machine ranged from 37 sec to 54 sec at a feeding rate of 5 kg min⁻¹ with drum speeds of 1400 r min⁻¹ as well as 1100 r min⁻¹. Generally, the results indicated (Figure 6) that the grating time of the machine tended to decrease with the increase of drum speed at the same feed rate because high drum speed had faster operated than lower drum speed which means grating time had an inverse relationship to the speed but a direct relationship to feed rate.

**Figure 6.** Effect of drum speed and feeding rate on grating time

The lowest grating time of 37 sec was observed at a speed of 1400 r min⁻¹ as well as a feeding rate of 5 kg min⁻¹, while the highest grating time was 54 sec observed at a speed of 1100 r min⁻¹ as well as a feeding rate of 5 kg min⁻¹. At the same feed rate, with increased drum speed from 1100 r min⁻¹ to 1400 r min⁻¹ grating time decreased from 54 sec to 37 sec.

Therefore, the drum speed of 1400 r min⁻¹ was comparatively quick as well as might grate a tuber within a short period, there was also a drum speed that had the lowest grating time among the other drum speeds. A similar trend for cassava grating machines was reported by [Esteves et al. \(2019\)](#).

Quality performance efficiency

Table 6 shows an analysis of variance for speed, feeding rate, as well as interaction effect on the quality performance efficiency of machine. Depend on a result obtained

(Table 6), an analysis of variance revealed that a speed, feeding rate, as well as interaction effect were significant at a 5% level since the p value was lower than 0.05 ($P < 0.05$). The findings suggested that the quality performance efficiency of a grating machine was influenced by the drum speed, feed rate, and interaction effect.

Table 6. Analysis of variance for quality performance efficiency of the grating machine.

Source	DF	Sum of squares	Mean squares	F-value	P-value	Remark
Block	2	1.292	0.6461			
Drum speed	3	85.135	28.3782	60.07	0.0000	Significant
Feed rate	2	162.865	81.4325	172.38	0.0000	Significant
Speed×Feed	6	21.905	3.6508	7.73	0.0001	Significant
Error	22	10.393	0.4724			
Total	35	281.589				

CV = 0.74, grand mean = 92.38, $P < 0.05$, significant at 5 % level.

As shown in Figure 7 it was founded that an average quality performance efficiency for grater ranged from 86.2% to 95.7%. With increased drum speed from 1100 r min⁻¹ to 1400 r min⁻¹, quality performance efficiency increased from 86.2% to 95.7%. The results shown (Figure 7) that the quality performance efficiency of the machine tended to increase with increase of speed as well as feeding rate which implied quality performance efficiency had a direct relationship to the speed as well as feeding rate of cassava tuber.

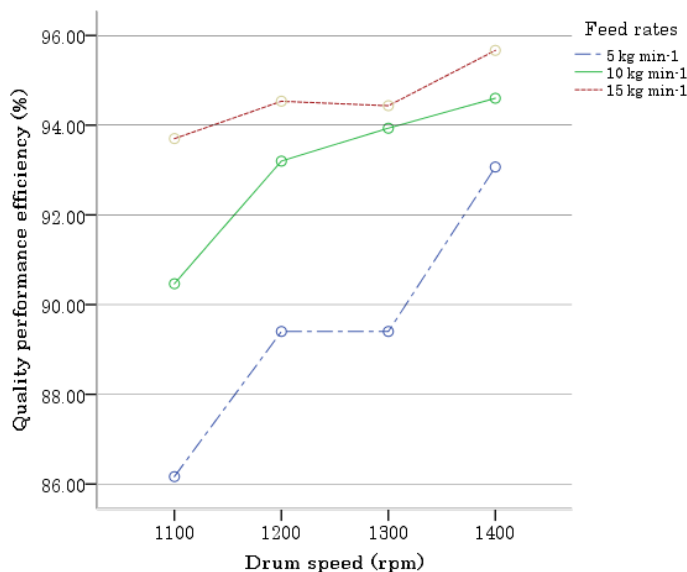


Figure 7. Effect of speed and feeding rate on quality performance efficiency.

The highest quality performance efficiency of 95.7% was obtained at a speed of 1400 r min⁻¹ as well as feeding rate of 15 kg min⁻¹, while the lowest quality performance efficiency was 86.2% obtained at a speed of 1100 r min⁻¹ as well as feeding rate of 5 kg min⁻¹. In comparison, [Ogunjirin et al. \(2020\)](#) reported a quality performance efficiency of 92.23% at 78.4 r min⁻¹ when grating cassava with a cassava grater. [Malomo et al. \(2014\)](#) reported a quality performance efficiency of 92.19% while evaluating a grater however the quality performance efficiency obtained in this study was higher.

Regression analysis

Regression analysis was conducted to predict how much variance was being accounted in the dependent variables by a set of independent variables. The regression analysis result for throughput capacity showed that 95% of throughput capacity was recorded both independent variables together, $F(2, 33) = 311.17$, $R = 0.974$, $p = 0.000$. The predicted throughput capacity was equal to $249.05 + 53.29V - 11.86F$. Also, regression analysis results for grating efficiency indicated that 70.14% of grating efficiency was accounted for by drum speed and feed rate together, $F(2, 33) = 38.77$, $R = 0.84$, $p = 0.000$. The predicted grating efficiency was equal to $82 + 2.58V + 2.30F$. Based on the regression analysis result, the percentage of mechanical loss showed that 70.1% of mechanical loss was contributed by drum speed and feed rate, $F(2, 33) = 38.76$, $R = 0.83$, $p = 0.000$. The estimated mechanical loss was equal to $18.03 - 2.66V - 2.25F$. Multiple linear regression analysis results showed that 82.8% of the quality performance efficiency was accounted for by drum speed and feed rate collectively, $F(2, 33) = 79.55$, $R = 0.91$, $p = 0.000$.

Economic cost analysis

The unit cost of an engine-operated cassava grating machine was determined by calculating the cost of different components and other costs. The costs of depreciation, interest on capital, fuel, and labor were computed as 2.8 EB h⁻¹, 2.5 EB h⁻¹, 20 EB h⁻¹, and 182 EB h⁻¹ using the straight-line method. A payback period for the engine-powered cassava grating machine was calculated as 1.05 years. The benefit cost ratio was computed as 1:2.3 which showed grating cassava using the cassava grater was economical for cassava producers. The estimated cost of the one unit of an engine-operated cassava grating machine was determined as 44,046 EB.

Table 1. Cost summary.

Numbers	Cost parameters	Costs (ETB)
I	Material cost	31,880
II	Material wasted (2.5%)	797
III	Machinery cost	1,170
IV	Wage	870
V	Overhead 5% (III+IV)	102
VI	Profits 10% (I+II+III+IV+V)	3,481.9
VII	Sell taxation 15% (I+II+III+IV+V+VI)	5,745.1
Selling price		44,046

CONCLUSION

The performance of the cassava grating machine was conducted at four levels of speeds and three levels of feed rates at a moisture content of 52.9% for cassava tuber. The machine was operated at optimum conditions of rotational speeds, feeding loads, vibration, temperature, and proper adjustment in order to attain maximum capacity and efficiency. Some physical properties of cassava tuber for Hawassa varieties related to its use of grater were determined. The machine was evaluated in terms of throughput capacity, grating efficiency, mechanical loss, grating time, as well as quality performance efficiency. From test results, it was observed that with increasing drum speed from 1100 r min⁻¹ to 1400 r min⁻¹, throughput capacity

increased from 272.5 kg h⁻¹ to 471.4 kg h⁻¹ while grating efficiency increased from 81.6% to 97.3% and the percentage of mechanical loss decreased from 18.4% to 2.45%. According to an analysis of variance, the speed, feeding rate, also their interaction effects were found to be significant at the 5% level. The grating machine's dependent variables were all influenced by main and interaction effects. Multiple linear regression analysis was carried out to predict how much variance was being accounted for in the dependent variable by a set of drum speed and feed rate.

DECLARATION OF COMPETING INTEREST

The author of this manuscript declares that there is no conflict of interest.

CREDIT AUTHORSHIP CONTRIBUTION STATEMENT

The author would like to declare that he solely developed all the sections.

ETHICS COMMITTEE DECISION

This article does not require any ethical committee decision.

REFERENCES

- Adetan DA, Adekoya LO, Aluko OB and Makanjuola GA (2005). An experimental mechanical cassava tuber peeling machine. *Journal of Agricultural Engineering and Technology (JAET)*, 13(113): 27-34.
- Amelework AB, Bairu MW, Maema O, Venter SL and Laing M (2021). Adoption and promotion of resilient crops for climate risk mitigation and import substitution: A case analysis of cassava for South African agriculture. *Frontiers in Sustainable Food Systems*, 5: 617783. <https://doi.org/10.3389/fsufs.2021.617783>
- AOAC 2005.pdf. (2005). Official Methods of Analysis of AOAC international. In: Horwitz, W., Ed., Association of Official Analytical Chemists, 17th Edition, AOAC International Suite 500, Gaithersburg.
- Apodi J, Akidiweasagadunga P and Kwablaamedorme S (2018). Design and construction of a manually operated cassava grating machine for the post harvest unit of the department of agricultural engineering of bolgatanga polytechnic. *International Journal of Advanced Research in Science, Engineering and Technology*, 5(10): 7091-7098.
- Bello SK, Lamidi SB and Oshinlaja SA (2020). Design and fabrication of cassava grating machine. *International Journal of Advances in Scientific Research and Engineering*, 6(10): 162-167. <https://doi.org/10.31695/IJASRE.2020.33915>
- Doydora KJ, Bodod R, Lira J and Zamoranos M (2017). Design, fabrication, and performance evaluation of electric motor driven cassava (*Manihot esculenta*) grater with juice extractor. *Philippine Journal of Agricultural Economics*, 1(1): 17-28. <https://doi.org/10.7719/pjae.v1i1.484>
- Edeh JC, Onwuka OS, Chukwu J. E and Nwankwojike BN (2022). Modeling and simulation of efficiency of cassava attrition peeling machine. *Agricultural Engineering International: CIGR Journal*, 24(2): 166-183.
- Esteves DU, Pantuhan GP, Serviñas MO and Malasador JS (2019). Design, fabrication and performance evaluation of motor-operated cassava grater. *Mindanao Journal of Science and Technology*, 17: 227-241.
- Fadeyibi A. and Ajao OF (2020). Design and performance evaluation of a multi-tuber peeling machine. *AgriEngineering*, 2(1): 55-71. <https://doi.org/10.3390/agriengineering2010004>
- Feyisa AS (2021). Current status, opportunities, and constraints of cassava production in Ethiopia: A review. *Journal of Agriculture and Food Research*, 11: 51.
- Gomez KA and Gomez AA (1984). Statistical procedures for agricultural research. *John Wiley & Sons*.

- Joshua SK and Simonyan KJ (2015). Some engineering properties of cassava tuber related to its peeling mechanization. *In Umudike Journal of Engineering and Technology (UJET)*, 1(1): 12-24.
- Krishnakumar T, Sajeev MS, Pradeepika C, Namrata AG, Sanket JM, Jeevarathinam G and Muthusamy V (2022). Physical and mechanical properties of cassava (*Manihot esculenta* Crantz) cultivars: Implications for the design of mechanical peeling machines. *Journal of Food Process Engineering*, 45(6): e13923. <https://doi.org/10.1111/jfpe.13923>
- Malomo O, Bello EK, Adekoyeni OO and Jimoh MO (2014). Performance evaluation of an automated combined cassava grater/slicer. *International Invention Journal of Biochemistry and Bioinformatics*, 2(3), 2408-2722.
- Moreno-Cadena P, Hoogenboom G, Cock JH, Ramirez-Villegas J, Pypers P, Kreye C, Tariku M, Ezui KS, Becerra Lopez-Lavalle LA and Asseng S (2021). Modeling growth, development and yield of cassava: A review. *Field Crops Research*, 267(March), 108140. <https://doi.org/10.1016/j.fcr.2021.108140>
- Musa SM, Samuel EB, Sani M and Mari E (2022). Cassava production, processing and utilization in Nigeria: A review. *African Scholar Journal of Biotechnology and Agricultural Research (JBAR-1)*, 6(1): 43-64.
- Ndaliman MB (2006). Development of cassava grating machine: A dual-operational mode. *Leonardo Journal of Sciences*, 9:103-110.
- Ndirika VIO and Oyeleke OO (2006). Determination of selected physical properties and their relationships with moisture content for millet (*Pennisetum glaucum* L.). *Applied Engineering in Agriculture*, 22(2): 291-297. <https://doi.org/10.13031/2013.20275>
- Nyamekye CA (2021). Health issues related to the production and consumption of cassava as a staple food. Norwegian University of Life Sciences, Master Theses.
- Ogunjirin OA, Bello MK, Oladipo NO and Jimoh RO (2020). Modification of ncam motorized cassava grating machine. *World Journal of Engineering Research and Technology*, 6(5): 209-222.
- Okoli IG and Okonkwo UC (2019). Design of an improved double barrel cassava grating machine. *International Journal of Engineering Research & Technology (IJERT)*, 10(2): 112-117.
- Okwuonu IC, Narayanan NN, Egesi CN, and Taylor NJ (2021). Opportunities and challenges for biofortification of cassava to address iron and zinc deficiency in Nigeria. *Global Food Security*, 28 (February 2020). <https://doi.org/10.1016/j.gfs.2020.100478>
- Philippine Agricultural Engineering Standards. (2004). PAES 219 (2nd Ed.) University of the Philippines at Los Baños College, Laguna 4031 Philippines: Agricultural Machinery Testing and Evaluation Center.
- Sarka S, Woldeyohannes D and Woldesilasie A (2017). Value chain analysis of cassava in Wolaita Zone, snnpr, Ethiopia. *Journal of Economics and Sustainable Development*, 8(5): 11-17.
- Temam M (2020). Development and evaluation of power-driven cassava grater and chipper machine. *International Journal of Engineering Research*, 3(11): 133-140. <https://doi.org/10.33329/ijoeer.8.5.1>



Turkish Journal of
Agricultural
Engineering Research
(Turk J Agr Eng Res)
e-ISSN: 2717-8420



Study on Dielectric Properties of Rice Husk Ash Stabilized Soil

Ogaga AKPOMEDAYE^a , Friday Elohor ODOH^{a*} ,
Helen JUWAH^b 

^aDepartment of Electrical Engineering, Delta State University of Science and Technology, Ozoro, NIGERIA

^bDepartment of Civil and Water Resources Engineering, Delta State University of Science and Technology, Ozoro, NIGERIA

ARTICLE INFO: Research Article

Corresponding Author: Friday Elohor ODOH, E-mail: fridoh4real33@gmail.com

Received: 1 December 2023 / Accepted: 7 April 2024 / Published: 30 June 2024

Cite this article: Akpomedaye O, Odoh FE and Juwah H (2024). *Study on Dielectric Properties of Rice Husk Ash Stabilized Soil. Turkish Journal of Agricultural Engineering Research, 5(1): 66-75.*
<https://doi.org/10.46592/turkager.1399039>

ABSTRACT

This study explored the impact of organic soil stabilizing agent on the engineering behaviors of subsoil commonly used for engineering applications in Nigeria. The soil obtained from a borrow pit and air-dried under laboratory conditions ($30\pm 5^\circ\text{C}$ and $81\pm 7\%$ relative humidity). The dried soil sample was stabilized with rice husk ash (RHA) at the rate of 2, 4, 6, 8 and 10% (by mass of the soil) and cured for 14 days under natural conditions. A J-band microwave at a frequency of 7.0 GHz was used to measure the dielectric properties, while the standard proctor compaction test was used to determine the maximum dry density "MDD" and optimal moisture content "OMC" of the soil samples. Results obtained from the study depicted that the RHA had a significant effect on both the electrical properties of the soil. It was noted from the findings that, as the quantity of RHA used in stabilizing the soil increased from 0 to 10%, MDD values declined non-linearly from 1.61-1.42 g/cm³, while the OMC values inclined in a non-linear pattern from 14.8 - 17.1%. Similarly, the study results indicated that the soil dielectric constant and loss increased from 3.41 to 5.13 and 0.91 to 1.44 respectively, as the RHA incorporated into the soil raised by 10%. Present findings offer valuable insights into the fields of civil and electrical engineering, especially in the context of soil treatment for engineering applications.

Keywords: Agricultural residues, Engineering properties, Environmental sustainability, Microwave frequency, Soil particles

INTRODUCTION

Soil is a complex composite material that consists of both organic and inorganic materials, which has various engineering properties and broad applications (Akhtar *et al.*, 2013; Akpokodje and Uguru, 2019). Soil electrical properties are



Copyright © 2024. This is an Open Access article and is licensed under a Creative Commons Attribution 4.0 International License (CC-BY-NC-4.0) (<https://creativecommons.org/licenses/by-nc/4.0/deed.en>).

relevant in electrical and civil engineering jobs, as the electrical characteristics of the soil has a significant impact on the design and performance of constructed/installed structures. Some soil geotechnical properties-moisture content, soil grain size, permeability and compaction level-are critical for understanding soil behaviors and play an essential role in various applications. They provide very useful information for agricultural and electrical engineering applications (Obukoeroro and Uguru, 2021). According to Gustavo Fano (2020), soil moisture content affects the soil electrical conductivity “EC”, resistivity and dielectric properties; therefore, ground water table and soil moisture content are essential parameters to be properly evaluated during the design of grounding systems and electrical wiring.

The dielectric properties of soils are usually influenced by the bulk density, textural properties, porosity and moisture content of the soil mass. Dielectric constant (ϵ') of soil generally decreases with increasing bulk and dry density of the soil, as soil with high maximum dry density tends to have fewer voids for air and water, which will result in a gradual reduction of the soil ϵ' level (Zhao and Ling, 2016). The volume of water in soil pores significantly increases the soil dielectric constant and electrical conductivity. Similarly, soils with higher fine-grains (clay) soils develop higher dielectric constant as compared to coarse-grained (sandy) soils. Fine particles usually have a higher effective contact surface area; thereby, providing more active areas for water molecules to interact with (Schoonover and Crim, 2015).

Soil dielectric properties can be systemically influenced by alteration of some crucial factors, such as: soil moisture content, temperature, compaction level, and other physicochemical properties. According to Syeda *et al.* (2020), soil dielectric properties can be seriously influenced by the mineral composition, organic matter content and salinity level of the soil. Moderate salinity has the potential of causing serious alteration in the soil electrical conductivity and dielectric properties, as it makes the soil to be more conductive; hence, increasing the EC and ϵ' of the soil (Patel *et al.*, 2018).

Though a number of studies had been done to appraise the dielectric properties of various soil types (Navar khele *et al.*, 2009; Kabir *et al.*, 2020; Kumar *et al.*, 2022; Muhammad *et al.*, 2022), there is still information dearth on the electrical properties of organic material stabilized soils. Therefore, the major aim of this experimental work is to investigate the impact of rice hush ash “RHA” on the electrical properties of poor quality soil. Findings obtained from this study will be useful in various engineering applications such as soil moisture sensing and geophysical investigations.

MATERIALS and METHODS

Soil collection and preparation

The virgin soil sample employed for this study was collected from an active borrow pit site (1.5-2 m depth) in Oleh community of Delta State, southern Nigeria. Borrow pit soils are commonly used for civil engineering works in Nigeria, as they are considered to be lateritic soil with applicable engineering properties

([Uguru *et al.*, 2022](#)). The soil was dried in the laboratory under natural environmental conditions (30±5°C and 81±7% relative humidity).

Rice husk ash (RHA)

The RHA which was produced with a muffle furnace was obtained from the farm structure laboratory of the Department of Agricultural Engineering, Delta State University of Science and Technology, Ozoro, Nigeria. The rice husk ash was sieved with a 150 µm gauge sieve to obtain a homogenous particle size.

Preparation of the stabilized soil samples

The soil was stabilized by using different RHA contents in accordance to the stabilization plans shown in Table 1. After the addition of the required amount of RHA, the modified soil samples were cured for a period of 14 days in ambient environmental conditions (30±5°C and 81±7% RH). During the curing period, the stabilized soil samples will experience both physical and chemical changes/reactions, leading to the desired stabilization effects - desired engineering properties ([Barman and Dash, 2022](#)).

Table 1. Stabilization plan of the soil samples.

Sample code	RHA quantity (% mass of the soil)
Control	0
Treatment 1	2
Treatment 2	4
Treatment 3	6
Treatment 4	8
Treatment 5	10

Laboratory analyses

Physical properties

Particle size distribution

The sieve analysis test of the virgin (control) soil sample was done by applying the wet method according to [ASTM D6913-04 \(2017\)](#) recommended procedures. The coefficient of uniformity (C_u) for the soil was determined using Equation 1, as outlined in the sieve analysis plot by [Uguru *et al.* \(2022\)](#).

$$C_u = \frac{D_{60}}{D_{10}} \quad (1)$$

Where: D_{60} and D_{10} correspond to the points where 60% and 10%, respectively, of the grains are finer in the sieve analysis.

Compaction test

The standard proctor compaction test was done on the soil samples in accordance with [ASTMD698-12 \(2021\)](#) approved guidelines. The procedure involved mixing the soil with water and subsequently placing it into a mold with a predetermined weight. The compaction process ensued with 75 blows from a rammer, administered in three

layers at a rate of 25 blows for each layer within the mold. The optimal moisture content (OMC) for each soil sample was obtained by plotting the maximum dry density (MDD) values against the corresponding moisture content values.

Electrical properties

Dielectric constant and loss

The dielectric constant and dielectric loss (ϵ'') of all the soil samples were determined in accordance with [ASTM D150 \(2018\)](#) approved guidelines, by using the microwave frequency of 7.0 GHz as described by [Syeda *et al.* \(2020\)](#), under laboratory temperature of $30\pm 5^\circ\text{C}$. During the testing procedure, the microwave signal is directed to the soil sample and the soil's electrical properties were measured accordingly. The dielectric constant (ϵ') of each soil sample was calculated through Equations 2.

$$\text{Dielectric constant} = \frac{C_a}{C_v} \quad (2)$$

Where: C_a : Soil sample capacitance, C_v : Free air capacitance.

Data analysis

The one-way analysis of variance (ANOVA) was used to analysis the influence of the RHA on the soil electrical properties.

RESULTS AND DISCUSSION

Physical properties

Soil particle size distribution

The results obtained from the particle size grading (sieve analysis) of the soil used as control, are presented in Figure 1. Figure 1 revealed that the soil had fine content of 21.2%, Coefficient of Uniformity (Cu) of 4.40 and Coefficient of Curvature (Cc) of 0.909. Soil particle sizes and their distribution pattern are fundamental soil attributes that affect its soil moisture content and electrical properties ([Hu *et al.*, 2011](#); [Uguru *et al.*, 2022](#)). Fine grained soils tend to have lower density and compaction degree, but higher dielectric properties when compared to their coarse particle size counterpart soils ([Chen *et al.*, 2018](#)). The higher dielectric properties of fine-grained soils could be linked to their higher potential to retain more water, and this property can have implications for various applications. The higher dielectric constant of fine-grained soils, indicative of higher water content, can influence the propagation of electromagnetic waves and affect the interpretation of subsurface features ([Owenier *et al.*, 2017](#)).

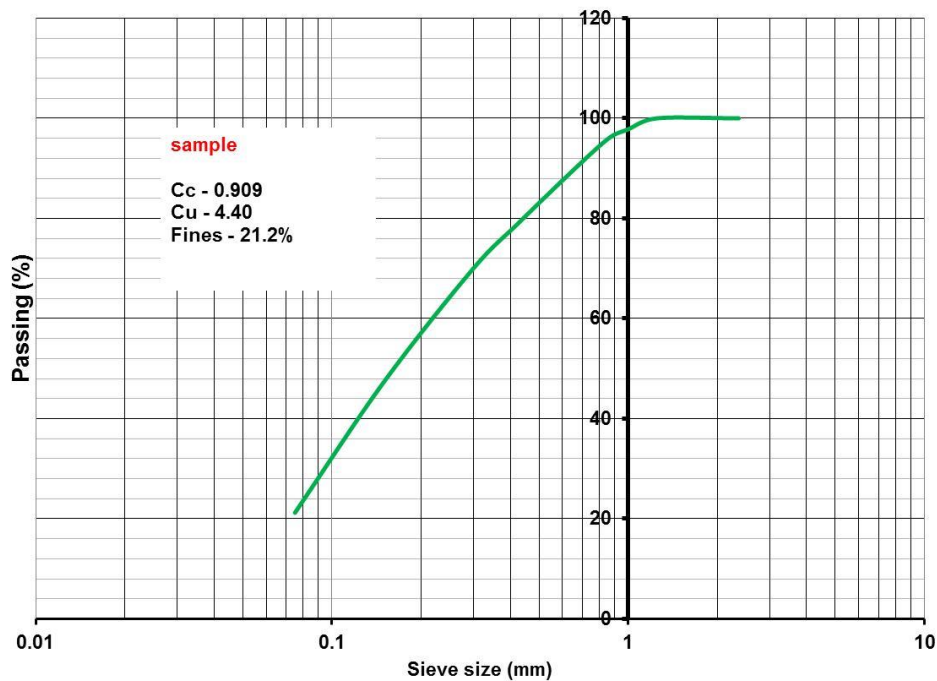


Figure 1. A plot of the natural/virgin soil sieve analysis.

Proctor compaction

The mean results of the stabilized soil samples MDD and OMC parameters are presented in Table 2. It was reliably observed from the findings that, when the RHA volume increased from 0 to 10%, their respective MDD value decreased from 1.61 to 1.42 g/cm³, and their OMC values increased from 14.8 to 17.1% respectively. This is an indication that RHA relatively decreased the density of all treated soil samples (Treatments 1 to 5), and consequently increased the available water content of the same soil. Similar results were obtained by [Ewa *et al.* \(2018\)](#) when a lateritic soil OMC increased from 18.3-21.63%, as the RHA increased from 0 to 20%. [Pushpakumara and Mendis \(2022\)](#) during their experimental studies into the suitability of green materials in stabilizing poor quality soils reported that, the addition of RHA to different soil samples relatively increased their OMC values. The increment observed in a soil sample OMC after stabilization can be linked to the high absorption rate of RHA; hence increasing the soil water holding capacity. RHA being a pozzolanic material has the capacity to increase the binding properties of the soil; hence resulting in an improved water retaining capability of the soil ([Okafor and Okonkwo, 2009](#)).

The difference in the OMC and MDD values obtained from this research when compared to other authors findings can be related to the chemical compositions of the different soil samples and RHA used for the experiment. According to [Rajeev *et al.* \(2022\)](#), pre-harvest and post-harvest management of crops significantly affects their engineering properties and chemical compositions. The higher OMC values of the stabilized fine-grained soil are attributed to their ability to retain more water, and this property can have implications for various civil and electrical engineering applications. The soil moisture content significantly affects its resistivity and dielectric properties. Higher optimal moisture content can lead to higher soil moisture content, potentially influencing the resistivity and dielectric constant of the

soil. These attributes have serious implications in the design, development and performance of electrical earthing systems, which are critical for the safety and reliability of electrical installations ([Uguru and Obukoeroro, 2020](#)).

Table 2. The MDD and OMC results of the various soil samples.

	MDD (g/cm ³)*	OMC (%)*
Control	1.61±0.09	14.8±0.13
Treatment 1	1.57±0.02	15.3±0.29
Treatment 2	1.54±0.04	15.9±0.55
Treatment 3	1.49±0.03	16.2±0.21
Treatment 4	1.45±0.04	16.7±0.42
Treatment 5	1.42±0.06	17.1±0.44

* n= 3; ± Standard deviation

Electrical properties

The results of the one-value ANOVA presented in Table 3 revealed that RHA had significant effect on the dielectric constant and dielectric loss of the soil samples ($P \leq 0.05$). This is an indication that the RHA can significantly altered the electrical behaviors of the soil samples.

Table 3. The ANOVA results of the impact of RHA of soil samples.

Source of Variation	SS	df	MS	F	P-value	F crit
Between Groups	48.084	2	24.0422	5.0104	0.0215*	3.682
Within Groups	71.976	15	4.798			
Total	120.060	17				

* = Significant at 95% confidence level

Dielectric constant

The results of the influence of the stabilizing therapies on the soil samples dielectric constant behavior are presented in Figure 2. Figure 2 obviously revealed that the soil ϵ' values increased non-linearly as the quantity of the soil stabilizing materials increased evenly from 2 to 10%. The ϵ' values for the soil samples amended with 0, 2, 4, 6, 8 and 10% RHA were 3.41, 3.95, 4.18, 4.33, 4.72 and 5.13, respectively. The findings clearly given by this study are signal that the correlation between the volume of RHA used in stabilizing the soil, and the dielectric constant is not a simple linear correlation. The rapid increment of dielectric constant levels in the soil containing with higher percentages of RHA depicted that, changes in the electrical characteristics of the soil can be duly linked to the addition of this material (RHA) to the soil. These observations are similar to previous reports of [Chaudhari \(2015\)](#), which stated that organic materials have a strong potential to improve (increase) the dielectric constant of poor soil samples. Similarly, [Muhammad *et al.* \(2022\)](#) stated that the incorporation of decaying agricultural materials into the soil considerably enhances most of its electrical properties, as reflected in the dielectric constant values. The increase in dielectric constant is an important indicator of changes in the soil electrical characteristics. Remarkably, higher dielectric constants have considerable impact on the soil water retention, nutrient availability, and other factors relevant to plant growth ([Zhang *et al.*, 2021](#)).

Additionally, the outcomes of the experimental revealed that soil OMC values increases as the ash content incorporated into the soil increase from 0 to 10%. This increase in moisture content corresponded to an elevation in the dielectric constant value of the soil.

Alteration in the soil moisture level and organic matter content can lead to indicative of variations in the soil dielectric constant values ([Park *et al.*, 2019](#)).

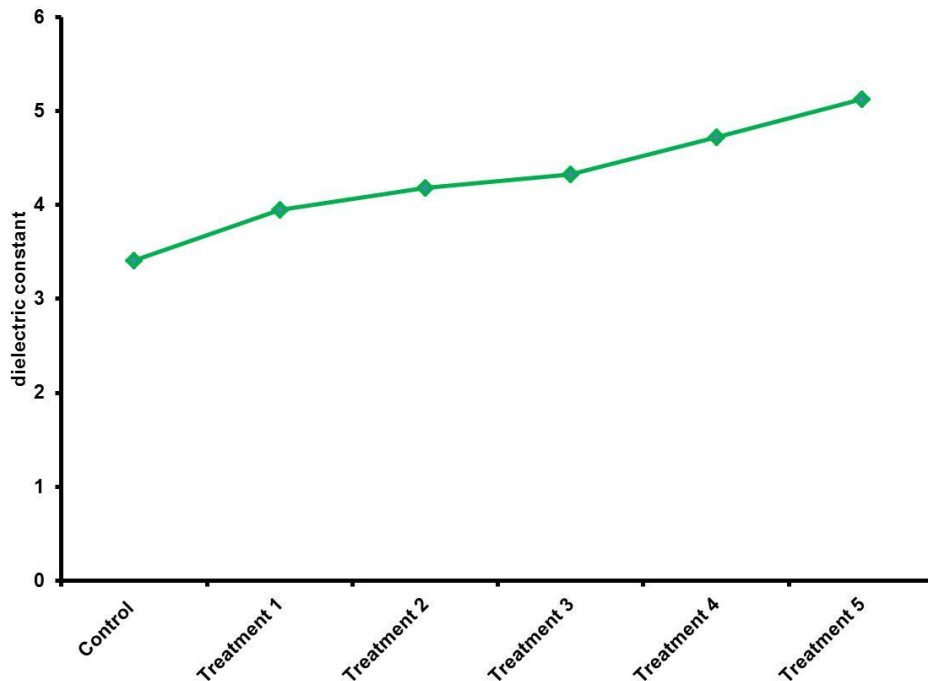


Figure 2. The dielectric constant of the soil samples.

Dielectric Loss

Figure 3 shows the plot of the Dielectric Loss values of the stabilized soil samples for engineering applications. The ϵ'' values for the control, Treatment 1, Treatment 2, Treatment 3, Treatment 4 and Treatment 5 soil samples were 0.91, 1.12, 1.25, 1.31, 1.36 and 1.44, respectively. This portrayed that the stabilizing agent (RHA) enhanced (increased) the ϵ'' levels in the soil specimens, and the ϵ'' increment was in direct proportion to the quantity of the RHA added to the soil. It can be observed from the findings that the reaction (effect of the RHA on the soil properties) was a dose-dependent relationship; because, when the amount of RHA incorporated into the soil increases, the dielectric loss factor values also increase proportionally in a non-linearly pattern. These findings (results) are comparable to those previously obtained by [Navar khele *et al.* \(2009\)](#), where they noted that the dielectric loss of soil increased with increasing organic materials in the soil increase despite the experimental microwave frequencies.

According to [Chaudhari \(2015\)](#), organic manure tends to have higher dielectric loss property when compared to inorganic materials; hence these materials (organic matter) have a higher potential of increasing the overall dielectric loss characteristic of the soil. Soil dielectric properties are highly dependent on the soil organic materials, water content and mineralogy level ([Szyplowska *et al.*, 2021](#)). Dielectric loss is more pronounced in the presence of moist environment; therefore organic

materials with higher water retention ability tend to increase the dielectric loss in the soil (Kumar *et al.*, 2022).

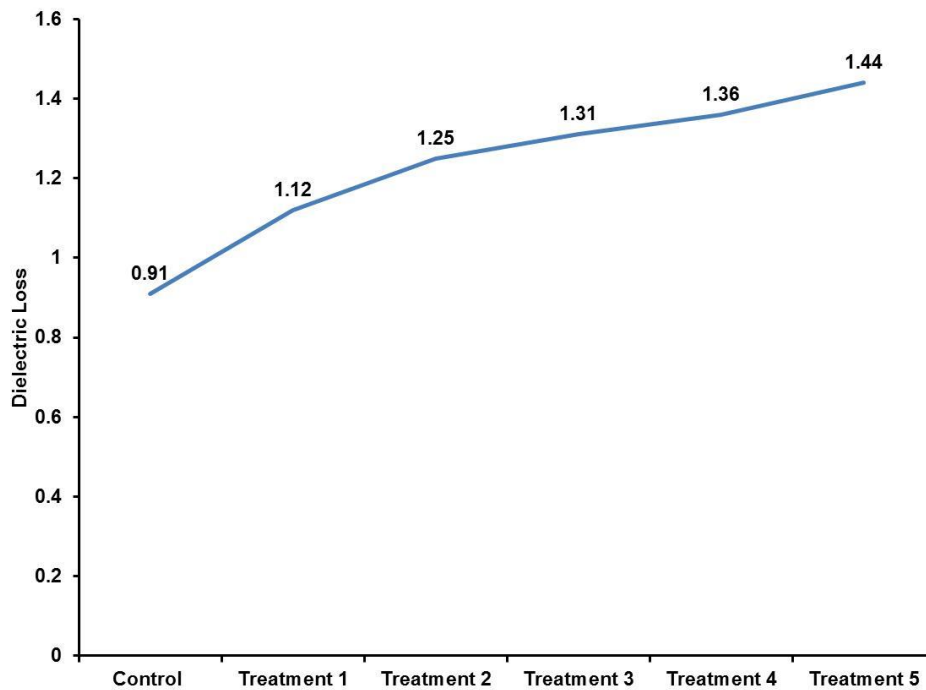


Figure 3. The dielectric loss vales.

CONCLUSION

The effect of rice husk ash on the dielectric properties of soil samples was duly investigated in this study. The soil was stabilized with RHA at the rate of 2, 4, 6, 8 and 10% (by the weight of the soil) and their (the stabilized soil samples) maximum dry density, optimal moisture content, dielectric constant and dielectric loss were determined in accordance with ASTM International approved guidelines. Findings obtained from this study revealed that the dielectric properties (ϵ' and ϵ'') of the soil increased unevenly as the quantity of the RHA incorporated into the soil increased from 0 to 10%. Similarly, the results portrayed that the OMC values increased non-uniformly as the RHA content in the soil increases uniformly, while the MDD values declined as the RHA volume into the soil increase. Outcomes of this research revealed that 10% RHA yield the optimal results. The information obtained from this research has serious valuable insights in the field of electrical engineering, especially in the context of sustainable soil improvement for electrical engineering practices.

DECLARATION OF COMPETING INTEREST

The authors declare that they have no conflict of interest

CREDIT AUTHORSHIP CONTRIBUTION STATEMENT

The authors declared that the following contributions are correct.

Ogaga Akpomedaye: Designed the research Methodology and writing of the original draft.

Friday Elohor Odoh: Data analysis and review of the original draft.

Helen Juwah: Designed the research and writing the original draft.

ETHICS COMMITTEE DECISION

This article does not require any ethical committee decision.

REFERENCES

- Akhtar MS, Ahmed M and HAQ Q (2013). Heavy metals in vegetable grown Korangi Area Karanchi, Pakistan, FUUAST. *Journal of Biology*, 3: 71-74.
- Akpokodje OI and Uguru H (2019). Bioremediation of hydrocarbon contaminated soil: assessment of compost manure and organic soap. *Transactions on Machine Learning and Artificial Intelligence*, 7(5): 13-23. <https://doi.org/10.14738/tmlai.75.7013>
- ASTM D6913-04 (2017). Standard Test Methods for Particle-Size Distribution (Gradation) of Soils Using Sieve Analysis. Available online at: <https://www.astm.org/d6913-04r09e01.html>
- ASTM D150 (2018). Standard Test Methods for AC Loss Characteristics and Permittivity (Dielectric Constant) of Solid Electrical Insulation. Available online at: <https://www.astm.org/d0150-18.html>
- ASTM D698-12(2021). Standard Test Methods for Laboratory Compaction Characteristics of Soil Using Standard Effort (12,400 ft-lbf/ft³ (600 kN-m/m³)). Available online at: <https://www.astm.org/d1557-12r21.html>
- Barman D and Dash SK (2022). Stabilization of expansive soils using chemical additives: A review. *Journal of Rock Mechanics and Geotechnical Engineering*, 14(4): 1319-1342. <https://doi.org/10.1016/j.jrmge.2022.02.011>
- Chaudhari HC (2015). Dielectric properties of soils with organic and inorganic matter at j-band microwave frequency. *International Journal of Remote Sensing & Geoscience*, 4(2): 15-19.
- Chen M, Wu G, Gan B, Jiang W and Zhou J (2018). Physical and compaction properties of granular materials with artificial grading behind the particle size distributions. *Advances in Materials Science and Engineering*, 2018: 1-20.
- Ewa D, Akeke GA and Okoi D (2018). Influence of rice husk ash source variability on road subgrade properties. *Nigerian Journal of Technology*, 37(3): 582-294. <https://doi.org/10.4314/njt.v37i3.4>
- Gustavo Fano W (2020). The electrical properties of soils with their applications to agriculture, geophysics, and engineering. *IntechOpen*. <https://doi.org/10.5772/intechopen.88989>
- Hu H, Tian F and Hu H (2011). Soil particle size distribution and its relationship with soil water and salt under mulched drip irrigation in Xinjiang of China. *Science China Technological Sciences*, 54: 1568-1574. <https://doi.org/10.1007/s11431-010-4276-x>
- Kabir H, Muhammad JK, Grahm B, Dorin G, Alexis P, Mohanvo J and Elsa A (2020). Measurement and modelling of soil dielectric properties as a function of soil class and moisture contents. *Journal of Microwaves Power and Electromagnetic Energy*, 54: 3-18. <https://doi.org/10.1080/08327823.2020.1714103>
- Kumar S, Ahalya N, Singh V, Patil PP, Raghavendra Rao AV, Nirmala Jyothsna A, Abhilash P, kushwah R and Palukaran Timothy S (2022). Exhibition of dielectric property based on soil class and moisture presence for Bengaluru District. *Advances in Materials Science and Engineering*, 2022: 1-9. <https://doi.org/10.1155/2022/6807204>
- Muhammad A, Zangina T, Suleiman AB, Mohammed J and Hafeez HY (2022). Determination of dielectric properties of cultivated and uncultivated land at Kafin Hausa LGA, Jigawa State, Nigeria. *Dutse Journal of Pure and Applied Sciences*, 8(2b): 98-104. <https://doi.org/10.4314/dujopas.v8i2b.11>
- Navar khele VV, Shaikh AA and Ramshetti RS (2009). Dielectric properties of black soil with organic and inorganic matters at microwave frequency. *Indian Journal of Radio & Space Physics*, 38: 112-115.
- Obukoeroro J and Uguru H (2021). Evaluating the geotechnical and electrical properties of soil samples around Delta State Polytechnic, Ozoro, Nigeria. *Applied Journal of Physical Science*, 3(1): 21-27. <https://doi.org/10.31248/AJPS2021.042>







- Okafor FO and Okonkwo UN (2009). Effects of rice husk ash on some geotechnical properties of lateritic soil. *Leonardo Electronic Journal of Practices and Technologies*, 15: 67-74.
- Owenier F, Hornung J and Hinderer M (2017). Substrate-sensitive relationships of dielectric permittivity and water content: implications for moisture sounding. *Near Surface Geophysics*, 16(2): 128-152. <https://doi.org/10.3997/1873-0604.2017050>
- Park CH, Montzka C, Jagdhuber T, Jonard F, De Lannoy G, Hong J, Jackson TJ and Wulfmeyer V (2019). A dielectric mixing model accounting for soil organic matter. *Vadose Zone Journal*, 18: 190036. <https://doi.org/10.2136/vzj2019.04.0036>
- Rajeev RT, Shukadev M, Adinath EK, Rokayya S, Al-Mushhin AAM, Mahmoud FM, Uguru H and Mahmoud H (2022). Effect of harvesting stages and storage temperature on quality attributes and post-harvest shelf-life of mango (*Mangifera indica*). *Journal of Biobased Materials and Bioenergy*, 16: 770-782. <https://doi.org/10.1166/jbmb.2022.2219>
- Patel VN, Chaudhary PD, Vankar HP, Rana VA, Vyas AD, and Gadani DK (2018). Variation of electrical parameters of soil with moisture and salinity over frequency range from 20 HZ TO 2 MHZ. *International Journal of Scientific Research and Reviews*, 7(1): Supplement, 457-471.
- Pushpakumara BHJ and Mendis WSW (2022). Suitability of rice husk ash (RHA) with lime as a soil stabilizer in geotechnical applications. *Geo-Engineering*, 13(4): 23-31. <https://doi.org/10.1186/s40703-021-00169-w>
- Schoonover JE and Crim JF (2015). An introduction to soil concepts and the role of soils in watershed management. *Journal of Contemporary Water Research & Education*, 154(1): 21-47. <https://doi.org/10.1111/j.1936-704X.2015.03186.x>
- Syeda RN, Abdullah BM, Khan AR and Shaikh YH (2020). Study of effect of potassium nitrate and ammonium sulphate on dielectric properties of soil at X and J-Band microwave frequencies. *Journal of Physics: Conference Series*, 1644(1): 012041-012049. <https://doi.org/10.1088/1742-6596/1644/1/012041>
- Szypłowska A, Lewandowski A, Yagihara S, Saito H, Furuhashi K, Szerement J, Kafarski M, Wilczek A, Majcher J, Woszczyk A and Skierucha W (2021). Dielectric models for moisture determination of soils with variable organic matter content. *Geoderma*, 401: 115288-115296. <https://doi.org/10.1016/j.geoderma.2021.115288>
- Uguru HE and Obukoeroro J (2020). A survey of residential and mini-industrial wiring systems in Nigeria: A case study of Bayelsa State, Southern Nigeria. *Journal of Engineering and Information Technology*, 7(7): 148-154. <https://doi.org/10.26765/DR-JEIT14202650>
- Uguru H, Akpokodje OI and Agbi GG (2022). Assessment of compressive strength variations of concrete poured in-site of residential buildings in Isoko District, Delta State, Nigeria. *Turkish Journal of Agricultural Engineering Research (TURKAGER)*, 3(2): 311-327. <https://doi.org/10.46592/turkager.1128061>
- Zhao Y and Ling D (2016). Study on a calibration equation for soil water content in field tests using time domain reflectometry. *Journal of Zhejiang University Science A*, 17: 240-252. <https://doi.org/10.1631/jzus.A1500065>
- Zhang YW, Wang KB, Wang J, Liu C and Shangguan Z.P (2021). Changes in soil water holding capacity and water availability following vegetation restoration on the Chinese Loess Plateau. *Scientific Reports*, 11(1): 9692- 9702. <https://doi.org/10.1038/s41598-021-88914-0>



Turkish Journal of
Agricultural
Engineering Research
(Turk J Agr Eng Res)
e-ISSN: 2717-8420



Gravimetric Characteristics and Friction Parameters of Common Bean (*Phaseolus vulgaris* L.)

Biniam Zewdie GHEBREKIDAN^{a*} , Adesoji Matthew OLANIYAN^b ,
Amana Wako KOROSO^a , Alemayehu Girma TADESSE^c ,
Dereje Alemu ANAWTE^c , Tamrat Lema NURGIE^c 

^aDepartment of Agricultural Machinery Engineering, School of Chemical, Mechanical & Materials Engineering,
Adama Science and Technology University, Adama, ETHIOPIA

^bDepartment of Agricultural and Bioresources Engineering, Faculty of Engineering, Federal University, NIGERIA

^cEthiopian Institute of Agricultural Research; Agricultural Engineering Research, Melkassa Agricultural Research
Center, Adama, ETHIOPIA

ARTICLE INFO: Research Article

Corresponding Author: Biniam Zewdie GHEBREKIDAN, E-mail: nzg2001nzg@gmail.com

Received: 3 April 2024 / Accepted: 23 May 2024 / Published: 30 June 2024

Cite this article: Ghebrekidan BZ, Olaniyan AM, Koroso AW, Tadesse AG, Anawte DA and Nurgie TL (2024). Gravimetric Characteristics and Friction Parameters of Common Bean (*Phaseolus vulgaris* L.). *Turkish Journal of Agricultural Engineering Research*, 5(1): 76-93. <https://doi.org/10.46592/turkager.1464050>

ABSTRACT

When designing appropriate machinery systems, equipment, and infrastructures for interacting with, cultivating, gathering, and agriculture-related processing, it is required to have an understanding of the engineering characteristics of agricultural products. This unpredictability makes it difficult to design or develop machines that can efficiently and effectively manage a wide range of product characteristics. Experimental analysis was used to accomplish the study's objective, which was to investigate the implications of variation on the gravimetric characteristics and frictional parameters of common bean (*Phaseolus vulgaris* L.) concerning the design of the threshing machine. The mean average values of gravimetric parameters were determined by analysing the experimental data: arithmetic mean diameter (7.042 ± 0.473 mm), geometric diameter (6.737 ± 0.463 mm), bulk density (781.20 ± 25.34 kg m⁻³), true density (1347.03 ± 143.0 kg m⁻³), porosity ($41.385 \pm 7.05\%$), width (6.316 ± 0.502 mm), thickness (4.962 ± 0.50 mm), projected area (49.194 ± 6.715 mm²), and volume of the seed (161.689 ± 3.778 mm³). The average moisture content values were found to be $11.214 \pm 1.185\%$ on a dry basis, the static coefficient of friction varied between 0.276 and 0.386 on the surface of iron sheets, 0.294 to 0.435 on stainless steel, 0.317 to 0.434 on galvanized iron, 0.321 to 0.451 on medium density fiberboard, 0.319 to 0.480 on aluminum, 0.310 to 0.470 on painted sheets, 0.320 to 0.440 on glass, 0.333 to 0.447 on plastic, and 0.374 to 0.575 on rubber. Perforated sheet surfaces showed the highest static coefficients of friction, followed by rubber, plastic, plywood, glass, aluminum, galvanized iron, painted sheet, stainless steel, and iron sheet surfaces. These data are not only required for predicting loads in agricultural storage structures but are also needed to establish useful sources for the development of machinery for handling, cleaning, storing, transporting and drying, among other things.

Keywords: Engineering properties, *Phaseolus vulgaris*, Static coefficient, Threshing machine



Copyright © 2024. This is an Open Access article and is licensed under a Creative Commons Attribution 4.0 International License (CC-BY-NC-4.0) (<https://creativecommons.org/licenses/by-nc/4.0/deed.en>).

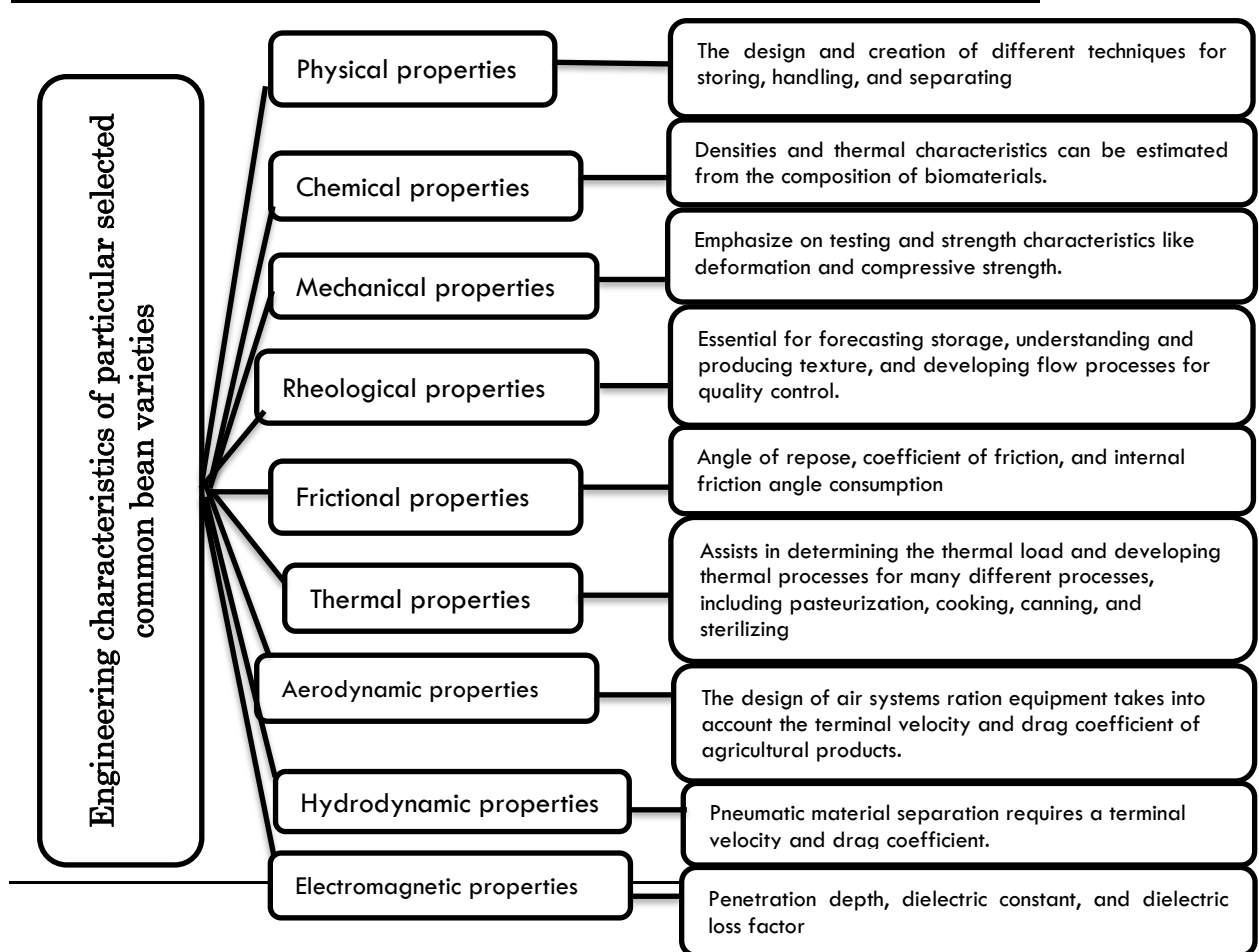
INTRODUCTION

The common bean is one of the primary worldwide sources of edible legumes (*Phaseolus vulgaris* L.). The leading producers are the US, China, Mexico, Brazil, India, and Mexico (FAO, 2020). In 2021, dry beans produced on 28 million hectares worldwide yielded over 20 million tons. Grain-based legumes are essential for nourishment for humans (Degirmencioglu *et al.*, 2019), particularly for low-income people in underdeveloped countries (Fernando, 2021). Compared to grains, their protein content is almost 2-3 times higher (Wodajo *et al.*, 2021), they are composed of a substantial amount of protein and are often referred to as "poor man's meat." For a sizable segment of the global populace, mostly in developing nations, they also provide an affordable and significant source of starch, dietary fiber, and protein (FAOSTAT, 2020).

According to Amsalu *et al.* (2018), Ethiopia has been producing and exporting common beans for more than 50 years. The country produces red, white, black, and mottled varieties of common beans (Abera *et al.*, 2020). The most widely available commercial kinds are pure red and white beans; as market demand increases, they are also being grown more frequently (Tekalign *et al.*, 2022). Due to the increased demand for these commodities in the local and international markets, in recent years, there has been a discernible increase in nationwide production area and volume (Kefelegn *et al.*, 2020). This illustrates how inefficient postharvest handling, primarily done by hand, persists in Ethiopia, considering the country's significant worldwide yield of common beans (Befikadu, 2018). To build appropriate systems, equipment, and infrastructures for interacting with, cultivating, gathering, and agriculture-related processing thus, comprehension of the engineering characteristics of agricultural products is essential (Table 1).

Bayano-Tejero *et al.* (2023) state that when designing, cleaning, sizing, and grading machines, the three main dimensions of length, breadth, and thickness must be considered (Samrawit, 2023). Aspect ratio (Omobuwajo *et al.*, 1999), projected area (Mirzabe *et al.*, 2013), roundness (Baryeh, 2002), sphericity and surface area (Mohsenin, 1986; Baryeh, 2002), arithmetic mean diameter and geometric mean diameter (Baryeh, 2002; Mpotokwane *et al.*, 2008), and Mohsenin (1986) computation of seeds' volume (V) were among the measurements taken.

When developing the seed metering mechanism of seed drills (Önal and Ertuğrul, 2011), as well as transportation, sorting and sizing systems, bean seed size is a critical parameter (Nciri *et al.*, 2014); Larger-seeded bean varieties absorb water more slowly and take longer to cook than smaller-seeded varieties (Sahin and Sumnu, 2006). During soaking, seed size affects electrical conductivity tests (Chhabra and Kaur, 2017).



Model developed by Author, 2024

Figure 1. Conceptual study model of engineering properties common bean seeds.

Surface area plays a crucial role in heat and mass transfer processes such as drying and various thermal applications. An agricultural product's surface area usually indicates how it will behave in a flowing fluid and how easy it will be to remove unwanted contaminants from the product while cleaning it with a pneumatic tool ([Omobuwajo *et al.*, 1999](#)). The surface area helps determine the agricultural products quality and quantity, color, respiration data, and aerodynamic calculations ([Singh and Heldman, 2009](#)).

The gravimetric parameters alter the rate of moisture transfer and heat transfer in the approach, which makes them crucial properties in drying and ventilation processes. The bulk density determines the conveyor capacity and amount of produce storage needed. When separating materials, the actual density is taken into account. Grain hopper and storage equipment sizing is determined by porosity ([Kakade *et al.*, 2019](#)). The engineering characteristics of agricultural materials are influenced by the moisture content, a gravimetric parameter ([Degirmencioglu and Srivastava, 1996](#); [Sahin and Sumnu, 2006](#); [Singh and Heldman, 2009](#); [Bhise *et al.*, 2014](#)). Equipment design that is effective, affordable, and efficient depends on having a comprehension of the traits of agricultural materials at varying moisture levels ([Chhabra and Kaur, 2017](#); [Bhise *et al.*, 2014](#)). When constructing storage and solid flow mechanisms ([Emrani and Berrada, 2023](#)) and material handling equipment ([Pawar *et al.*, 2023](#)),

another essential consideration to take into account is the coefficient of resistance (Bako and Aguda, 2023). An essential factor in predicting pressure from seeds on walls (Amin *et al.*, 2004) is the coefficient of friction (Bhise *et al.*, 2014) between the seed and the wall.

Hence, agricultural products have inherent variability in their engineering parameters, including moisture contents, size, shape, surface area, sphericity, density (both bulk & true), porosity, volume of seed, coefficient (both static & dynamic), and angle of repose (Jahanbakhshi, 2018; Ertuğrul *et al.*, 2022). This variability poses challenges in designing, modification, improvement, or development of machines efficiently and effectively. A lack of thorough data, inconsistent testing procedures, and a poor comprehension of the relationship between the agricultural product and the machine are a few additional challenges (Elijah *et al.*, 2018). The aim of this article is to find out how the gravimetric and frictional characteristics of common beans (*Phaseolus vulgaris* L.) influence the design of a thresher for a particular bean variety. This will help to establish the convenient reference data required to develop equipment for handling, cleaning, storing, transportation, drying, and other processes involving the seed.

MATERIALS and METHODS

Materials

Awash Melkassa Research Center, Oromia regional State, Ethiopia, provided seven improved varieties of common beans that grow in several regions of the country: Awash-1, Awash-2, Awash-Tikur, Awash Meten, Nasir, SER-119, and SER-125 (Figure 2). For further investigation, the sample seeds were manually picked and cleaned of foreign elements such as dust, stones, dirt, immature seeds, damaged seeds, and other contaminants. Then, in an airtight plastic vessel, the healthy seeds that had been chosen were kept at 5°C. The seeds were allowed to attain the room temperature before the test began.



Figure 2. Awash Melkassa Research Center's national common bean research programs improved varieties.

Instrumentation

Digital caliper: With the following specifications: Mitutoyo 500-197 model; Mitutoyo brand; Measurement Range: 0-200 mm; Resolution: 0.0005 in; Repeatability: 0.01 mm or 0.0005 in.

Electronic balance: This analytical electronic balance and digital scale (Figure 3) has the following features: Brand Name-JYCTD; stainless steel and ABS; made in China from 100 to 2000 grams is its capacity. Units: 0.01g, lb, oz, g, and ct precisely, it can support up to 5 kg of load. TARE, CAL, PCS, POWER, and UNIT are function buttons.

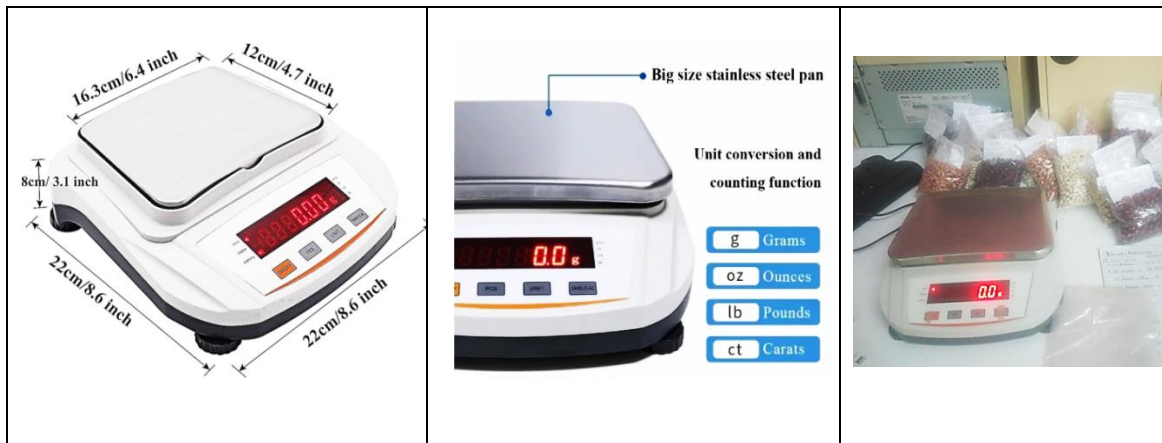


Figure 3. Digital scale analytical electronic balance (Readability (0.01g) Chinese origin).

Grain moisture meter: The approximate dimensions of the device are 19.0 x 12.5 x 8.0 cm, and its weight, including batteries, is 700 g (Figure 4). Using two 1.5 V AA type batteries (LR6) as the power source, the sample volume is 270 ml, and the power consumption ranges from 15,2 mA to 84 mA when the backlight intensity is set; manual filling of the measurement chamber with a special dispenser; Accuracy of moisture measurement is $\pm 1\%$ in the range up to 10% and $\pm 1.5\%$ in the range above 10%, and it may rise in proportion to sample moisture; and accuracy is $\pm 0.5^\circ\text{C}$ / $\pm 0.9^\circ\text{F}$. The temperature measurement range is -10°C to $+ 85^\circ\text{C}$ / 14°F to 185°F ; the temperature indication resolution is 0.1°C / 0.1°F . 10°C to 35°C , or 50°F to 95°F , is the recommended temperature range for operation; 5°C to 45°C , or 41°F to 113°F , is the recommended temperature range for storage.



Figure 4. Grain moisture meter (Model: GMM mini DRAMINSKI, which is Origin Poland).

Laboratory

All of the tests were carried out at the Agricultural Engineering Laboratories at Melkassa Agricultural Research Center (MARC); Haramaya University; and Adama Science & Technology University's; Science, Technology, Engineering, & Mathematics (ASTU STEM) Center's Chemistry laboratory.

Experimental procedure

Finding the dimensional characteristics

The dimensions of seven hundred (100 for each variety) randomly chosen bean seeds were determined. Using an electronic vernier caliper with a precision of 0.01 mm, the three fundamental axial dimensions of *Phaseolus vulgaris* were measured. *Phaseolus vulgaris* mean diameters were computed as geometric mean (D_g), arithmetic mean (D_a), square mean (D_s), and equivalent mean (D_{eq}) were determined using Equations (1-5) ([Fraser *et al.*, 1978](#); [Mohsenin, 1986](#); [Baryeh, 2002](#); [Haciseferogullari *et al.*, 2003](#); [Altuntas and Yildiz, 2007](#); [Sundaram *et al.*, 2014](#)).

$$\text{Geometric Mean Diameter, mm} \quad D_g = \sqrt[3]{L \times W \times T} \quad (1)$$

$$\text{Arithmetic Mean Diameter, mm} \quad D_a = \frac{L + W + T}{3} \quad (2)$$

$$\text{Square Mean Diameter, mm} \quad D_{sq} = \sqrt{LW + WT + TL} \quad (3)$$

$$D_{eq} = \frac{D_g + D_a + D_s}{3} \quad (4)$$

$$\text{Equivalent Mean Diameter, mm} \quad D_{eq} = \left[\frac{L(W + T)^2}{4} \right]^{\frac{1}{3}} \quad (5)$$

Using Equations 6–14 adopted by [Mohsenin \(1986\)](#); [Baryeh \(2002\)](#); [Gupta *et al.* \(2007\)](#); [Sirisomboon *et al.* \(2007\)](#); [Mirzabe *et al.* \(2013\)](#), the surface area, projected area, specific surface area, transverse surface area, cross-section area, and volume of the seeds were calculated.

	$A_s = \pi D_g^2$	(6)
Surface Area seed, mm ²	$A_s = (36\pi)^{\frac{1}{3}} V^{\frac{2}{3}}$	(7)
	$A_s = \frac{\pi B^2 L^2}{2L-B}$; B = (WT) 0:5	(8)
Projected Area, mm ²	$A_p = \left(\frac{\pi}{4}\right) L * W$	(9)
Specific Surface Area, mm ²	$S_s = A_s \rho_b / m$	(10)
Transverse Surface area, mm ²	$A_t = \left(\frac{\pi}{4}\right) T * W$	(11)
Cross-Section Area, mm ²	$CSA = \frac{\pi}{4} \left[\frac{(L + W + T)^2}{3} \right]$	(12)
	$V = \frac{\pi}{6} D_g^3 = \frac{\pi}{6} LWT$	(13)
Volume of the seed, mm ³	$V = \frac{\pi B^2 L^2}{6(2L-B)}$; B = (WT) 0:5	(14)

Where, B = (WT) 0:5; the seeds' width, W, and thickness, T, are measured in mm.

Using the algorithms described by several references ([Mohsenin, 1986](#); [Omobuwajo *et al.*, 1999](#); [Baryeh, 2002](#); [Chhabra and Kaur, 2017](#); [Saparita *et al.*, 2019](#)), the flakiness ratio, aspect ratio, shape index, shape factor, sphericity, and roundness of the common beans were computed using the following Equations 15-22.

Flakiness Ratio	$R_f = T/W \times 100\%$	(15)
-----------------	--------------------------	------

Aspect Ratio	$R_a = W/L \times 100\%$	(16)
--------------	--------------------------	------

Shape Index	$SI = L/\sqrt{(W * T)}$	(17)
-------------	-------------------------	------

Shape Factor	$SF = 4\pi P_A / P^2$	(18)
--------------	-----------------------	------

	$\varphi = \frac{D_g}{L}$	(19)
--	---------------------------	------

Sphericity	$\varphi = \left(\frac{WT}{L^2}\right)^{1/3}$	(20)
------------	---	------

Roundness	$R = \left\{ \frac{W/L + T/L + T/W}{3} \right\}$	(21)
-----------	--	------

	$R = \left\{ \frac{1/E_w + 1/E_t + 1/E_v}{3} \right\}$	(22)
--	--	------

Using the following Equations 23, 24, and 25 adopted by ([Mohsenin, 1986](#)), the elongation at the width orientation ([Gupta *et al.*, 2007](#)), elongation at the thickness

orientation ([Mirzabe *et al.*, 2013](#)), and elongation at the vertical orientation ([Chhabra and Kaur, 2017](#)) of the *Phaseolus vulgaris* were determined.

$$\text{Elongation at the width orientation} \quad E_w = L/W \quad (23)$$

$$\text{Elongation at the thickness orientation} \quad E_t = L/T \quad (24)$$

$$\text{Elongation at the vertical orientation} \quad E_v = W/T \quad (25)$$

Determination of gravimetric parameters

The true density and seed volumes were determined using the liquid displacement technique. Water was not utilized since the seed absorbs water more readily than toluene (C₇H₈). To measure the amount of toluene displaced from the weighted seed, the amount of the product that was displaced was measured using a graduated scale on the cylinder. Once the weight of the seeds was divided by the volume of displaced toluene, their true density was found. Bulk density, true density, and porosity were calculated using Equations 26-32 ([Mohsenin, 1986](#); [Desphande *et al.*, 1993](#); [Omobuwajo *et al.*, 1999](#); [Singh and Heldman, 2009](#); [Saparita *et al.*, 2019](#)).

$$100 \text{ seed weight} = \left(\frac{100 - \text{MC records}}{(100 - 10)} \right) \times 100\% \quad (26)$$

Thousand Seed Mass (TSM)

$$\text{TSM} = \frac{\text{Weight of sample, g}}{\text{Number of grains in sample}} \times 10 \quad (27)$$

Bulk Density, kgm⁻³

$$\rho_b = \frac{\text{weight of sample (g)}}{\text{volume of occupied (cm}^3\text{)}} \quad (28)$$

True Density, kgm⁻³

$$\rho_t = \frac{\text{weight of the sample (g)}}{\text{volume of toluene displaced (cm}^3\text{)}} \quad (29)$$

Density Ratio, (%)

$$R_\rho = \left(\frac{\rho_b}{\rho_t} \right) \times 100(\%) \quad (30)$$

$$\varepsilon = \left(1 - \frac{\rho_b}{\rho_t} \right) \times 100(\%) \quad (31)$$

Porosity, (%)

$$\varepsilon = 1 - R_d \times 100(\%) \quad (32)$$

Determination of angle of repose

Two cylindrical diameter containers, one hollow and placed on top of a closed side, were used in the setup for the experiment for measurements of the repose angle (Figure 5). Conical-shaped beans began to trickle down the closed container when the hollow container was gradually removed in an upward orientation. Using Equation 33 as provided by [Baryeh \(2002\)](#), [Mohsenin \(1986\)](#), and [Saparita *et al.* \(2019\)](#), likewise the repose angle (α) and the apex height were taken into consideration were computed using the trigonometry rule.

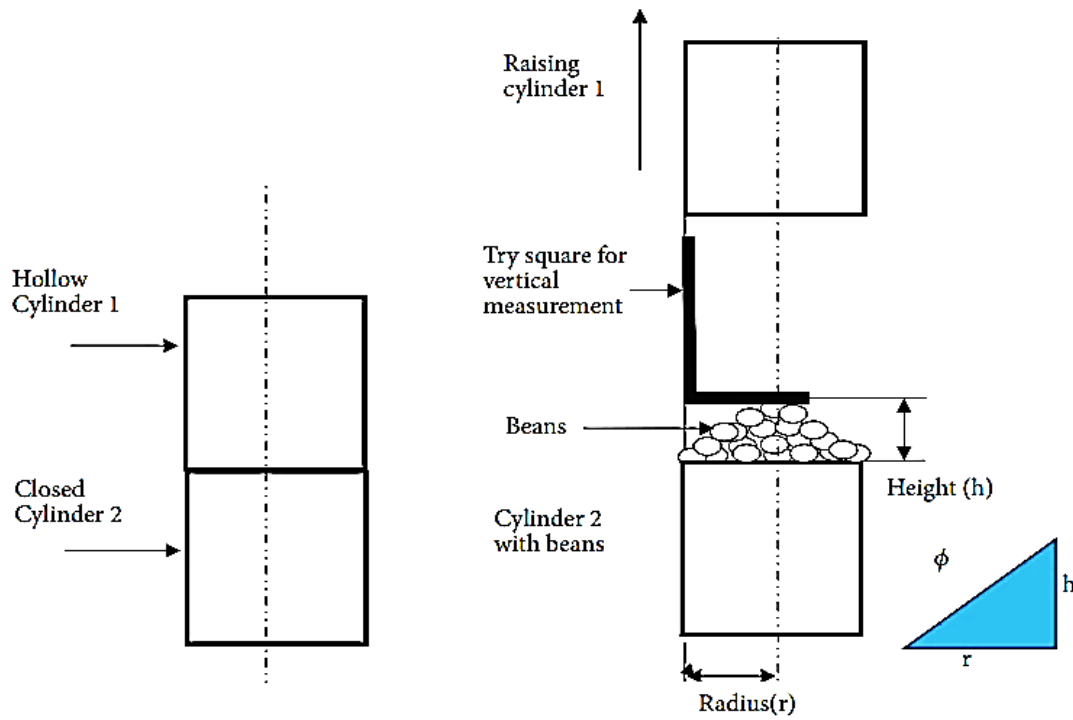


Figure 5. Repose angle measurements in an experimental setup.

Coefficient of static friction determination

Ten surfaces' coefficient of static friction was computed using the inclined plane approach (Figure 6). The angle of inclination (ϕ) was found using the protractor attached to the apparatus after the table had been gently raised to the horizontal at which the seeds began to slide. Equation 34 was utilized to compute the static friction coefficient (μ), following the method outlined by [Mohsenin \(1986\)](#) and [Saparita *et al.* \(2019\)](#), albeit with some adjustments.

Angle of repose $\phi = \tan^{-1} [h/b]$ (33)

Coefficient of static friction $\mu = \tan \phi$ (34)

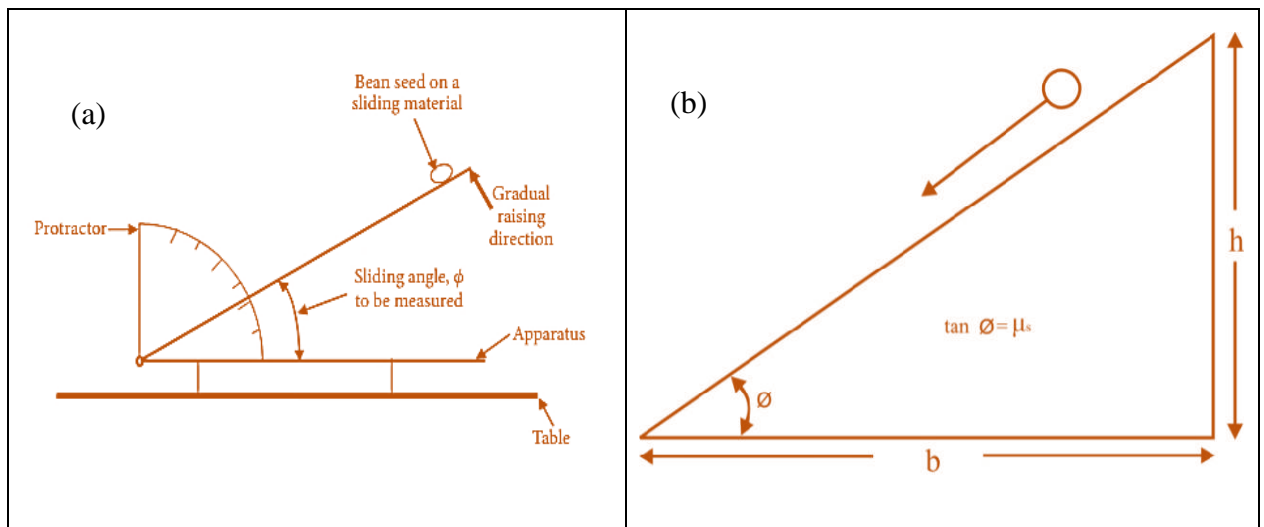


Figure 6. A setup for measuring (a) and computing (b) the coefficient of sliding friction of common beans using the inclined plane method.

Statistical Analysis

The standard deviation (SD) and mean of the results were displayed. Using IBM SPSS Statistics 27.0.1_IF026 and the Statistical Package for Social Science, version 22, way analysis of variance (ANOVA) was performed on the data.

RESULTS AND DISCUSSION

Dimensional characteristics

Table 1 shows a summary of the measured and determined dimensional parameters tested across multiple bean types (Awash-1, Awash-2, Awash Tikur, Awash Meten, Nasir, SER-119, and SER-125) are shown in the table along with their respective means, standard deviations (STDEV), and coefficients of variation (CV%). The findings verified that the seeds' longitudinal dimensions ranged from 7.841 to 11.894 mm, with an average mean value (amv) of 9.847 ± 0.802 mm; their width varied from 5.061 to 7.746 mm, with an amv of 6.316 ± 0.502 mm; their seed thickness ranged from 3.547 to 6.013 mm, with an amv of 4.962 ± 0.500 mm; their elongation of width (Ew) varied from 1.208 to 1.881 mm, with an amv of 1.560 ± 0.120 mm; their elongation of thickness (Et) varied from 1.558 to 2.710 mm, with an amv of 2.007 ± 0.234 mm; and their elongation of vertical (Ev) varied from 1.042 to 1.687 mm, with an amv of 1.284 ± 0.124 mm. The significance of axial dimensions in machine design was emphasized by [Mohsenin \(1986\)](#). However, symmetric projections towards process equipment adaption can be made by comparing the results with previous research on other seeds.

The seeds' arithmetic mean diameter ranged from 5.664 to 8.142 mm, with an amv of 7.042 ± 0.473 mm; their geometrical mean diameter varied from 5.379 to 7.763 mm, with an amv of 7.715 ± 0.69 mm; their square mean diameter varied from 9.559 to 13.749 mm, with an amv of 11.914 ± 0.805 mm; their equivalent mean diameter varied from 6.871 to 9.885 mm, with an amv of 8.565 ± 0.579 mm; their roundness ranged from 0.537 to 0.760 mm, with an amv of 0.651 ± 0.047 ; their sphericity varied from 0.595 to 0.803 with an amv of 0.789 ± 0.072 ; their flakiness ratio varied from 0.594 to 0.966 with an amv of 0.649 ± 0.052 ; their aspect ratio varied from 0.539 to 0.847, with an amv of 0.649 ± 0.052 mm; cross-sectional area varied from 76.403 to 156.528 mm² with the mean value of 117.793 ± 15.576 mm², the projected area ranged from 32.827 to 67.175 mm² with the amv of 49.194 ± 6.715 mm², the transverse surface area varied from 14.828 to 34.343 mm² with the mean value of 24.699 ± 3.809 mm², and the seed volume varied from 83.752 to 245.872 mm³ with the mean value of 162.689 ± 3.777 mm³, respectively. The values should be given for arithmetic, geometric, and sphericity were comparable to those of [Ozturk *et al.* \(2009\)](#), [Amin *et al.* \(2004\)](#), and [Kumar and Sharma, \(2021\)](#); Nonetheless, they were lower than those reported by [Cetin \(2007\)](#) and [Altuntas and Yildiz \(2007\)](#), but greater than common beans ([Ozturk *et al.*, 2009](#)) and lower than red kidney beans with speckles ([Isik and Unal, 2011](#)). The relative variability within each parameter is revealed by the coefficient of variation (CV%). Each variety's relative variability is shown by the dimensions parameters (L, W, and T), which often have lower CV% values (between 5 and 10%). On the other hand, some metrics show larger CV% values (up to 20%), indicating greater variability in these features. These parameters include volume (V), surface

area (As), and shape index (SI). With regard to sorting, processing, and packing, among other uses, this data offers a thorough grasp of the dimensions and shape-related characteristics of the various bean varieties.

Table 1. Mean and Coefficient of Variation of measured and determined dimensional parameters.

Varieties	Awash - 1			Awash - 2			Awash Tikur			Awash Meten		
parameter	Mean	STDEV	CV (%)	Mean	STDEV	CV (%)	Mean	STDEV	CV (%)	Mean	STDEV	CV (%)
L, mm	8.263	0.616	7.461	8.605	0.756	8.78a*	10.392	0.793	7.627	9.188	0.982	10.69a*
W, mm	5.910	0.639	10.82b*	6.107	0.439	7.19b*	6.651	0.466	7.01b*	6.091	0.653	10.72b*
T, mm	4.926	0.472	9.57c*	5.247	0.480	9.14c*	5.138	0.549	10.69c*	4.948	0.395	7.98c*
Da mm	6.366	0.414	6.506d*	6.653	0.463	6.95d*	7.394	0.411	5.564	6.742	0.604	8.96d*
Dg, mm	6.207	0.420	6.77e*	6.501	0.449	6.9e*	7.067	0.401	5.673	6.510	0.558	8.57e*
Dsq, mm	10.880	0.723	6.640	11.384	0.786	6.901	12.506	0.695	5.556	11.463	1.005	8.766
Deq, mm	7.818	0.518	6.626	8.179	0.565	6.910	8.989	0.500	5.561	8.238	0.722	8.76f*
φ, %	0.754	0.055	7.34g*	0.757	0.037	4.86g*	0.682	0.042	6.147g*	0.711	0.033	4.67g*
V, mm ³	126.992	26.097	20.550	143.913	0.047	0.033	184.855	0.034	0.018	144.509	0.091	0.063
As, mm ²	121.534	16.525	13.597	132.703	0.632	0.476	156.952	0.505	0.322	133.069	0.978	0.735
Ap,mm ²	38.380	5.404	14.079	41.397	5.738	13.862	54.379	6.757	12.426	44.363	9.095	20.501
At, mm ²	23.001	4.260	18.523	25.234	3.493	13.844	26.857	3.649	13.587	23.772	3.843	16.166
SI,	1.544	0.166	10.76h*	1.523	0.111	7.30h*	1.788	0.166	9.274	1.676	0.116	6.94h*
CSA, mm ²	95.839	12.597	13.144	104.732	14.265	13.620	129.134	14.407	11.156	107.896	18.998	17.607
Varieties	Nasir			SER-119			SER-125					
parameter	Mean	STDEV	CV (%)	Mean	STDEV	CV (%)	Mean	STDEV	CV (%)			
L, mm	10.039	0.665	6.620	10.770	0.876	8.138	11.676	0.930	7.963			
W, mm	6.452	0.538	8.336b*	6.438	0.398	6.178	6.568	0.379	5.766			
T, mm	4.647	0.634	13.642c*	4.778	0.552	11.559c*	5.050	0.418	8.273c*			
Da mm	7.046	0.439	6.234	7.329	0.519	7.087	7.764	0.462	5.953			
Dg, mm	6.686	0.490	7.331e*	6.910	0.505	7.303e*	7.281	0.416	5.721			
Dsq, mm	11.877	0.802	6.752	12.304	0.876	7.116	12.985	0.746	5.746			
Deq, mm	8.536	0.575	6.733	8.848	0.632	7.143	9.344	0.540	5.775			
φ, %	0.668	0.053	7.976g*	0.643	0.028	4.359g*	0.625	0.029	4.666g*			
V, mm ³	156.555	0.062	0.039	172.843	0.067	0.039	202.157	0.038	0.019			
As, mm ²	140.365	0.754	0.537	149.939	0.800	0.533	166.446	0.545	0.327			
Ap,mm ²	50.910	6.039	11.862	54.595	6.763	12.388	60.335	7.207	11.945			
At, mm ²	23.723	4.764	20.080	24.227	3.615	14.923	26.082	3.037	11.643			
SI,	1.854	0.223	12.013h*	1.948	0.126	6.483h*	2.032	0.151	7.438h*			
CSA, mm ²	117.365	14.608	12.447	127.114	17.209	13.538	142.471	16.949	11.897			

*a, b, c, d, e, f, g, h is a higher degree of relative variability, STDEV =standard Deviation, CV=Coefficient of Variation, L = length, W=width, T=thickness, Da =arithmetic mean diameter, Dg=geometric mean diameter, Dsq=square mean diameter, Deq=equivalent mean diameter, Ra=aspect Ratio, R_f=flakiness ratio, φ=sphericity, V=volume, As = surface area, Ap=Projected Area, At=Area of transverse surface, R=Roundness, SI=Shape Index, CSA=Cross-Section Area

Gravimetric characteristics

Table 2 presents an overview of the outcomes for the gravimetric characteristics that were measured and determined. The statistical description of the gravimetric properties of the selected *Phaseolus vulgaris* (common bean) varieties based on the information provided in the table. The average moisture content values were found to be $11.214 \pm 1.185\%$ on a dry basis, mass of one thousand seed (227.714 ± 41.339 kg), bulk density (781.20 ± 25.34 kg m⁻³), true density (1347.03 ± 143.0 kg m⁻³), and porosity ($41.385 \pm 7.05\%$) for selected varieties. Similar trends were reported for common beans by (Amin *et al.*, 2004), faba beans by (Altuntas and Yildiz, 2007), barbania beans by (Cetin, 2007), white speckled red kidney beans by (Isik and Unal, 2011), and for red bean grain and common bean seed by (Saparita *et al.*, 2019). Nevertheless, compared to the studies of Altuntas and Yildiz (2007) and Cetin (2007), these increases in the bulk and dimensions of the size variants as influenced by moisture content were smaller. The research indicates that whereas bulk density and density ratio exhibit somewhat lesser variability, the *Phaseolus vulgaris* cultivars exhibit relatively significant variability in moisture content, thousand seed mass, porosity, and true density.

Table 2. Statistical description of gravimetric properties of selected *Phaseolus vulgaris*.

Variety	Mc, db%	TSM, g	Porosity, %	Bulk density, kg m ⁻³	True density, kg m ⁻³	Density ratio
Awash-1	13.00	177.00	44.230	795.200	1425.860	0.558
Awash-2	10.90	174.00	32.930	817.600	1219.020	0.671
Awash-Tikur	9.30	256.00	46.553	740.800	1386.045	0.534
Awash Meten	11.20	206.00	29.559	759.200	1077.786	0.704
Nasir	10.40	246.00	45.716	782.600	1441.667	0.543
SER-119	11.90	271.00	44.462	795.400	1432.167	0.555
SER-125	11.80	264.00	46.249	777.600	1446.667	0.538
Mean	11.214	227.714	41.385	781.200	1347.030	0.586
STDEV	1.185	41.339	7.048	25.343	143.031	0.070
CV%	10.569a*	18.154b*	17.029c*	3.244d*	10.618e*	12.024f*

Mc = Moisture content, TSM =Thousand seed mass; CV = coefficient of variance; "a*", "b*", "c*", "d*", "e*", and "f*" indicates higher relative variability or Significant at $P \leq 0.05$:

Static coefficient of friction

Table 3 shows static coefficient of friction for different sliding surface materials with a single seed/minimum value and the remaining seeds/maximum value sliding on a selected surface. The static coefficient of friction on the iron sheet surface varied from 0.276 to 0.386 with average mean value (amv) of 0.355 ± 0.129 , on the stainless steel from 0.294 to 0.435 with amv of 0.385 ± 0.107 , on the galvanized iron from 0.317 to 0.434 with amv of 0.392 ± 0.109 , on the MDF sheet from 0.321 to 0.451 with amv of 0.388 ± 0.115 , on the aluminum from 0.319 to 0.480 with amv of 0.786 ± 0.462 , on the perforated sheet from 0.462 to 1.048, on the painted sheet from 0.310 to 0.470 with amv of 0.412 ± 0.125 , on the glass from 0.320 to 0.440 with amv of 0.395 ± 0.088 , on the plastic from 0.333 to 0.447 with amv of 0.396 ± 0.085) and on the rubber from 0.374 to 0.575 were amv of 0.529 ± 0.161 , respectively.

The moisture content and the coefficient of friction generally have a proportional relationship on all surfaces. Perforated sheet surfaces showed the highest static coefficients of friction, followed by rubber, plastic, plywood, glass, aluminum, galvanized iron, painted sheet, stainless steel and iron sheet surfaces. Similar patterns have been found for black-eyed peas ([Desphande *et al.*, 1993](#)), cumin seed ([Singh and Heldman, 2009](#)), red kidney beans, soybeans, unshelled peanuts, black-eyed peas ([Mohsenin, 1986](#)), and lentil seeds ([Saparita *et al.*, 2019](#)).

Table 3. Statistical description frictional properties of *Phaseolus vulgaris* on various types of sliding surface materials.

Surface		Angle of inclination (θ),degrees			Coefficient of friction (μ_s)		
		Min.	Max.	Avg.	Min	Max.	Avg.
Iron sheet	Mean	14.786	24.000	19.393	0.264	0.446	0.355
	Variance	5.358	6.259	5.303	0.002	0.003	0.002
	CV%	15.656a*	10.424	11.874	16.353d*	11.713e*	12.855f*
Stainless steel	Mean	15.381	22.476	18.929	0.275	0.414	0.345
	Variance	2.571	4.328	3.138	0.001	0.002	0.001
	CV%	10.426	9.256	9.358	10.989d*	10.361e*	10.211f*
Galvanized Iron	Mean	17.476	25.095	21.286	0.315	0.469	0.392
	Variance	4.291	2.323	2.340	0.002	0.001	0.001
	CV%	11.853	6.073	7.186	12.520d*	6.945e*	7.803f*
Plywood, MDF	Mean	15.905	26.000	20.952	0.285	0.488	0.387
	Variance	6.101	2.704	3.553	0.002	0.001	0.001
	CV%	15.529	6.324	8.996	16.528d*	7.169e*	9.707f*
Aluminum	Mean	17.905	27.286	22.595	0.324	0.517	0.420
	Variance	8.508	7.238	6.925	0.003	0.003	0.003
	CV%	16.291	9.860	11.646	17.094d*	11.431e*	12.734f*
Perforated sheet	Mean	24.571	46.619	35.595	0.459	1.113	0.786
	Variance	10.026	92.127	33.888	0.004	0.132	0.039
	CV%	12.887	20.589	16.354	14.263d*	32.644e*	25.118f*
Painted sheet	Mean	17.619	26.000	21.810	0.318	0.489	0.403
	Variance	6.831	6.778	6.124	0.002	0.003	0.002
	CV%	14.834	10.013	11.347	15.709d*	11.219e*	12.313f*
Glass	Mean	17.048	25.333	21.190	0.307	0.474	0.391
	Variance	3.757	6.000	4.217	0.001	0.003	0.002
	CV%	11.369	9.669	9.691	12.103d*	10.987e*	10.676f*
Plastic/Maica	Mean	17.238	25.238	21.238	0.311	0.472	0.391
	Variance	8.323	2.545	4.647	0.003	0.001	0.002
	CV%	16.736	6.321	10.150	17.744d*	7.139e*	10.920f*
Rubber	Mean	18.905	30.857	24.881	0.345	0.599	0.472
	Variance	23.138	7.698	13.673	0.009	0.004	0.006
	CV%	25.444a*	8.992	14.862	27.358d*	10.943e*	16.509f*

CV = coefficient of variance; "a*", "d*", "e*", and "f*" indicates Significant at $P \leq 0.05$: It suggests that the values have a wider spread around the mean, indicating more diversity or fluctuation.

Table 3 includes a number of materials that are frequently used for sliding surfaces, such as rubber, plywood/MDF, aluminum, perforated sheet, painted sheet, glass, stainless steel, galvanized iron, and plastic/Maica. Specifications for each surface material include the lowest, maximum, and average angles of inclination. Significant variance in the sliding behavior across the surfaces is indicated by the average angle of inclination, which varies from 18.929° (stainless steel) to 35.595° (perforated sheet). According to [Mohsenin \(1986\)](#), the angle of repose for common bean seed was determined to be between 27.1° and 35.4°, which are still below the maximum angle of repose of 45° for the majority of agricultural commodities. A lower range of values, from 6.073% to 16.736%, is indicated by the coefficient of variation for the angle of inclination, indicating reasonably consistent values within each surface material. The perforated sheet's average coefficient of friction is 0.786, whereas the average coefficient of friction for stainless steel is 0.345, indicating the considerable variation in frictional qualities between the surfaces. The coefficient of variation for the coefficient of friction varies more, from 6.945% to 32.644%, suggesting that there is more variety in the behavior of the friction within each surface material. The asterisk-designated CV% values ("a*", "d*", "e*", and "f*") in the table indicate statistical significance at the $p \leq 0.05$ level. In summary, this extensive table offers significant insights into *Phaseolus vulgaris*'s frictional characteristics on a range of sliding surface materials. These insights may find application in agricultural engineering, processing, and handling systems. In order to build and optimize handling and transportation systems for this agricultural commodity, it is vital to take into account the notable differences in the angle of inclination and coefficient of friction among the various surface types, as highlighted by the data.

CONCLUSION

In this study, the engineering properties of *Phaseolus vulgaris* seeds are determined that may provide opportunities to design construct and develop harvesting, handling, and processing machinery for *Phaseolus vulgaris* seeds by considering their physical and frictional characteristics. In this process, the gravimetric variables impact the exchange rate between heat and moisture, making them essential characteristics in drying and ventilation processes. The bulk density establishes the required amount of produce storage and the conveyor capacity. The true density of a material is considered throughout the separation process. The size of grain hoppers and storage equipment must be determined by taking into account the porosity. The engineering qualities of the agricultural materials are influenced by the moisture content, one gravimetric parameter. Designing affordable, efficient, and successful equipment requires an understanding of the characteristics of agricultural materials at varying moisture levels. Perforated sheet surfaces showed the highest static coefficients of friction, followed by rubber, plastic, plywood, glass, aluminum, galvanized iron, painted sheet, stainless steel and iron sheet surfaces. These data are frequently needed to establish a convenient reference required to develop equipment for handling, cleaning, storing, transporting, drying, and other processes, as well as for predicting loads in agricultural storage structures and resolving flow issues in agro-processing. More research ought to be done to investigate the enhanced *Phaseolus vulgaris* cultivars' moisture-dependent engineering characteristics.

ACKNOWLEDGMENTS

Biniam Zewdie Ghebrekidan, the author, expresses gratitude to the Department of Agricultural Engineering & Food Process Engineering from Awash Melkassa Agricultural Research Center; Haramaya University; and Science, Technology, Engineering, & Mathematics (ASTU STEM) CENTER, Chemistry laboratory from Adama science & Technology University for the provision of the improved common bean seed varieties and laboratory facilities, respectively.

DECLARATION OF COMPETING INTEREST

The author(s) must declare that they have no conflict of interest

CREDIT AUTHORSHIP CONTRIBUTION STATEMENT

Biniam Zewdie Ghebrekidan: Conceptualization (lead); Data curation (lead); Formal analysis (equal); Funding acquisition (equal); Investigation (equal); Methodology (equal); Resources (equal); Supervision (equal); Validation (equal); Writing-original draft (equal).

Adesoji Matthew Olaniyan: Data curation (equal); Methodology (equal); Supervision (equal); Writing-review & editing (equal).

Amana Wako Koroso: Investigation (equal); Supervision (equal); Writing-review & editing (equal).

Alemayehu Girma Tadesse: Data curation (lead); Formal analysis (equal); Writing-review & editing (equal).

Dereje Alemu Anawte: Formal analysis (equal); Investigation (equal); Methodology (equal); Validation (equal); Visualization (equal).

Tamrat Lema Nurgie: Conceptualization (equal); Software (equal); Supervision (equal); Writing-review & editing (equal).

ETHICS COMMITTEE DECISION

This article does not require any ethical committee decision.

REFERENCES

- Abera TA, Heiskanen J, Pellikka PK, Adhikari H and Maeda EE (2020). Climatic impacts of bushland to cropland conversion in Eastern Africa. *Science of the Total Environment*, 717: 137255. <https://doi.org/10.1016/j.scitotenv.2020.137255>
- Altuntaş E and Yıldız M (2007). Effect of moisture content on some physical and mechanical properties of faba bean (*Vicia faba* L.) grains. *Journal of Food Engineering*, 78(1): 174-183. <https://doi.org/10.1016/j.jfoodeng.2005.09.013>
- Amanuel T, Tadele T and Belay A (2022). Registration of milkesa, large-red seed food type common bean (*Phaseolus vulgaris*) varieties for Midland Areas of Bale and East Bale, Southeast Ethiopia. *Journal of Plant Sciences*, 10(1): 46-50. <https://doi.org/10.11648/j.jps.20221001.17>
- Amin MN, Hossain MA and Roy KC (2004). Effects of moisture content on some physical properties of lentil seeds. *Journal of Food Engineering*, 65(1): 83-87. <https://doi.org/10.1016/j.jfoodeng.2003.12.006>

- Amsalu B, Negash K, Shiferaw T, Tumssa K, Tsegaye D, Claude RJ and Mukankusi CM (2018). Progress of common bean breeding and genetics research in Ethiopia. *Ethiopian Journal of Crop Science*, 6(3): 15-26.
- Bako T and Aguda AC (2023). Effect of moisture content on the engineering properties of African yam bean (*Sphenostylis stenocarpa*) seed. *Journal of Horticulture and Postharvest Research*, 6(1): 15-26. <https://doi.org/10.22077/jhpr.2022.5285.1276>
- Baryeh EA (2002). Physical properties of millet. *Journal of Food Engineering*, 51(1): 39-46. [https://doi.org/10.1016/S0260-8774\(01\)00035-8](https://doi.org/10.1016/S0260-8774(01)00035-8)
- Bayano-Tejero S, Karkee M, Rodríguez-Lizana A and Sola-Guirado RR (2023). Estimation of harvested fruit weight using volume measurements with distance sensors: A case study with olives in a big box. *Computers and Electronics in Agriculture*, 205: 107620. <https://doi.org/10.1016/j.compag.2023.107620>
- Befikadu D (2018). Postharvest losses in Ethiopia and opportunities for reduction: A review. *International Journal of Sciences: Basic and Applied Research (IJSBAR)*, 38: 249-262.
- Betelhem A, Menbere B, Amsalu N, Ruelle ML, Alex M, Zemedu A and Zerihun W (2020). Diversity, use and production of farmers' varieties of common bean (*Phaseolus vulgaris* L., Fabaceae) in Southwestern and Northeastern Ethiopia. *Genetic Resources and Crop Evolution*, 67(2): 339-356. <https://doi.org/10.1007/s10722-019-00877-4>
- Bhise SR, Kaur A and Manikantan MR (2014). Moisture dependent physical properties of wheat grain (PBW 621). *International Journal of Engineering Practical Research*, 3(2): 40-45. <https://doi.org/10.14355/ijep.2014.0302.03>
- Cetin M (2007). Physical properties of barbutia bean (*Phaseolus vulgaris* L.). *Journal of Food Engineering*, 80(1): 353-358. <https://doi.org/10.1016/j.jfoodeng.2006.06.004>
- Chhabra N and Kaur A (2017). Studies on physical and engineering characteristics of maize, pearl millet and soybean. *Journal of Pharmacognosy and Photochemistry*, 6(6): 1-5.
- Degirmencioglu A and Srivastava AK (1996). Development of screw conveyor performance models using dimensional analysis. *Transactions of the ASAE*, 39(5): 1757-1763. <https://doi.org/10.13031/2013.27695>
- Degirmencioglu A, Mohtar RH, Daher BT, Ozgunaltay-Ertugrul G and Ertugrul O (2019). Assessing the sustainability of crop production in the Gediz Basin, Turkey: A water, energy, and food nexus approach. *Fresenius Environmental Bulletin*, 28(4): 2511-2522.
- Dereese W, Shimelis A and Belay D (2021). Geometric characteristics and mass-volume-area properties of haricot beans (*Phaseolus vulgaris* L.): Effect of variety. *International Journal of Food Properties*, 24(1): 885-894. <https://doi.org/10.1080/10942912.2021.1937210>
- Deshpande SD, Bal S and Ojha TP (1993). Physical properties of soybean. *Journal of Agricultural Engineering Research*, 56(2): 89-98. <https://doi.org/10.1006/jaer.1993.1063>
- Dubale B (2018). Postharvest losses in Ethiopia and opportunities for reduction: A review. *International Journal of Sciences: Basic and Applied Research (IJSBAR)*, 38: 249-262.
- Elijah O, Rahman TA, Orikumhi I, Leow CY and Hindia MN (2018). An overview of internet of things (iot) and data analytics in agriculture: Benefits and challenges. *IEEE Internet of things Journal*, 5(5): 3758-3773. <https://doi.org/10.1109/JIOT.2018.2844296>
- Emrani A and Berrada A (2023). Structural behavior and flow characteristics assessment of gravity energy storage system: Modeling and experimental validation. *Journal of Energy Storage*, 72: 108277. <https://doi.org/10.1016/j.est.2023.108277>
- Ertugrul Ö, Yilar M, Kır H and Kömekçi C (2022). Some physical, chemical, and germination properties of *Peganum harmala* L. seeds. *Journal of Food Process Engineering*, 45(2): e13967. <https://doi.org/10.1111/jfpe.13967>
- FAO (2020). Food and Agriculture Organization crop production and trade data, Available at <http://www.fao.org/faostat/en/#data/QC>, Access: October 19, 2023.
- FAOSTAT (2020). Food and agriculture data: Crops and livestock products. <https://www.worldatlas.com/articles/the-world-s-top-dry-bean-producing-countries>. Access: October 19, 2023.
- Fernando S (2021). Production of protein-rich pulse ingredients through dry fractionation: A review. *LWT*, 141: p.110961. <https://doi.org/10.1016/j.lwt.2021.110961>
- Fraser BM, Verma SS and Muir WE (1978). Some physical properties of faba beans. *Journal of Agricultural Engineering Research*, 23(1): 53-57. [https://doi.org/10.1016/0021-8634\(78\)90079-3](https://doi.org/10.1016/0021-8634(78)90079-3)

- Gupta RK, Arora G and Sharma R (2007). Aerodynamic properties of sunflower seed (*Helianthus annuus* L.). *Journal of Food Engineering*, 79(3): 899-904. <https://doi.org/10.1016/j.jfoodeng.2006.03.010>
- Haciseferoğulları H, Gezer İ, Bahtiyarca Y and Mengeş HO (2003). Determination of some chemical and physical properties of Sakız faba bean (*Vicia faba* L. Var. major). *Journal of Food Engineering*, 60(4): 475-479. [https://doi.org/10.1016/S0260-8774\(03\)00075-X](https://doi.org/10.1016/S0260-8774(03)00075-X)
- Isik E and Unal H (2011). Some engineering properties of white kidney beans (*Phaseolus vulgaris* L.). *African Journal of Biotechnology*, 10(82): 19126-19136. <https://doi.org/10.5897/AJB11.1341>
- Jahanbakhshi A (2018). Determine some engineering properties of snake melon (*Cucumis melo* var. flexuosus). *Agricultural Engineering International: CIGR Journal*, 20(1): 171-176.
- Kakade A, Khodke S, Jadhav S, Gajabe M and Othzes N (2019). Effect of moisture content on physical properties of soybean. *International Journal of Current Microbiology and Applied Sciences*, 8(4): 1770-1782. <https://doi.org/10.20546/ijcmas.2019.804.206>
- Kefelegn N, Mekibib F and Dessalegn Y (2020). Genetic advancement and variability of released common bean (*Phaseolus vulgaris* L.) varieties from 1974–2009 GC in Ethiopia. *Advances in Agriculture*, 2020, 1-7. <https://doi.org/10.1155/2020/1315436>
- Kumar N and Sharma AK (2021). Study on engineering properties of chickpea (*Cicer arietinum*) seeds in relation to design of threshing mechanism. *The Pharma Innovation*, 10(9): 455-458.
- Mirzabe AH, Khazaei J, Chegini GR and Gholami O (2013). Some physical properties of almond nut and kernel and modeling dimensional properties. *Agricultural Engineering International: CIGR Journal*, 15(2): 256-265.
- Mohsenin NN (1986). Physical properties of plant and animal materials: structure, physical characteristics and mechanical properties (2. rev. and updated ed). *New York: Gordon and Breach Science Publisher*.
- Mpotokwane SM, Gaditlhatlhelwe E, Sebaka A and Jideani VA (2008). Physical properties of bambara groundnuts from Botswana. *Journal of Food Engineering*, 89(1): 93-98. <https://doi.org/10.1016/j.jfoodeng.2008.04.006>
- Nciri N, El-Mhamdi F, Ismail HB, Mansour AB and Fennira F (2014). Physical properties of three white bean varieties (*Phaseolus vulgaris* L.) grown in Tunisia. *Journal of Applied Science and Agriculture*, 9(11 Special): 195-200.
- Omobuwajo TO, Akande EA, and Sanni LA (1999). Selected physical, mechanical and aerodynamic properties of African breadfruit (*Treculia africana*) seeds. *Journal of Food Engineering*, 40(4): 241-244. [https://doi.org/10.1016/S0260-8774\(99\)00060-6](https://doi.org/10.1016/S0260-8774(99)00060-6)
- Ozturk I, Kara M, Yildiz C and Ercisli S (2009). Physico-mechanical seed properties of the common Turkish bean (*Phaseolus vulgaris*) cultivars ‘Hinis’ and ‘İspir’. *New Zealand Journal of Crop and Horticultural Science*, 37(1): 41-50. <https://doi.org/10.1080/01140670909510248>
- Önal İ and Ertuğrul Ö (2011). Seed flow and in-row seed distribution uniformity of the top delivery type fluted roller for onion, carrot and canola seeds. *Journal of Agricultural Sciences*, 17: 10-23.
- Pawar P, Shinde V, Raut A, Suke S, Kolpe K and Manna A (2023). An automated combined system for crop prediction and yield prediction using deep hybrid learning technique. In 2023 7th International Conference on Computing, Communication, Control and Automation (ICCUBEA) (pp. 1-5). IEEE.
- Sahin S and Sumnu SG (2006). Physical properties of foods: Springer science & Business media. *Journal of Applied Science and Agriculture*, 9(1):185-200.
- Samrawit T (2023). Design and numerical analysis of rice grading machine for Ethiopian rice varieties (Doctoral dissertation, Bahir Dar University).
- Saparita R, Hidajat DD and Kuala SI (2019). Statistical analysis on the geometric, physical and mechanical properties of dried robusta coffee cherry resulting from natural system processing. *In IOP Conference Series: Earth and Environmental Science*, 251(1): 012041. <https://doi.org/10.1088/1755-1315/251/1/012041>
- Singh RP and Heldman DR (2009). Psychrometrics. In Introduction to Food Engineering, 4th ed, ed. R. P. Singh, and D. R. Heldman, 9, 571-593. Burlington, MA, USA: Academic Press.
- Sirisomboon P, Kitchaiya P, Pholpho T and Mahuttanyavanitch W (2007). Physical and mechanical properties of *Jatropha curcas* L. fruits, nuts and kernels. *Biosystems Engineering*, 97(2): 201-207. <https://doi.org/10.1016/j.biosystemseng.2007.02.011>
- Sundaram PK, Singh AK and Kumar S (2014). Studies on some engineering properties of faba bean seeds. *Journal of AgriSearch*, 1(1): 4-8.

- Tekalign A, Tadesse T and Asmare B (2022). Registration of Hora, small-red seed food type common bean (*Phaseolus vulgaris*) varieties for Midland Areas of Bale and East Bale, Southeast Ethiopia. *Plant*, 10(1): 36-39. <https://doi.org/10.11648/j.jps.20221001.17>
- Wodajo D, Admassu S and Dereje B (2021). Geometric characteristics and mass-volume-area properties of haricot beans (*Phaseolus vulgaris* L.): Effect of variety. *International Journal of Food Properties*, 24(1): 885-894. <https://doi.org/10.1080/10942912.2021.1937210>



Turkish Journal of
Agricultural
Engineering Research
(Turk J Agr Eng Res)
e-ISSN: 2717-8420



Development of a Solar-Powered Barley Sprouting Room

Ahmed Shawky EL-SAYED^{a*} , AbdelGawad SAAD^a ,
Mohamed Ali Ibrahim AL-RAJHI^b , Maisa Moneir MEGAHED^a 

^aDepartment of Agricultural Bioengineering Systems, Agricultural Engineering Research Institute (AENRI),
Agricultural Research Center (ARC), Dokki, Giza, EGYPT

^bDepartment of Mechanization of Livestock and Fish Production, Agricultural Engineering Research Institute
(AENRI), Agricultural Research Center (ARC), Dokki- Giza, EGYPT

ARTICLE INFO: Research Article

Corresponding Author: Ahmed Shawky EL-SAYED, E-mail: ahmedshawkyelsayed85@gmail.com

Received: 13 April 2024 / **Accepted:** 28 May 2024 / **Published:** 30 June 2024

Cite this article: El-Sayed AS, Saad A, Al-rajhi MAI and Megahed MM (2024). *Development of a Solar-Powered Barley Sprouting Room. Turkish Journal of Agricultural Engineering Research, 5(1): 94-116.*
<https://doi.org/10.46592/turkager.1467904>

ABSTRACT

The study aims to develop a sprouting room for barley powered by solar energy instead of traditional alternating-current rooms to suit remote areas. The cooling, lighting, and irrigation systems were developed and replaced with another that operates on 12 V DC. An air-cooling device based on the Peltier module has been developed as an alternative to air conditioning devices. Four cooling units of the air cooler were tested with three lighting durations of 6, 9, and 12 h and three irrigation rates of 1.7, 1.85, and 2 m³ ton⁻¹. The measurements included evaluating the performance of the developed air cooler device. The vegetative and quality characteristics and a chemical analysis of sprouted barley for the solar-powered room compared to the room before the modification was estimated. The solar room's productivity and electrical energy consumption rates were calculated, and an economic evaluation of the development was conducted. The maximum electrical power consumption for the solar-powered sprouting room was 63.275 kWh ton⁻¹, compared with 117.19 kWh ton⁻¹ for the alternating current-managed room before modification. The interaction between the DC air cooling, lighting and irrigation used achieved standard rates for the vegetative and quality characteristics of the barley produced. The maximal productivity from sprouted barley was 1.22 tons per 7 days with an increment ratio over control of 31.97%. The net earnings for the developed sprouting room were maximized relative to the significant decrease in electrical production costs. The developed sprouting room fits the livestock sector by providing good economical alternative fodder sources.

Keywords: Arduino, Controller, Cooler, Panel, Remote, Strips



INTRODUCTION

Addressing the rising demand for food and livestock feed, particularly in urban areas, is crucial, with the global population expected to reach 10 billion by 2050 ([Ghorbel *et al.*, 2021](#)). This increase will also drive higher demands for energy and water resources which are inevitably interrelated ([Degirmencioglu *et al.*, 2019](#)). Hydroponic systems offer efficient, high-moisture forage production methods, especially valuable in arid desert regions facing fodder scarcity like Egypt ([Mariyappillai *et al.*, 2020](#)). Barley sprouting via hydroponic systems ensures a steady supply of green fodder, conserving water, reducing labor, and minimizing reliance on chemical inputs. This paper explores managing barley sprouting rooms with solar-powered solutions, offering a sustainable approach to meet modern agriculture's evolving demands.

The benefits of barley sprouts for year-round green fodder production underscore their significance in sustainable agriculture. Compared to conventional methods, barley sprouting requires approximately 80% less water and typically lasts only 7-8 days ([Farghaly *et al.*, 2019](#)). Additionally, 50 m² of sprouting rooms yield the same productivity as 2.94 hectares of alfalfa cultivation annually ([Hegab, 2018](#)). Barley sprouts provide nutrient-rich forage options, particularly beneficial for ruminants such as cattle, sheep, and goats due to their protein, vitamin, and enzyme content ([Helal, 2015](#)). Protein-rich fodder can strain breeders financially. Additionally, the pesticide-free nature of sprouted fodder enhances animal immunity, reduces disease risk, and helps alleviate thirst, especially in the summer ([Basko, 2009](#)). Unlike concentrated feed, Barley sprouts' natural yeasts aid in cellulose digestion without causing bloating or acidity in animals, leading to improved animal specifications, fertility, and reproduction rates ([Izydorczyk and Edney, 2017](#)).

However, constructing sprouting rooms poses financial challenges for small-scale breeders, necessitating innovative cost-reducing solutions while maintaining production quality. These rooms rely on hydroponic systems, requiring artificial factors such as lighting, irrigation, and temperature control, which can escalate production costs due to electricity consumption and fuel expenses for generators in areas without electricity ([Basko, 2009](#)). Hydroponic systems are essential in barley sprouting rooms, yielding ample plant material quickly. [Kumari *et al.* \(2018\)](#) also discovered that incorporating fresh barley sprouts into livestock diets can enhance health, reduce heat stress, and improve birth rates. Technological advancements in sprouting methods have enhanced economic competitiveness, which is crucial in regions with limited forage production ([Adegbeye *et al.*, 2020](#)).

Precise water and nutrient level control is crucial to managing increasing costs and securing expected profits. [Dung *et al.* \(2010\)](#) maintained a consistent temperature of 25°C and continuous lighting over a 7-day barley sprouting period using a hydroponic unit in a temperature-controlled environment, employing fluorescent lamps with an average light intensity of about 615 lux. The results showed fresh sprouts weighed about 3.7 times their pre-steeped weight after seven days. For optimal synthesis and release of plant bioactive compounds, longer sprouting durations (3 to 5 days) and higher processing temperatures (25 to 35°C) are usually necessary. Nutritional changes during sprouting offer various health benefits ([Lemmens *et al.*, 2019](#)). Proteins convert into essential amino acids, carbohydrates into sugars, and fats into essential fatty acids. This enzymatic activity

increases, enhancing digestibility compared to dry seeds ([Shit, 2019](#)). Producing hydroponic green forage through sprouting takes 8-15 days and minimal land ([Bazeley and Hayton, 2013](#); [Gebremedhin, 2015](#)). From one kilogram of seeds, approximately 6 to 10 kilograms of fresh green sprouts can be generated annually ([Soufan *et al.*, 2023](#)). These sprouts, consisting of germinated seeds with intertwined roots and green shoots, are consumed entirely by livestock. Barley seeds, being affordable and widely available, are preferred. They maintain a crude protein content of 16-17% with over 85% in vitro digestibility, and high levels of vitamin E and beta-carotene, promoting animal fertility ([Atlas, 2004](#)). Hydroponic fodder production drastically reduces water usage. For instance, it requires about 3 liters of water per kilogram of fresh hydroponic feed, compared to 73 liters under conventional field conditions ([Sharma *et al.*, 2018](#); [Ramteke *et al.*, 2019](#)).

Hydroponic techniques are recognized as a successful alternative for sustainable livestock farming ([Ramteke *et al.*, 2019](#)). The chemical composition of hydroponically germinated barley fodder is influenced by the harvesting duration, with the seventh day identified as optimal ([Akbag *et al.*, 2014](#)). Chlorophyll indicates nitrogen levels in plants, which is crucial for plant health ([Marsh, 2016](#)). Sprouting under net houses yields superior physical characteristics and chemical analysis. However, high construction costs for sprouting rooms hinder widespread adoption, particularly in Egypt. The high expenses for temperature control, lighting, and irrigation, which are reliant on electrical power, significantly raise production costs. The high electricity consumption of sprouting rooms increases production expenses and burdens owners ([Alrajhi and Elsayed, 2023](#)). Power outages also lead to substantial losses from sprouted barley spoilage. In the remote areas sprouting rooms, owners must buy electric generators, which are considered additional costs due to their cost, fuel prices, and environmental pollution from combustion exhausts. The use of solar energy to manage sprouting rooms is considered a new matter that can be relied upon to save electrical energy consumption and achieve sustainable agricultural development.

Therefore, the research aims to manage barley sprouting rooms with solar energy to operate alternative DC-developed cooling, lighting, and irrigation systems using solar-powered energy stored in rechargeable batteries to fit remote areas lacking electricity sources. The objectives include: 1) Developing a DC air cooler device and electronic circuit for the automatic control of the cooling, lighting, and irrigation systems in the sprouting room. 2) Studying the engineering production factors influencing the efficiency of the developed sprouting rooms. 3) Conducting an economic analysis of the developed system compared to the pre-developed sprouting room.

MATERIALS and METHODS

Experimental procedure

Experiments were conducted in the barley solar-powered sprouting room on the barley (*Hordeum vulgare* L.) variety Giza 133 from November 2023 to March 2024. The experiments were conducted on a private farm in the Qalabsho city of Dakahlia Governorate, with coordinates 31° 43' 08" and 31° 32' 55". This desert area was

chosen to conduct experiments on the solar-powered barley sprouting room. The average hours of daily solar radiation during the experimental period ranged from 9.2 to 10 hours per day at an average temperature of 25°C and a relative humidity of 75%. The experiments were conducted in a completely randomized block design using five experimental replicates. A barley grain amounting to 625 kg was used to produce 5 tons of sprouted barley. A primary experiment was done to test the developed DC air cooler device separately under the effect of using four levels for cooling units (C1, C2, C3, and C4) with four settled air temperatures (T1, T2, T3, and T4) of 20, 21, 22, and 23°C. The developed solar-powered sprouting room experiments included testing four cooling unit levels for the developed air cooler (C1, C2, C3, and C4). Three durations of the developed LED lighting system were tested (L1, L2, and L3) at 6, 9, and 12 h per day. Three different irrigation rates of the developed irrigation system (I1, I2, and I3) of 1.7, 1.85, and $\text{m}^3 \text{ton}^{-1}$ were tested.

General description

The solar-powered sprouting room

A solar-powered barley sprouting room has been developed. All electrical systems operate with 12 volt direct current, as shown in Figure 1. The developed room is suitable for sprouting barley in remote areas without a local electricity network. Dual solar panels (12V-100W), a charging circuit, and dual electrical DC batteries (12V-120A) were installed to operate the developed sprouting room, as shown in Figure 1. A closed room was used for sprouting barley with geometric dimensions of 6 m long, 2.75 m wide, and 2 m high, which produces 1 ton of sprouted barley weekly. All AC 220 volts, 50-60 Hz air conditioners, irrigation pumps, and lighting systems were replaced. A developed air cooling device that operates on 12V DC was utilized (Figure 1, No. 2). Fluorescent white LED strips run with 12V DC (24W per reel length of 5 m) were also installed for lighting the solar bowered sprouting room, as shown in Figure 1, No. 7. The LED strip width was 12 mm. The LED type was SMD 5050, with a brightness of 670 lm m^{-1} . The used LED strip type has a life span of 50000 h, a LED density of 60 LEDs m^{-1} , and ambient working temperatures of -20 to +45 °C. Brushless DC water pumps model 1238-B operate on a direct current of 12 V, as shown in Figure 1, No. 5. The used pump body size is 37.5*35*25.5mm (length*width*height), with a net weight of 66 g. The water pump has a maximum flow rate of 240 L h^{-1} , a maximum power consumption of 3.6 W (0.35 A), a maximum height lift of 3 m, and a lifespan of 30,000 hours. A sprinkler irrigation network hose equipped with equally distributed sprinklers was fixed over the sprouting trays, as shown in Figure 1, No. 6.

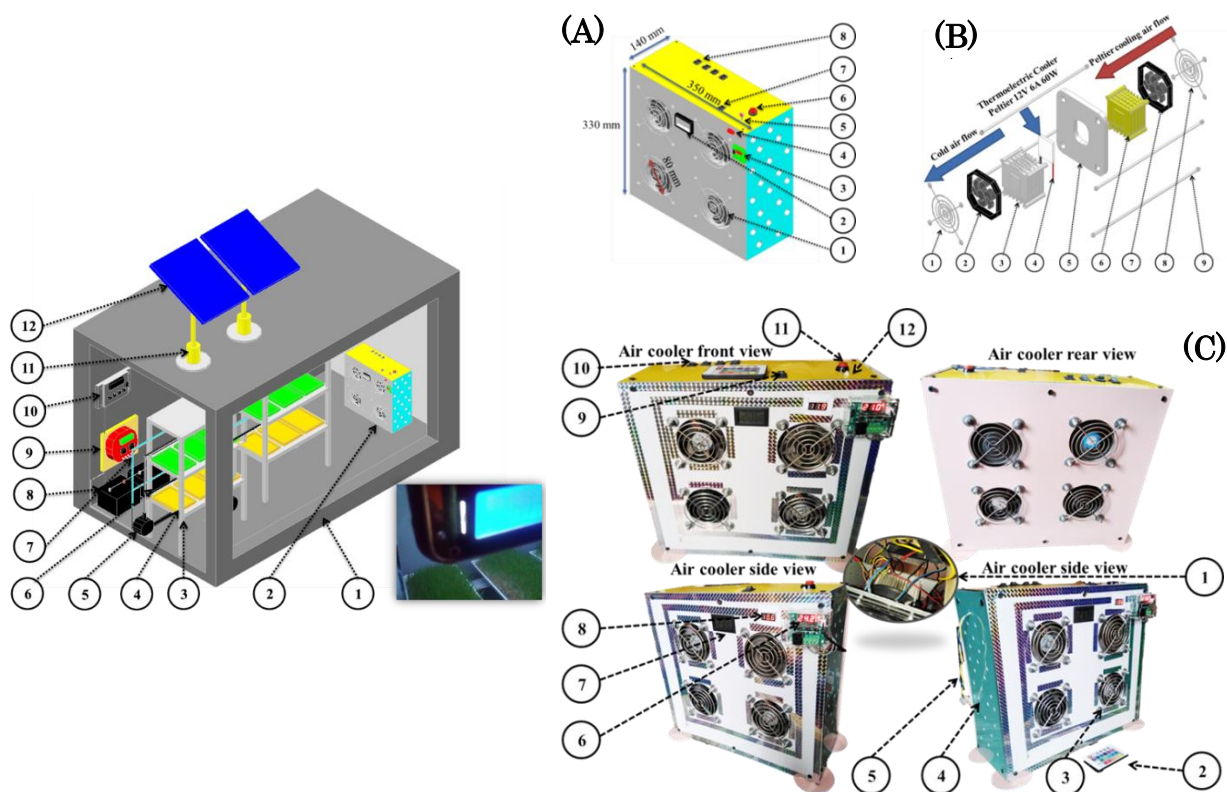


Figure 1. Isometric view of the solar-powered sprouting room.

(1-sprouting room; 2-developed DC air cooler device; 3-barley rack holder; 4-barley racks; 5-DC water pump; 6-water nozzles hose; 7- LED strip lights; 8- DC 12V & 120A batteries; 9-arduino controller; 10-solar charger controller; 11- solar guidance motor; 12- 12V &100 W solar panel).

Figure 2. The developed DC air cooler device.

(A) Air cooler isometric view: (1- air cooling unit; 2- digital thermostat; 3- temperature controller W1209; 4- volt indicator; 5- infrared receiving lens; 6- temperature controller press switch; 7- main on/off switch; 8- cooler unit switches); (B) the cooler forming unit: (1-shield mesh; 2-cold air exit fan; 3-aluminum heat sink; 4-peltier module; 5- fiberboard peltier holder; 6-copper heat sink; 7-peltier cooling fan; 8-shield mesh; 9-screw) and (C) air cooler views: (1-inlet cooler unit; 2-remote control; 3-shield mesh; 4-air vents; 5- power supply cable; 6-temperature controller W1209; 7-digital thermostat; 8-volt indicator; 9-main on/off switch; 10-cooler unit switches; 11-temperature controller press switch; 12-infrared receiving lens).

Solar power supply components

Two 100 W solar panels with an open and maximum circuit voltage of 21.6 and 17.3 V were used to supply the sprouting room with electrical energy. The solar panels were fixed on the top room surface, as shown in Figure 1. The short circuit and working current for the solar panels were 6.17 and 5.78 A, respectively, with an output tolerance of $\pm 3\%$. The working temperature range for the solar panels was -40 to $+80^{\circ}\text{C}$. The solar panels were connected in parallel, as shown in Figure 1, No. 12. Every solar panel was mounted by a rotating hollow shaft holder that followed the sun's rays using a solar guidance motor, as shown in Figure 1 No. 11. A solar charger controller (Figure 1, No. 10) with a capacity of 20 A and an overcharge protection range of 14.4 to 28.8 V was used to save the generated electrical energy to dual DC batteries (12V and 120A), as shown in Figure 1, No. 8. The solar charger controller and the DC batteries were fixed inside the sprouting room, as shown in Figure 1. The two dual solar panels (200W) generated 16.67A, which was enough to

operate the sprouting rooms' DC electrical systems for lighting, cooling, and irrigating.

The developed DC air cooler device

The air cooler device cools the barley sprouting room instead of using an air conditioner. As shown in Figure 2A, the geometric dimensions of the developed air cooler device are 350 mm wide, 330 mm long, and 140 mm thick. The air cooling device weighs 5200 g. The air-cooling device consumed power of 0.255 kW and 12 V DC at entire unit operation. The air cooler device is in the shape of a rectangular box and is easy to move inside the sprouting room according to the position of the sprouted barley tray holder. The outer frame of the air-cooling device is made of 5 mm-thick compressed fiber and is lined with aluminum panels on both sides to resist moisture and heat.

Figure 2C No. 4, shows that the air cooler device is equipped with side ventilation holes to prevent the internal components from heating up. The cooler device contains four separate air cooling units to distribute cold air, each of which can be operated separately. Every air cooling unit consumed 0.06 kW and 12 VDC. As in Figure 2C No. 10, there are four buttons to operate the cooling units. Each air cooling unit, as shown in Figure 2B, consists of a pair of fans, a pair of cooling heat sinks, a peltier, two shield meshes, and four screws. Each 12V, 6A, 60W (40×40 mm) peltier module unit (Figure 2B No. 4) is installed inside a square perforated fiberboard holder 120 mm long and 5 mm thick (Figure 2B No. 5). The hot side of the peltier is installed opposite the copper heat sink (Figure 2B No. 6) because the heat transfer coefficient of copper is higher.

Therefore, the hot side of the peltier is cooled efficiently. The peltier cooling fan is installed opposite the copper heat sink. It draws air internally into the copper heat sink to cool the peltier so that its temperature does not exceed 38°C (Figure 2B No. 7). The aluminum heat sink and cold air cooling fan are installed from the cold side of the peltier, as shown in Figure 2B, No. 2 and 3. Circular holes with a diameter of 80 mm were made to install the cooling units in the air cooling device, as shown in Figure 2A. The used fans have a diameter of 120 mm and a 25 mm depth, a rotation speed of 2000 RPM, an operating voltage of 12V (0.3A; 3.6W), and an airflow of 65.41 m³ h⁻¹ with a noise level of 36 dBA. Each cooling unit was installed using four 7-mm screws with a length of 140 mm axially, as shown in Figure 2B No. 9. A pair of shield meshes were used on the cooling units, front and back, as in Figure 2B No. 1 and 8.

The operation of the air cooling device is controlled using the remote control (Figure 2C No. 2). An infrared receiving circuit was installed to operate the device, as shown in Figure 2C No. 12. The infrared receiving lens was installed on top of the air cooling device, as shown in Figure 2A No. 5. A voltage indicator (Figure 2C No. 8) has been installed to show the electrical voltage consumed during operation. A thermal controller, model W1209, was used to control the cooling temperatures of the device, as shown in Figure 2C No. 6. The probe for the thermal controller was installed internally and connected to the aluminum heat sink for cooling. The temperature controller W1209 has measurement control accuracy with 0.1 runs at 12 V (0.42 W) and is supplied with a one-channel relay module with a capacity of 10 A. Room cooling temperatures can be controlled from 21 to 23 °C by programming

the temperature controller using its buttons. There is a separate red button (Figure 2A No. 6) to operate the thermal controller. A main button to turn off and turn on the cooling device was used, as shown in Figure 2A No. 7. A digital air thermostat was installed to indicate the room temperatures, as shown in Figure 2C No. 7.

Arduino controller

The operating timing of the irrigation pumps and LED light strips was controlled using an electronic control board with an Arduino, as shown in Figure 3. The Arduino controller consumes electrical power of 1.5 W. The Arduino controller circuit contains a pair of 12V, 125A relays to connect and disconnect the continuous electrical current for the irrigation and lighting systems. The Arduino Nano microcontroller circuit is programmed to control operating time ranges to minimize human intervention. The electronic controller has a digital screen that shows the room's operating programs that can be changed as needed, as shown in Figure 3. The number of used lightning LED strips, irrigation pumps, and other operating electrical systems for electrical energy consumption is listed in Table 1.

Table 1. Solar-powered sprouting room operating systems electrical power consumption.

Sprouting room operating systems	Consumed energy; W	Used system units numbers	Operating period; h day ⁻¹	Total consumed energy; kW.h day ⁻¹	Total consumed energy; kW.h ton ⁻¹ (7 days)
1 Lightening LED strip (5 m length)	24	10	6; 9 and 12	1.44; 2.16 and 2.88	10.08; 15.12 and 20.16
2 Irrigation pump	3.6	7; 8 and 9	1	0.0252; 0.0288 and 0.0324	0.177; 0.202 and 0.227
3 Air cooler device 1, 2, 3 and 4 cooling units	63.75, 127.5, 191.25 and 255	1	24	1.53; 3.06; 4.59 and 6.12	10.71; 22.12; 32.13 and 42.84
4 Arduino controller	1.5	1	24	0.036	0.252
Consumed electrical energy in the solar-powered sprouting room				Maximum: 63.275 kW.h ton ⁻¹ Minimum: 21.219 kW.h ton ⁻¹	
Consumed electrical energy in the traditional AC sprouting room				117.19 kW.h ton ⁻¹	
Reduction ratio in the consumed energy				46.01 to 81.89%	

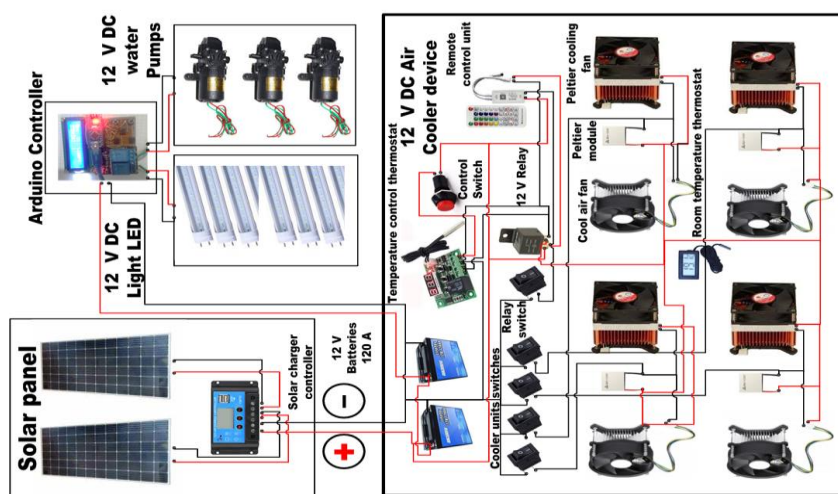


Figure 3. Schematic drawing for the electrical circuit for the solar-powered sprouting room.

Measurements

Air cooler device performance evaluation

Precise sensors were positioned throughout the sprouting chamber, over the barley sprouting trays, and between the racks to measure the temperature distribution therein. A data logging system allowed for real-time monitoring and continuous temperature recording. The cooling load was determined according to Equation 1. ([Remeli *et al.*, 2020](#))

$$Q = UA(T_o - T_i) + Q_{int} + Q_{sol} + Q_{vent} \quad (1)$$

$$Q_{vent} = \rho \times Cp \times V \times (T_o - T_i) \quad (2)$$

Where: Q is the total cooling load in Watt; U is the overall heat transfer coefficient $W m^{-2}K^{-1}$; A is the cooling surface area in m^2 ; T_i is the desired room temperature in $^{\circ}C$; T_o is the outside temperature in $^{\circ}C$; Q_{int} is the internal gain heat, W; Q_{sol} is the gain solar heat, W; Q_{vent} is the ventilation heat gains or losses due to air changes, W; ρ is the density of air, $1.225 kg m^{-3}$ at sea level; Cp is the specific heat capacity of air $1005 J kg^{-1}C^{-1}$; V is the volume of exchanged air, $m^3 h^{-1}$.

The energy efficiency ratio (EER) for the developed DC air cooler device was estimated as presented in Equation 3.

$$EER = \frac{q_c}{E} \quad (3)$$

Where: q_c is the output cooling energy, Btu; E is the electrical energy consumption Watt-hour; Wh.

The coefficient of performance (COP) of the peltier air cooling units was determined from Equation 4 ([Parmar *et al.*, 2022](#)).

$$COP = \frac{Q_c}{P_{el}} \quad (4)$$

Where: Q_c is the heat absorbed on the cold side, Btu; P_{el} is the input power, kW.

Lighting Intensity LI (lux):

Using a calibrated spectrometer, lighting intensity, expressed in lux, measures the quantity of light that reaches a surface inside the cultivation area, according to [Grubisic *et al.* \(2018\)](#).

Lighting Uniformity LU (%):

The cultivation area's uniformity of light distribution is evaluated by lighting uniformity. The coefficient of variation (CV), which is determined by dividing the standard deviation by the mean of light intensity as given in Equation (5), is used to quantify the lighting uniformity percentage, according to [Asiabanpour *et al.* \(2018\)](#).

$$CV = \frac{\sigma}{\mu} \times 100\% \quad (5)$$

Where: σ is the standard deviation of light intensity measurements; μ is the mean of light intensity measurements; and CV is the coefficient of variation, expressed as a percentage.

Vegetative characteristics of barely sprouted yield

Following an 8-day seeding period, the freshly sprouted barley was harvested, and measurements were taken of the root and shoot lengths (cm), total fresh and dry yields (kg m^{-2} and kg m^{-2}), the conversion factor (kg kg^{-1}) [the ratio of the produced yield to the initial planted seed weight], and chlorophyll content (mg m^{-2}). A digital atLEAF model chlorophyll meter was used to measure the amount of chlorophyll.

Chemical and quality analysis of barely sprout yield

Fresh samples (leaves and roots) were gathered, weighted, and oven-dried for 48 hours at 70°C in an air-forced oven before being stored for chemical analysis. As per [Jones and Case \(1990\)](#), powdered dried samples were digested in H_2SO_4 to identify their nitrogen content, which was then calculated using the Kjeldahl method. N was multiplied by 5.83 to determine the crude protein ([Merrill and Watt, 1955](#)). Samples were burned for four hours at 550°C in a muffle furnace (Protherm, PFL 110/10 MODEL), according to [AOAC \(1990\)](#) to ascertain the amount of ash. Flame photometry was used to determine potassium ([Ryan 1996](#)).

Productive (P), ton

The productivity of the constructed solar-powered sprouting room per ton during the seven-day sprouting period was estimated in order to evaluate the efficacy of the system modifications.

Specific energy consumption (SE), kW.h ton⁻¹

The generated energy from the used solar panels was estimated for the sprouting room as presented in Equation 6 ([Sharma and Puri, 2023](#)). The electrical daily power consumption rates (kW.h day^{-1}) were determined for each operating system in the developed solar-powered sprouting rooms (cooling, lighting, and irrigation). Then, the total electrical power consumed during the production of 1 ton of sprouted barley over seven days was estimated as presented in Equation 7 ([Hunt, 1983](#)).

$$E = A \times r \times H \times PR \quad (6)$$

$$SE = \frac{\text{consumed power (kW.h)}}{\text{Productivity (Ton.h}^{-1})} \text{ kW.h ton}^{-1} \quad (7)$$

Where: E = energy, kWh; A = total solar panel area, m^2 ; r = solar panel yield or efficiency; %; H = annual average solar radiation on titled panels (shaded, not included); PR = performance ratio (coefficient for losses) (0.75).

Cost economic analysis

The production cost (Pr. C) estimation for producing 1 ton from sprouted barley in the developed solar-powered sprouting room was determined as presented in Equation 8. The total operating costs, which included all production costs (grains

cost + electrical power cost + repair and maintenance cost + interest cost + depreciation cost + taxes and insurance costs + labor costs + development price/10 years), were estimated. The production cost for the developed solar-powered sprouting room was compared with the traditional AC sprouting room before the development to calculate the cost reduction ratio (R.C) as presented in Equation 9. (Oida, 1997)

$$Pr.C = \frac{\text{Total operating costs USD}}{\text{Productivity ton}} \text{ USD ton}^{-1} \quad (8)$$

$$R.C = \frac{Pr.C_2 - Pr.C_1}{Pr.C_2} \times 100 \quad (9)$$

Where: $R.C$ = the cost reduction ratio, %; $Pr.C_1$ & $Pr.C_2$ = the developed and traditional sprouting room production costs, USD ton^{-1} .

Profit net earn (NE) for the developed managed sprouting room was determined from Equation 10.

$$NE = \text{Total production costs per ton} - \text{production price per ton USD} \quad (10)$$

Statistical analysis

The experimental data was analyzed using Costat 2019, SPSS 2020, and Minitab 2020. An ANOVA was conducted to measure the interaction between the experimental variables and their effect on the selected measurements at a significance probability of $P < 0.05$. The least significant difference (LSD) was estimated at 0.05 for all variables. Linear regression analysis was performed to derive linear regression equations to determine the experimental variables that most influenced the measurements.

RESULTS AND DISCUSSION

Air cooler device performance evaluation

The forming units of the developed air cooler were tested before assembling the integrated electrical systems. The device was designed based on the cooling needs of the newly developed barley sprouting room. Figure 4 displays the effect of operating the number of cooling units in the developed air-cooling device and their impact on the sensing temperatures inside the sprouting room. There is a proportional relationship between the number of air-cooling units used and the sensing temperatures. The more cooling units are used, the smaller the difference between the perceived temperatures and the temperatures set by the digital thermostat.

The air cooler device was tested at four temperatures: 20, 21, 22, and 23 °C, which is considered the appropriate temperature range for the barley sprouting room, in agreement with Lin *et al.* (2009). There are five different types of temperatures measured inside the sprouting room. The sensing temperature (ST) is the mean temperature measured by a group of thermal sensors distributed within the room and connected to the data logger. The air cooler device sets a temperature CT that could be adjusted from 20 to 23 °C according to the needs of the sprouting room. The device thermostat temperature DT is measured by the built-in digital thermostat of

the air cooler device. The ambient air temperature (RT) inside the sprouting room is the average temperature of the atmospheric air during the cooling process. The temperature over the barley trays (TRT) is the average temperature over the barley trays. The temperature between the sprouting tray racks (KT) is the average between the sprouting rack stands. When cooling units increase, there is a direct proportional relationship between DR, TR, TRT, and KT. The cooling efficiency increases exponentially when the temperature controller is set at 20 °C. The energy efficiency ratio of the developed air cooling device, EER, was measured at 1.76 when the device was fully operational, while the efficiency coefficient for the cooling units, COP, was 0.516.

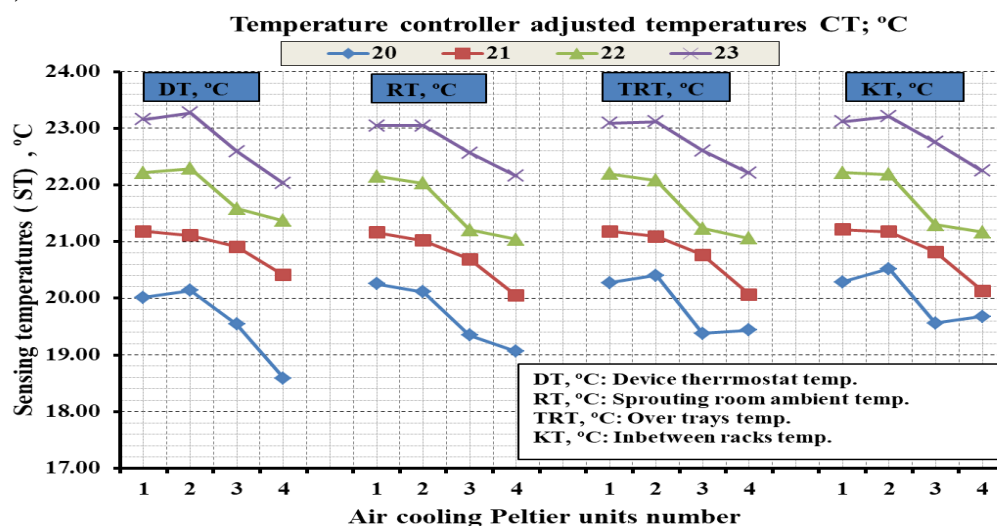


Figure 4. The effect of air cooling Peltier units on the sensing temperatures in the solar-powered sprouting room.

Table 2. The different temperature differences inside the solar-powered sprouting room.

CT °C	ΔDT °C				ΔRT °C			
	1	2	3	4	1	2	3	4
20	+0.02	+0.14	-0.46	-1.41	+0.26	+0.11	-0.65	-0.4
21	+0.18	+0.11	-0.09	-0.59	+0.16	+0.02	-0.31	-0.95
22	+0.22	+0.29	-0.42	-0.63	+0.15	+0.03	-0.8	-0.96
23	+0.15	+0.27	-0.41	0.03	+0.05	-0.43	-0.43	-0.84
	ΔTRT °C				ΔKT °C			
20	+0.27	+0.4	-0.62	-0.56	+0.29	+0.52	-0.44	-0.32
21	+0.18	+0.09	-0.33	-0.93	+0.21	+0.18	-0.18	-0.87
22	+0.2	+0.08	-0.77	-0.94	+0.22	+0.19	-0.70	-0.83
23	+0.09	+0.12	-0.39	-0.79	+0.12	+0.21	-0.25	-0.75

Where: CT: temperature controller adjusted temperature°C; AC unit N.: the used air cooling units number; ΔDT °C: the difference between CT (thermocontroller temp.) and DT (device thermostat temp.); ΔRT °C: the difference between CT (thermocontroller temp.) and RT (ambient sprouting room temp.); ΔTRT °C: the difference between CT (thermocontroller temp.) and TRT (over sprouting trays temp.); ΔKT °C: the difference between CT (thermocontroller temp.) and KT (inbetween racks temp.).

As listed in Table 2, the cooling efficiency improves significantly when the cooling units used are increased by 3 and 4 units, respectively. The negative differences between the temperature differences at which the device was set show a significant improvement in of air cooling efficiency. This is due to the difference in the accuracy and sensitivity of the electronic components. All positive and negative differences did not exceed the correct ones for the temperatures. This is due to adjusting the current intensity, the voltage difference used, and the power needs of the cooling device at the standard level in agreement with [Buchalik and Nowak \(2022\)](#); [He *et al.* \(2024\)](#).

Lighting intensity and uniformity

Figure 5 shows the effect of the number of cooling units used at the lighting levels and irrigation rates tested on both the intensity and uniformity of lighting inside the solar-powered sprouting room. An inverse relationship exists between increasing the number of cooling units used and the intensity (LI) and uniformity (LU) of lighting at the lighting duration and irrigation rates. Figure 5A shows the lowest values of LI, 1200, and 1266.67 lux, respectively, at the maximum number of cooling units used for the advanced air cooler C4, at L 6h and I 2 m³ ton⁻¹. The maximum values of LI were 2201.0 and 2178.78 lux at the lowest number of C1, the highest lighting duration was 12 h, and the lowest I was 1.7 m³ ton⁻¹. Figure 5B shows a direct proportional relationship between the number of cooling units and the lighting uniformity at different lighting durations and irrigation rates. The highest LU 87.67 and 87.66%, values were recorded at C4, L 12h, and I 1.7 m³ ton⁻¹. The lowest values for LU were 74.33 and 75.0%, respectively, at C1, L 6h, and I 2 m³ ton⁻¹. Statistically, there was high significance at $P < 0.05$ for both LI and LU, respectively, for the interaction between the levels of the experimental variables tested. Linear regression Equations (11&12) for Li and LU show the gradual effect of the number of cooling units, lighting durations, and irrigation rates on the averages of the inferred values, as shown in Figure 6 A&B.

$$[LI, \text{lux}] = -146.273[C \text{ No.}] + 98.757[L, \text{h}] + 635.674 [I, \text{m}^3 \text{ ton}^{-1}] \quad R^2= 0.878 \quad (11)$$

$$[LU, \%] = 3.113[C \text{ No.}] + 1.560[L, \text{h}] + 31.980 [I, \text{m}^3 \text{ ton}^{-1}] \quad R^2= 0.894 \quad (12)$$

The greater the number of cooling units, the more it affects the consumption of electrical energy and leads to a relative reduction in the intensity and uniformity of the lighting diffusion without affecting the productivity and quality of the sprouted barley. The uniformity of lighting increases significantly with the increase in the operating time of the lighting as a result of the improvement in the luminance of the LED lamp strip with the rise in the operating time. The increase in uniformity of lighting increased directly with the increase in cooling units due to balancing the electrical system's consumption inside the sprouting room, in agreement with [Nelson and Bugbee \(2014\)](#). Proper thermal management strategies, periodic maintenance, and cleaning routines may help for a significant improvement in lighting performance, by [Lee *et al.* \(2021\)](#).

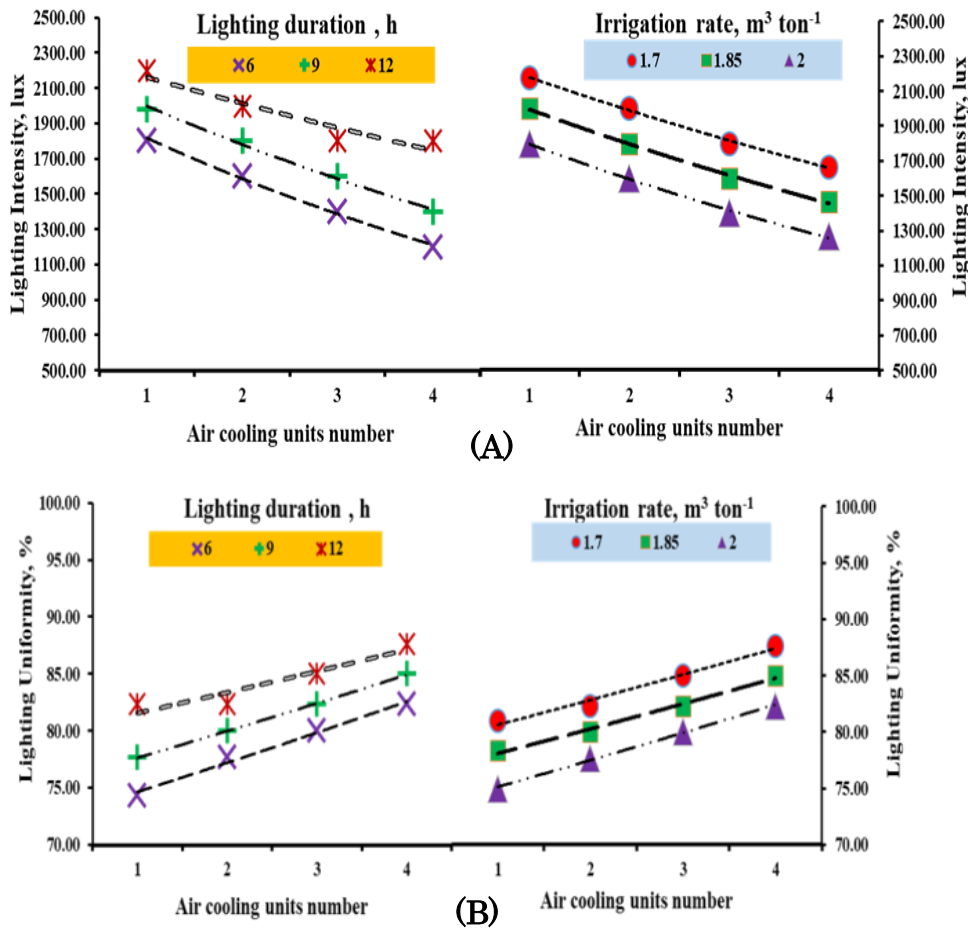


Figure 5. The effect of air cooling units at the various lighting durations and irrigation rates on (A) lighting intensity and (B) lighting uniformity.

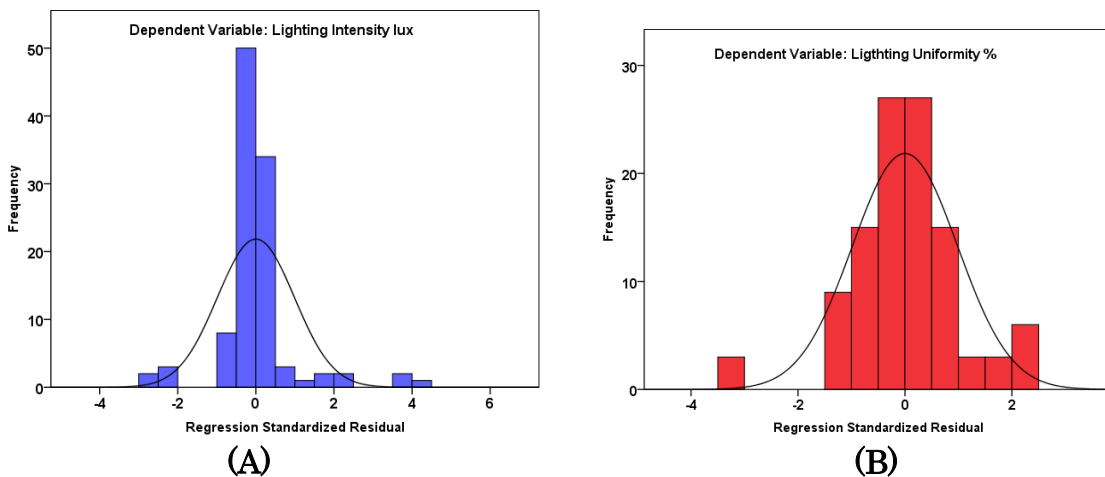


Figure 6. Regression standardized residual frequency for (A) lighting intensity and (B) lighting uniformity.

Sprouted barely vegetative characteristics

Table 3 presents the means and standard deviations for selected vegetative traits influenced by the studied factors, including the number of air cooling units, lighting duration, and irrigation rates, along with a control group. Increasing the number of air cooling units, lighting durations, and irrigation rates led to significant improvements in vegetative characteristics for the solar-powered sprouting room over the control room. The maximal root and shoot lengths (8.86 and 22.83 cm) were

estimated at C4, L3, and I3 with an increment ration over the control of 40.90 and 23.65%, respectively. The highest fresh and dry yield mean values were 33.32 and 7.86 kg m⁻², which were estimated at the highest levels of C, L, and I, respectively, with increment ratios over control at 32.32 and 47.58%, respectively. The maximum conversation factor of 8.52 kg kg⁻¹ was recorded for the maximum studied factor levels with an increment ratio over control with 39.91%. The maximum measured chlorophyll content was 40.18 mg m⁻², recorded for the maximum C, L, and I with an increment ratio of 14.88% over the control.

Statistically, the measured measurements had a high significant probability with the interaction with the studied variables at $P < 0.05$, as listed in Table 3. The results of the vegetative characteristics were because higher levels of cooling provided by additional Peltier modules positively impacted the growth and productivity of barley sprouts. Longer exposure to light positively affected the growth and development of barley sprouts, leading to enhanced productivity. Higher irrigation water rates facilitated better growth and productivity of barley sprouts, potentially by providing optimal hydration and nutrient uptake, in agreement with [Farghaly *et al.* \(2019\)](#). Overall, the results demonstrate the significant influence of the studied factors on the vegetative characteristics of barley sprout yield. The findings underscore the importance of optimizing environmental conditions, such as cooling, lighting, and irrigation, to maximize the productivity and quality of barley sprouts, thereby contributing to the advancement of sprout production techniques, in agreement with [Elsoury *et al.* \(2015\)](#).

Table 3. Means and standard deviations for sprouted barely vegetative characteristics.

Factors		Root length, cm	Shoot length, cm	Fresh yield, kg m ⁻²	Dry yield, kg m ⁻²	Conversion factor, kg kg ⁻¹	Chlorophyll content, mg m ⁻²
Air cooling units No.	C ₁	7.14±.97 ^a	15.14±1.44 ^a	24.53±2.10 ^a	4.67±0.32 ^a	5.80±0.23 ^a	36.98±0.78 ^a
	C ₂	7.71±.19 ^b	16.99±1.34 ^b	28.48±1.60 ^b	5.65±0.19 ^b	6.74±0.33 ^b	38.59±0.97 ^b
	C ₃	8.60±0.90 ^c	19.31±1.73 ^c	31.72±2.37 ^c	6.95±0.44 ^c	7.46±0.23 ^c	39.47±0.53 ^c
	C ₄	8.11±1.29 ^d	22.83±2.19 ^d	33.32±2.64 ^d	7.86±0.14 ^d	8.52±0.26 ^d	40.18±0.44 ^d
LSD 0.05		0.160	0.136	0.124	0.056	0.057	0.079
Lighting durations, h	L ₁	7.22±1.54 ^a	17.14±3.14 ^a	28.17±4.36 ^a	6.03±1.30 ^a	6.84±1.03 ^a	38.35±1.51 ^a
	L ₂	8.17±0.88 ^a	18.49±2.71 ^b	29.53±4.05 ^b	6.26±1.20 ^b	7.15±1.01 ^b	38.69±1.36 ^b
	L ₃	8.28±0.80 ^b	20.06±3.53 ^c	30.84±3.22 ^c	6.56±1.25 ^c	7.39±1.03 ^c	39.37±1.10 ^c
LSD 0.05		0.138	0.117	0.107	0.049	0.050	0.069
Irrigation rates, m ³ ton ⁻¹	I ₁	7.20±1.20 ^a	17.43±3.20 ^a	27.40±2.86 ^a	6.16±1.26 ^a	7.04±1.05 ^a	38.23±1.41 ^a
	I ₂	7.78±0.92 ^b	18.58±3.23 ^b	30.08±4.09 ^b	6.31±1.26 ^b	7.13±1.05 ^b	38.94±1.36 ^b
	I ₃	8.68±1.02 ^c	19.69±3.28 ^c	31.07±4.14 ^c	6.38±1.27 ^c	7.22±1.03 ^c	39.24±1.23 ^c
LSD 0.05		0.138	0.117	0.107	0.049	0.050	0.069
Control		5.13±1.03	17.43±3.20	22.55±2.94	4.12±0.31	5.12±0.17	34.20±0.32
R²		0.860	0.896	0.898	0.895	0.893	0.893
P< 0.05		0.00***	0.00***	0.00***	0.00***	0.00***	0.00***

^{a-d} the means with no common subscript within each column differed significantly ($P \leq 0.05$)

Sprouted barely chemical and quality vegetative analysis

The studied factors, including the number of air-cooling units, lighting duration, and irrigation rates significantly influenced the chemical and quality analysis of sprouted barley. Table 4 presents the mean values and standard deviations for nitrogen (N), phosphorus (P), potassium (K), and protein content across different experimental conditions. Also, Figure 7 demonstrates the interaction effect between the studied variables on the sprouted barley chemical analysis. As shown in Figure 7 (A&B) and Table 2, the maximum mean values for N, P, K, and protein content were 3.55, 0.84, 1.83, and 20.67%, respectively, with increment ratios over control of 11.55, 25.0, 7.10, and 12.87%. Statistically, there was a high significant probability for the measured chemical and quality measurements at $P < 0.05$, as listed in Table 4. The results obtained for the chemical and quality analyses were because greater cooling capacity, lighting durations, and irrigation rates positively impact the nutrient uptake and synthesis processes in barley sprouts, resulting in higher nutrient content in the harvested sprouts, in agreement with [Bakeer *et al.* \(2015\)](#); [Wang *et al.* \(2023\)](#).

Table 4. Means and standard deviations for sprouted barely chemical analysis.

Factors		N, %	P, %	K, %	Protein content %
Air cooling units No.	C ₁	3.34±0.09 ^a	0.64±0.02 ^a	1.73±0.01 ^a	19.48±0.52 ^a
	C ₂	3.39±0.03 ^b	0.70±0.02 ^b	1.77±0.02 ^b	19.79±0.15 ^b
	C ₃	3.46±0.02 ^c	0.78±0.02 ^c	1.78±0.01 ^c	20.19±0.11 ^c
	C ₄	3.55±0.03 ^d	0.84±0.02 ^d	1.83±0.03 ^d	20.67±0.15 ^d
LSD 0.05		0.0226	0.0044	0.0074	0.132
Lighting duratiosn, h	L ₁	3.40±0.10 ^a	0.72±0.08 ^a	1.76±0.04 ^a	19.83±0.58 ^a
	L ₂	3.45±0.08 ^a	0.74±0.08 ^b	1.78±0.04 ^b	20.09±0.48 ^a
	L ₃	3.46±0.08 ^b	0.76±0.08 ^c	1.79±0.04 ^c	20.16±0.47 ^b
LSD 0.05		0.0017	0.0038	0.0064	0.114
Irrigation rates, m ³ ton ⁻¹	I ₁	3.43±0.10 ^a	0.73±0.08 ^a	1.77±0.04 ^a	19.98±0.56 ^a
	I ₂	3.44±0.09 ^a	0.74±0.08 ^b	1.78±0.04 ^a	20.03±0.53 ^a
	I ₃	3.44±0.09 ^a	0.75±0.08 ^c	1.78±0.04 ^b	20.07±0.50 ^a
LSD 0.05		0.0017	0.0038	0.0064	0.114
Control		3.04±0.05	0.63 ±0.01	1.70±0.01	18.01±0.21
R ²		0.859	0.893	0.825	0.859
P < 0.05		0.00***	0.00***	0.00***	0.00***

^{a-d} the means with no common subscript within each column differed significantly ($P \leq 0.05$).

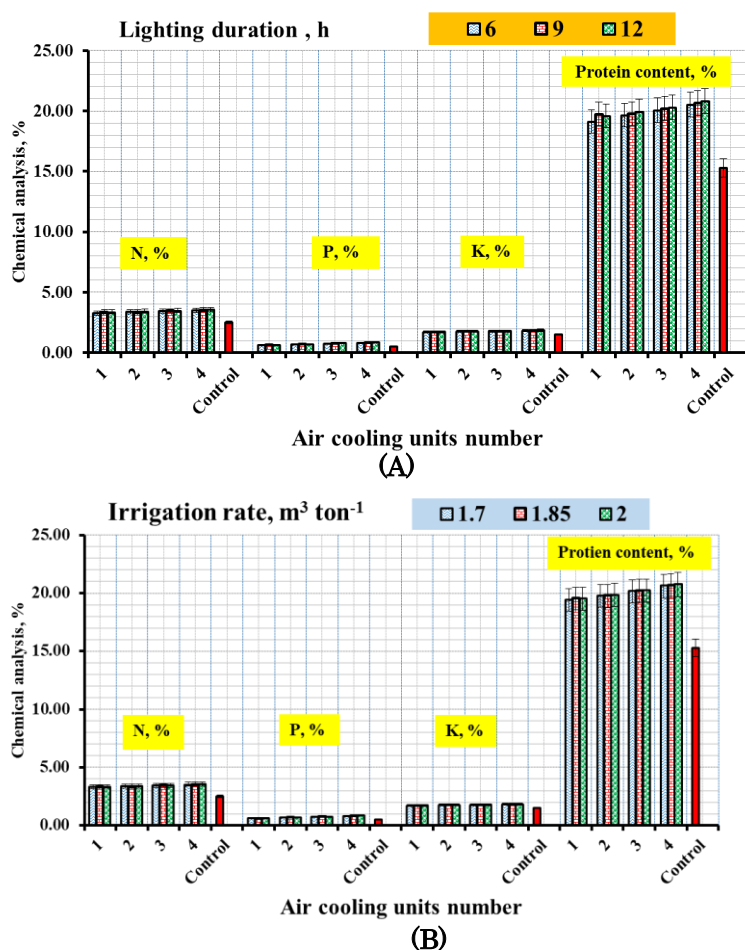


Figure 7. Effect of air cooling unit number on the sprouted barley chemical analysis at (A) lighting durations and (B) irrigation rates.

The solar-powered sprouting room productivity

Figure 8 shows the effect of the number of cooling units C on the productivity P of the solar-powered sprouting room and control (*the sprouting room operated by alternating current before modification*) at different lighting durations L and different irrigation rates I. There is a direct proportional relationship between increasing the number of cooling units and productivity when increasing lighting durations and irrigation rates. The lowest productivity recorded for the sprouted barley crop at the end of the sprouting cycle after seven days in the solar-powered room was 0.91 and 0.94 tons at C 1, L 6 h, and I 1.7 m³ton⁻¹, as shown in Figure 8. The highest values of P were 1.22 and 1.21 tons, respectively, at the highest number of air cooling units (C4), the highest lighting duration (12 h), and the highest irrigation rate (2 m³ ton⁻¹). The maximum productivity of the control was 0.83 tons when using the AC-managed sprouting room before modification. The control productivity decreased by 31.97% compared to the maximum productivity of the solar-powered room. Significantly higher productivity rates were achieved compared to the control due to controlling all optimal production factors for barley sprouting, including cooling, lighting, and irrigation, in agreement with [Ahamed et al. \(2023\)](#). Statistically, there is a high significance $P < 0.05$ for the interaction between C, L, and I and their effect on P, as shown in the regression linear Equation (13), which shows the significance of the interaction between the levels of the experimental variables tested.

$$[P, \text{ton}] = 0.0905 [C \text{ No.}] + 0.0142 [I, \text{h}] + 0.399 [I \text{ m}^3 \text{ ton}^{-1}] \quad R^2 = 0.898 \quad (13)$$

Figure 8C shows the regression line between the observed and expected values of productivity, which shows a significant increase in productivity for the solar culture room due to the development of cooling, lighting, and irrigation systems compared to the room before the modification. The data reveal notable enhancements in productivity across all configurations, indicating the efficacy of employing multiple Peltier modules in augmenting agricultural output. The significant productivity improvements underscore the effectiveness of the development interventions implemented within the system. These improvements may encompass various enhancements, including optimizing energy utilization, refining environmental conditions, and augmentation of growth-promoting factors facilitated by the Peltier modules. The escalating trend in productivity improvement with increasing Peltier modules suggests a positive correlation between system scalability and productivity. Scaling up the number of modules likely enables more efficient utilization of resources, finer control over environmental parameters, and better adaptation to varying cultivation needs, thereby resulting in amplified productivity enhancements. These findings affirm the potential of Peltier-based systems as a viable approach for enhancing agricultural productivity (Remeli *et al.*, 2020). Moreover, they underscore the importance of strategic system design and development to unlock the full potential of such technologies in agricultural contexts. The positive correlation between irrigation water usage rates and productivity levels suggests that achieving an optimal balance in water application is crucial for maximizing agricultural output while minimizing resource waste (Elzanaty *et al.*, 2021).

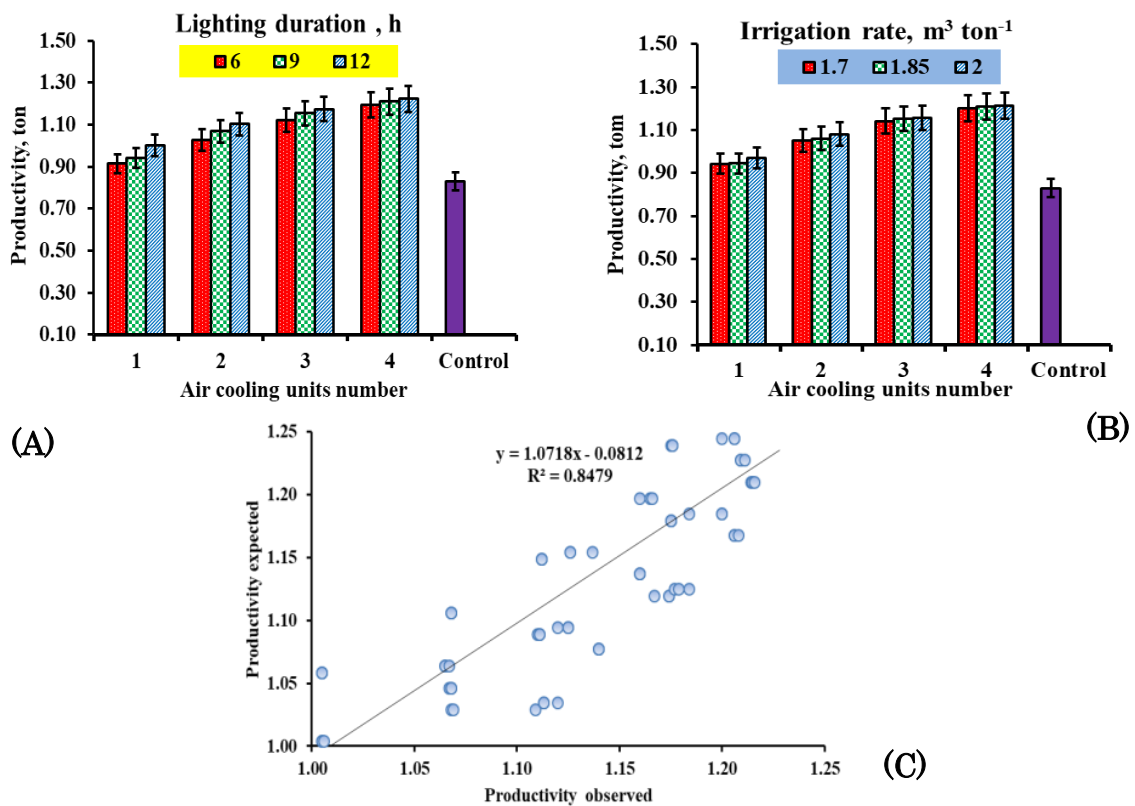


Figure 8. Effect of air cooling unit number on the solar-powered sprouting room productivity at (A) the lighting durations, (B) the irrigation rates, and (C) the productivity observed and expected values.

Solar-powered sprouting room-specific power consumption

Figure 9 shows the effect of the number of cooling units used for the developed air-cooling device and its impact on electrical energy consumption rates (SE) at the lighting durations used and irrigation rates. A direct, proportional relationship exists between the number of air cooling units used and SE at (C, L, and I). The greater the number of air cooling units used, the higher the rates of electrical energy consumption. As the duration of the lighting operation increases with the increase in irrigation rates, this leads to an increase in the rate of energy consumed, as shown in Figure 9. There is a significant difference between the decrease in consumption rates of the solar-powered sprouting room and the control, as shown in Figure 9 (B and D). The maximum electrical energy rates consumed by the solar-powered sprouting room at C4, L 12h, and I 2 m³ ton⁻¹ were 63.37 and 58.35 kWh ton⁻¹, as shown in Figures 9 (A and B). The lowest levels of electrical energy consumed by the solar-powered sprouting room were 21.24 and 26.26 kWh.ton⁻¹, at the lowest values of C1, L12h, and I1.7 m³ ton⁻¹, as in Figures 9 (B and D). The control rates for the room powered by alternating current increased to 117.19 kWh ton⁻¹, with an increment ratio of 45.93% over the maximum energy consumption rate in the solar-powered sprouting room. Statistically, all variables and their interaction were highly significant at P < 0.05. It also appears in the linear regression Equation (14) that the maximum factor that directly impacts the electrical energy consumption rates of the solar-powered sprouting room is the number of cooling units, followed by the lighting levels and irrigation rates for the experimental treatments.

$$[(SE), \text{kWh ton}^{-1}] = 10.642 [C \text{ No.}] + 1.675 [L, \text{h}] + 0.440 [I, \text{m}^3 \text{ton}^{-1}] \quad R^2=0.899 \quad (14)$$

The low energy levels consumed per ton of sprouted barley for the solar-powered room are due to the development of 12-volt DC cooling, lighting, and irrigation systems. The use of advanced cooling devices instead of air conditioning devices has had a strong positive impact on reducing electrical energy consumption rates, in agreement with [Elmorsy *et al.* \(2013\)](#). The developed lighting systems and water pumps that operate with direct current instead of traditional lighting systems (tube lamps) or large water pumps also led to a significant reduction in the rates of specific energy consumption per ton of sprouted barley, in agreement with the results of [Afzalinia and Karimi \(2020\)](#).

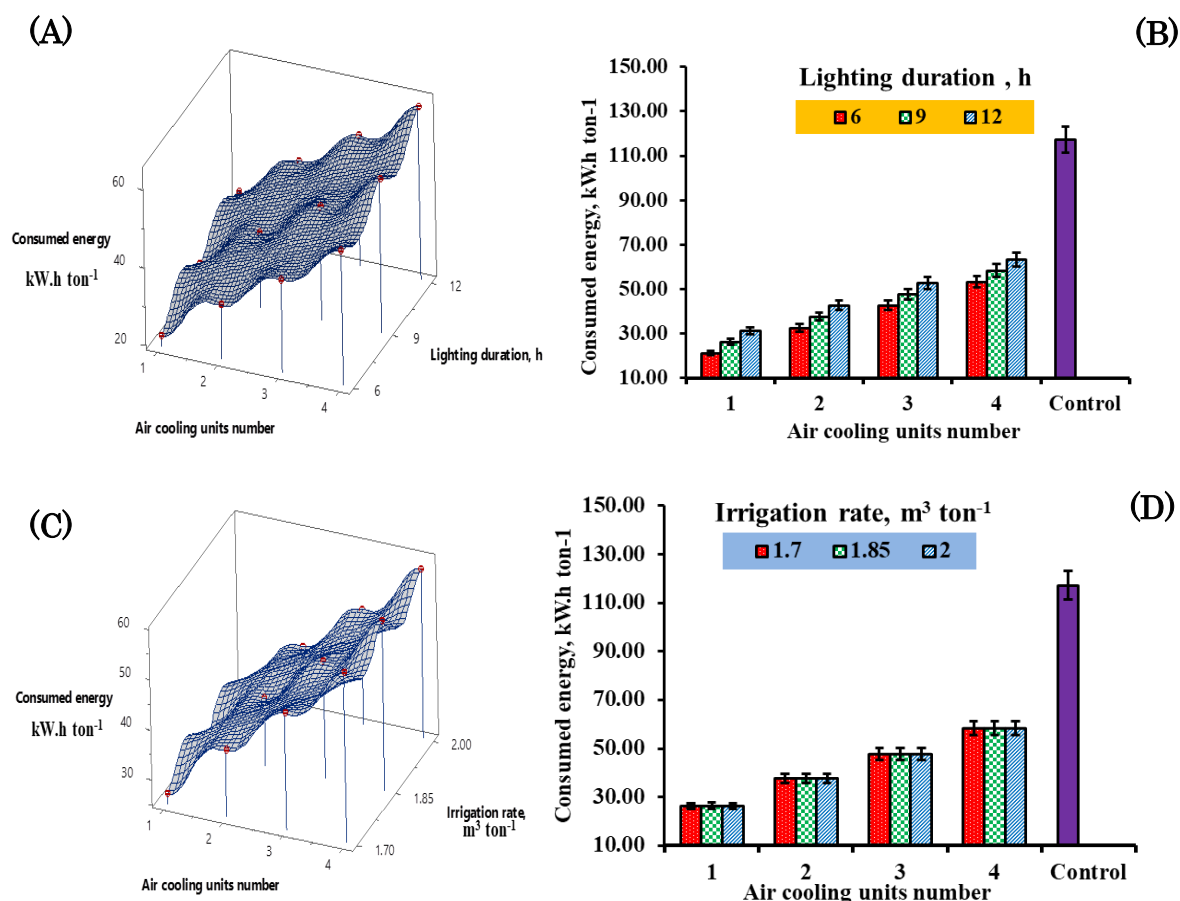


Figure 9. Effect of air cooling units number on the consumed electrical energy for (A&B) the solar-powered and control sprouting rooms at the lighting durations and (C&D) the solar-powered and control sprouting rooms at the various irrigation rates.

Financial economic analysis for the solar-powered sprouting room

Table 5 lists detailed mean average values of the production cost for the sprouted barley produced in the solar-powered and control sprouting rooms before modification. The cost of electrical energy per ton of sprouted barley decreased by 36.56% for the solar-powered room compared to the control room. The mean average price of the barley produced in the sprouting room was estimated after the germination cycle lasted one week for the experimental replicates. The price of the developed system, 14.67 USD for 10 years, was divided and added to the total costs of production to restore capital. There is a significant increase in net earnings of 33.32% compared to the control due to the lower cost of electrical energy and higher productivity within the same sprouting period, in agreement with [Ghorbel and Kosum \(2022\)](#). The ratio of electrical costs to total production costs was 3.77% for the solar-powered room compared with 8.56% for the control room, as listed in Table 5. The decrease in production costs is due to using solar energy instead of alternating current while replacing power-saver cooling, lighting, and irrigation systems. The production cost included the price of seeds and their treatments, maintenance costs, taxes, and the annual depreciation rate, in addition to labor wages, as demonstrated in Table 5. It could be recommended to acquire solar-powered barley sprouting rooms for animal production breeders to reduce production costs.

Table 5. Mean and standard deviation of the economic analysis.

xFactors		Electricity cost; USD ton⁻¹	Total costs; USD ton⁻¹	Barley price; USD ton⁻¹	Net earn; USD ton⁻¹	
Air cooling units No.	1	0.84±0.13 ^a	35.59±0.13 ^a	60.34±2.69 ^a	9.75±2.58 ^a	
	2	1.21±0.13 ^b	35.96±0.13 ^b	67.41±2.37 ^b	16.46±2.25 ^b	
	3	1.53±0.13 ^c	36.28±0.13 ^c	72.84±1.45 ^c	21.56±1.33 ^c	
	4	1.87±0.13 ^d	36.62±0.13 ^d	76.50±0.92 ^d	24.88±0.80 ^d	
Lighting durations , h	6	1.20±0.39 ^a	35.95±0.39 ^a	67.36±6.79 ^a	16.41±6.41 ^a	
	9	1.36±0.39 ^b	36.11±0.39 ^b	69.23±6.58 ^b	18.12±6.20 ^b	
	12	1.52±0.39 ^c	36.27±0.39 ^c	71.22±5.39 ^c	19.96±5.01 ^c	
Irrigation rates, m³ ton⁻¹	1.7	1.36±0.41 ^a	36.11±0.41 ^a	68.64±6.55 ^a	17.53±6.15 ^a	
	1.85	1.36±0.41 ^b	36.11±0.41 ^b	69.15±6.76 ^b	18.04±6.36 ^b	
	2	1.36±0.41 ^c	36.11±0.41 ^c	70.02±6.05 ^c	18.91±5.65 ^c	
P value < 0.05		0.00***	0.00*	0.00***	0.00***	
R²		0.885	0.836	0.898	0.898	
Mean value (solared)		1.36±0.40	36.11±14.67	69.27±6.42	18.49±6.03	
Control (AC room)		3.72±0.30	43.47±0.30	55.80±3.42	12.33±1.55	
Total developmen t price	146.70 USD	Solar system 50 USD	Air cooling devis 50.50 USD	Lighting system 10.5 USD	Irrigation system 20.5 USD	Arduino controller 15.2 USD

Notice: USD equal 47.16 L.E during the experiments time. a-d the means with no common subscript within each column differed significantly (P≤0.05).

CONCLUSION

Developing a solar-powered sprouting room leads to achieving sustainable agricultural development. Utilizing the developed air cooling device, it achieved superior thermal adaptation in the solar-powered room. Increasing the operating air cooling units via air cooler devices significantly improved nutrient uptake and synthesis. Four cooling units with a lighting duration of 12 hours and an irrigation rate of 2 m³ ton⁻¹ were the optimal production levels within the solar-powered sprouting room. Using the extended duration of 12 hours for lighting positively influenced the sprouted barley growth rate and productivity. Significant improvements in vegetative characteristics and chemical analysis were indicated for the sprouted barley in the developed sprouting room over the traditional AC-managed room before modification. The total electrical energy consumption rates for the solar-powered sprouting room decreased by 46.01% compared to the control, which led to a reduction in total production costs and an increase in the net profit of the developed system. Solar-powered sprouting rooms can be adopted as an excellent economical alternative to traditional greenhouses, suitable for remote areas and small livestock farmers.

DECLARATION OF COMPETING INTEREST

The authors declare that they have no conflict of interest.

CREDIT AUTHORSHIP CONTRIBUTION STATEMENT

Ahmed Shawky El-Sayed: Design, conceptualization, methodology refinement, data collection, manuscript drafting.

AbdelGawad Saad: Methodology refinement, data analysis, manuscript review and editing.

Mohamed Ali Ibrahim Al-Rajhi: Methodology refinement, data analysis, manuscript review and editing.

Maisa Moneir Megahed: Guidance, economic evaluation, manuscript review for scientific rigor.

ETHICS COMMITTEE DECISION

This article does not require any ethical committee decision.

REFERENCES

- Adegbeye MJ, Reddy PRK, Obaisi AI, Elghandour MMY, Oyebamiji KJ, Salem AZM and Camacho-Díaz LM (2020). Sustainable agriculture options for production, greenhouse gasses and pollution alleviation, and nutrient recycling in emerging and transitional nations-An overview. *Journal of Cleaner Production*, 242: 118319. <https://doi.org/10.1016/j.jclepro.2019.118319>
- Afzalnia S and Karimi A (2020). Barley cultivars and seed rates effects on energy and water productivity of green fodder production under hydroponic condition. *Indian Journal of Agricultural Research*, 54(6): 792-796. <https://doi.org/10.18805/ijare.a-554>
- Ahamed MS, Sultan M, Shamshiri RR, Rahman MM, Aleem M and Balasundram SK (2023). Present status and challenges of fodder production in controlled environments: A review. *Smart Agricultural Technology*, 3: 100080. <https://doi.org/10.1016/j.atech.2022.100080>
- Akbag HI, Turkmen OS, Baytekin H and Yurtman IY (2014). Effects of Harvesting Time on Nutritional Value of Hydroponic Barley Production. *Turkish Journal of Agricultural and Natural Sciences*, 1(Special Issue-2): 1761–1765. <https://dergipark.org.tr/en/pub/turkjans/issue/13311/160977>
- Alrajhi MAI and Elsayed AS (2023) Developing Sterilization and Lighting Systems for Sprouting Rooms Using Ozone and Optical Fibers. *Yuzuncu Yil University Journal of Agricultural Sciences*, 33(4): 556-570. <https://doi.org/10.29133/vyutbd.1261911>
- AOAC (1990). Association official Analytical chemists. 15th edn. Wash. Dc, U.S.A. <https://doi.org/10.1002/0471740039.vec0284>
- Asiabanpour B, Estrada A, Ramirez R and Downey MS (2018). Optimizing natural light distribution for indoor plant growth using PMMA optical fiber: simulation and empirical study. *Journal of Renewable Energy*, 2018(1): 1-10. <https://doi.org/10.1155/2018/9429867>
- Atlas Global Crop. LTD. (2004). Feeding animals to feed people. Retrieved from: World Wide Web: www.atgloco.com.
- Bakeer GAR, Hegab K, El-Beairy U and Elsayy W (2015). Effect micro irrigation systems, irrigation period and seed thickness on barley sprout production. *Misr Journal of Agricultural Engineering*, 32(2): 589-610. <https://doi.org/10.21608/mjae.2015.98600>
- Basko I (2009). Food therapy to reduce the stress of summer climate changes. *American Journal of Traditional Chinese Veterinary Medicine*, 4(1): 77-83. <https://doi.org/10.59565/001c.83752>
- Bazeley K and Hayton A (2013). Practical cattle farming. *Crowood Press LTD, Ramsbury, Marlborough, Wiltshire*. WWW.Crowood.com.
- Buchalik R and Nowak G (2022). Technical and economic analysis of a thermoelectric air conditioning system. *Energy and Buildings*, 268: 112168. <https://doi.org/10.1016/j.enbuild.2022.112168>
- Degirmencioglu A, Mohtar RH, Daher BT, Ovgunaltay-Ertugrul G, and Ertugrul O (2019). Assessing the sustainability of crop production in the Gediz Basin, Turkey: a water, energy, and food nexus approach. *Fresen Environ Bull*, 28(4): 2511-2522. <https://doi.org/10.7546/crabs.2019.08.18>

- Dung DD, Godwin IR and JV Nolan (2010). Nutrient content in Sacco digestibility of barley grain and sprouted barley. *Journal of Animal and Veterinary Advances*, 9(19): 2485-2492. <https://doi.org/10.3923/javaa.2010.2485.2492>
- Elmorsy A T, Abul-Soud M and Emam M S A (2013). Localized hydroponic green forage technology as a climate change adaptation under Egyptian conditions. *Research Journal of Agriculture and Biological Sciences*, 9(6): 341-350.
- Elsoury H A, Aboukarima A M and Bayomi M I (2015). Effect of natural lighting, combination of soaking and irrigation, and seeding rate on barley green fodder production under farmer's domestic room conditions. *Misr Journal of Agricultural Engineering*, 32(1): 257-280. <https://doi.org/10.21608/mjae.2015.98722>
- Elzanaty TM, Elmesery AEA, Zabady FIM and Mashhour AMA (2021). Applications of magnetized and electrostatic water on irrigation water use efficiency and barley fodder yield under hydroponic system. *Al-Azhar Journal of Agricultural Engineering*, 1(1): 73-85. <https://doi.org/10.21608/azeng.2021.209954>
- Farghaly MM, Abdullah MA, Youssef IM, Abdel-Rahim IR and Abouelezz K (2019). Effect of feeding hydroponic barley sprouts to sheep on feed intake, nutrient digestibility, nitrogen retention, rumen fermentation and ruminal enzymes activity. *Livestock Science*, 228: 31-37. <https://doi.org/10.1016/j.livsci.2019.07.022>
- Gebremedhin W K (2015). Nutritional benefit and economic value of feeding hydroponically grown maize and barley fodder for Konkan Kanyal goats. *IOSR Journal of Agriculture and Veterinary Science*, 8: 24-30. <https://doi.org/10.9790/2380-08722430>
- Ghorbel R and Koşum N (2022). Hydroponic fodder production: an alternative solution for feed scarcity. *In 6th International Students Science Congress Proceedings*. <https://doi.org/10.52460/issc.2022.005>
- Ghorbel R, Chakchak J, Malayoğlu HB and Cetin NS (2021). Hydroponics “Soilless Farming”: The Future of Food and Agriculture—A Review. *Proceedings of the 5th International Students Science Congress Proceedings, Rome, Italy, 20-22*. <https://doi.org/10.52460/issc.2021.007>
- Grubisic M, Van Grunsven, RH, Manfrin A, Monaghan MT and Hölker F (2018). A transition to white LED increases ecological impacts of nocturnal illumination on aquatic primary producers in a lowland agricultural drainage ditch. *Environmental pollution*, 240: 630-638. <https://doi.org/10.1016/j.envpol.2018.04.146>
- He Z, Zuazua RA and Martin GC (2024). Current-dependent temperature change model of a thermoelectric window frame. *Applied Thermal Engineering*, 123081. <https://doi.org/10.1016/j.applthermaleng.2024.123081>
- Hegab K (2018). Light uniformity improvement inside the sprouting environment and product evaluation. *Misr Journal of Agricultural Engineering*, 35(2): 743-766. <https://doi.org/10.21608/mjae.2018.95829>
- Helal HG (2015). Sprouted barley grains on olive cake and barley straw mixture as goat diets in Sinai. *Advances in Environmental Biology*, 9(22): 91-102.
- Hunt D (1983). Farm power and machinery management 8th Ed. Iowa state Univ., Ames, USA.
- Izydorczyk MS and Edney M (2017). Barley: Grain-quality characteristics and management of quality requirements. In *Cereal grains* (pp. 195-234). *Woodhead Publishing*. <https://doi.org/10.1016/b978-0-08-100719-8.00009-7>
- Jones JB and Case VW (1990). Sampling, handling, and analyzing plant tissue samples. *Soil testing and plant analysis*, 3, 389-427. <https://doi.org/10.2136/sssabookser3.3ed.c15>
- Kumari S, Pradhan P, Yadav R and Kumar S (2018). Hydroponic techniques: A soilless cultivation in agriculture. *Journal of pharmacognosy and phytochemistry*, 7(1S): 1886-1891.
- Lee H, Zhao X and Seo J (2021). A study of optimal specifications for light shelves with photovoltaic modules to improve indoor comfort and save building energy. *International Journal of Environmental Research and Public Health*, 18(5), 2574. <https://doi.org/10.3390/ijerph18052574>
- Lemmens E, Moroni AV, Pagand J, Heirbaut P, Ritala A, Karlen Y and Delcour JA (2019). Impact of cereal seed sprouting on its nutritional and technological properties: A critical review. *Comprehensive Reviews in Food Science and Food Safety*, 18(1): 305-328. <https://doi.org/10.1111/1541-4337.12414>
- Lin R, Horsley RD and Schwarz PB (2009). Methods to determine dormancy and preharvest sprouting resistance in barley. *Crop science*, 49(3), 831-840. <https://doi.org/10.2135/cropsci2007.11.0652>
- Mariyappillai A, Arumugam G and Raghavendran VB (2020). The techniques of hydroponic system. *Acta Scientific Agriculture*, 4(7): 79-84. <https://doi.org/10.31080/asag.2020.04.0858>

- Marsh BH (2016). An Investigation of Current Potato Nitrogen Fertility Programs' Contribution to Ground Water Contamination. *International Journal of Agricultural and Biosystems Engineering*, 10(3), 138-144. <https://doi.org/10.5281/zenodo.1111889>
- Merrill AL and Watt BK (1955). Energy value of foods: basis and derivation (No. 74). Human Nutrition Research Branch, *Agricultural Research Service, US Department of Agriculture*.
- Nelson JA and Bugbee B (2014). Economic analysis of greenhouse lighting: light emitting diodes vs. high intensity discharge fixtures. *PloS one*, 9(6), e99010. <https://doi.org/10.1371/journal.pone.0099010>
- Oida A (1997). Using personal computer for agricultural machinery management. Kyoto University. Japan. JICA publishing. Farm Machinery and Equipment, 5th ed. Graw Hill of Publ., New York, NY, USA.
- Parmar N, Sharma N, Arora A, Goyal D and Buddhi D (2022). Hybrid thermoelectric air cooler for building cooling. *Materials Today: Proceedings*, 69, 309-316. <https://doi.org/10.1016/j.matpr.2022.08.540>
- Ramteke R, Doneria R and Gendley MK (2019). Hydroponic techniques for fodder production. *Acta Scientific Nutritional Health*, 3(5), 127-132.
- Remeli MF, Bakaruddin NE, Shawal S, Husin H, Othman MF and Singh B (2020). Experimental study of a mini cooler by using Peltier thermoelectric cell. In IOP Conference Series: *Materials Science and Engineering* (Vol. 788, No. 1, p. 012076). IOP Publishing. <https://doi.org/10.1088/1757-899x/788/1/012076>
- Ryan J (1996). A soil and plant analysis manual adapted for the West Asia and North Africa region.
- Sharma N and Puri V (2023). Solar energy fundamental methodologies and its economics: A review. *IETE Journal of Research*, 69(1), 378-403. <https://doi.org/10.1080/03772063.2020.1822762>
- Sharma N, Acharya S, Kumar K, Singh N and Chaurasia OP (2018). Hydroponics as an advanced technique for vegetable production: An overview. *Journal of Soil and Water Conservation*, 17(4), 364-371. <http://dx.doi.org/10.5958/2455-7145.2018.00056.5>
- Shit N (2019). Hydroponic fodder production: An alternative technology for sustainable livestock production in India. *Exploratory Animal & Medical Research*, 9(2).
- Soufan W, Azab O, Al-Suhaibani N, Almutairi KF and Sallam M (2023). Plasticity of Morpho-Physiological Traits and Antioxidant Activity of Hydroponically Sprouted *Hordeum vulgare* L. When Using Saline Water. *Agronomy*, 13(4), 1135. <https://doi.org/10.3390/agronomy13041135>
- Wang L, Sun C, Luan H and Semiroumi DT (2023). Investigating the effectiveness of LED lighting in the production of rich sprouts for food purposes. *Heliyon*, 9(4): e14964. <https://doi.org/10.1016/j.heliyon.2023.e14964>



Turkish Journal of
Agricultural
Engineering Research
(Turk J Agr Eng Res)
e-ISSN: 2717-8420



A Review of Hybrid and Green House Type Solar Dryers

Promise ETIM^{a*} , Akindele ALONGE^b , David ONWE^b , Inimfon OSSOM^b 

^aDepartment of Agricultural Engineering, Akwa Ibom State University, Ikot Akpaden, Mkpát Enin, Akwa Ibom State, NIGERIA

^bDepartment of Agricultural and Food Engineering, University of Uyo, Uyo, Akwa Ibom State, NIGERIA

ARTICLE INFO: Review Article

Corresponding Author: Promise ETIM, E-mail: promiseetim@aksu.edu.ng

Received: 1 August 2023 / Accepted: 6 January 2024 / Published: 30 June 2024

Cite this article: Etim P, Alonge A, Onwe D and Ossom I (2024). A Review of Hybrid and Green House Type Solar Dryers. *Turkish Journal of Agricultural Engineering Research (TURKAGER)*, 5(1): 117-130. <https://doi.org/10.46592/turkager.1332828>.

ABSTRACT

Solar drying is a renewable, efficient, cheap, and sustainable method of preserving agricultural produce. Recent trends in hybrid and greenhouse-type solar dryers were studied. The study revealed that hybrid and greenhouse-type dryers are robust and efficient because they are mostly embedded with heat generating and circulation systems. They are designed to accommodate large-scale drying of fruits and vegetables with higher rates of drying, reduced drying time and some other specific advantages. Findings also revealed that hybrid and greenhouse type solar dryers are mostly designed for optimum retention of heat to compensate for periods with low illumination. The study also gave insight into design challenges peculiar to these types of dryers, and further revealed that most of the fabrications were based on assumptions, with limited data as references. This review also highlights the cost of procurement, uniformity of airflow, sizing of blower and material selection as some of the factors limiting the utilization of hybrid and greenhouse type solar dryers for drying of fruits, vegetables, and other staple crops.

Keywords: Solar drying, Greenhouse solar dryers, Hybrid solar dryers, Fruits, Vegetables

INTRODUCTION

Drying is essential for the preservation of food, reducing microbial loads, and maintaining the physical and textural properties of the food. According to a survey by [FAO \(2017\)](#), between 40 to 60% of staple crops, fruits and vegetables harvested is lost annually in most parts of Africa, due to the inability of local food producers to develop adequate technology for post-harvest handling of their produce. However, this may not be the case in other climes as they have over time deployed sustainable means of drying and preserving harvested products. Solar drying is a superior alternative to open sun drying, as the latter is characterized by theft, infestation by



animals, hygienic concerns, etc. These shortcomings are addressed to some reasonable extent when products are dried using hybrid and greenhouse type solar dryers, because of the enclosed nature of the dryers. [Mohammed *et al.* \(2020\)](#) compared traditional solar drying systems to improved solar drying systems using some fruits as case studies. Their study revealed that the solar systems tested have the potential of preserving the quality and sensory properties of the dried fruits better than open sun drying, which were reported to be contaminated because of their exposure to the atmosphere. [Udomkun *et al.* \(2020\)](#) examined solar dryers for agricultural products in Asia and Africa, using an innovative landscape approach. Their findings revealed that solar drying is cost-effective and capable of preserving the quality of harvested products in sub-Saharan Africa and Asia. They also concluded that despite the high initial cost required for its development; hybrid and greenhouse type solar dryers come with huge economic returns.

Hybrid and greenhouse type solar dryers are robust and generally enhance the drying process better than open sun drying. The dryers are mostly embedded with heating medium and blower to enhance circulation of hot air within the drying chamber for rapid drying of products. Several researchers have worked on hybrid and greenhouse type solar dryers and reported higher efficiencies as against other systems like indirect, direct, and mixed mode solar dryers, because some of the systems are developed to work round the clock, despite low radiation and temperature ([Almuhanna, 2012](#); [Cesar *et al.*, 2015](#); [Barade *et al.*, 2016](#); [Madhava *et al.*, 2017](#); [Etim *et al.*, 2019](#); [Mohsen *et al.*, 2019](#)). [Janjai and Bala \(2012\)](#) observed that recent developments and use of solar dryers such as greenhouse type solar dryers, roof based integrated dryers, and tunnel type dryers in drying agricultural products such as fruits, vegetables, species, medicinal plants, and fish have greatly improved their quality.

This review will attempt to outline some of the developments in hybrid and greenhouse-type solar dryers and highlight gaps for possible research opportunities in the future.

SOME RECENT ADVANCEMENTS IN HYBRID SOLAR DRYERS

Various kinds of solar dryers were developed in the last three and half decades. These include: Active direct solar dryers ([Alonge and Uduak, 2014](#)); and active indirect solar dryers ([Alonge and Jackson, 2014](#)) as shown in Figures 1 and 2 respectively. A combined direct-indirect solar dryer (Figure 3) also known as mixed mode was developed by [Alonge *et al.* \(2020\)](#) and used for drying of fruits and vegetables. This dryer had similar features to dryers developed by [Afzal *et al.* \(2023\)](#) and [Duque-Dussán *et al.* \(2023\)](#).



Figure 1. A direct active solar dryers ([Alonge and Uduak, 2014](#)).



Figure 2. Indirect active solar dryers ([Alonge and Jackson, 2014](#)).



Figure 3. Mixed mode solar dryer ([Alonge et al., 2020](#)).

[Amer et al. \(2010\)](#) designed a hybrid solar dryer for bananas and tested it for its performance. A heat exchanger was attached to the dryer for optimal air circulation. The drying time of the product was reduced by almost 50% when compared to open drying. [Poonia et al. \(2018\)](#) fabricated a (Pressure, Volume/Temperature) PV/T hybrid solar dryer. The system was designed to combine both electrical and thermal energy for the drying process. The dryer as shown in Figure 4, consisted of a collector unit, drying chamber, (Direct Current) D.C. fan, (Photovoltaic) P.V. panel, and a PCM chamber, which aided storage of thermal energy. The PV panel attached to the dryer supplied the blower with the required power to ensure optimum circulation of air in the drying chamber. Three mathematical models, namely: Henderson and Pabis, Lewis and Page, were used to predict the drying process.



Figure 4. PV/T hybrid solar dryer ([Poonia et al., 2018](#)).

[Murali et al. \(2020\)](#) designed a hybrid solar dryer for shrimp drying. The study focused on designing a solar system that will ensure continuous drying operation irrespective of the time of the day. The drying and maximum collector efficiency obtained were 37.09% and 42.37%, respectively. The drying time was reduced by more than half when compared to the open sun experiment. [Yahya \(2016\)](#) developed a solar-assisted heat-pump dryer integrated with a biomass furnace for drying red chilli. The dryer had a blower with a capacity of 0.75kW used in the circulation of air and had three layers of drying as shown in Figure 5. The dryer reduced the time of drying by 82% when placed side aside with open sun drying. The performance of the dryer was computed as a function of the rate of drying, moisture removal rate, and efficiency of the dryer. The performance of the dryer was dependent on components such as solar collector, heat pump and biomass furnace. Their study however reported some degree of uncertainty in experimental data due to factors like selection of instrument and conditions of the environment. [Etim et al. \(2023\)](#) reported similar concerns.



Figure 5. Solar assisted heat pump dryer integrated with biomass furnace ([Yahya, 2016](#)).

[Aremu et al. \(2020\)](#) developed a hybrid solar dryer and tested it for performance. The system was embedded with a collector, drying chamber and three trays of 1.3×1.4

m dimension. Four solar photovoltaic (PV) cells, which served as a heating element charged the tubular battery and powered the blower. The dryer was observed to have reduced the time of the drying and achieved better efficiency as compared to open sun experiments and other dryers tested without attaching the external energy source. [Hussien *et al.* \(2017\)](#) developed a photovoltaic hybrid solar dryer. The dryer was embedded with a drying chamber, racks, trays, heater, blower, solar panel, D.C. battery, and charge controller. The drying chamber was of 0.30 m³ volume and the distance within the trays was 0.1 m. Materials considered were mild, galvanized steel and plywood. Figure 6 shows a picture of the dryer as constructed, with solar panels attached to supply the power needed to activate the blower. The hybrid solar dryer reported an increase in drying chamber temperature from 38 to 62°C, while the temperature of the control experiment (open sun) did not exceed of 45°C during the peak period of solar radiation (12-2pm). They argued that the efficiency of dryers could be enhanced by combining solar and heating element coils powered by a PV panel as compared to biomass heating sources.



Figure 6. A hybrid photovoltaic (PV) solar dryer ([Hussien *et al.*, 2017](#)).

[Padhi and Bhagoria \(2013\)](#) developed a mixed-mode forced convective solar dryer. A smooth and rough plate solar collector was attached to the dryer. The roughness of the absorber underside enhanced heat transfer within the drying chamber. The dryer was observed to have achieved drying within four days, as against eight days which was the case of the control experiment (open sun). [Yunus and Al-Kayiem \(2013\)](#) simulated a hybrid solar dryer. They averred that the dryer's performance was dependent on effective thermal heat flow in the inner chamber of the dryer. The simulation process was considerably in agreement with data from the experiment, although the high temperature spot showed the low circulation of air, portraying the design as faulty. [Etim *et al.* \(2020\)](#) designed an air indirect mode solar dryer. The focus of their design was to examine the effect of the air inlet vent on the performance of the dryer. It was repeated that the dryer performance was dependent on the air inlet area. They observed that the dryer was able to reduce the drying time by 40%. The solar dryer was optimized for efficiency, and a further reduction of the drying time by 65% was achieved ([Etim *et al.*, 2021](#)).

[Shaikh and Kolekar \(2015\)](#) reviewed several hybrid solar dryers and made quite the same significant observations. They observed that in most underdeveloped countries, farmers depend hugely on open sun for drying harvested products. They argued that practices of this sort affect the quality of dried products, enhance the infestation by

impurities, and promote uneven drying rates. They observed that the high cost associated with hybrid mode solar dryers, despite its ease of fabrication and usage, has led to a deviation of interest from advancing the use of the system for drying agricultural products, one of such being a hybrid solar dryer developed by [Saravanan *et al.* \(2014\)](#) as shown in Figure 7. They advised the use of low-cost materials that are particular to the environment of the drying for the fabrication of hybrid solar dryers to enhance acceptability and usage. Similar observation was made by [Lamrani *et al.* \(2022\)](#).

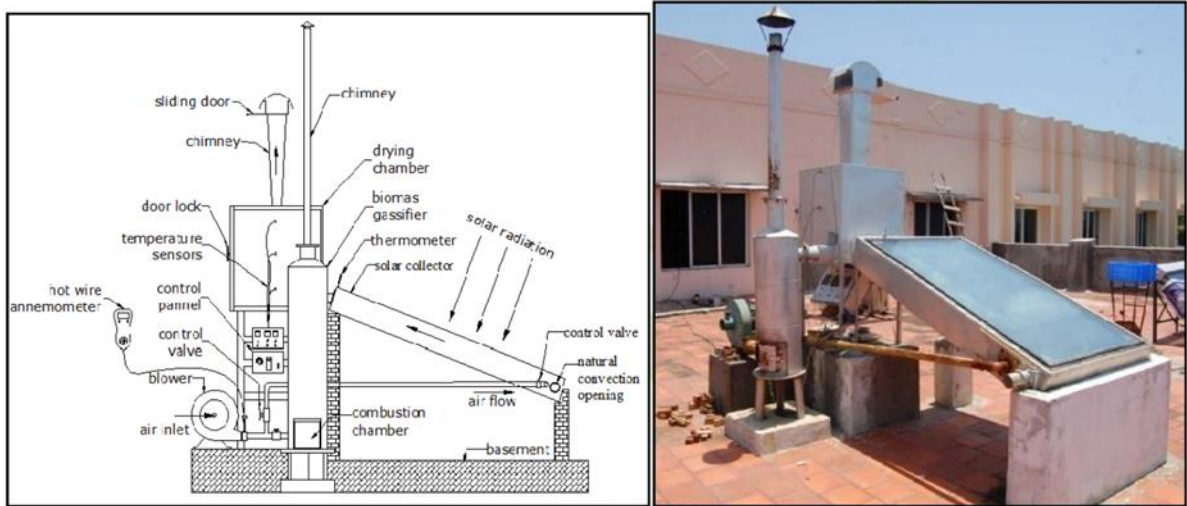


Figure 7. Hybrid solar dryer ([Saravanan *et al.*, 2014](#)).

SOME RECENT ADVANCEMENT IN GREEN HOUSE TYPE SOLAR DRYERS

[Prakash and Kumar \(2014\)](#) designed, developed, and tested a greenhouse type dryer modified with conditions of natural convection. Their study was aimed at examining the performance of the dryer based on factors such as heat loss, diffusion, heat transfer, and thermal efficiency. To preserve heat, the wall of the dryer was designed with an opaque feature.

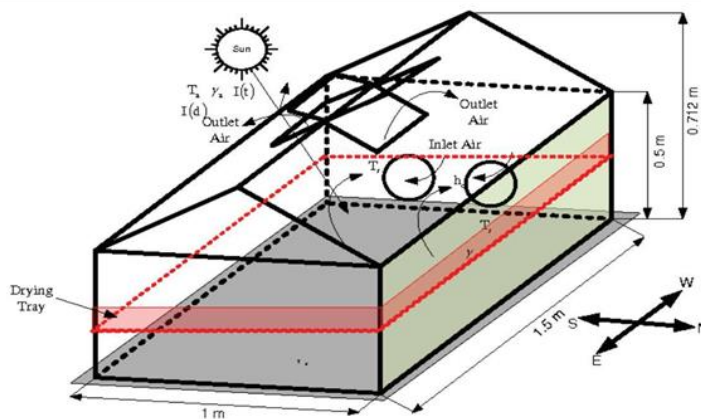


Figure 8. Skeletal view of a modified greenhouse type developed by [Parkash and Kumar \(2014\)](#).

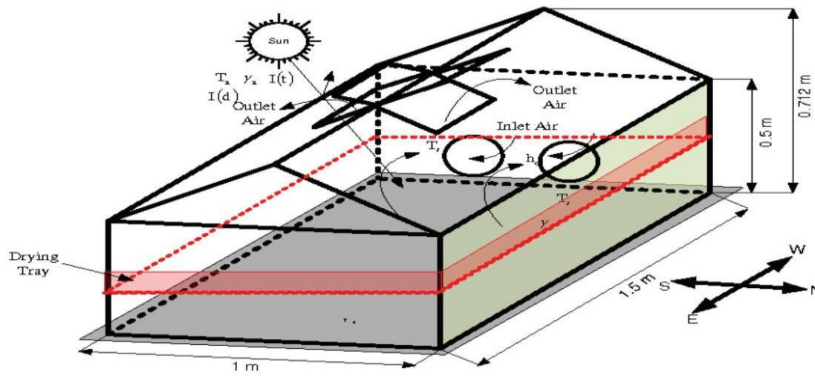


Figure 9. Skeletal view of a modified greenhouse type with a black PVC cover material, developed by [Parkash and Kumar \(2014\)](#).

Two sets of experiments were conducted for the respective dryers, the first seeing the greenhouse rest of a sandy ground (Figure 8). The floor of the dryer was covered with a sheet of black plastic (Figure 9). The latter was discovered to be more efficient than the former, because the black PVC aided the retention of heat inside the dryer.

[Barnwal and Tiwari \(2008\)](#) designed, constructed, and tested a hybrid photovoltaic integrated greenhouse dryer for performance. The solar radiation incident on the glass of the PV module produced the heat required to increase the temperature of the greenhouse for smooth operation. The radiation was converted to a DC electric system, which was used to power a blower for efficient circulation of hot air within the chamber. They also designed a similar system but used polythene as a collector/covering material in place of glass and it was operated by a non-convective force principal. Both dryers are shown in Figure 10.

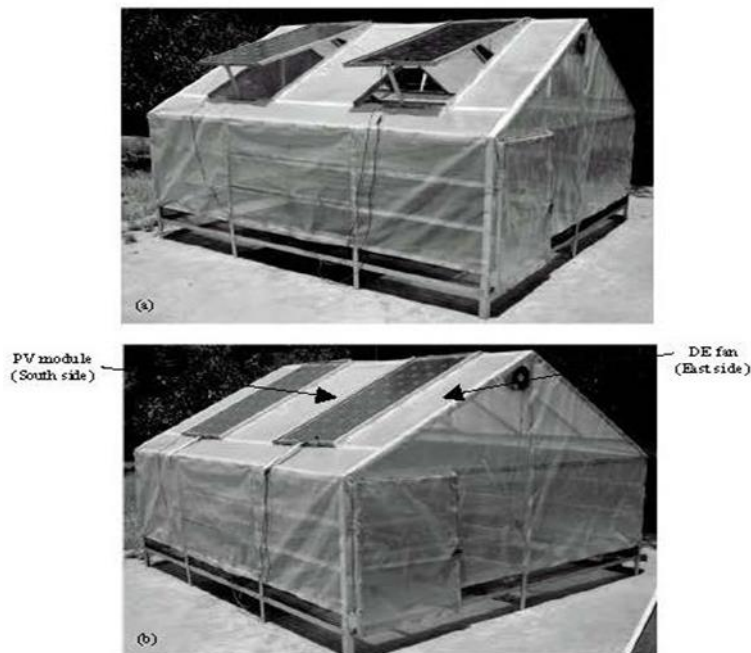


Figure 10. Natural convection and forced convection hybrid photovoltaic integrated greenhouse dryer ([Barnwal and Tiwari, 2008](#)).

It was observed that the forced convective drying system was of slight advantage than the natural convection type, as there was even distribution of hot air inside the dryer which also helped in maintaining the desired drying temperature. They concluded that the thermal loss efficiency of the dryer was reduced by 80%.

[Nguimdo and Noumegnie \(2020\)](#) designed an automatic hybrid solar dryer for households for staple crops in Cameroon. They posited that post-harvest losses in the Central African nation were because of drying systems that could help in preserving the quality of what is harvested by locals. The efficiency obtained from the hybrid system was higher than that of the passive solar system. The variation was attributed to the more efficient circulation of hot air in the drying chamber aided by the blower.

[Hempattarauwan *et al.* \(2019\)](#) designed a parabolic green-house type dryer for drying of cayene pepper and tested it for its performance. The dryer was of base area of 48 m² and height of 3.25m. It was designed to dry between 100 to 200 kg of the product in less than 50% of the time that would have been taken to dry a similar quantity of product using the open sun drying method. The dryer, which was embedded with a 50W solar cell module, powered three DC fans, and was also observed to have had more reliability in terms of preservation of the final quality of the product as against natural convection means of drying.

[Janjai \(2012\)](#) developed a greenhouse type solar dryer for small-scale drying in the Food Industry. The dryer was made of a parabolic roof structure covered with polycarbonate sheets on a concrete floor. The width of the dryer was 8m, length 20m and height was 3.5m. The dryer (1000 kg loading capacity) was fitted with nine 15W D.C. fans powered with the aid of a 50W P.V. module to ventilate the dryer. Experimental data averred that the temperature in the drying chamber increased 35 to 65°C while drying was achieved between two to three days, relatively shorter than what should have been obtained if the products were dried using natural sun drying. [Puello-Mendez *et al.* \(2017\)](#) comparatively studied the drying of cocoa beans in rural communities of Colombia. The dryer used (Figure 11) was 2.0 m in width, 5.0 m in length and 2.2 m in height. The cover material used was polyethylene film of 2.0 mm thickness.

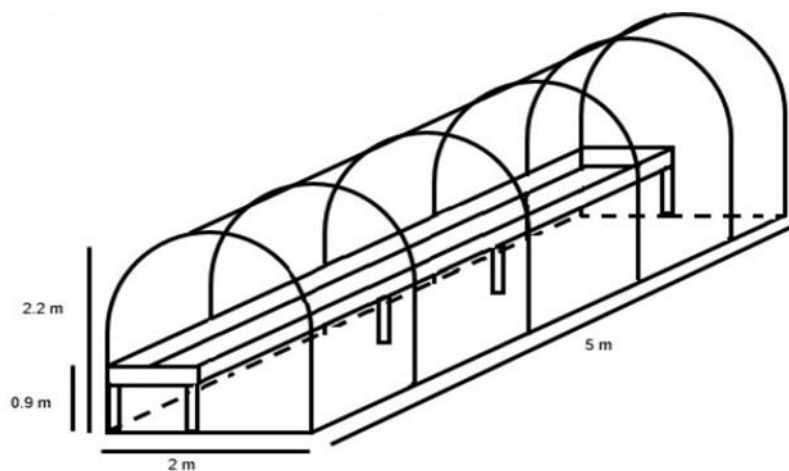


Figure 11. Interior view of a Green House type solar dryer developed by [Puello-Mendez *et al.* \(2017\)](#).

The dryer was observed to have reduced the duration of drying by two days when compared to the six days required to dry the same amount of product (2 kg) using natural sun. The moisture level of the product reportedly decreased rapidly within 48 hours of consistent drying, but gradually decreased on the third and fourth day, with corresponding increases in the drying time.

[Ndirangu *et al.* \(2020\)](#) analysed various designs of existing solar green-house type dryers in Kenya and appraised their performance. Eighteen dryers were assessed in the process and the length, width and height averaged 8.12, 3.95, and 2.37m, respectively. The analysis was based on key factors including: the design; construction materials; configuration and cost-benefit ratio. It was reported that more than 20% of the dryers were characterized by losses above 10% due to environmental conditions, ventilation concerns and spillage. About 65% of the dryers were reported to have been made of gable roof structure (Figure 12), while 23% were of parabolic shape. The remainder could not be traced to any specific shape configuration. They opined that the gable of type-solar dryer was preferred to others because of its simplicity to construct, ease of maintenance, cost, and other common features.

[Kaewkiew *et al.* \(2012\)](#) investigated the performance of a large-scale greenhouse type solar dryer for drying chilli. The dryer was 8.0 m in width, 20.0 m in length and a height of 3.5 m. It was parabolic in shaped. The experiment conducted using 500 kg of chili revealed that the moisture level reduced from an initial 74% (wet basis) to a final moisture level of 9 % (wet basis) within 72 hours of drying. When compared to open sun drying, the product could only reduce its moisture content to 66% within the same time frame. The positioning of the trays in the dryer had no significant effect on the quality of the final product.

[Nurhasanah *et al.* \(2018\)](#) developed a green-house-type dryer for red onion bulb leaves. The dryer was 6 m long, 3 m wide, and 6 m height. The roof was made of transparent fiber glass equipped with an aeration wall. A heat exchanger was also embedded into the dryer to optimize the flow of hot air within the dryer for faster drying of the product. Experiments conducted revealed that 1000 kg of red onion bulb leaf with an initial moisture level of 87% reduced to 14% (wet basis) within 35 hours. This was economical for large scale operations, as against open sun drying which would require double the time. Another significant advantage of the dryer as reported was its ability to work optimally irrespective of seasonal variation.

[Roman-Roldan *et al.* \(2019\)](#) analysed the heat transfer properties of a greenhouse solar type dryer embedded with an air heating system. The dryer (Figure 12) was of 6 m width, 5 m length and 4 m height. The dryer had two inlets and two outlet points to enhance the circulation of hot air during the drying process. The system was observed to have been 60% more efficient than the control experiment (open sun) and recommended for drying the products withintemperature not more than 70°C.



Figure 12. Greenhouse solar dryer embedded with air solar heating device showing air inlet (a) and outlet (b) ([Roman-Roldan et al., 2019](#)).

[Intawee and Janjai \(2011\)](#) have designed and evaluated the greenhouse solar dryer made with polyethylene as cover material. The dryer was of 7.5 m width, 20.0 m length and a height of 3.7 m. It was designed to handle 1000 kg of product per batch. Six number direct current fans were attached to the dryer for optimal circulation of hot air within the drying chamber. The blowers were powered using three 50W solar cell modules. Readings from the experiments were taken with the aid of a digital data logger. The dryer (Figure 13) was used to dry chili and banana and the result from the experiments showed that the moisture level of the product (chili) reduced from 76% (wet basis) to 10% (wet basis) within 72 hours, whereas, the moisture content of chili of the product exposed to open sun experiment could not be reduced to 44% within the same period (72 hours). Similar result was recorded for banana samples which were also subjected to drying on the dryer.

RESEARCH GAPS



Figure 13. Interior view of a greenhouse dryer for drying chilli (a) and banana (b) ([Intawee et al., 2011](#)).

This review has highlighted a few gaps, which are rather technical and a complete deviation from the initial installation cost, which researchers attribute limited utilization of hybrid and greenhouse-type dryers to. From the study, most designs based the width, length and height of greenhouse-type dryers on assumptions, without necessary recourse to the quantity of product to be dried and considerations for the design of the drying chamber. In some cases, the dimensions (length, width

and height) informed the sizing of the drying chamber, and considerations not made for loading and unloading of the product in the dryer.

Another critical concern observed was the uniformity of the air flow in the drying chamber. From the several studies examined, the positioning of the blowers (DC fans) may not affect the overall performance of the dryer, but aid in the fast drying of product in segments where they were placed, while drying gets optimal in other segments of the chamber with time.

Adequate sizing of the blower is also key. It was observed that the blowers used for the dryers reviewed were based on assumption. The air-flow rate within the drying chamber and outside should have been considered in many of the designs, to allow for proper sizing of the fans. The fans should also be dependent on the capacity of the dryer and should be used as the basis for determining the amount of power required for optimal operation.

Most of the greenhouse type dryers were of parabolic shape, while a few preferred the roof type. Most of the fabricators preferred the parabolic type because of its initial cost and maintenance options. The parabolic shaped dryers were reported to be more efficient because of their configuration, which aids in more direct penetration of solar radiation. Most of the dryers were observed to have been constructed with polyethylene, as against more heat-retaining materials like Perspex. The choice of cover material is of relevance, given environmental and other factors. In summary, the design of most greenhouse type solar dryers is based on assumptions and factors the design engineer considered relevant for the design.

CONCLUSION

Hybrid and greenhouse type solar dryers are more efficient than passive and active solar drying systems. These systems should be utilized to minimize post-harvest related losses in fruits and vegetables. Local materials that are more efficient and available can be deployed to serve the purpose since the cost of acquiring some of the materials reviewed was relatively higher. The initial cost of acquiring a hybrid and greenhouse type is significantly high. However, it is strongly recommended that farmers who are into production of crops of similar characteristics, which require drying and removal of moisture content for prolonged shelf life, should form themselves into cooperatives and acquire a large scale dryer to help in cost reduction and profit maximization. Similarly, prior attention should be paid to the dimensions, sizing of air heating and circulation medium when designing a hybrid and greenhouse-type solar dryer to ensure optimal performance.

ACKNOWLEDGEMENTS

The authors hereby acknowledge the Tertiary Education Trust Fund (TETFund) through the National Research Fund (NRF) Intervention of 2020 for sponsoring the research on production and packaging of Zobo tea. An Active solar dryer for drying of Zobo leaves and calyx was built through this fund.

DECLARATION OF COMPETING INTEREST

The authors declare that they have no conflict of interest.

CREDIT AUTHORSHIP CONTRIBUTION STATEMENT

Promise ETIM: Investigation, conceptualization, writing-original draft, review, and editing

Akindede ALONGE: Investigation, conceptualization, writing-original draft, review, and editing

David ONWE: Writing-original draft, review, and editing

Inimfon OSSOM: Writing-original draft, review, and editing.

ETHICS COMMITTEE DECISION

This article does not require any ethical committee decision.

REFERENCES

- Afzal A, Iqbal T, Ikram K, Anjum MN, Umair M, Azam M, Akram S, Hussain F, Ameen Ul Zaman M, Ali A and Majeed F (2023). Development of a hybrid mixed-mode solar dryer for product drying. *Heliyon*, 9(3): e14144. <https://doi.org/10.1016/j.heliyon.2023.e14144> PMID: 36915557; PMCID: PMC10006682.
- Alonge AF and Jackson NI (2014). Development of an indirect forced convection solar dryer for cassava chips. *Journal of Agricultural Engineering and Technology (JAET)*, 22 (4): 89-100. Available online at <https://jaet.com.ng/index.php/Jaet/article/view/47>
- Alonge AF and Uduak US (2014). Development of A direct active solar dryer and its use in drying chester leaves (*Heinsia crinita*). *Journal of Agricultural Engineering and Technology (JAET)*, 22(4):110-120. Available online at <http://www.jaet.com.ng/index.php/Jaet/article/view/49>
- Alonge AF, Ukonne IN and NI Jackson (2020). Development of a mixed mode passive solar dryer. *Nigerian Journal of Solar Energy*, 31 (1): 80 – 89.
- Amer BMA, Hossain MA and Gottschalk K (2010). Design and performance evaluation of a new hybrid solar dryer for banana. *Energy Conversation and Management*, 51(4): 8130-820. <https://doi.org/10.1016/j.enconman.2009.11.016>
- Aremu OAI, Odepidan KO, Adejuwon SO and Ajala AL (2020). Design, fabrication and performance evaluation of hybrid solar dryer. *International Journal of Research and Innovation in Applied Science*, 5(3): 159-164.
- Almuhanna EA (2012). Utilization of a solar greenhouse as a solar dryer for drying dates under the climatic conditions of the eastern province of Saudi Arabia. *Journal of Agricultural Science*, 4(3): 237 – 246. <http://dx.doi.org/10.5539/jas.v4n3p237>
- Barnwal P and Twari A (2008). Design, construction and testing of hybrid photovoltaic integrated greenhouse dryer. *International Journal of Agricultural Research*. 3(2): 110-120. <https://doi.org/10.25125/engineering-journal-IJOER-MAY-2017-4>
- Cesar LE, Isaac PF and Artuto N (2015). Drying of strawberry in a direct and indirect solar dryer (Effects of drying methods on total phenolic content). *International Journal of Advances in Agricultural & Environmental Engineering*, 2(2): 61-63. <http://dx.doi.org/10.15242/IJAEE.ER12150176>
- Duque-Dussán, E, Sanz-Urbe, JR, and Banout, J (2023). Design and evaluation of a hybrid solar dryer for postharvesting processing of parchment coffee. *Renewable Energy*, 215. <http://dx.doi.org/10.1016/j.renene.2023.118961>

- Etim PJ, Eke AB and Simonyan K.J (2019). Effect of air inlet duct and grater thickness on cooking banana drying characteristics using active indirect mode solar dryer. *Nigerian Journal of Technology*, 38(4): 1054-1063. doi: <http://dx.doi.org/10.4314/njt.v38i4.31>
- Etim PJ, Eke AB and Simonyan K.J (2020). Design and development of an active indirect solar dryer for cooking banana. *Scientific African*. e00463. doi: <https://doi.org/10.1016/j.sciaf.2020.e00463>
- Etim PJ, Eke AB, Simonyan KJ, Umani, KC and Udo S (2021). Optimization of solar drying process parameters of cooking banana using response surface methodology. *Scientific African*. e00964. doi: <https://doi.org/10.1016/j.sciaf.2021.e00964>
- Etim PJ, Olatunji MO, Ekop IE, Alonge AF and Offiong UD (2023): Optimization of air inlet features of an active indirect mode solar dryer: A response surface approach. *Clean Energy Technologies*, 1(1): 12-22. <https://doi.org/10.14744/cetj.2023.0003>
- FAO (2017). Drying construction for solar dried fruits and vegetables production. www.teca.fao.org/read/4502. Accessed 28-10-2020.
- Hussien JB, Hassan MA, Kareem KB and Filli, KB (2017). Design, construction and testing of a hybrid photovoltaic (PV) solar dryer. *International Journal of Engineering Research and General Science*, 3(5): 1-14. <https://doi.org/10.25125/engineering-journal.IJOER-MAY-2017-4>
- Intawee P and Janjai, S. (2011). Performance evaluation of a large-scale polyethylene covered greenhouse solar dryer. *International Energy Journal*, 12: 39-52.
- Janjai S (2012). A green house type solar dryer for small-scale dried food industries: Development and dissemination. *International Journal of Energy and Environment*, 3(3): 383-398.
- Janjai S and Bala BK (2012). Solar Drying Technology. *Food Engineering Reviews*, 4: 16-54. <https://doi.org/10.1007/s12393-011-9044-6>
- Kaewkiew J, Nabnean S and Janjai S (2012). Experimental investigation of the performance of a large-scale greenhouse type solar dryer for drying chilli in Thailand. *Procedia Engineering*, 32: 433-439. <https://doi.org/10.1016/j.proeng.2012.01.1290>
- Lamrani B, Elmrabet Y, Mathew I, Bekkioui N, Etim PJ, Chahboun A, Draoui, A and Ndukwu, MC (2022). Energy, economic analysis and mathematical modelling of mixed-mode solar drying of potato slices with thermal storage loaded V-groove collector: Application to Maghreb region. *Renewable Energy*, 200(22): 48-58. <https://doi.org/10.1016/j.renene.2022.09.119>
- Madhava M, Kumar S, Rao DB, Smith DD and Kumar HVH (2017). Performance evaluation of photovoltaic ventilated hybrid greenhouse dryer under no-load condition. *Agricultural Engineering International: CIGR Journal*, 19(2): 93-101.
- Mohammed S, Edna M and Siraj K (2020). The effect of traditional and improved solar drying methods on the sensory quality and nutritional composition of fruits: A case of mangoes and pineapples. *Helvion*. <https://doi.org/10.1016/j.helivon.2020.e04163>
- Mohsen HA, El-Rahmam AA and Hassan HE (2019). Drying of tomato fruits using solar energy. *Agricultural Engineering International: CIGR Journal*. 21(4): 204-215.
- Murali S, Amulya PR, Alfiya PV, Delfiya DS, Aniesrani S and Manoj P (2020). Design and performance evaluation of solar-LPG hybrid dryer for drying shrimps. *Renewable Energy*, 147(1): 2417-2428. <https://doi.org/10.1016/j.renene.2019.10.002>
- Ndirangu SN, Kanali CL, Mutwiwa UN, Kituu GM and Ronoh EK (2020). Analysis of designs and performance of existing greenhouse solar dryers in Kenya. *Journal of Postharvest Technology*, 6(1): 27-35.
- Nguimdo LA and Noumegmie, VAK (2020). Design and implementation of an automatic indirect hybrid solar dryer for households and small industries. *International Journal of Renewable Energy Research*, 10(3): 1415-1421.
- Nurhasanah A, Suparlan S and Mokhtar S (2018) Technical and economic analysis of a plant scale green-house dryer for red onion bulb. *Integrative Food, Nutrition and Metabolism*, 4(2): 1-5. <https://doi.org/10.15761/IFNM.1000175>
- Padhi C and Bhagoria J (2013). Development and performance evaluation of mixed-mode solar dryer with forced convection. *International Journal of Energy and Environmental Engineering*, 4:23. doi: <http://www.journal-ijeee.com/content/4/1/23>
- Poonia S, Singh AK and Jain D (2018). Design, development and performance evaluation of a photovoltaic/thermal (PV/T) hybrid solar dryer for drying of ber (*Zizyphus Mauritania*) fruit. *Cogent Engineering*, 5: 1. <https://doi.org/10.1080/23311916.2018.1507084>

- Prakash O and Kumar A (2014). Design, development and testing of a modified green house dryer under conditions of natural convection. *Heat transfer Research*, 45(5): 433-451. <https://doi.org/10.1615/HeatTransRes.2014006993>
- Puello-Mendez J, Meza-Castellar P, Cortés L, Bossa L, Sanjuan E, Lambis-Miranda H and Villamizar L (2017). Comparative study of solar drying of cocoa beans: Two methods used in colombian rural areas. *Chemical Engineering Transactions*, 57: 1711-1716. <https://doi.org/10.3303/CET1757286>
- Roman-Roldan N, Lopez-Ortiz A, Ituna-Yudonago J, Garcia-Valladares O and Pilatowsky-Figueroa I (2019). Computational fluid dynamics analysis of heat transfer in a greenhouse solar dryer chapel-type coupled to an air solar heating system. *Energy Science & Engineering*, 7: 1123–1139. <https://doi.org/10.1002/ese3.333>
- Saravana D, Wilson V and Kuamarasamy S (2014). Design and thermal performance of the solar biomass hybrid dryer for cashew drying. *Facta Universitatis Mechanical Engineering*, 12(3): 277-288.
- Shaikh TB and Kolekar AB (2015). Review of hybrid solar dryers. *Int'l Journal of Innovations in Engineering Research and Technology*, 2(8): 1-7. <https://doi.org/10.5281/zenodo.1469961>
- Udomkun P, Romuli S, Schock S, Mahayothee B, Sartas M, Wossen T, Njukwe E, Vanlauwe, B and Muller J (2020). Review of solar dryers for agricultural products in Asia and Africa: An innovation landscape approach. *Journal of Environmental Management*, 268: 1-14. <https://doi.org/10.1016/j.jenvman.2020.110730>
- Yahya M (2016). Design and performance evaluation of a solar assisted heat pump, dryer integrated with Biomass furnace for Red chilli. *International Journal of Photoenerg*, 1-14. <https://doi.org/10.1016/j.renene.2019.10.002>
- Yunus YM and Al-Kayiem HH (2013). Simulation of hybrid solar dryer. IOP Conf. Ser: Earth Environ. Sci. 16: 012143. <http://dx.doi.org/10.1088/1755-1315/16/1/012143>

TURKISH JOURNAL OF AGRICULTURAL ENGINEERING RESEARCH

TURKAGER



2024

e-ISSN:2717 - 8420

<https://dergipark.org.tr/tr/pub/turkager>

